FR 81-11-1246

FINAL REPORT

ON THE

CANCELLATION OF SURFACE REVERBERATION

FROM A BISTATIC SONAR

January 20, 1982

Prepared Under

Contract Number N00024-80-C-6292

For The

Naval Sea Systems Command Code 63R

Hughes Aircraft Company
Ground Systems Group
Fullerton, California

82 06 28 365

Final Report
on the
Cancellation of Surface Reverberation
From a Bistatic Sonar

January 20, 1982

Prepared Under
Contract Number N00024-80-C-6292
for the
Naval Sea Systems Command
Code 63R

By
P.L. Feintuch
F.A. Reed
N.J. Bershad

Hughes Aircraft Company
Ground Systems Group
Fullerton, CA.

FOREWORD

This report documents the effort performed under contract number N00024-80-C-6292 for the Naval Sea Systems Command Code 63R, and covers the period from October 1980 to September 1981. The study has considered the use of LMS adaptive cancellation to suppress convergence zone surface reverberation in a bistatic sonar. The work was directed by Mr. Daniel Porter of NAVSEA Code 63R.

ABSTRACT

This report considers the cancellation of surface reverberation from the convergence zone (CZ) using an LMS multiple canceller structure. In CZ operations, this surface reverberation is often the limiting factor in the detection of low doppler targets. The multiple reference canceller approach is bistatic in that hydrophones spatially separated from the active sonar transmit/receive array are used as references to cancel the CZ surface reverberation. When the target is submerged below the CZ, providing spatial separation of the target and surface, it may be possible to spatially reject the CZ surface reverberation but not the target, allowing detection.

The first phase of the study, reported in this document, concentrates on the ability of the canceller to reject the reverberation in the absense of signal. The CZ surface reverberation is modeled as an extended source with range extent limited by the width of the CZ and horizontal extent limited by the horizontal directivity of the transmitter. When viewed from typical convergence zone ranges, this source appears to have narrow angular extent. Using the narrow extended source model, expressions are developed for the second order statistics of the canceller output. It is shown that the solution to the spatial cancellation problem with a narrow, extended source is functionally equivalent to the linear prediction of a bandlimited, temporal sequence. This equivalence not only allows use of the results of linear prediction theory in the spatial case, but provides an intuitive feel for the parametric behavior of the spatial canceller.

Using the analytical results, the cancellation achieved is examined as a function of the reverberation and canceller parameters. It is shown that as the number of references, K, is increased, the cancellation improves rapidly

up to some threshold value, say, $K=K_0$, the improvements diminish rapidly. Given the computational cost of adding a reference, the use of $K > K_0$ references may not be justified. The value of K_0 is determined approximately, and provides a design guide for the selection of the number of references in any given sonar situation. Significantly, effective cancellation of the reverberation can be achieved using less than four references. Extensive curves showing the parametric dependencies of the cancellation on the design parameters are given as design tools. The report also describes several configurations of the LMS canceller structure for use in the non-stationary reverberation environment and discusses their performance.

The second phase of this study will focus on two areas: the incorporation of a plane wave signal in the model; and the verification of the extended source model as representative of the CZ surface reverberation. This report on the first phase of the study includes some initial determination of the response of the canceller to the signal. These results must be extended to include the effect of the primary array and the detailed characteristics due to separation of the target and the reverberating surface. The performance of the canceller will ultimately be evaluated in terms of the improvement in detection performance provided by the canceller over that achieved without the canceller. Again, this will be examined as a function of the canceller design parameters, reverberation extent, and the spatial separation between surface and target.

To assess the validity of the analytical models, a computer simulation of the multiple canceller structure will be developed. This will first be tested against computer generated data simulating the active sonar in the CZ detection mode. More importantly, the simulation will be run on actual

data from sea tapes to be provided by the Navy. Any changes to the models necessitated by the simulation runs will be made in the analysis and the effect of these changes on canceller performance examined.

TABLE OF CONTENTS

LIST OF ILLUSTRATIONS

LIST OF ILLUSTRATIONS (Continued)

LIST OF ILLUSTRATIONS (Continued)

LIST OF ILLUSTRATIONS (Continued)

LIST OF ILLUSTRATIONS (Continued)

LIST OF ILLUSTRATIONS (Continued)

LIST OF ILLUSTRATIONS (Continued)

LIST OF ILLUSTRATIONS (Continued)

1.0 INTRODUCTION

1.0 INTRODUCTION

This is the final report on the first phase of a study of a technique for processing against surface reverberation from the convergence zone in an active sonar. When attempting to detect a low doppler, submerged convergence zone (CZ) target, this backscatter of the transmitted waveform from the surface above the target can be the limiting background noise. The concept involves bistatic or multistatic operation, in which reference hydrophones spatially separated from the primary transmit/receive array of the sonar are used to suppress the reverberation in the primary array output. This is done using a Least Mean Square (LMS) adaptive multiple canceller structure, which has been used in the past to suppress point interference in the output of a beamformer[1]. The CZ surface reverberation, however, appears as a narrow extended acoustic interference, so this study addresses the performance of the multiple canceller concept with extended sources.

The most common (and most practical) algorithm for the implementation of spatial noise cancellation is the Least Mean Square (LMS) algorithm described in [2]. Define the inputs to the algorithms as

$$d(n) = \text{desired input at } n^{th} \text{ sample time}$$

$$x(n) = \text{reference input at } n^{th} \text{ sample time.}$$

The LMS algorithm stores the M-dimensional data vector

$$\underline{X}(n) = [x(n), x(n-1), \ldots x(n-M+1)]^T \tag{1-1}$$

and computes the filter output,

$$\dot{y}(n) = \underline{W}^T(n) \, \underline{X}(n) \tag{1-2}$$

with

1

$$\underline{W}(n) = \left[W_0(n), W_1(n), \ldots, W_{M-1}(n) \right]^T$$

the weight vector of length M. The weights are updated recursively to minimize the mean squared value of the error signal, defined as

$$\epsilon(n) = d(n) - y(n) \tag{1-3}$$

This is done by means of a gradient descent approach in which the actual gradient of the mean squared error is replaced by an estimate of the gradient extracted from the data vector, $\underline{X}(n)$. This yields the very simple weight update equation

$$\underline{W}(n+1) = \underline{W}(n) + \mu\epsilon(n)\underline{X}(n) \tag{1-4}$$

where μ is a weight update coefficient that controls the rate of convergence and stability of the algorithm.

When the inputs to the LMS adaptive structure are zero mean random sequences that are at least wide sense stationary, the weights given by (1-1) can be shown to converge in the mean to the discrete Wiener filter provided μ is sufficiently small to assure stability[3]. That is, if E[x] denotes the expected value of x and

$$\left. \begin{array}{l} E[d(n)] = E[x(n)] = 0 \\[2ex] R_{xx} = E[\underline{X}(n)\,\underline{X}^T(n)] \\[2ex] \text{and} \\[2ex] \underline{r}_{dx} = E[d(n)\,\underline{X}(n)] \end{array} \right\} \quad k = 0, 1, \ldots K-1 \tag{1-5}$$

then

$$\lim_{n \to \infty} E[\underline{W}(n)] = R_x^{-1}\,\underline{r}_{dx} \tag{1-6}$$

2

under the appropriate conditions on μ. Reference [3] shows that (1-6) occurs if

$$0 < \mu < 1/\lambda_{max} \qquad (1-7)$$

where λ_{max} is the largest eigenvalue of the covariance matrix, R_{xx}. Further, it is shown that the mean of the weights of the adaptive filter approach the Wiener solution, (1-6), approximately exponentially with the time constant

$$\tau_I \approx \frac{1}{\mu \lambda_{min}} \qquad (1-8)$$

where τ_I is expressed in iterations of the filter and λ_{min} is the smallest eigenvalue of the covariance matrix, R_{xx}.

Because the weights are computed from the random input data in (1-4), they are themselves random, and exhibit fluctuations about the discrete Wiener solution, (1-6). Therefore, the power in the error, $\varepsilon(n)$, is greater than the error that would be achieved by the Wiener weights. This increase in error power due to algorithm noise is termed the misadjustment [3] of the algorithm. In general, due to the recursive nature of (1-4), even the second order statistics of the weights cannot be determined analytically in closed form. As will be discussed below, one way of approximating the weight variance is to develop a frequency domain model for the adaptive filter, as in [4], and to then use [5].

Now, consider using this LMS adaptive filter to adaptively cancel a single plane wave interference from the output of a beam steered in the direction of a signal of interest. A single hydrophone is chosen as a reference, providing the reference input to the LMS algorithm, $x(n)$. The desired input, $d(n)$, is the output of the beam steered toward the signal.

which is assumed to arrive from a different angle than the interference. Because the interference dominates both the reference hydrophone and beam outputs, the adaptive filter minimizes the mean squared value, or power, in $\epsilon(n)$ primarily by eliminating the interference component. It does this by attempting to insert a delay in the reference input equal to the propagation delay between the phase center of the primary array and the reference hydrophone, plus a gain equal to the primary array gain. The interference component of the filter output is then nearly coherent with the primary array output, so that the interference is cancelled in the error waveform, which serves as the canceller output. In order to cancel the signal, the filter would have to adapt to the propagation delay and array gain for the signal, which differ from those for the interferences because the arrival angles differ. In doing this, the structure would pass the much stronger interference, increasing the mean squared error. The adaptive algorithm therefore converges to a solution which cancels the interference but passes the signal. In a spatial sense, this can be viewed as steering a null in the beam response in the direction of the plane wave interference. Generally, the signal will be somewhat attenuated by the cancellation process, but this will be tolerable in view of the much greater rejection of the interference.

If the interference must be modelled as more than one, say K, plane wave sources, then, in general, K spatially separated references will be needed to allow spatial nulls to be steered in the direction of each. The LMS algorithm can be configured to use K reference inputs as follows. Let

$$x_k(n) = k^{th} \text{ reference input at } n^{th} \text{ sample time } (k = 0, 1, \ldots K-1)$$

and let the algorithm store the K data vectors of length M,

$$\underline{X}_k(n) = [x_k(n), x_k(n-1), \ldots x_k(n-M+1)]^T, \quad k = 0, 1, \ldots K-1 \tag{1-9}$$

The LMS algorithm computes

$$y_k(n) = \underline{W}_k^T(n) \underline{X}_k(n), \quad k = 0, 1, \ldots K-1 \tag{1-10}$$

where $\underline{W}_k(n)$ is the kth weight vector, with the error given by

$$\epsilon(n) = d(n) - \sum_{k=0}^{K-1} y_k(n), \quad k = 0, 1, \ldots K-1 \tag{1-11}$$

The weights are updated according to

$$\underline{W}_k(n+1) = \underline{W}_k(n) + \epsilon(n) \underline{X}_k(n), \quad k = 0, 1, \ldots K-1 \tag{1-12}$$

Note that each implementation of (1-10) is a non-recursive digital filter

with time varying weights, so the multiple reference LMS algorithm can be

represented as shown in Figure 1-1. Each reference input is passed through

a non-recursive digital filter, the filter outputs used to form the error, $\epsilon(n)$,

by (1-13), then the error fed back to update the filter weights according to

(1-4).

In many practical situations, the computational requirements of implement-

ing (1-16), (1-17), and (1-18) are prohibitive, and the cancellation must be

done using the so-called frequency domain LMS algorithm [4, 6]. The fre-

quency domain algorithm first Fast Fourier Transforms (FFT's) the reference

and primary inputs, forming
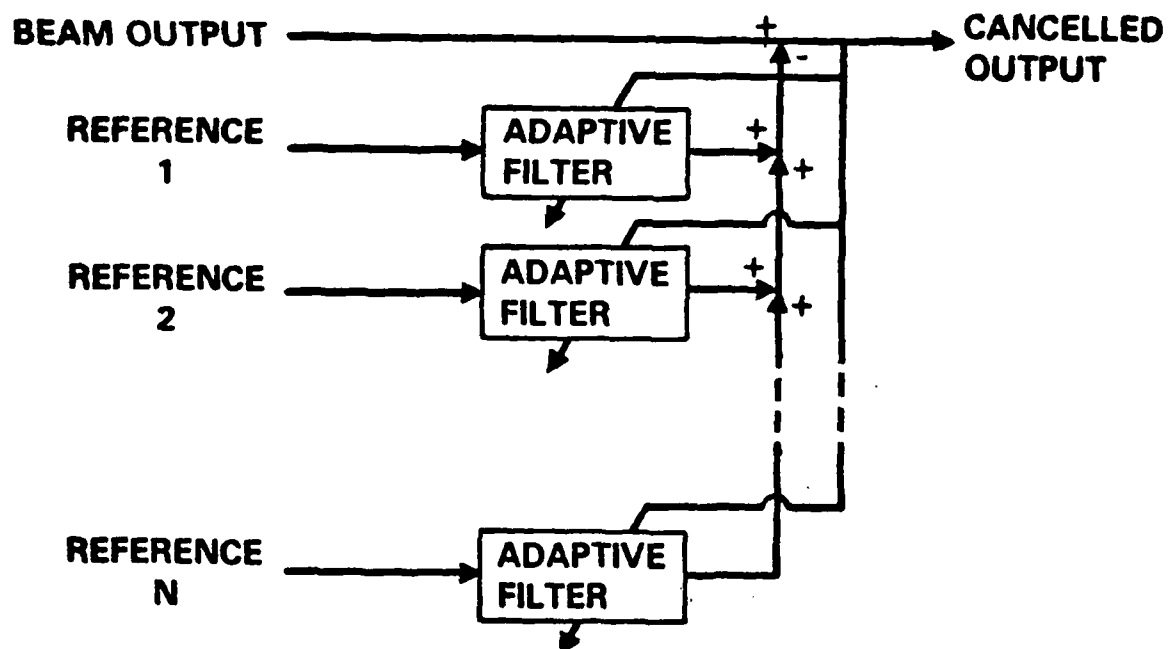
Figure 1-1. Multiple Reference LMS Algorithm

$D_i(n)$ = i^{th} FFT coefficient at time n

$$= \sum_{m=0}^{M-1} d(m + nM) \, e^{-j \frac{2\pi}{M} mi} \qquad (1\text{-}13)$$

and

$X_{ik}(n)$ = i^{th} FFT coefficient of kth reference at time n

$$= \sum_{m=0}^{M-1} x_k(m + nM) \, e^{-j \frac{2\pi}{M} mi} \qquad (i = 0, \, 1, \, \dots M\text{-}1) \quad (1\text{-}14)$$

where M is again the dimension of the $\underline{X}_k(n)$ data vectors. A single tap complex LMS algorithm is then performed independently in each frequency bin. Let

$F_{ik}(n)$ = the frequency domain weight in the ith FFT bin for the kth reference at time n

Then the LMS filter output in the ith bin for the kth reference at time n is

$$Y_{ik}(n) = F_{ik}(n) \, X_{ik}(n) \qquad (1\text{-}15)$$

and the error in the ith FFT bin (used to update all K filters) is

$$E_i(n) = D_i(n) - \sum_{k=0}^{K-1} Y_{ik}(n) \qquad (1\text{-}16)$$

The complex LMS algorithm [7] gives the updated weights as

$$F_{ik}(n+1) = F_{ik}(n) + E_i(n) \, X_{ik}^*(n) \qquad (1\text{-}17)$$

If required, the time domain canceller output can be obtained by inverse FFTing the $E_i(n)$.

While this algorithm gives significant computational savings over the time domain approach, it is not an exact implementation of the time domain algorithm and can give different results, even in relatively simple cases [4]. A number of practical cancellation problems have been solved using the frequency domain approach, however [8, 9]. When it can be used, it has some analytical advantages in that it may be possible to determine the variance of the frequency domain weights as well as the mean using [8]. This allows the effects of algorithm noise to be considered analytically.

The CZ surface reverberation differs from interferences usually associated with LMS spatial cancellation in three ways:

(1) Extent; The first CZ will nominally appear at a range of 30 miles and have a width of approximately 2 miles, so that it appears to have a narrow vertical angular extent. In addition, most modern active sonars have horizontal directivity, so that only a horizontal sector of the CZ is illuminated. The reverberating CZ surface therefore appears as an extended source in both horizontal and vertical angles. Within this sector, the reverberation is made up of a multitude of individual reflections, often regarded as uncorrelated [10]. The surface may therefore be regarded as narrow extended source exhibiting no correlation from angle to angle. This study therefore addresses the performance of the canceller with such a source.

(2) Non-stationarity: In the active sonar environment, the input

statistics to the canceller are markedly non-stationary, consist-

ing of a transmit period followed by periods of reverberation

from various sources, intervals of ambient noise only, and signal

returns. Although the derivation of the LMS adaptive canceller

assumes stationarity of the inputs, it has often been applied in

non-stationary situations by making its convergence time short

enough to track the non-stationarities. An approach to the ap-

plication of the LMS algorithm in the reverberation environment

is also developed in this study and its performance analyzed.

(3) Noise Related to Signal: In most applications of the adaptive

canceller, the signal and noise are derived from different

sources, and are therefore uncorrelated. In the detection of a

target against the background of CZ surface reverberation, the

noise consists of many reflections of the transmitted waveform.

Since reflections of the waveform also make up the signal, the

signal and noise are related. This will not be of central interest

here, since this report concentrates on the signal absent case.

Suppose that instead of consisting of one or more discrete plane wave

sources, the interference is truly extended in that it is distributed in

angle over some finite sector. Given the argument that the adaptive can-

celler is steering nulls in the overall response pattern in the direction of the

interference, it would seem that an extended source could never be completely

cancelled. However, as more and more references are added (K increased),

steering an increasing number of nulls to the interference, it seems clear

that the amount of additional cancellation achieved per added reference would eventually become quite small. Since the computational cost of adding a reference is significant (requiring an additional LMS adaptive filter), at some point the improvement will not be worth the cost. This study examines the performance of the multiple canceller approach with extended sources using a Wiener filter model. The amount of cancellation achieved is examined as a function of the source extent, the number of references, and their location with respect to the primary array. Of particular interest is the following

    a. The degree of cancellation theoretically achieveable for an extended source

    b. The selection of the number of references for a given source extent, taking into account both cancellation performance and computational cost.

The Final Report is divided into three sections, the first of which is this Introduction. Section 2 summarizes the results of the study, describes the general approach used, and discusses the models of the adaptive canceller and extended interference source. The detailed development of the models and the derivations of the results given in Section 2 are included as Appendices A through K. Section 3 presents the general conclusions of the study as to the applicability of the LMS cancellation technique to the rejection of surface reverberation from the convergence zone. It also discusses areas where additional study is needed.

2.0 SUMMARY OF RESULTS

2.0 SUMMARY OF RESULTS

This section presents the results of the study in summary form without detailed derivations, which are included in the Appendices. Where results are best illustrated by the use of graphs, typical cases are shown here and the complete set of curves given in the Appendices. Section 2.1 discusses the application of the LMS algorithm in the non-stationary reverberation environment. Section 2.2 develops the model for the extended interference source and relates it to surface reverberation from the convergence zone. In Section 2.3, the frequency domain Wiener filter model for the adaptive canceller is derived. Section 2.4 shows that there exists an equivalence between the linear prediction of a bandlimited temporal random process and the cancellation of an extended source. This equivalence is used to apply a number of results from linear prediction theory to the problem of interest here. The general results of Section 2.4 are then specialized to a source that is uniformly distributed in angle and spatially uncorrelated in Section 2.5. This model is shown to be a reasonable model for CZ surface reverberation. Performance predictions for the multiple canceller in this enviornment are presented, and design criteria given for selection of hydrophone spacing and number of references. Section 2.6 discusses the performance of the canceller with a source producing an exponential CSD at the hydrophone outputs, and compares this performance to that achieved with the uniform source of Section 2.5. Section 2.6 investigates at the effects of the non-stationarity of the reverberation on the performance of the adaptive canceller. Finally, Section 2.7 takes a preliminary look at the response of the array to a plane wave signal in the presence of an extended source.

2.1 Cancellor Structure for Application in the Non-Stationary Reverberation Environment. As pointed out in the Introduction, the development of the LMS canceller structure is based upon the stationarity of the inputs, although the adaptive algorithm itself has been applied to non-stationary problems [9, 11]. This is done by making the time constant of the adaptation process short enough that the weights can "track" the non-stationarities. This requires use of value of μ larger than would be needed in a stationary environment with a resulting increase in algorithm noise. There is therefore a trade-off between the ability of the algorithm to follow input dynamics and the algorithm noise.

The application of the LMS canceller approach being considered here departs from this usual approach to non-stationary inputs. The active sonar environment, taken as a whole, is markedly non-stationary, consisting of periods during which reverberation from various sources (surface, bottom, convergence zone, etc) dominates the noise field. Between these periods of reverberation the ambient noise field will be the main limitation on sonar performance. However, within a period of reverberation from a particular source, the reverberation is often regarded as a stationary random process. Hence, it may be possible to avoid the need for increasing μ to track input dynamics by adapting the weights only when the convergence zone (CZ) reverberation is present. During these periods, the reverberation dominates the ambient noise component and the signal, so it should be possible to detect its presence reliability.

These considerations suggest the following canceller structure. Because the propagation distance to the CZ is so much greater than that associated

with other forms of reverberation, it is possible to exclude all other rever-
beration from influencing the canceller by freezing the weights for T_w sec-
onds after each transmission. After T_w seconds, it can be assumed that the
input to the canceller is either ambient noise or CZ surface reverberation
(possibly with a target present). The presence of the reverberation is then
determined by a simple energy detection in the reverberation band of the
primary array output, and the weights adapted only during its presence.
This structure is shown schematically in Figure 2-1. If the detector can de-
termine the presence of the CZ reverberation perfectly, the weights only
adapt in the presence of the reverberation. Given that this reverberation is
stationary, as assumed above, the inputs as seen by the weight adaptation
process are stationary at all times, so that they converge to the optimal
weights that would occur if the reverberation were always present. The
selection of μ can be made solely on the basis of acceptable algorithms mis-
adjustment. False alarms in the detector will cause the weights to adapt
in an ambient noise background, which will degrade the effectiveness of the
canceller. False dismissals in the detector will result in the weights being
frozen during the presence of the CZ reverberation, so that the algorithm
will take longer to change. It is anticipated, though, that the high rever-
beration to ambient noise ratio associated with this problem will allow detector
operation at a low probability of error.

An alternative approach can be based on the well known fact [10] that
the LMS adaptive algorithm adapts much more rapidly in an environment
producing correlation between its inputs (such as reverberation from any

13
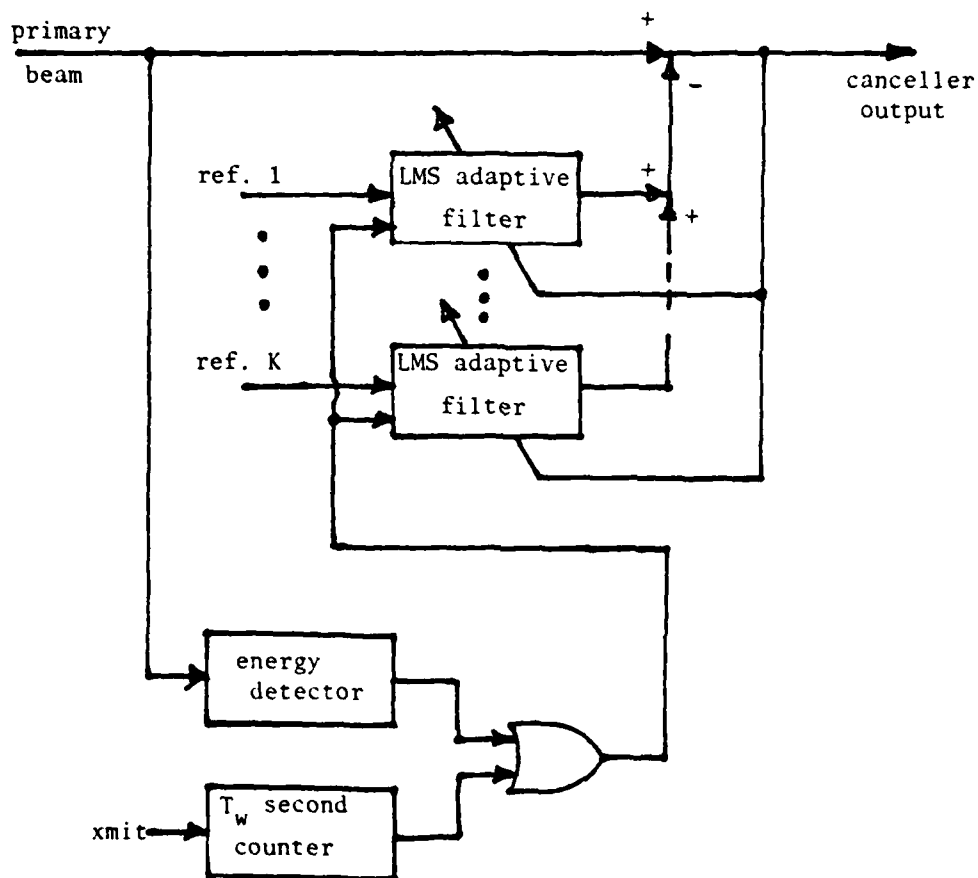
Figure 2-1. Multiple Canceller Structure for Application
to CZ Surface Reverberation

source) than to one producing uncorrelated inputs (such as ambient noise field would). That is, the filter "learns" the correlation properties of an input rapidly in comparison to the way it "forgets" those properties once the correlation disappears. Therefore, in order to maintain the properties of the convergence zone reverberation in the filter weights, it is first essential that all other forms of reverberation be excluded from the adaptation process by inhibiting the adaptation of the weights for T_w seconds after each transmission. From the point of view of the adaptive weights, then, the input consists of the intervals $[nT + T_w, (n+1)T]$ for $n = 1, 2, \ldots$ concatenated together to form a continuous input sequence. This concatenated input is then sampled every T seconds to produce the inputs $x(n)$ and $d(n)$. The question is how much the adaptation in ambient noise only, albeit slow, degrades the operation of the canceller when the reverberation actually commences. This is considered in Section 2.7.

2.2 Model for the Acoustic Field. The majority of the results of this study are based upon a far field extended source model developed in Appendix A for the particular array geometry shown in Figure 2-2. In this geometry, the K reference hydrophones are configured in a line array with an inter-hydrophone spacing of d feet. These K references are to be used in an LMS canceller to suppress an extended interference from the output of a single omnidirectional hydrophone located md feet from the nearest reference and colinear with the reference line array. In this model, the transmit/ receive array of the sonar has been replaced by a single omnidirectional hydrophone. The impact of this simplification is discussed later.
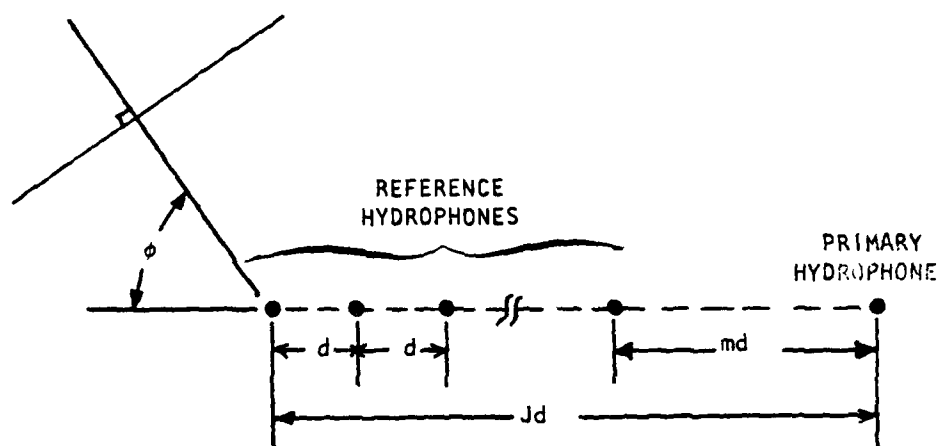
Figure 2-2. Array Geometry for Far Field Model

The extended interference is assumed to be distributed in a horizontal plane that contains the line array, as shown in Figure 2-2. The acoustic energy arriving at the array from the interference at any angle, ϕ, is assumed to produce a plane wave across the entire array (including references and primary). This requires that the distance to any point on the interference be large in comparison to the array dimensions so that the wavefront curvature is negligible. As is usually done with plane wave models, it is also assumed that the propagation losses from a point on the source to any hydrophone is the same, so that the difference in propagation to different hydrophones is characterized in terms of delay only. The common propagation losses can be lumped with the source characteristics.

Statistically, it is assumed that the acoustic energy arriving at each angle, ϕ, from the interference is a zero mean, stationary random process. In the general model, the arrivals from two angles, ϕ_1, and ϕ_2, are allowed to be correlated, producing a cross-spectral density (single frequency correlation) between the arrivals of $S_I(\phi_1, \phi_2, \omega)$. Thus the spectral density of the intererence at any arrival angle, ϕ, is $S_I(\phi, \phi, \omega)$. In addition to the interference, the acoustic field is assumed to have an isotropic background, producing zero mean noise at the output of each hydrophone. This noise is assumed to be uncorrelated from hydrophone to hydrophone and to have spectral density $\sigma_n^2(\omega)$.

Next, in Appendix A.1 the model is restricted to narrow extended interferences that are distributed over a narrow angular sector $[\phi_0 - \Phi, \phi_0 + \Phi]$. This allows an approximation leading to a two-dimensional Fourier transform relationship between the source angular distribution and the cross-spectral

density (CSD) of the hydrophone outputs. Appendix A.2 adds the additional assumption of a spatially uncorrelated interference, for which

$$S_I(\phi_1, \phi_2, \omega) = S_I(\phi_1, \omega) \delta(\phi_1 - \phi_2) \qquad (2\text{-}1)$$

In this case, the CSD between the outputs of the pth and q^{th} reference hydrophones is given by

$$s_e(p, q, \omega) = e^{-j\frac{\omega d}{c}(p-q)\cos\phi_0} \int_{-\phi}^{\phi} S_I(\phi_0 + \phi, \omega)\, e^{+j\frac{\omega d}{c}(p-q)\,\phi\sin\phi_0}\, d\phi$$
$$+ \sigma_n^2(\omega)\, \delta_{pq} \qquad (2\text{-}2)$$

which is again a Fourier transform relationship. Expression (2-2) is exploited in Section 2.4, which describes some general results for the multiple canceller structure.

Although it is not immediately apparent that this simple, far field model can be used to model surface reverberation from the convergence zone, Appendix B considers two source geometries representative of this reverberation and shows that they reduce to the form of the far field model under very reasonable assumptions. Suppose that the sonar transmitter has a horizontal beamwidth of $2\theta_1$ degrees, so that it only illuminates a sector of the annulus comprising the convergence zone, which has inside radius R_I and outside radius R_0. The illuminated sector is assumed to be centered about the angle θ_0, and the transmitter/receiver is located D feet below the surface, as shown in Figure 2-3. The reference hydrophones are placed d feet apart

18
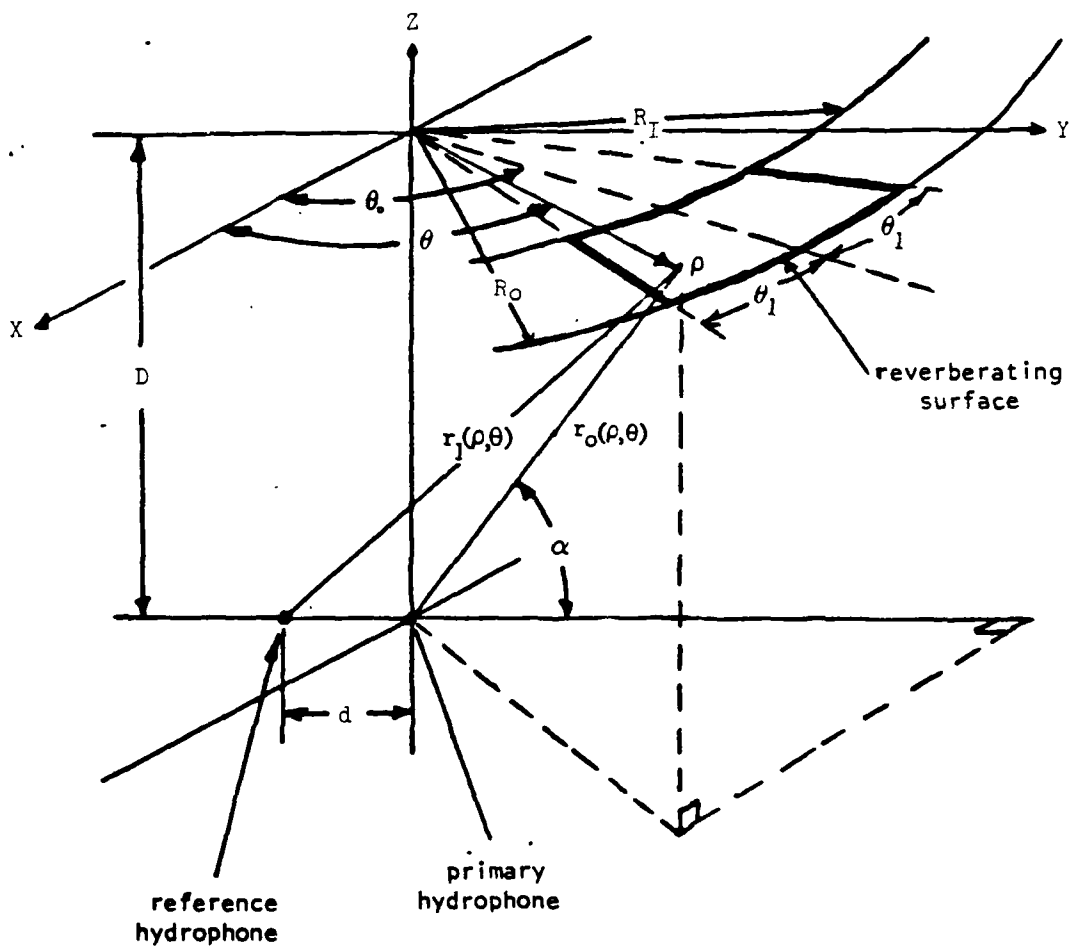
Figure 2-3. Geometry for Surface Model with Straight Line Propagation

along the negative y axis, with the distance between the primary and the closest reference md feet. The reverberation from each point on the sector of the annulus is assumed to propagate via a straight line (direct) path to the hydrophones, and can be regarded as a plane wave across the array. The ambient noise is assumed to produce noise with spectral density $\sigma_n^2(\omega)$ which is uncorrelated from hydrophone to hydrophone. This can be viewed as a model of the convergence zone surface reverberation, except that the propagation paths are direct rather than along the refracted paths associated with the convergence zone. It is shown in Appendix B that when the reverberation is spatially uncorrelated, the shape of the propagation paths does not affect the hydrophone CSD except in terms of the overall interference strength (this is incorporated in the interference spectrum). The assumption that the reverberation is uncorrelated from point to point is commonly made in active sonar (see, for example, Van Trees [9]) and will be made here.

Now, let $S_I(\rho, \theta, \omega)$ be the spectral density of the reverberation from the point on the surface at range ρ and angle θ, with the propagation losses incorporated in the source. It is assumed that this spectral density is separable in range,

$$S_I(\rho, \theta, \omega) = S_{Ir}(\rho, \omega) \, S_{Ia}(\theta, \omega) \tag{2-3}$$

Then under the additional assumptions that θ, is small enough that

$$\cos \theta_1 \approx 1$$

$$\sin \theta_1 \approx \theta_1 \tag{2-4}$$

and that $D \ll \rho$, the CSD between the pth and q^{th} hydrophones in the array is

$$s_e(p,q,\omega) = \sigma_n^2(\omega)\,\delta_{pq} + e^{-j\frac{\omega d}{c}(p-q)\cos\theta_o}\,G_r(\omega)$$

$$\int_{-\theta_l}^{\theta_l} S_{Ia}(\theta+\theta_o,\omega)\,e^{+\varphi_o\,j\frac{\omega d}{c}(p-q)\,\theta\sin\theta_o}\,d\theta \qquad (2\text{-}5)$$

with

$$G_r(\omega) = \int_{R_I}^{R_o} S_{Ir}(\rho,\omega)\,\rho^2\,d\rho \qquad (2\text{-}6)$$

Comparing (2-5) with (2-2) shows that the model illustrated in Figure 2-3 produces the same form for the hydrophone output CSD as the far field source with $S_I(\phi+\phi_o,\omega)$ replaced by the angular source spectral density $S_{Ia}(\theta+\theta_o,\omega)$ and with the additional factor $G_r(\omega)$. This additonal factor can just be regarded as part of the source spectral density in the far field model of Appendix A. Hence, the far field model developed in Appendix A can be applied to the CZ surface reverberation problem.

Appendix B also develops a second model for the CZ reverberation that utilizes the assumption of plane wave arrivals at the array from each point on the source, but distributes these arrivals on the horizontal sector, θ $\epsilon [\theta_0 - \theta_1, \theta_0 + \theta_1]$, and the vertical sector, $\phi \epsilon [\phi_0 - \Phi, \phi_0 + \Phi]$ as shown in Figure 2-4. When the reflections from each point on the surface are uncorrelated, the arrivals from different angles will also be uncorrelated. As before, the horizontal extent is limited by the horizontal directivity of the
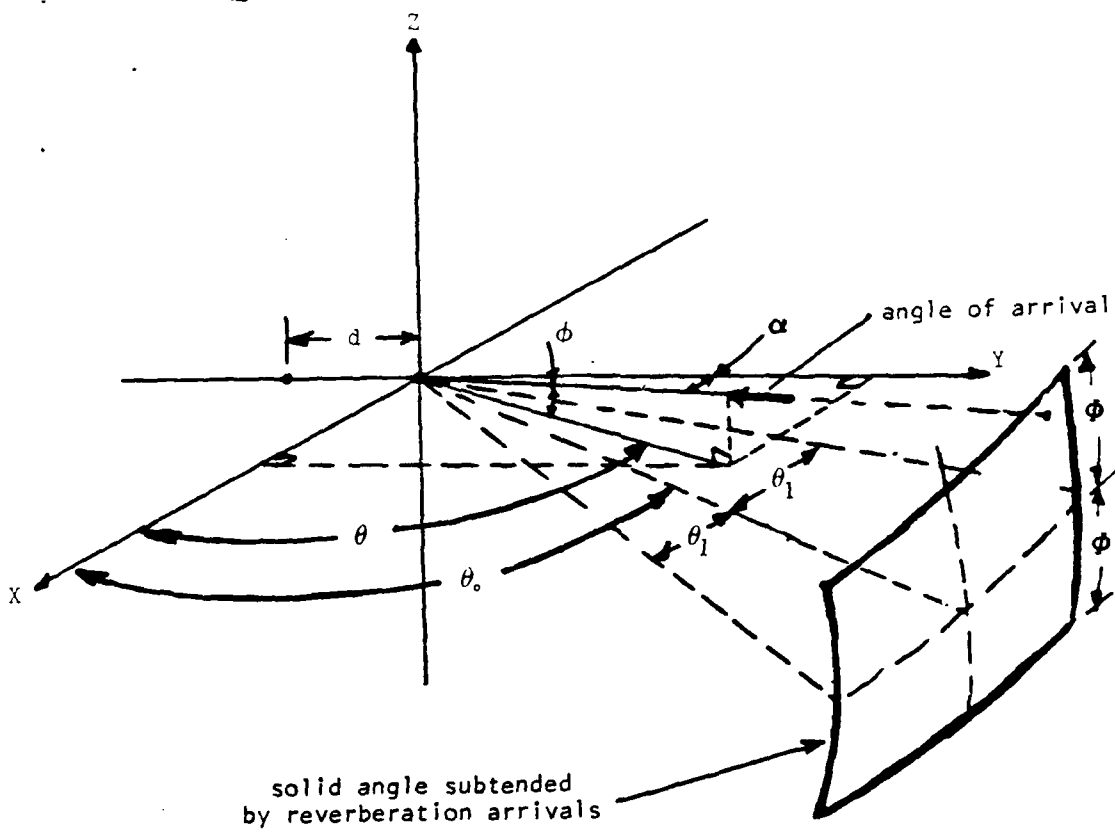
Figure 2-4. Geometry for Vertical Arrival Model

transmitter. The vertical sector comprises those angles producing CZ propagation. Let $S_I(\theta, \phi, \omega)$ be the spectral density of the arrival at horizontal angle, θ, and vertical angle, ϕ, and assume that

$$S_I(\theta, \phi, \omega) = S_{Ih}(\theta, \omega)\, S_{Iv}(\phi, \omega) \qquad (2\text{-}7)$$

That is, $S_I(\theta, \phi, \omega)$ is separable into a horizontal density, $S_{Ih}(\theta, \omega)$, and a vertical density, $S_{Iv}(\phi, \omega)$. It is assumed that θ_1 is small in the sense of (2-4), and that

$$\max\ [\phi_0 - \Phi, \phi_0 + \Phi] << 1 \qquad (2\text{-}8)$$

so that $\cos[\max[\phi_0 - \Phi, \phi_0 + \Phi]] \approx 1$. This requires that the vertical arrivals be clustered near horizontal, and is consistent with CZ arrivals in a surface ship sonar. Then the CSD of the outputs of the pth and q^{th} hydrophone is

$$s_e(p,q,\omega) \approx \sigma_n^2(\omega)\, \delta_{pq} + e^{-j\frac{\omega d}{c}(p-q)\cos\theta_0}\, G_\phi(\omega)$$

$$\int_{-\theta_1}^{\theta_1} S_I(\theta, \omega)\, e^{j\frac{\omega d}{c}(p-q)\,\theta \sin\theta_0}\, d\theta \qquad (2\text{-}9)$$

where $G_\phi(\omega) = \displaystyle\int_{\phi_0 - \Phi}^{\phi_0 + \Phi} S_{IV}(\phi, \omega)\, \phi^2 d\phi$

Again, comparison of (2-9) with (2-4) reveals that the model of Figure 2-6 produces the same hydrophone CSD as the far field model of Appendix A, so that the latter can be used to study the CZ surface reverberation problem.

An important special case of the far field model is that of uniform source spectral density

$$S_I(\phi, \omega) = \begin{cases} \sigma_I^2(\omega), & \phi \in [\phi_0 - \Phi, \phi_0 + \Phi] \\ 0, & \text{otherwise} \end{cases} \qquad (2\text{-}10)$$

23

The hydrophone output CSD then becomes

$$s_e(p,q,\omega) = \sigma_n^2(\omega)\,\delta_{pq} + \sigma_I^2(\omega)\,\frac{\sin\left[\frac{\omega d}{c}(p-q)\Phi\sin\phi_0\right]}{\frac{1}{2}\frac{\omega d}{c}(p-q)\sin\phi_0}$$

$$e^{-j\frac{\omega d}{c}(p-q)\cos\theta_0} \qquad\qquad (2\text{-}11)$$

Note that for the surface model (Figure 2-3) and the vertical arrival model
(Figure 2-4), (2-10) is replaced by

$$S_{Ia}(\theta,\omega) = S_{Iv}(\theta,\omega) = \begin{cases} \sigma_I^2(\omega), & \theta\in[\theta_0 - \theta_1,\ \theta_0 + \theta_1] \\[2mm] 0, & \text{otherwise} \end{cases}$$

This requires that the reverberation intensity does not vary as a function
of bearing within the transmitter main lobe.

It is important to note the behavior of the hydrophone output CSD,
$s_e(p,q,\omega)$, as the extended source approaches end fire, $\phi_0 = 0$. When $\phi_0 = 0$,
(2-2) reduces to

$$s_e(p,q,\omega) = \sigma_n^2(\omega)\,\delta_{pq} + \left[\int_{-\Phi}^{\Phi} S_I(\phi_0 + \phi,\,\omega)\,d\phi\right] e^{-j\frac{\omega d}{c}(p-q)} \qquad (2\text{-}12)$$

which is exactly the CSD produced by a single end fire plane wave with
spectral density

$$\left[\int_{-\Phi}^{\Phi} S_I(\phi_0 + \phi,\,\omega)\,d\phi\right]$$

Similarly, when $\phi_0 = 0$, (2-11) becomes

24

$$s_e(p,q,\omega) = \sigma_n^2 \delta_{pq} + 2\Phi\sigma_I^2(\omega) e^{-j\frac{\omega d}{c}(p-q)} \qquad (2\text{-}13)$$

which is again the hydrophone CSD of an end fire plane wave. Further, (2-11) indicates that as the source approaches endfire, its hydrophone output CSD broadens in terms of the difference (p-q), so that it looks like the CSD is that of a narrower source. It is as if the effective extent of the source is $2\Phi\sin\varphi_0$ rather than the actual source extent of 2Φ. It is important to show that this apparent narrowing of the extended source near end fire is a characteristic of the physical problem of cancelling an extended source using a line array of references, and not just an anomaly introduced by the model or by approximations within the model.

Although analysis of the general case has not been completed, a number of numerical evaluations of the exact hydrophone output CSD have been made for the special case of a uniform source. These agree very well with the CSD derived using the narrow source approximation, given by (2-11) in the case where $\sigma_n^2(\omega) = 0$. This tends to support the validity of the model near end-fire in the uniform source case, and suggest that the apparent source comparession actually occurs.

In most cases of interest, the primary sensor will not be a single omnidirectional hydrophone but an array of hydrophones steered in some particular direction. Appendix I investigates the applicability of the single hydrophone model to this more realistic case. It considers a primary input derived from

a line array of N hydrophones spaced every d_p feet and located a distance Ld feet from the reference array as shown in Figure 2-5. The results show that the equivalent model of Figure 2-6, in which the primary array is replaced by a single directional hydrophone, produces the same statistics for the reference and primary inputs if

> (a) the single primary hydrophone is placed Ld feet from the reference array

> (b) the primary hydrophone has the same directional response, $H(\phi)$ as the primary array

> (c) the ambient noise component of the primary hydrophone output has spectral density

$$\sigma_z^2(\omega) = \left[\sum_{n=0}^{N-1} a_n^2 \right] \sigma_n^2(\omega) \tag{2-14}$$

where a_n is the shading applied to the nth hydrophone and $\sigma_n^2(\omega)$ is the spectral density of the output of a single hydrophone on in the primary array being replaced. Hence, in the computation of the spectral density of the primary hydrophone output and the cross-spectral density between the primary and the references (as required to evaluate the canceller performance, Section 2.3), the source CSD function $S_I(\phi, \omega)$ i.e. modified by the response, $H(\phi)$.

2.3 Model for the Adaptive Canceller. In this study, the performance of the adaptive canceller is analyzed under the assumption that the inputs to the canceller are stationary random processes. This requires that the
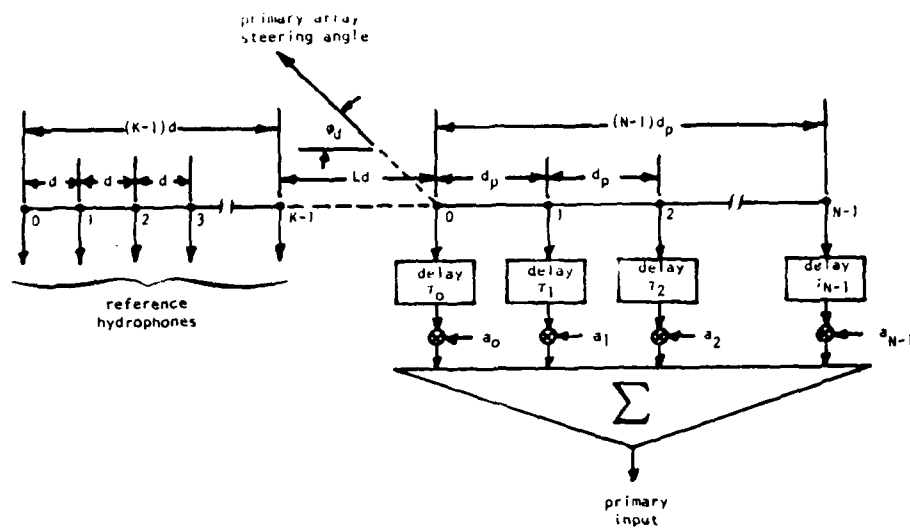
Figure 2-5. Use of a Line Array as the Primary Input
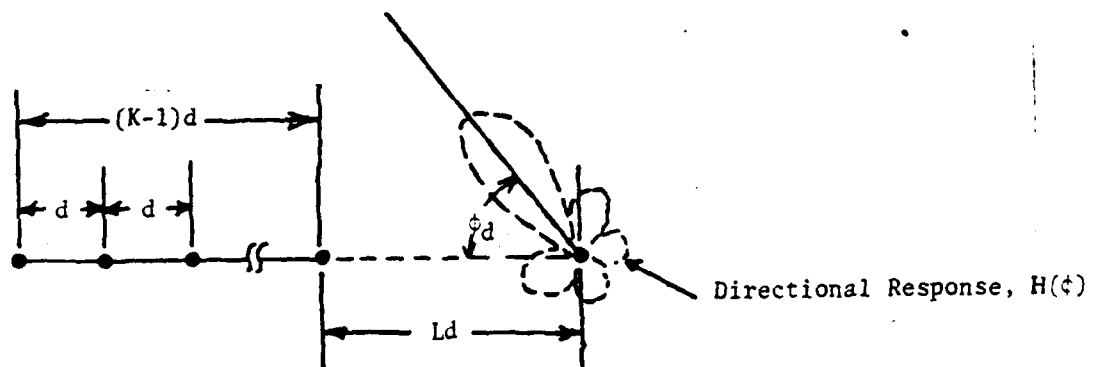
Figure 2-6. Equivalent Model for Primary Hydrophone Array

27

weights only be adapted during the time when the reverberation is present. Section 2.1 described a canceller configuration in which the weights are frozen except when a detector indicates that the CZ surface reverberation is present. The analysis which is discussed here therefore applies to this canceller structure when the detector determines the presence of the reverberation with no errors. Also described in Section 2.1 is a second configuration of the adaptive canceller to reverberation in which the weights continue to adapt when only ambient noise is present. The performance of this canceller configuration will therefore be degraded somewhat from the performance predicted using the stationary input canceller model. If the adaptation in ambient noise is very slow and the length of time during which only ambient noise is present is relatively short, then the results using the stationary model will be a good approximation to the actual performance of the second canceller configuration. The degree to which the performance of these two canceller configurations is degraded from the stationary model is discussed in Section 2.7 and analyzed in detail in Appendix J.

The multiple LMS adaptive canceller structure of Figure 1-1 is analyzed by replacing each of the LMS adaptive filters with a continuous Wiener filter. In a stationary environment, the LMS adaptive filter converges in the mean to the discrete Wiener filter. In turn, the discrete Wiener filter will be a good approximation to the continuous Wiener filter if the sampling rate high enough and the filter long enough for the discrete impulse response to approximate that of the continuous filter. This will be the case in any well designed adaptive canceller. Therefore, the mean of the converged LMS adaptive filter weights (which comprise its impulse response) will be well

approximated by the continuous Wiener filter. The actual weights (impulse response) of the converged LMS adaptive canceller randomly fluctuate about the mean weights, and these fluctuations increase the canceller output power above that of the discrete Wiener filter. However, these fluctuations can be made arbitrarily small in a stationary environment by making the feedback coefficient, μ, small. The use of the continuous Wiener filter to model the LMS adaptive canceller can therefore be regarded as neglecting the effects of sampling, finite filter length, and algorithm noise, all of which will be small in a well-designed canceller. Obviously, the Wiener filter analysis also applies only to the converged LMS canceller, and provides no information as to its transient response.

Appendix C derives the transfer functions of the Wiener canceller illustrated in Figure 2-7 in terms of the second order statistics of the hydrophone outputs. These are characterized in the frequency domain by $S_{11}(\omega)$ the power spectral density of the primary hydrophone output, $S_e(\omega)$, the cross-spectral density (CSD) matrix of the K reference hydrophone outputs, defined as

$$S_e(\omega) = \left(s_e(p, q, \omega) \right) \quad \begin{array}{l} p = 0, 1, \ldots K-1 \\ q = 0, 1, \ldots K-1 \end{array} \qquad (2\text{-}15)$$

with $s_e(p, q, \omega)$ the CSD between the outputs of the pth and q^{th} hydrophones as given in Section 2.2, and by $\underline{s}_1(\omega)$, the CSD vector between the primary and the references. With the primary hydrophone is md feet from the nearest reference, as shown in Figure 2-2,

$$S_{11}(\omega) = s_e(K + m - 1, K + m - 1, \omega) \qquad (2\text{-}16)$$
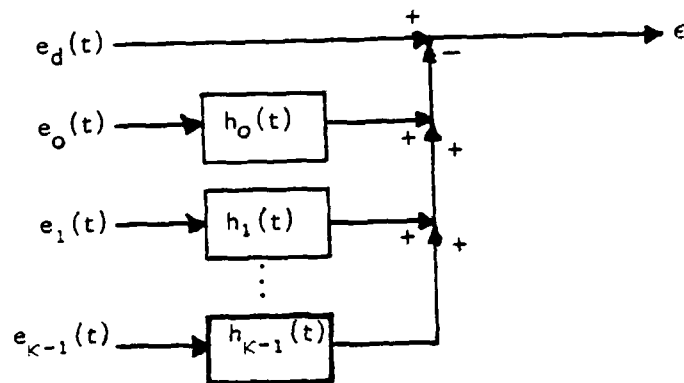
Figure 2-7. Multiple Reference Canceller

and

$$\underline{s}_1(\omega) = [s_e(0, K+m-1), s_e(1, K+m-1), \ldots, s_e(K-1, K+m-1)]^T$$

(2-17)

In this notation, the transfer functions of the K filters in Figure 2-12 are given by

$$\underline{H}^o(\omega) = [H_0(\omega), H_1(\omega), \ldots, H_{k-1}(\omega)]^T = S_e^{-1}(\omega) \, \underline{s}_1(\omega)$$

(2-18)

and the power spectral density of the canceller output is

$$E_K(m, \omega) = S_{11}(\omega) - \underline{s}_1^+(\omega) \, S_e^{-1}(\omega) \, \underline{s}_1(\omega)$$

(2-19)

where the subscript K on $E_K(m, \omega)$ indicates that K references are used in the canceller and m is the distance from the reference array to the canceller in units of d feet. Since the models described in Section 2.2 provide $s_e(p, q, \omega)$, (2-15), (2-16), and (2-17) can be used to evaluate the canceller output spectrum (2-19). This is the primary vehicle for the analyses reported here.

2.4 <u>Results From Linear Prediction Theory</u>. Proceeding from the general models developed in Appendices A and B, and from the canceller model derived in Appendix C, Appendix D shows that the Least Mean Square cancellation of a spatially uncorrelated, narrow extended source is equivalent to the linear minimum mean square error prediction of a bandlimited random process in noise. This equivalence allows direct application of known results from linear prediction theory to the extended source cancellation problem of interest in this report. The most useful of these results involve the irreducible canceller output spectrum, defined as

$$E_{\infty}(m, \omega) = \lim_{K \to \infty} E_K(m, \omega) \tag{2-20}$$

Recall from Section 2.1 that the acoustic field model requires that the plane wave assumption be valid across the entire receiving array, which will be violated as $K \to \infty$ (since the length of the reference array becomes infinite). Therefore, $E_{\infty}(m, \omega)$ must be regarded as a lower bound to the canceller output spectrum.

When m=1, so that the entire array is uniformly spaced with spacing, d, the irreducible canceller output spectrum is shown to be given by

$$E_{\infty}(1, \omega) = \exp\left[\frac{1}{2\pi} \int_{-\pi}^{\pi} \log H_e(\alpha, \omega) \, d\alpha\right] \tag{2-21}$$

where $H_e(\alpha, \omega)$ is the wave number-frequency spectrum (WNFS) of the hydrophone outputs. For a narrow source of angular extent, 2Φ, this is related directly to the source spectral density, $S_I(\phi, \omega)$, as follows

$$H_e(\alpha, \omega) = \sigma_n^2(\omega) + \sum_{k=-\infty}^{\infty} \frac{1}{\gamma} S_I \left(\frac{\alpha+2\pi k}{2\pi} + \phi_0, \omega\right) \text{Rect} \left[\frac{\alpha+2\pi k}{2\pi w}\right], \alpha \in [-\pi, \pi] \tag{2-22}$$

where

$$\gamma = \frac{d}{\lambda} \sin \phi_0 \quad \text{and } W = \gamma \Phi$$

When $w < 1/2$, (2-22) reduces to

$$H_e(\alpha, \omega) = \sigma_n^2(\omega) + \frac{1}{\gamma} S_I \left(\frac{\alpha}{2\pi\gamma} + \phi_0, \omega\right) \text{Rect} \left[\frac{\alpha}{2\pi\gamma\Phi}\right] \tag{2-23}$$

The condition that $W \le 1/2$ therefore eliminates spatial aliases from the WNFS, and, as such, can be regarded as a sampling cirterion.

An important footnote to equation (2-21) is that when $\log [H_e(\alpha,\omega)]$ is not integrable, the right hand side must be replaced by zero. Appendix D shows that if there is no ambient noise and the criterion $\gamma \Phi \leq 1/2$ is met, then $E_\infty(1,\omega) = 0$, so that at least asymptotically, the extended source can be cancelled to zero. However, when ambient noise is present,

$$E_\infty(1,\omega) > \sigma_n^2(\omega) \qquad (2-24)$$

so that the extended source can never be cancelled to the ambient noise floor.

When there is no ambient noise present, not only can the irrducible canceller output power, $E_\infty(1,\omega)$, be shown to be zero, but the canceller output spectrum, $E_K(1,\omega)$, can be shown to approach zero asymptotically in K, the number of references. That is, $E_K(1,\omega)$ is asymptotic to

$$L(K) = G(\omega)[\sin(\pi\gamma\Phi)]^{2K+1} \qquad (2-25)$$

where $G(\omega)$ depends upon the source extent, Φ, the sampling parameter, γ, and upon the WNFS of the hydrophone output, but not upon K ($G(\omega)$ is given by equation D-61 of Appendix D). The rate at which this asymptotic approaches zero does not depend upon the shape of the source, as can be seen from (2-25). It is pointed out in Section 2.5 that even for relatively small K, L(K) is a good approximation to $E_k(1,\omega)$. Further, L(K) will be useful in predicting the value of $E_k(1,\omega)$ when ambient noise present, as developed in Appendix K.

The more general case of $m > 1$ is also considered in Appendix D. It is shown that if the irreducible canceller output spectrum for $m=1$, that is $E_\infty(1,\omega)$, is zero, then

$$E_{\alpha}(m,\omega) = 0 \qquad m > 1 \qquad\qquad (2\text{-}26)$$

This means that if the output spectrum gives asymptotically to zero with K for m=1, then it will do so for m > 1, too. Although there is no result analogous to (2-25) for m > 1 indicating exponential behavior, numerical results discussed in Section 2.5 suggest that $E_k(m,\omega)$ also goes to zero exponentially but at a slower rate. As in the case of m=1, the irreducible output spectrum is always non-zero when ambient noise is present, so this result applies only to the noise free case. It is also shown that $E_{\infty}(m,\omega)$ is a non-decreasing sequence in m, so that the irreducible output spectrum, which places a floor on the cancellation performance, cannot decrease as the references are moved farther from the primary (m increases). In fact, for the cases of interest here, $E_{\infty}(m,\omega)$ always increases with m.

Appendix D also develops an implicit expression for the cancellation floor, $E_{\infty}(m,\omega)$, in terms of the source spatial distribution, $S_I(\phi,\omega)$. It is shown that

$$E_{\infty}(m,\omega) = \sum_{k=0}^{m-1} \left| C_k(\omega) \right|^2 \qquad\qquad (2\text{-}27)$$

where

$$C_0(\omega) = \exp\left\{ \frac{1}{2\pi} \int_{-\pi}^{\pi} \log\left[H_e(\alpha,\omega) \right] d\alpha \right\} \qquad\qquad (2\text{-}28)$$

and the remaining C_k's satisfy

$$\sum_{n=0}^{\infty} C_n^*(\omega)\, z^n = \exp\left\{ \frac{b_0(\omega)}{2} + \sum_{n=1}^{\infty} b_n(\omega)\, z^n \right\} \qquad\qquad (2\text{-}29)$$

with

$$b_n(\omega) = \frac{1}{2\pi} \int_{-\pi}^{\pi} \log[H_e(\alpha,\omega)] \, e^{-jn\alpha} \, d\alpha \qquad (2\text{-}30)$$

Again, $H_e(\alpha,\omega)$ is the hydrophone output WNFS given by (2-22) or (2-23) in terms of $S_I(\phi,\omega)$. The implicit relationship, (2-29), can be solved explicitly for small m (see Appendix D, supplement II), but the expressions are quite complicated and give little insight into the canceller performance.

2.5 Results for a Uniform Spatially Uncorrelated Interference. Suppose that the model shown in Figure 2-3 is used to represent the surface reverberation from the CZ. A reasonable model for the reverberation is that the intensity of the reverberation does not vary with bearing in the mainlobe of the transmitted signal, so that, using (2-3)

$$S_{Ia}(\theta,\omega) = \begin{cases} \bar{\sigma}_I^2(\omega), & \theta \varepsilon [\theta_0 - \theta_1, \theta_0 + \theta_1] \\ 0, & \text{otherwise} \end{cases} \qquad (2\text{-}31)$$

where θ_1 is assumed small in the sense of (2-4). Incorporating two way cylindrical spreading loss into the source characteristics suggests that

$$S_{Ir}(\rho,\omega) = \frac{1}{2\rho} \qquad (2\text{-}32)$$

so that the reverberation falls off linearly with range. Then from (2-6),

$$G_r(\omega) = \frac{1}{4}\left[R_0^2 - R_I^2\right] \qquad (2\text{-}33)$$

and the hydrophone output CSD is

35

$$S_e(p,q,\omega) = \sigma_n^2(\omega)\,\delta_{pq} + e^{-j\frac{\omega d}{c}(p-q)\cos\theta_0}\,\frac{1}{4}\left[R_0^2 - R_I^2\right]\sigma_I^2(\omega)$$

$$\cdot\left[\frac{\sin\frac{\omega d}{c}(p-q)\,\vartheta_1\sin\theta_0}{\frac{1}{2}\frac{\omega d}{c}(p-q)\sin\theta_0}\right] \tag{2-34}$$

which is just a straight forward extension of (2-11) using (2-5). Hence the uniform source model developed in Appendix A can be used to investigate the performance of the canceller with CZ surface reverberation if the source spectrum, $\sigma_I^2(\omega)$, in (2-10) is replaced by $\sigma_I^2(\omega)\left[R_0^2 - R_I^2\right]/4$.

Appendix F uses uniform source model and the results of Appendix D to determine the cancellation floor, $E_\infty(1,\omega)$, for the CZ surface reverberation modelled as in (2-34). A significant result is the existence of a spatial sampling criterion relating the hydrophone spacing

$$\gamma = \frac{d}{\lambda}\sin\phi_0 \tag{2-35}$$

and the source extent, θ_1. It is shown that if

$$\gamma\theta_1 \geq \frac{1}{2} \tag{2-36}$$

then only very slight cancellation is possible. One the other hand, if

$$\gamma\theta_1 < \frac{1}{2} \tag{2-37}$$

then the cancellation floor is given by

$$F_\infty(1,\omega) = \frac{\sigma_n^2(\omega)}{2W}\left[1 + \frac{INR}{2W}\right]^{2W}, \quad \gamma\theta_1 < \frac{1}{2} \tag{2-38}$$

where

36

$$INR = \frac{1}{2}\left[R_0^2 - R_I^2\right] \theta_1 \sigma_I^2(\omega) \Big/ \sigma_n^2(\omega) \qquad (2\text{-}39)$$

is the interference to noise ratio at the array, and

$$W = \gamma \theta_1 \qquad (2\text{-}40)$$

Using (2-38), the cancellation floor relative to the input power, $\sigma_n^2(\omega)(1+INR)$, is

$$\frac{E_\infty(1,\omega)}{\sigma_n^2(\omega)(1+INR)} = \frac{[1+INR]}{2W}^{-1}\left[1 + \frac{INR}{2W}\right]^{2W}, \quad W < \frac{1}{2} \qquad (2\text{-}41)$$

This is plotted in Figure 2-8 for values of W between 0 and 0.5, and for INR's of 40, 30, and 20 dB. It can be seen that only when W is small is cancellation to near the ambient noise floor possible.

A *second useful result derived in Appendix F for the uniform source* case is an asymptote in K for $E_K(1,\omega)$ when the ambient noise is not present. This is developed using the form of the Strong Szego Limit Theorem [12] discussed in Appendix D. It is shown that for $\sigma_n^2(\omega) = 0$ and $W < 1/2$, $E_k(1,\omega)$ is asymptotic in K to

$$A(K) = \frac{2\Theta \sigma_e^2(\omega)}{2W} [\sin \pi W]^{2K+1} \qquad W < \frac{1}{2} \qquad (2\text{-}42)$$

that is asymptotically, $E_K(1,\omega)$ decreases asymptotically with K. Although the noise free case is not of practical interest, it will be shown later that A(K) is useful in describing the canceller behavior in the noise present case.

The results of Figure 2-8 indicate that the cancellation can be made arbitrarily close to the noise floor by making d small, which moves the references closer together. However, it should be noted that as d gets

37

FIGURE 2-8: Irreducible Canceller
Output Power vs W for
Sin x/x CSD

INR=20 dB

INR=30 dB

INR=40 dB

38
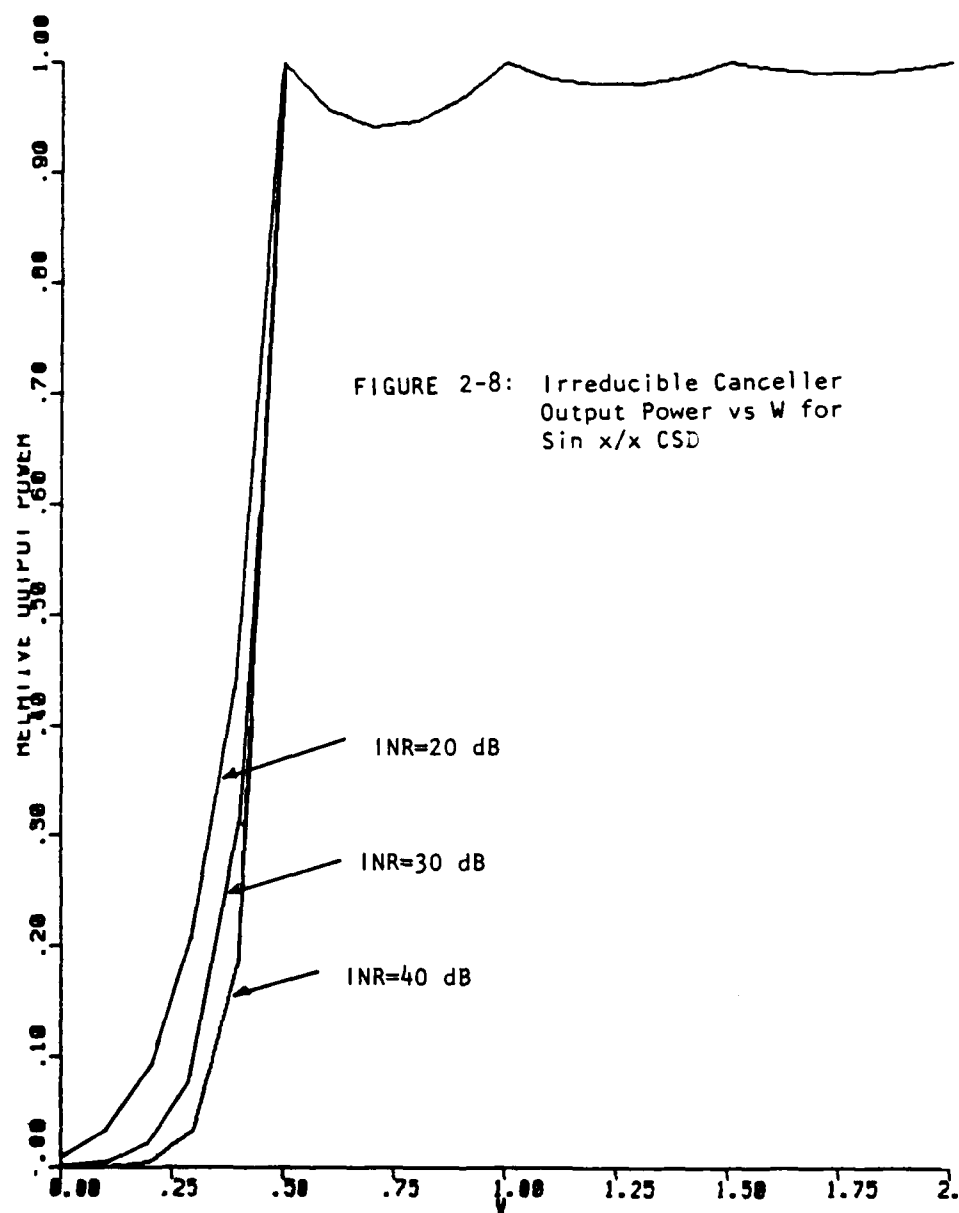
smaller, the references are also moving closer to the primary in this model, accounting for some of the cancellation improvement. A meaningful examination of the performance therefore requires evaluation of $E_\infty(m, \lambda)$, where the reference are md feet from the primary. This would allow determination of the cancellation floor as the references are moved closer together but maintained a constant distance from the primary. Although Appendix D developed an expression, (2-29), which allows explicit determination of $E_\infty(m, \omega)$, the expressions are very complex and yield no insight.

An alternative approach is to evaluate $E_K(m, \omega)$ numerically, using the results developed in Appendix E. Using the fact that the eigenvalues and eigenvectors of the reference hydrophone output CSD matrix can be expressed in terms of the Discrete Prolate Spheroidal Sequences (DPSS's) and their associated eigenvalues [13], it is shown that

$$E_K(m, \omega) = \sigma_n^2(\omega) + 2\vartheta_1 \sigma_e^2(\omega)$$

$$\left\{ 1 - \frac{1}{2W} \sum_{k=0}^{K-1} \left[\frac{2\vartheta_1 \lambda_k(K,W)}{2W\sigma_n^2(\omega) + 2\vartheta_1 \sigma_e^2(\omega)\lambda_k(K,W)} \right] \lambda_k(K,W) \right.$$

$$\left. \left[V_{K+m-1}^{(k)}(K,W) \right]^2 \right\}$$

(2-43)

where k is the number of references, as before, and

$$\left\{ V_m^{(k)}(K,W) \right\}_{m = \ldots -1, 0, 1, \ldots} = k^{th} \text{ DPSS}$$

$\lambda_k(K,W) =$ eigenvalue associated with the kth DPSS.

The DPSS and their eigenvalues are easily evaluated on the computer, which allows numerical evaluation of $E_K(m, \omega)$ from (2-42). Appendix K

includes extensive plots of $E_K(m,\omega)$ as a function of K for various m and values of W from 10^{-4} to 5×10^{-1}. Interference-to-noise ratios of 40 dB, 30 dB, and 20 dB are given, as well as some results in the ambient noise free case.

In the ambient noise free case, plots show that the asymptote, A(K), given in (2-42), is an excellent approximation to $E_k(1,\omega)$ even for small K, that is

$$E_k(1,\omega) \approx \frac{2\theta_1 \sigma_e^2(\omega)}{2W} [\sin \pi W]^{2K+1}, \qquad \begin{cases} \sigma_n^2(\omega) = 0 \\ W < \frac{1}{2} \end{cases} \qquad (2\text{-}43)$$

Recall from Section 2.4 that an extended source cannot be cancelled to the ambient noise floor, but approaches some cancellation floor, $E_\infty(1,\omega) > \sigma_n^2(\omega)$. However, it seems reasonable that the noise present case should behave approximately like (2-43) if the interference to noise ratio is high and the cancellation achieved, $E_K(1,\omega)$ is well above the cancellation floor, $E_\infty(1,\omega)$. This conjecture is shown to be valid by comparison with numerical results later.

The numerical results from Appendix K for the ambient noise present case are typified by Figures 2-9 through 2-11, which show the 40 dB INR for $W = 10^{-1}$, 10^{-2}, and 10^{-3} respectively, and by Figures 2-12, 2-13, and 2-14 which show the same cases for INR = 20 dB. Also shown on these figures (and the others in Appendix K) are the cancellation floor, $E_\infty(1,\omega)$, computed using (2-41) and the approximate value of $E_K(1,\omega)$ in the noise free case from (2-43). Note that $E_\infty(1,\omega)$ is indistinguishable from the noise floor for $W = 10^{-2}$. It can be seen that the canceller output spectrum, $E_K(1,\omega)$, approaches the floor quite rapidly at first, following the asymptote, (2-42). However, there is a pronounced inflection point above which the cancellation floor is approached slowly. This point is very significant from the
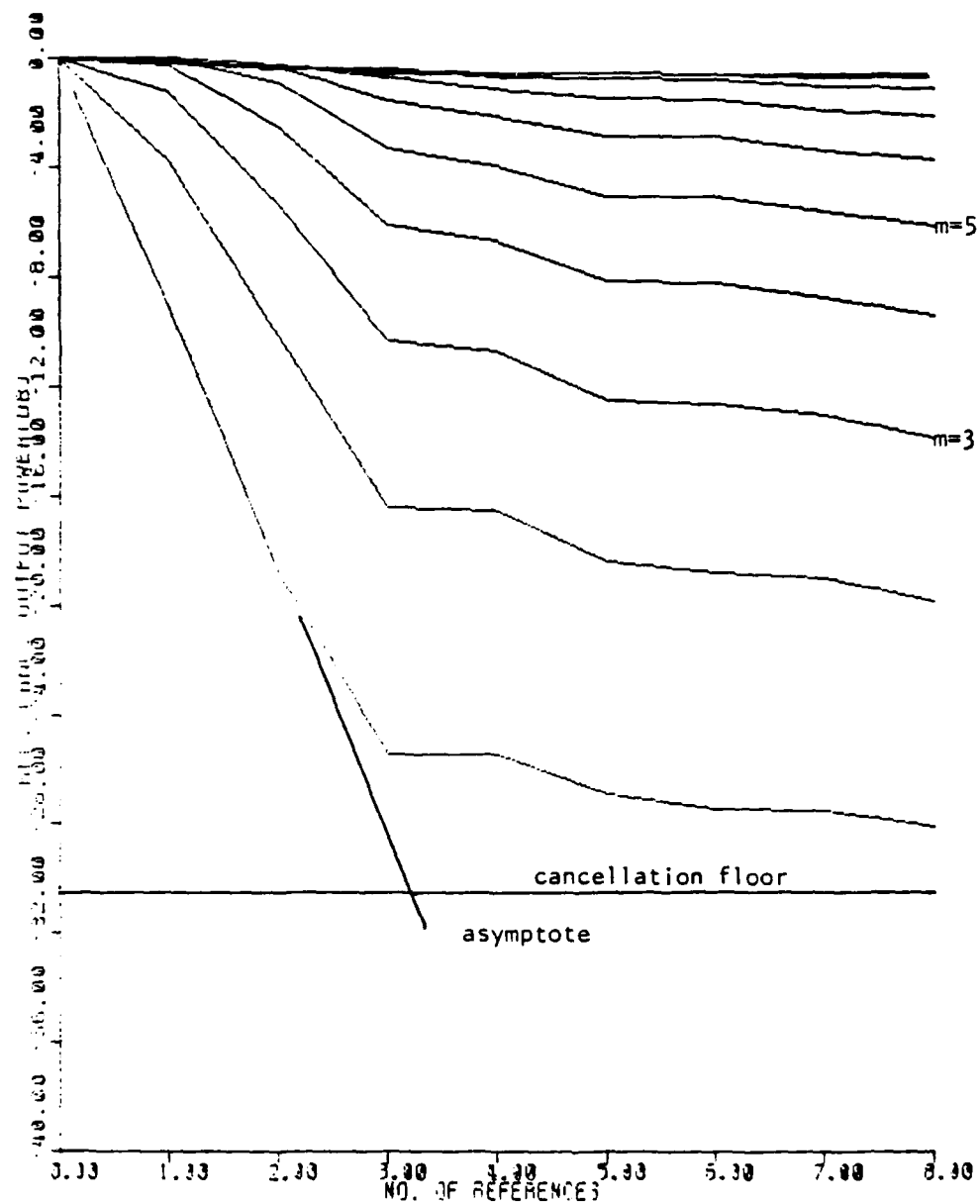
Figure 2-9. Canceller Output Spectrum vs. K for $W = 10^{-1}$, INR = 40 dB
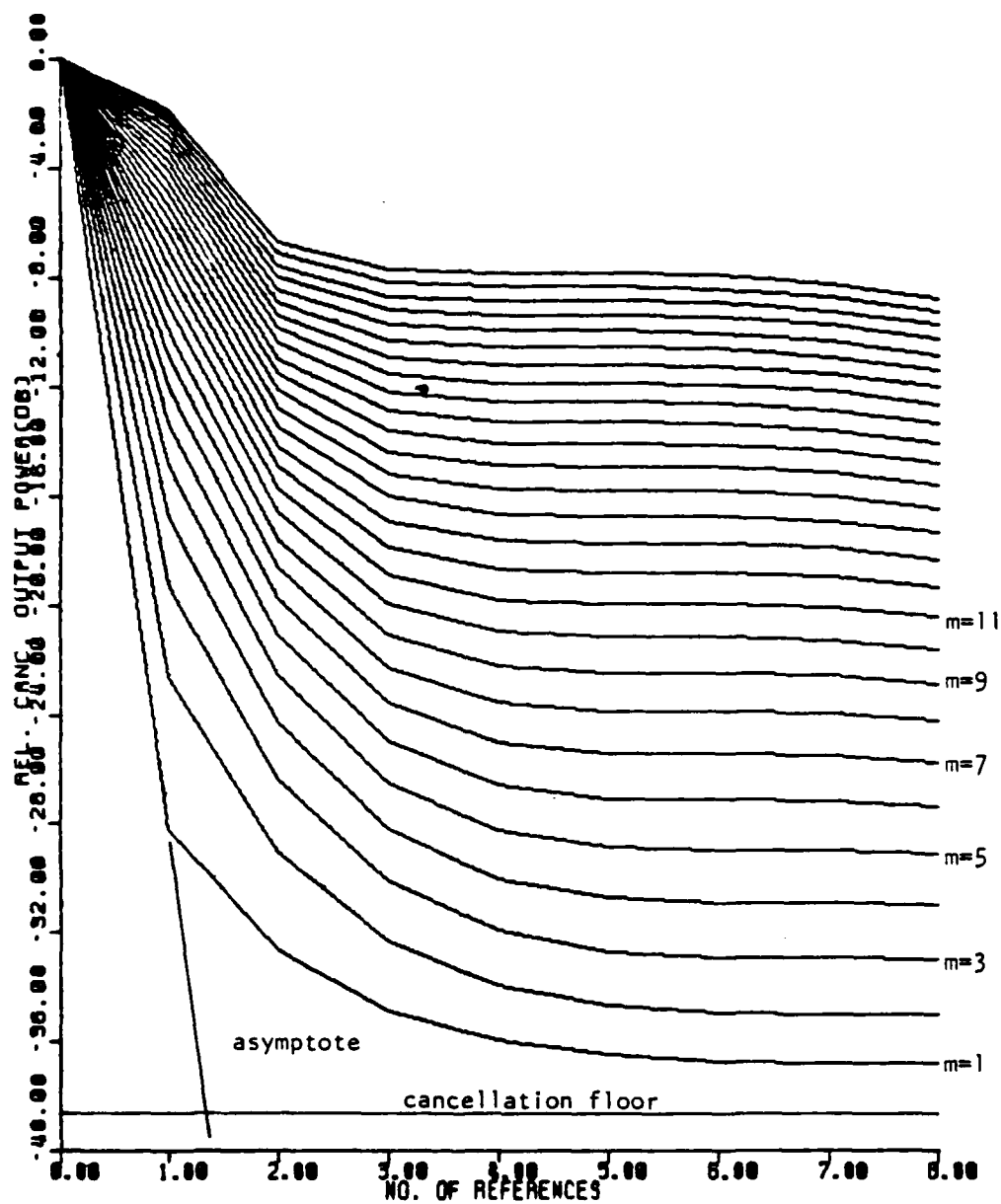
Figure 2-10.   Canceller Output Spectrum vs. K for W = 10^{-2}, INR = 40 dB
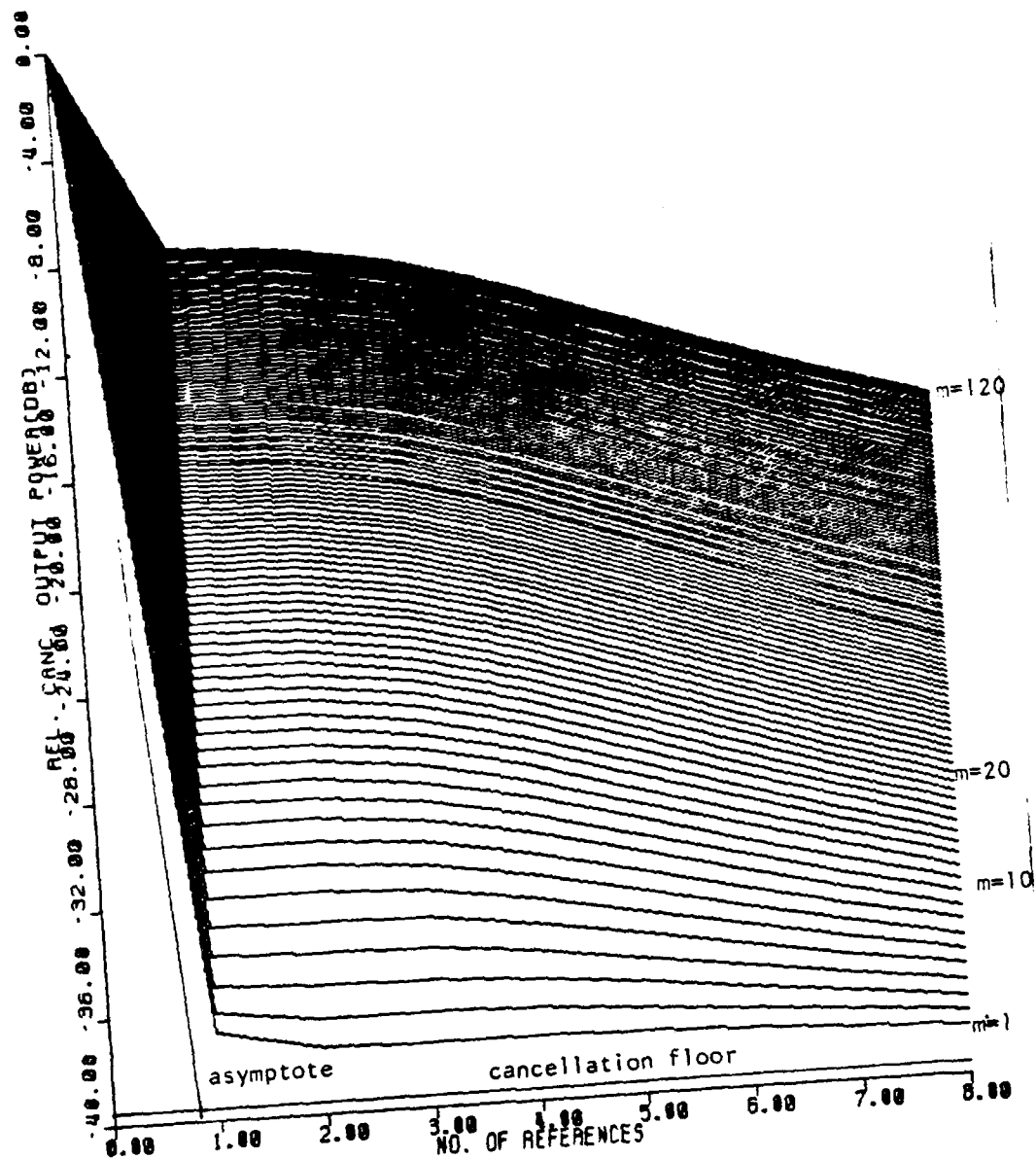
Figure 2-11. Canceller Output Spectrum vs. K for $W = 10^{-3}$, INR = 40 dB

43
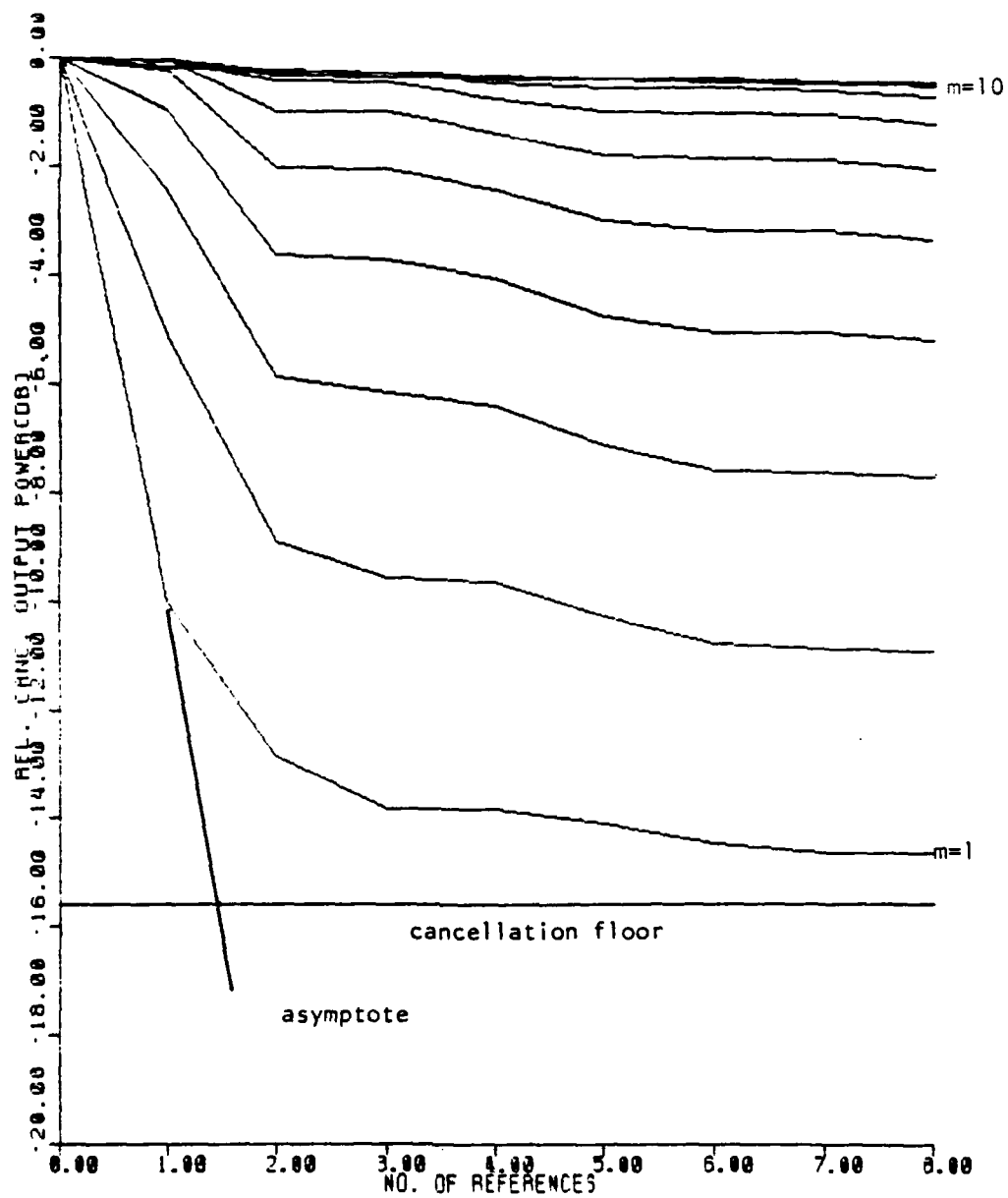
Figure 2-12. Canceller Output Spectrum vs. K for $W = 10^{-1}$, INR = 20 dB
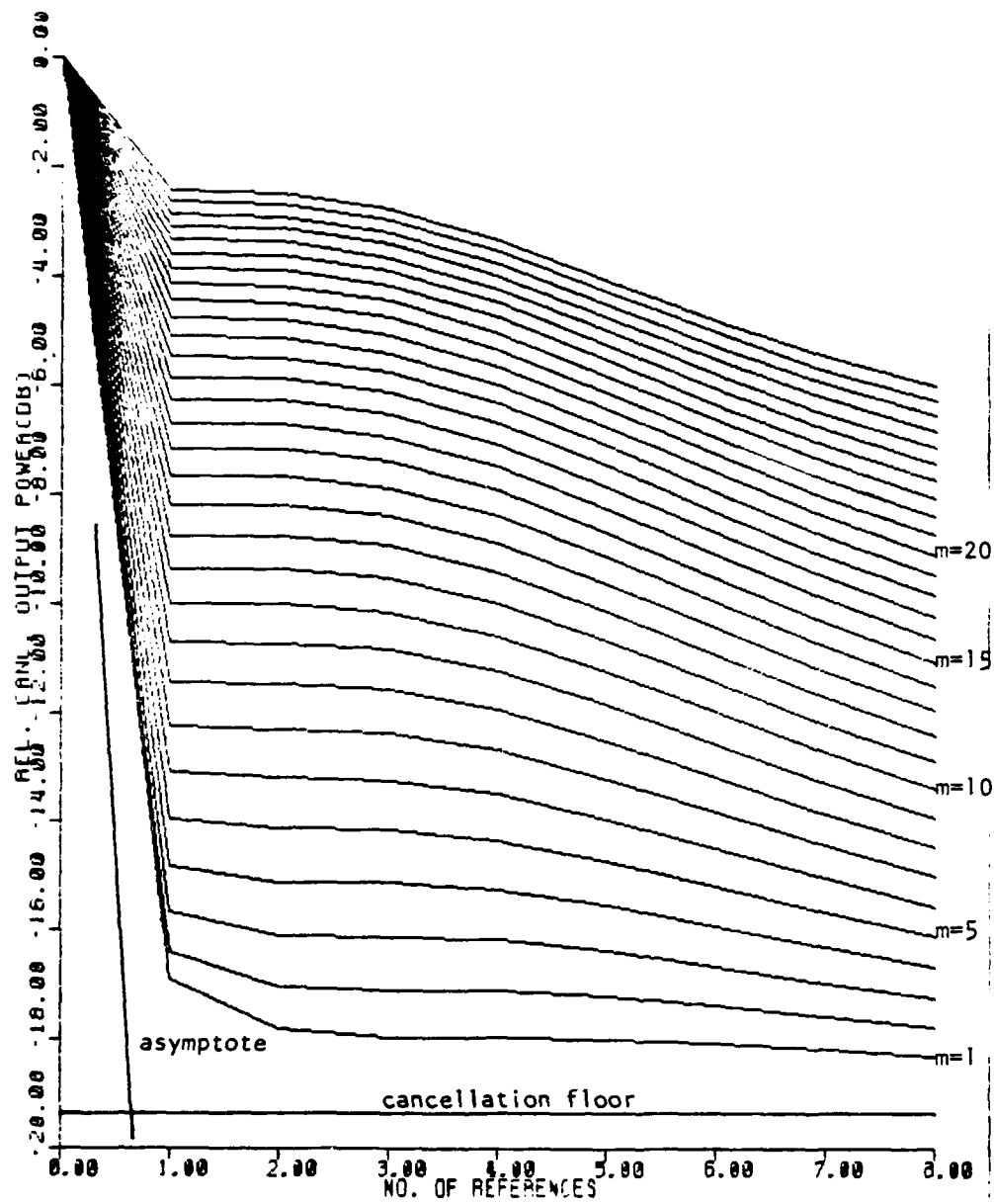
Figure 2-13.   Canceller Output Spectrum vs. K for $W = 10^{-2}$, INR = 20 dB
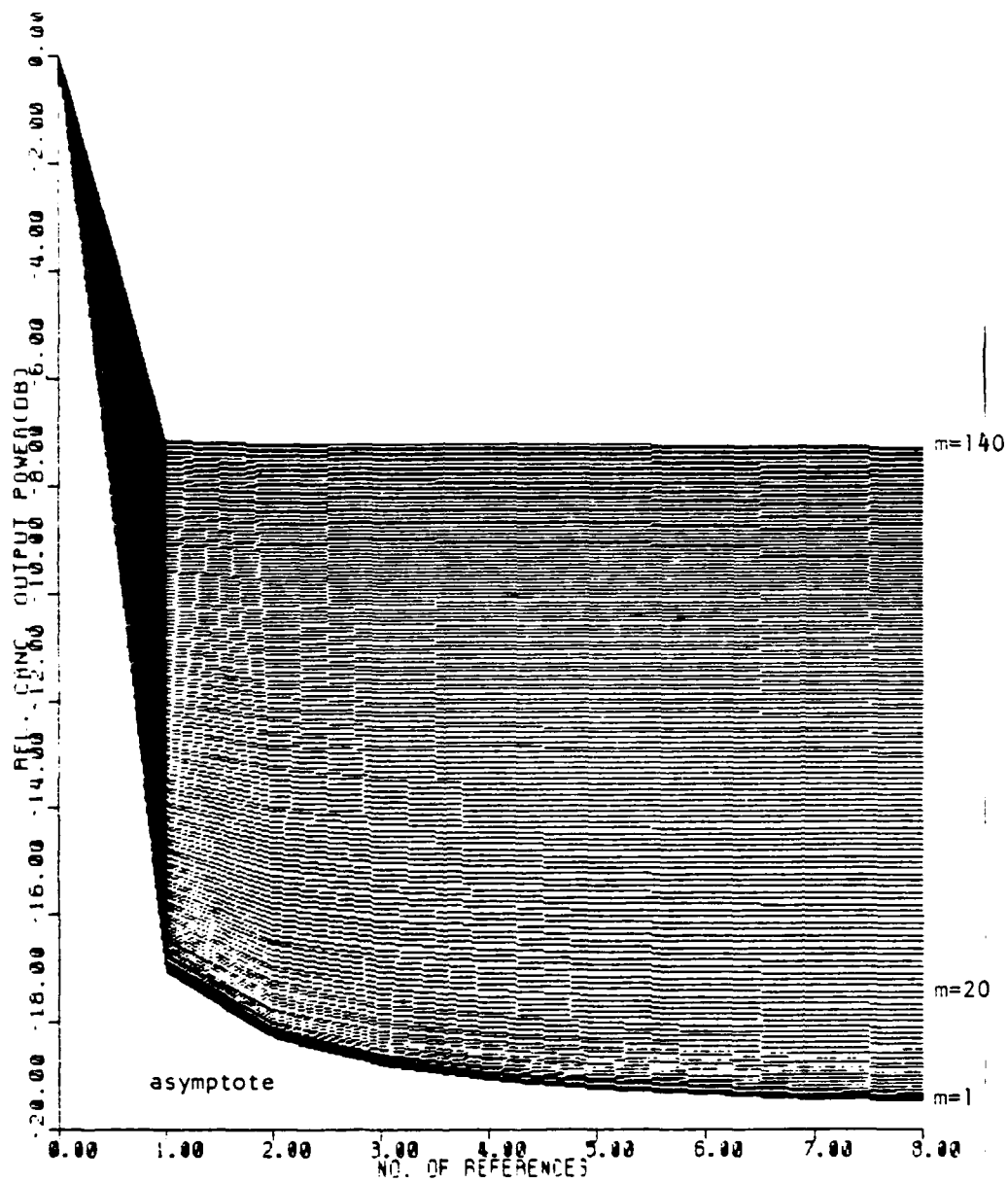
Figure 2-14. Canceller Output Spectrum vs. K for $W = 10^{-3}$, INR $= 20$ dB

46

point of view of the cost of cancellation improvement per dB. Suppose the inflection occurs at $K = K_0$. Then there is a definite "law of diminishing returns" in using more than K_0 references, since each additional reference incurs the computational cost of another LMS adaptive filter, regardless of the additional cancellation it provides. For example, in Figure 2-15, use of 2 references achieves about 33 dB of cancellation, while use of 6 additional references only improves the cancellation 3-4 dB.

It is shown in Appendix K that this inflection point occurs at approximately

$$K_0 = [K_I] \qquad (2\text{-}44)$$

where $[x]$ is the smallest integer greater than or equal to x and

$$K_I = \frac{1}{2} \left\{ [\log(\sin \pi W)]^{-1} \left[(2W-1) \log \frac{INR}{2W} \right] -1 \right\}, \quad W < \frac{1}{2} \qquad (2\text{-}45)$$

The parameter K_I is just the intersection of the asymptote, (2-42) and the cancellation floor (2-41). Choosing $K = K_0$ (for m=1) does not mean that further cancellation is not possible, but that this additional cancellation is costly.

The number, K_I, provides insight as to how the number of references required in a given situation changes with W and with INR. From (2-45), it can be seen that K_I is linear in 10 log (INR), which is the interference-to-noise ratio in dB. The slope of K_I with respect to 10 log (INR) is

$$\frac{d K_I}{d (10 \log (INR))} = \frac{1}{20} \frac{2W-1}{\log (\sin \pi W)} \qquad (2\text{-}46)$$
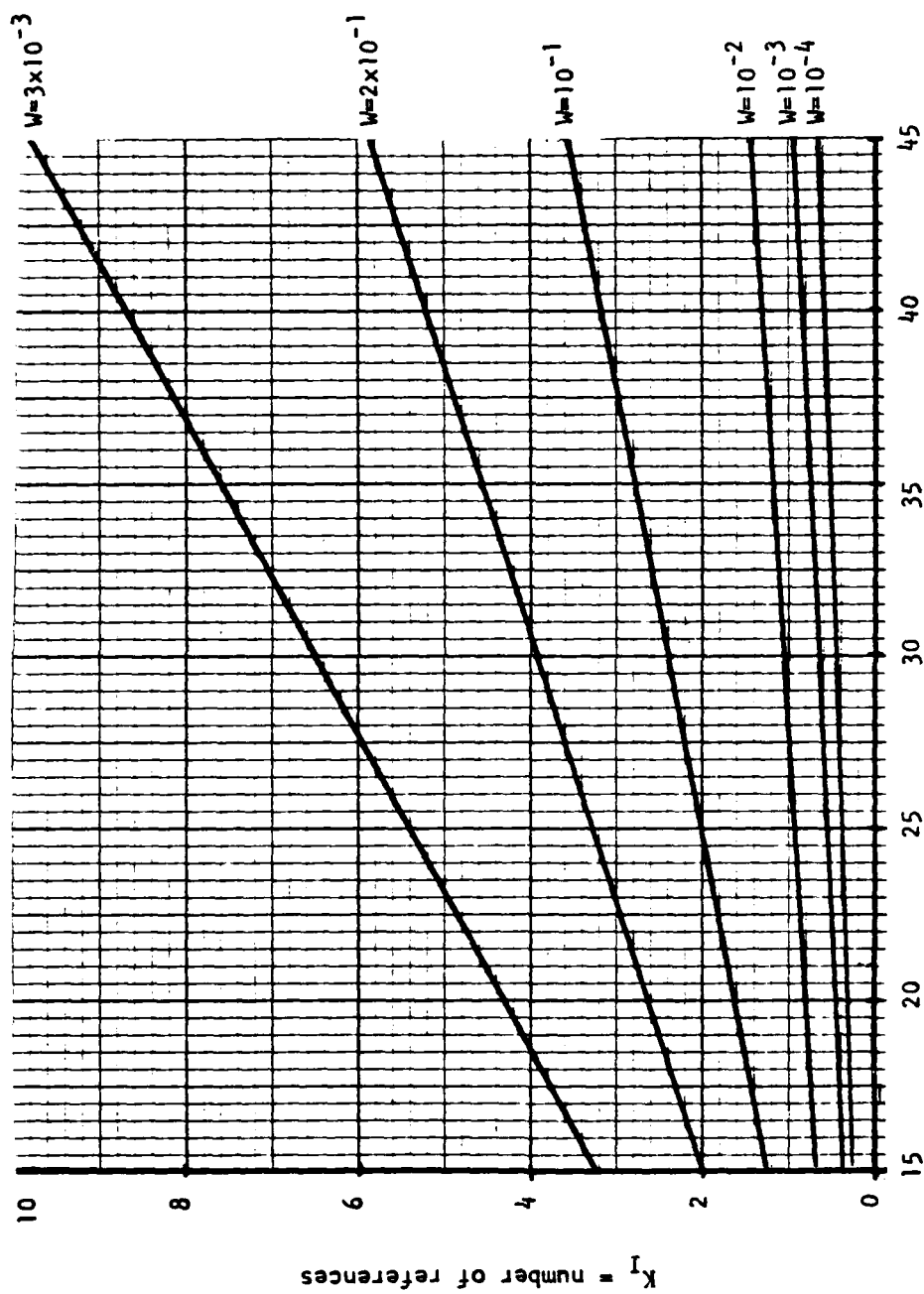
Figure 2-15. Change in K_I as a Function of INR
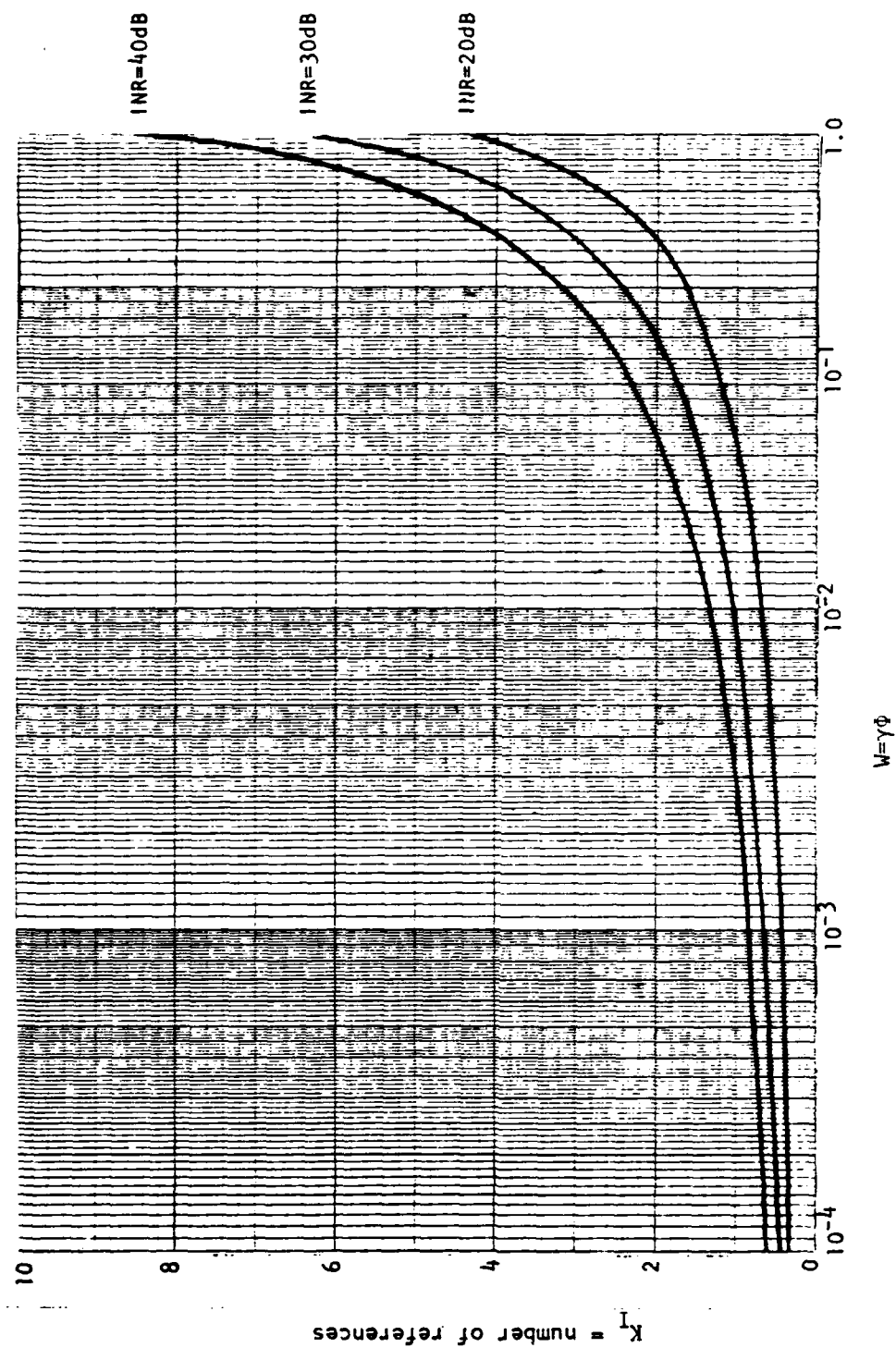
Figure 2-16. Change in K_I as a Function of W

49

so that approximately $(2W-1)/(20 \log (\sin \pi W))$ references are required per dB of INR. Figure 2-15 shows K_I plotted as a function of $10 \log (INR)$ for various W. The dependence on the interference-to-noise ratio is quite weak when $W \leq 0.01$, that is, when the interferences are very narrow.

The dependence of I_I on W is more complicated as shown in Figure 2-16, which shows K_I plotted as a function of W for INR = 20, 30, and 40 dB. For small W (say, $W < 10^{-2}$) the dependence of K_I on W is very weak, regardless of INR. As W increases above 10^{-2}, the value of K_I begins to increase rapidly with W, going asymptotically to infinity at $W = 1/2$. Recalling that no cancellation is possible when $W = 1/2$, it would be expected that $K_I \to \infty$ at this point.

Now, suppose the criterion $K = K_0$ is used to select the number of references used in a given situation. Figure 2-17 shows that the cancellation achieved is within several dB of the cancellation floor, (2-41) for this choice of K. In fact, it can be seen that the value of $E_{K_0} (1, \omega)$ is very nearly log (INR) dB above the floor, so that

$$E_{K_0} (1, \omega) \approx (INR)^{0.1} E_{\infty}(1, \omega) = 2 \theta_1 \sigma_e^2(\omega) (INR)^{-.9} \left[1 + \frac{INR}{2W} \right]^{2W}$$

(2-47)

provided that $(INR)^{0.1} E_{\infty} (1, \omega) \leq 2^{\theta_1} \sigma_e^2 (\omega) + \sigma_n^2 (\omega)$. This condition just assures that the approximation is not used when it would produce an arrarent increase in the interference power relative to the uncancelled primary output. If INR $>>$1 and $W < 1$, as it will be in all cases of interest, (2-47) can be approximated as

$$E_{K_0} (1, \omega) \approx 2^{\theta_1} \sigma_e^2 (\omega) (INR)^{2W-.9} (2W)^{-2W}$$

(2-48)
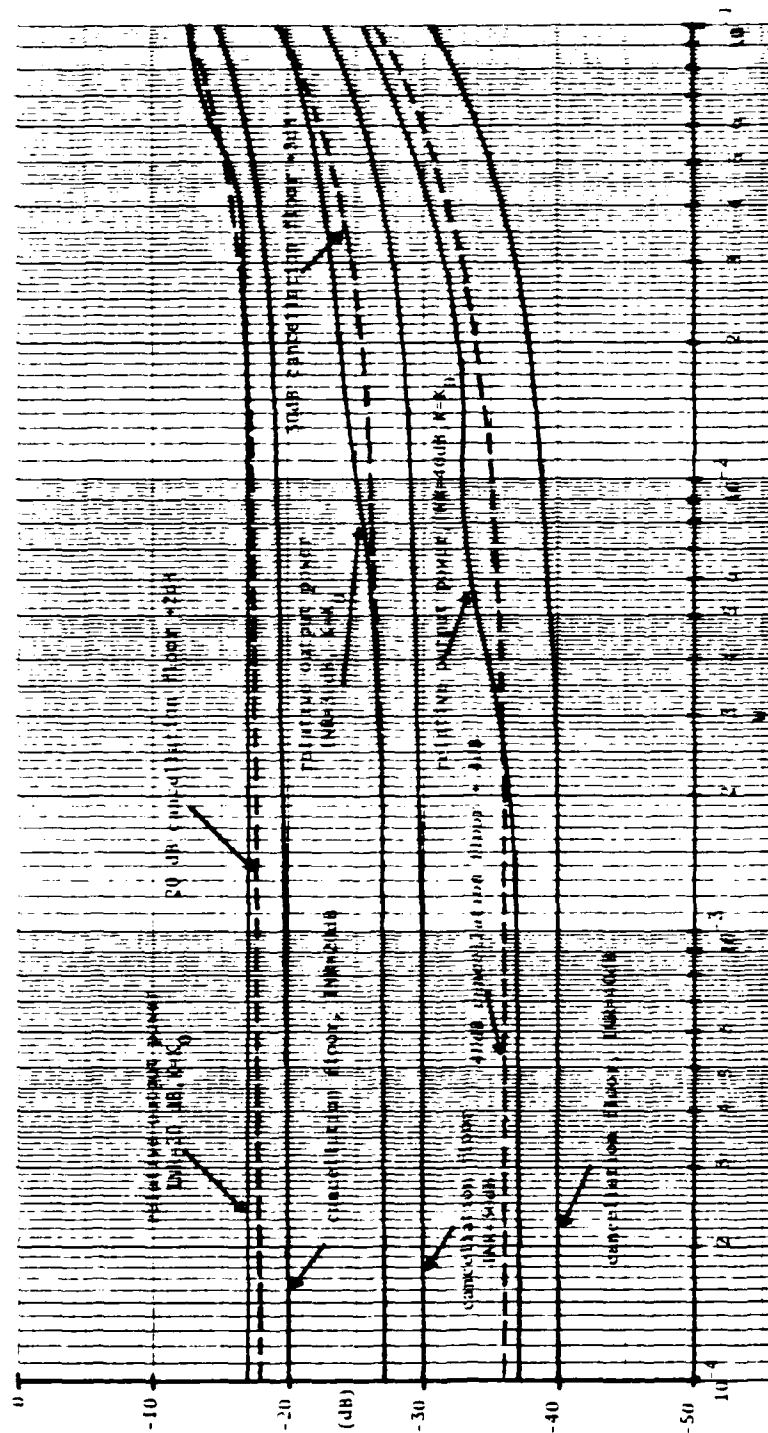
Figure 2-17. Relative Canceller Output Power and Approximation When $K = K_o$

51

For $0 \leq W \leq 1$, $(2W)^{-2W}$ is within about 1.6 dB of unity, so

$$E_{K_0}(1,\omega) \approx 2\theta_1 \sigma_e^2(\omega)(INR)^{2W-.9} \qquad (2-49)$$

The cancellation achieved is then approximately

$$C_{K_0}(1,\omega) = \frac{E_{K_0}(1,\omega)}{\sigma_n^2(\omega) + \theta_1\sigma_e^2(\omega)} \approx \frac{(INR)^{2W+0.1}}{1 + INR} \approx (INR)^{2W-.9}$$

for $INR \gg 1$. Expressed in dB, there yields

$$10 \log C_{K_0}(1,\omega) \approx -0.9\,[10 \log(INR)] + 2W\,[10 \log INR] \qquad (2-51)$$

The interference rejection in dB varies approximately linearly with both the interference to noise ration in dB and the paramter W. This result is valid over the range $10^{-4} \leq W \leq 0.45$ and $10^2 \leq INR \leq 10^4$.

Examination of the numerical results of Appendix K shows for any given selection of K and W, the curves of $E_k(m,\omega)$ for $m > 1$ have roughly the same shape as that of $E_k(1,\omega)$ and, in particular, have the same inflection point in K. Therefore, the value of K_0 given above is suitable as a guide to the selection of the number of references, K, even when $m > 1$. For some values of W, however, $E_k(m,\omega)$, $m > 1$, falls off somewhat faster with $K > K_0$ than $E_K(1,\omega)$ does. For example, in Figure 2-10, with $m=1$ and $K_0=2$ yielding about 33 dB of cancellation. Six additional references ($K=8$) gives only 3-4 dB more cancellation, so choosing $K = K_0$ seems justified. However, for the same case with $m=5$, $K = K_0 = 2$ provides 22 dB of cancellation, while using only 2 more references gives 6 dB more cancellation. Thus, K_0 appears to be a rougher guideline when it is used for $m > 1$. Of course, there will always be some ambiguity as to how much rejection must be provided by a

52

reference to justify its use. Certainly in any given design situation, K_0 can be used as a "rule of thumb," with final choice of K made by referral to the curves given in Appendix K.

The numerical procedure for calculating E_K (m, ω) as given in Appendix K allow assessment of the effects of changing the hydrophone spacing, d, while holding the distance from the primary to the closest reference (md) constant. If d is divided by Δ (reducing hydrophone spacing), then m is multiplied by Δ to make md constant. The results of this are shown in Figures 2-18, 2-19, 2-20, and 2-21. These curves show $E_K(m,\omega)$ as a function of K for various values of Δ, where

$$m = \Delta$$

and

$$W = W_o/\Delta \quad = \quad \frac{(d_o/\Delta)}{\lambda} \; \theta_1 \sin\theta_o \qquad (2\text{-}52)$$

Hence, the curves can be interpreted as varying spacing d, while holding md constant. Figures 2-18, 2-19, 2-20, and 2-21 use W_o = .1, .05, .005, and .001 respectively, and vary m over the range indicated on the figures. The plots are all for an INR of 40 dB. Recall that as m was increased for fixed W and K (that is, as the reference array is moved farther from the primary with fixed spacing between reference hydrophones) the canceller output spectrum increased monotonically. The situation is quite different when the reference spacing is changed holding the distance to the primary constant. The behavior is not monotonic, and the E_K (m,ω) may increase or decrease dependint upon W_o and K. The details of this behavior cannot be predicted from the analytical results at present, and will be investigated further in the next phase of the study.

53

Figure 2-18
Canceller Output Spectrum vs K
$W_o = .1$
INR = 40 dB
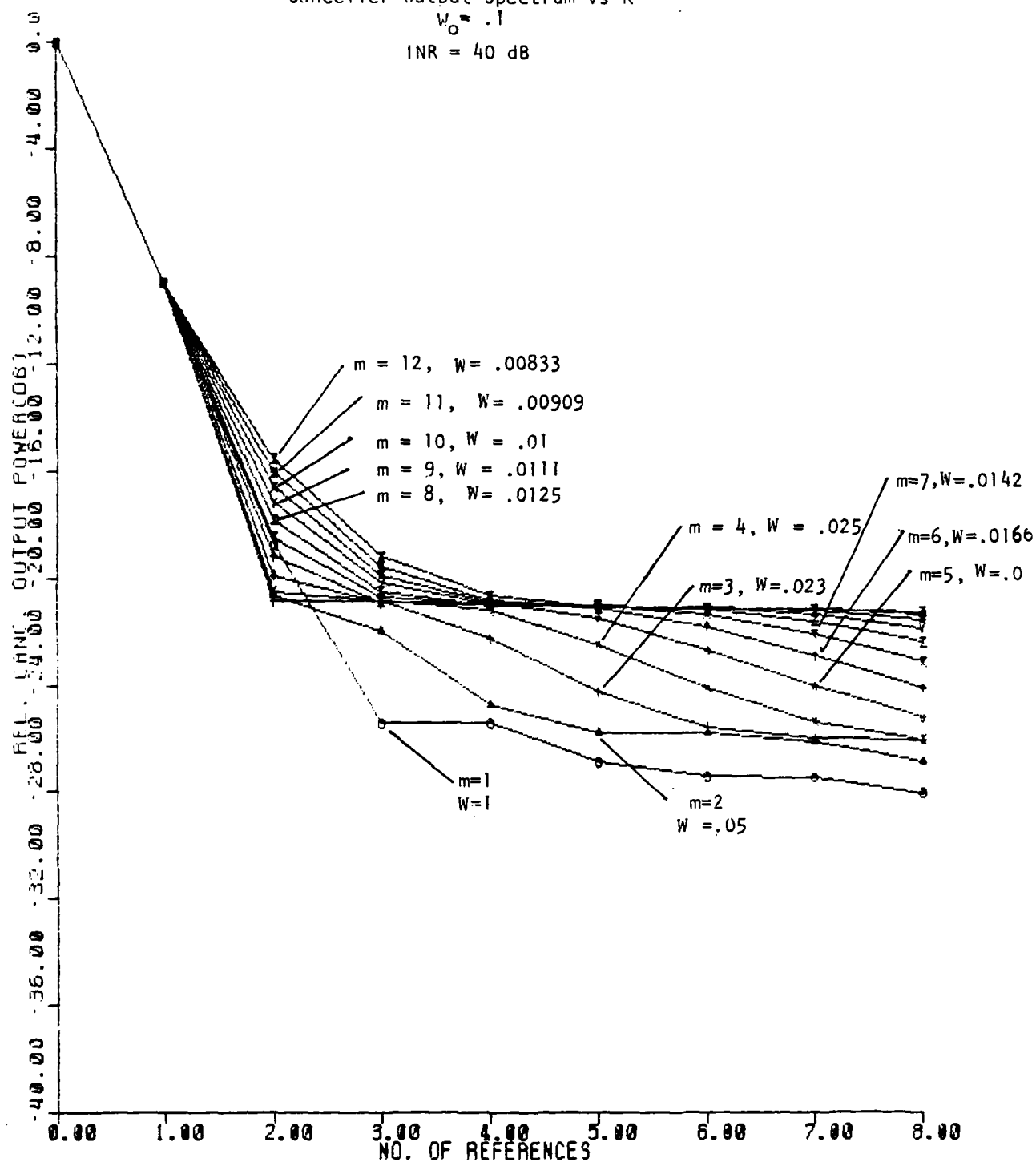
Figure 2-18.   Canceller Output Spectrum vs. K for W_o = 0.1, INR = 40 dB

54

Figure 2-19
Cancel ler Output Spectrum vs K
$W_o = .05$

INR = 40 dB

m = 7, W = .00714
m = 6, W = .00833
m = 5, W = .01
m = 4, w = .0125
m = 3, W = .0166

m = 2, W = .025
m = 1, W = .05

NO. OF REFERENCES
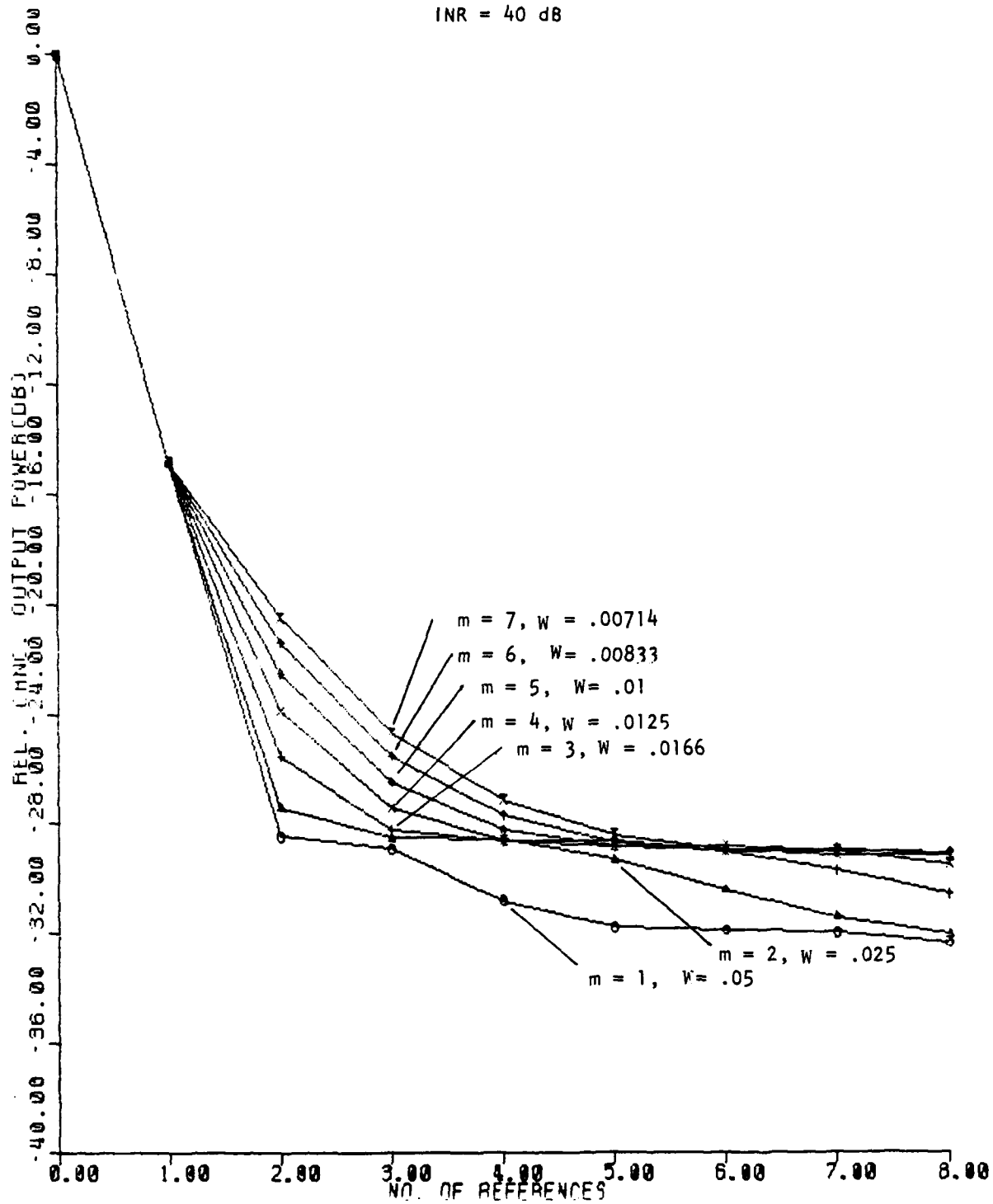
Figure 2-19. Canceller Output Spectrum vs. K for W_o = 0.05, INR = 40 dB

Figure 2-20
Canceller Outputs Spectrum vs K
$W_O = .005$
INR = 40 dB
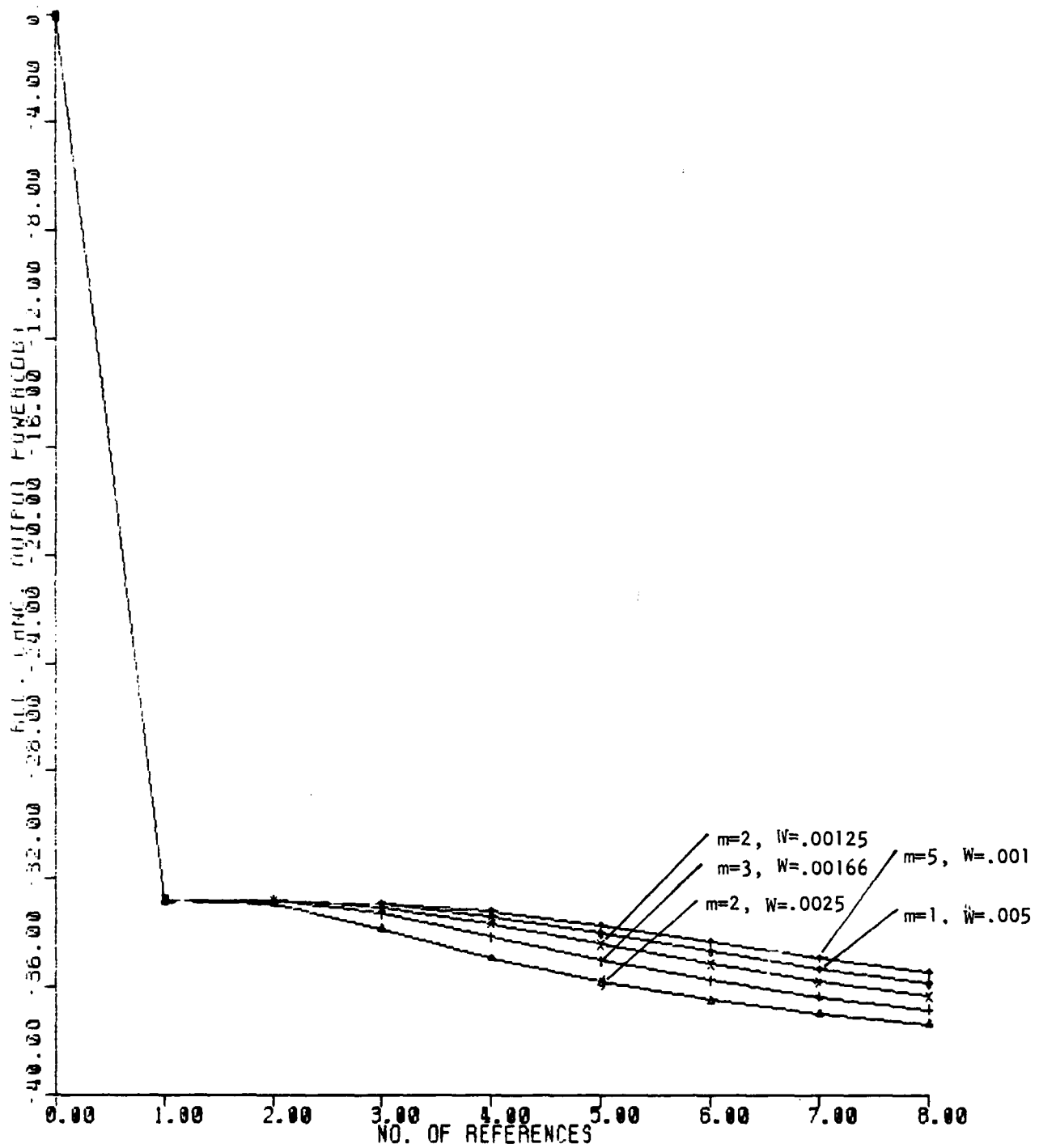
Figure 2-20.   Canceller Output Spectrum vs. K for $W_o = 0.005$, INR = 40 dB

Figure 2-21
Canceller Output Spectrum vs K
$W_o = .001$

INR = 40 dB

m = 1
W = .001

m = 2, W = .0005

m = 3, 4, 5
W = .00033, .00025, .0002

NO. OF REFERENCES
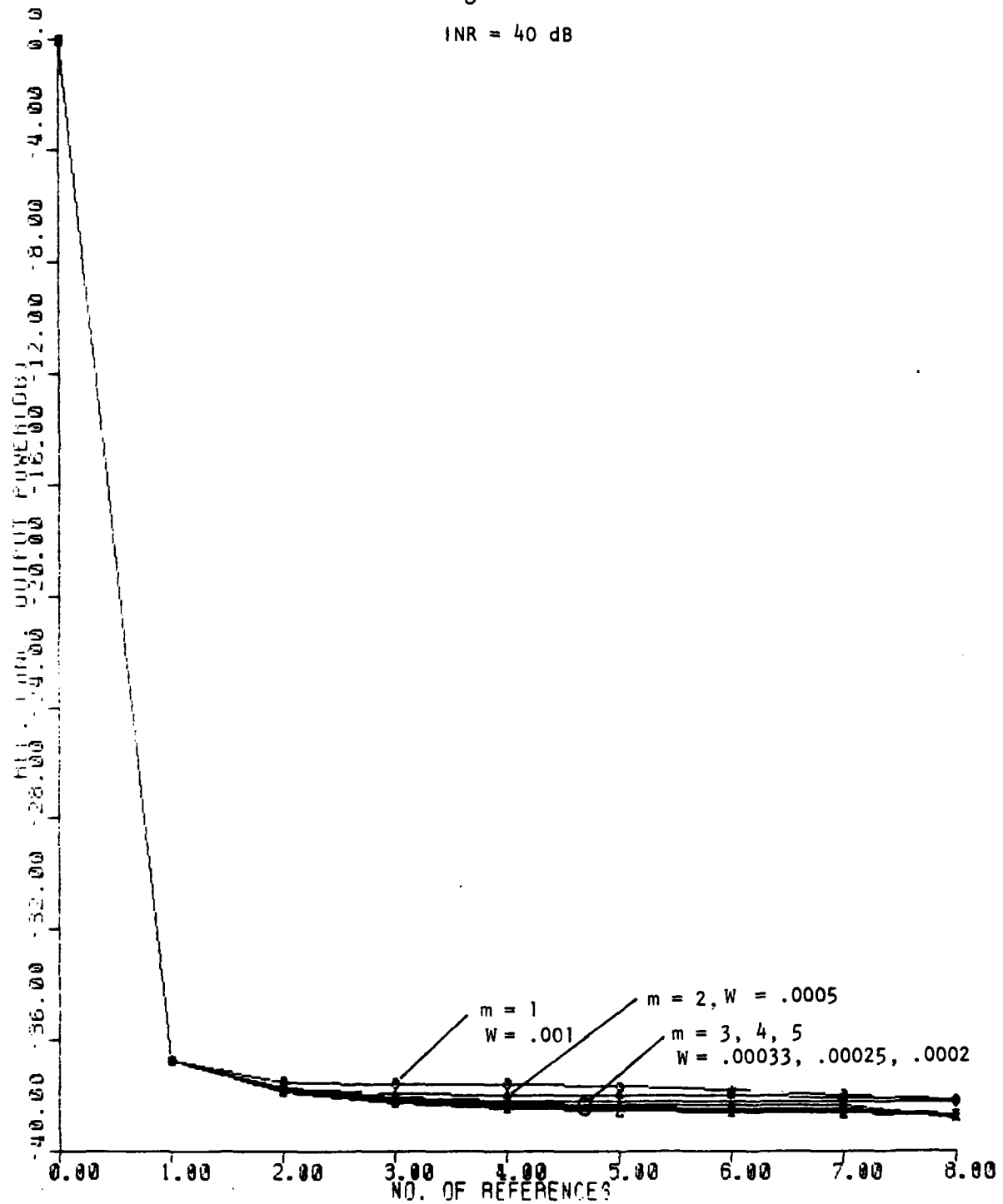
Figure 2-21.   Canceller Output Spectrum vs. K for W_o = 0.001, INR = 40 dB

2.6 Cancellation for an Extended Interference Producing an Exponential Hydrophone Output CSD.

It is quite common in the study of bandlimited temporal random processes to model the process as having an exponential correlation function.

$$\rho(\tau) = \sigma^2 e^{-B|\tau|} \tag{2-53}$$

where σ^2 is the power of the process and where B is the bandwidth. This correlation function has the advantage of being representative of many physical processes while having nice analytical properties. In particular, given a sequence of N samples, uniformly spaced in time, of such a process, the correlation matrix of the N samples is invertible explicitly (this is discussed thoroughly in Appendix G). It therefore seemed reasonable to consider a source producing an exponential hydrophone output CSD and the performance of the canceller with such an interference.

Appendix G assumes the same hydrophone geometry as Figure 2-2, but assumes that the extended interference produces the hydrophone output CSD

$$s_e(p,q,\omega) = \sigma_n^2(\omega) \delta_{pq} + \sigma_I^2(\omega) e^{-B(\omega)|p-q|d} \tag{2-54}$$

between the outputs of the pth and q^{th} references, where $B(\omega)$ is a spatial bandwidth. Using the results of Appendix D and the special properties of the CSD matrix produced by (2-54), the irreducible canceller output power, $E_\infty(m,\omega)$, can be determined in closed form for arbitrary m. It is shown that

$$E_\infty(m,\omega) = \sigma_I^2(\omega) \left\{ \left[\beta(1-\rho^{2m}) + (1-\rho^{2m}) \right. \right.$$

$$\left. \left. - \frac{2\beta^2 \rho^m}{\beta(1+\rho^2)+(1-\rho^2)+\sqrt{[\beta(1+\rho^2)+(1-\rho^2)]^2-(2\beta\rho)^2}} \right\} \right. \tag{2-55}$$

where

$$\rho = e^{-B(\omega)d} \tag{2-56}$$

and

$$\beta = \frac{\sigma_n^2(\omega)}{\sigma_I^2(\omega)} \tag{2-57}$$

In the interference only (ambient noise free) case, $\beta = 0$ and (2-55) reduces to

$$E_\infty(m,\omega) = \sigma_I^2(\omega)(1-\rho^{2m}) = \sigma_I^2(\omega)(1 - e^{-2mB(\omega)d}), \sigma_n^2(\omega) = 0 \tag{2-58}$$

From Appendix G, however, (2-58) is just the cancellation that would be achieved using a single reference placed md feet from the primary. Therefore, use of more than one reference ($K > 1$) does not improve canceller performance. This is a fundamental difference between the uniform interference discussed in Section 2.5 and the one producing the exponential CSD of (2-54). Recall that for the uniformly distributed source

$$\lim_{K\to\infty} E_K(m,\omega) = 0$$

The difference in the behavior of $E_K(m,\omega)$ for the two hydrophone output CSD's can be explained in terms of the special nature of the exponential CSD. It can be shown that the sequence of hydrophone outputs, taken at a single frequency (in the interference only case), are a first order Markov sequence. As a result, the optimal canceller uses only the closest reference, regardless of how many are possible.

Figures 2-22 and 2-23 plot the irreducible canceller output power relative to the input power given by (2-55) as a function of ρ for values of

10 log $(1/\beta)$ of 40 and 20 dB, respectively. It can be seen that cancellation to near the noise floor, $\sigma_n^2(\omega)$, requires that the primary and references be very highly correlated. This is again due to the Markov nature of the hydrophone outputs under the exponential CSD. At high interference to noise ratio, the optimal canceller uses only the reference closest to the primary and the output power is proportional to $(1 - \rho^{2m})$. Additional references have no effect, so the canceller depends completely on the proximity of the closest references to the primary to achieve cancellation. Hence, ρ must be very close to unity to produce cancellation to near the noise floor.

The canceller performance with the exponential hydrophone output CSD can be compared with that achieved in the presence of a uniform interference (producing a sin x/x shaped CSD) by noting that the parameter $B(\omega)d$ in the exponential case plays the same role as

$$ W = \frac{d}{\lambda} \Phi \sin\phi_o $$

in the uniform case. Appendix G makes the following observations:

    (a) If $W \gtrsim 1/2$ in the sin x/x case, virtually no cancellation is achievable, as already observed in Section 2.5. No such sampling criterion is present in the exponential case, but cancellation is still severely limited for $B(\omega)d \geq 1/2$. Either CSD requires a value of W much smaller than $1/2$ if the canceller is to produce cancellation in the 10 to 40 dB range.

    (b) The optimal canceller produces better results for the exponential CSD for W larger than approximately 0.4. However, in the important region of small W, producing more than 10 dB of

60
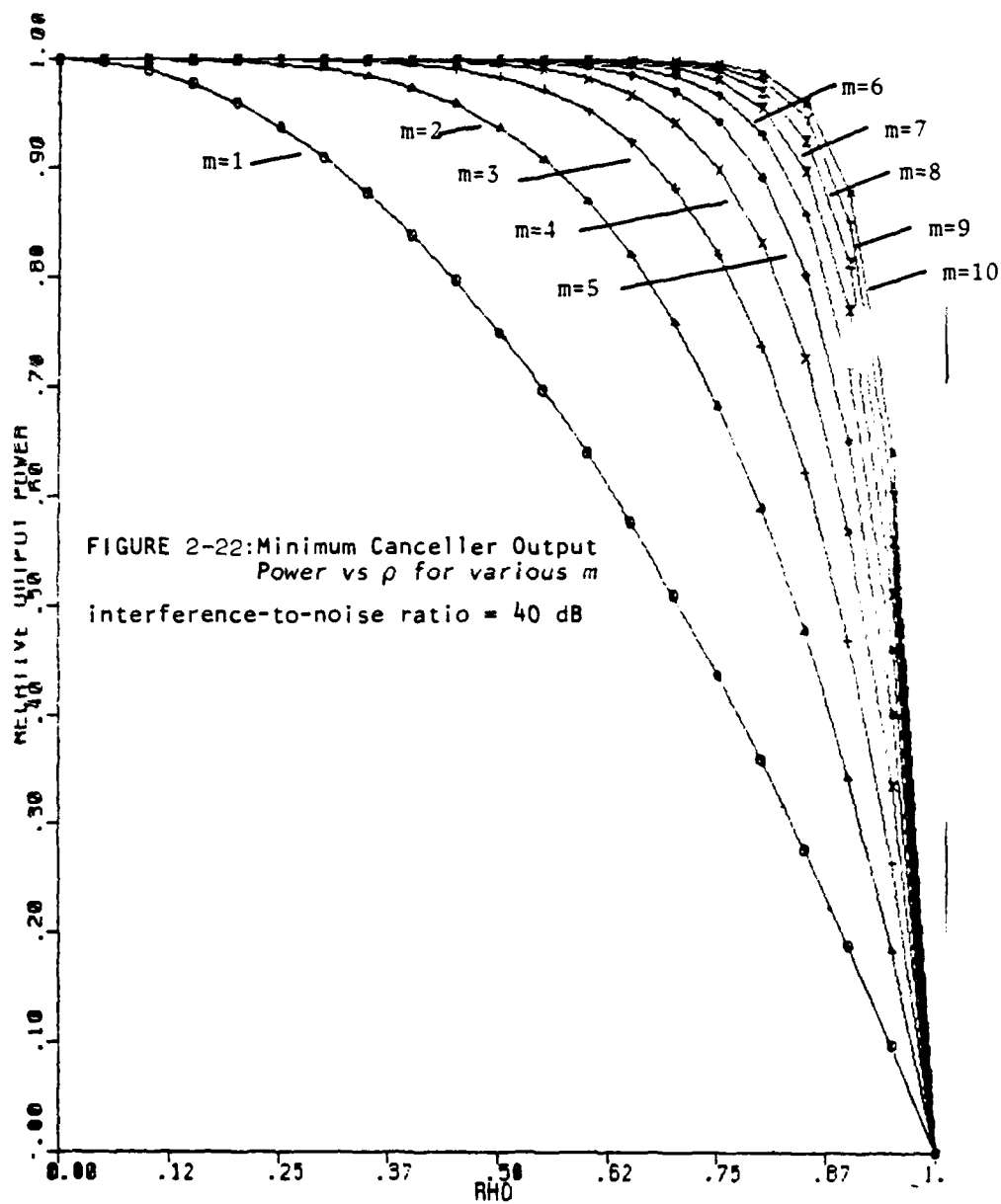
FIGURE 2-22:Minimum Canceller Output
Power vs ρ for various m
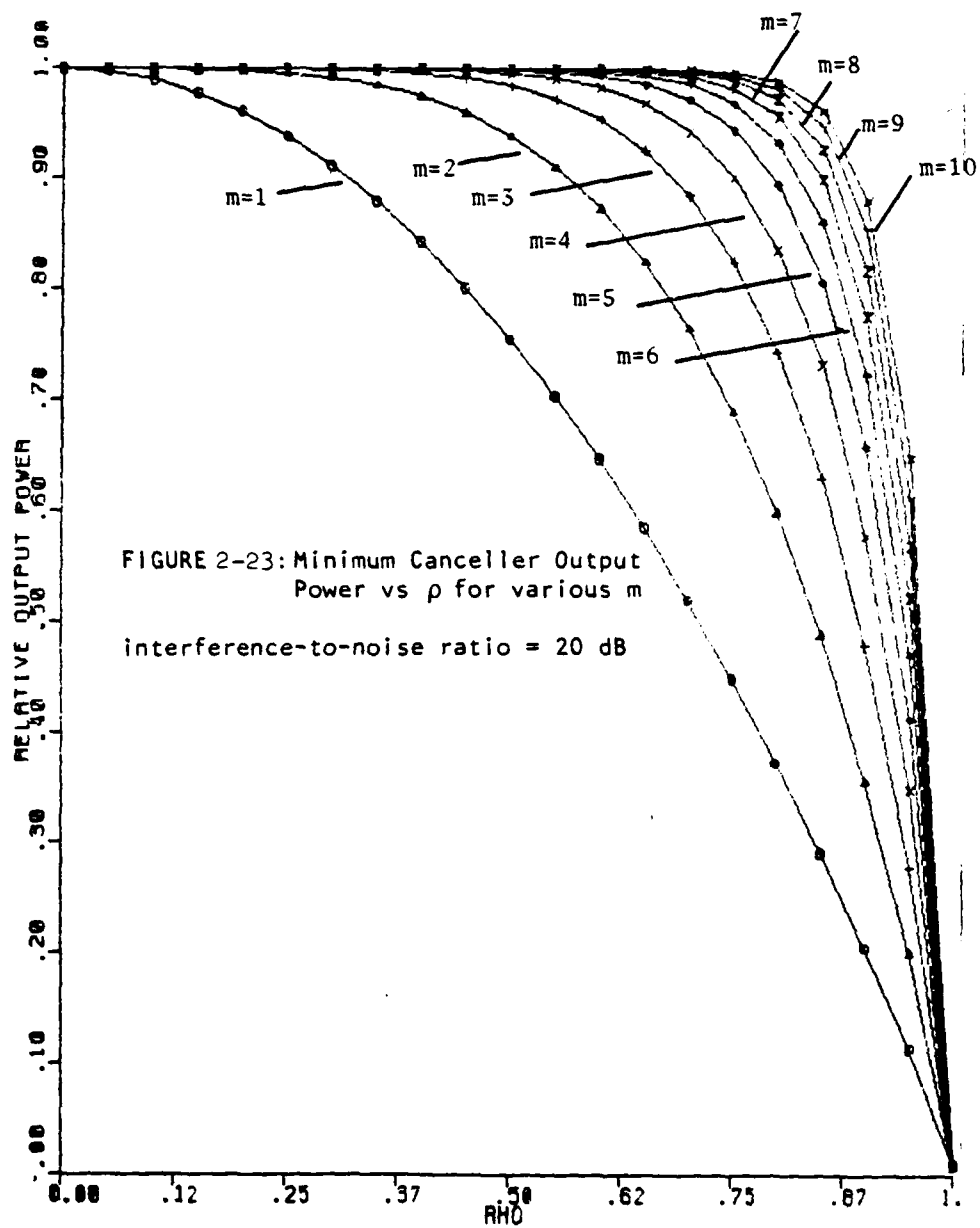
interference-to-noise ratio = 40 dB

FIGURE 2-23: Minimum Canceller Output
Power vs ρ for various m

interference-to-noise ratio = 20 dB

62

cancellation, the canceller is better able to reject the sin x/x source. This is due to the Markov property of the exponential source, as discussed above.

Summarizing, the exponential CSD produces significantly different results than the sin x/x case, as noted above. The differences between the two reflect a Markov property inherent in the double exponential CSD. It is likely that the differences also result from the fact that the sin x/x CSD is produced by an angle limited source, while the exponential case results from a source distributed on $(-\pi, \pi)$. Like the sin x/x CSD, the source producing the exponential CSD cannot be cancelled to an ambient noise floor for m=1. Further, the minimum canceller output power is shown to increase with m, just as the numerical results indicated for the sin x/x. However, the parametric behavior of the canceller with the two CDS's differs sufficiently that the exponential case cannot be used to predict the canceller performance with the sin x/x CSD.

2.7 <u>Effects of Reverberation Non-stationarity on Canceller Behavior.</u>
Section 2.1 considered two methods of applying the LMS adaptive canceller to the non-stationary reverberation environment. Both methods held the weights fixed for an interval of time after transmission in order to assure that the canceller was not operating during periods of reverberation from other sources. This is critical because the highly correlated inputs to the canceller during these periods would severely degrade cancellation of the CZ reverberation if the weights were not frozen. Once the initial time interval has passed (and all other sources of reverberation died out), the question arises as to the effects of ambient noise on canceller performance.

The first method discussed in Section 2.1 seeks to avoid canceller adaptation in ambient noise completely. It does this by using an energy detector in the reverberation band to determine when the CZ reverberation is present, and only allowing the weights to adapt during this time. Given the fact that the reverberation dominates the ambient noise (and signal, if present), this detection should be very reliable.

However, it is well known that the LMS algorithm adapts much more rapidly in an environment producing correlation between its inputs (such as reverberation) than to one producing uncorrelated inputs (like ambient noise does). That is, the filter "learns" the correlation properties of an input much more quickly than it "forgets" those properties once the correlation disappears. The second approach discussed in Section 2.1 takes advantage of this by operating the adaptive canceller continuously after the initial time interval has passed. Thus, the weights adapt during the period of ambient noise alone, as well as when the CZ reverberation is present. Since the filter "forgets" slowly, the degradation due to adaptation in the presence of the ambient noise will be tolerable if the period of ambient noise is not too long. This approach eliminates the need for (and cost of) the reverberation detector.

The latter approach is considered in Appendix J. A pulsed model for the adaptive canceller input is developed then used to derive an expression for the mean weights and man square error (canceller output power) in such an acoustic field in the absence of signal. It is shown that if the reference hydrophone cross-spectral density matrix due to interference has a dominant eigen value, λ_{max} (as it will for a plane wave or narrow interference and

high INR). then the transient response of the system is determined by $\mu(P_n + \lambda_{max} D_c)$, where P_n is the ambient noise power and where D_c is the duty cycle of the reverberation, i.e.,

$$D_c = \frac{\text{time CZ reverberation is present in one transmit cycle}}{\text{time canceller is adapting during one transmit cycle}}$$

Hence, the transient response is determined by the noise power plus the time average of the eigenvalue over the adaptation time.

It is also shown that the pulsed character of the input produces an increase in the steady state canceller output power above that which would occur if adaptation only occurred in the presence of CZ reverberation. Note that the canceller reaches a steady state, time varying solution in response to the non-stationary input. For a single plane wave interference. this maximum increase is shown to be

$$\gamma_{max} = \frac{[1 - (1-\mu P_n)^{k-p}]^2}{[1 - (1-\mu P_I)^p (1-\mu P_n)^{k-p}]} \tag{2-59}$$

where P_I is the interference power, is is the total number of samples in the period during which filter adapts in one transmit cycle, and p is the number of samples within k that the reverberation is present. This has been shown numerically to be a monotone increasing function of μ, so the increase in canceller output power can be made arbitrarily small by decreasing μ. However, it will generally be required that the canceller converge within several pings, so that μ will be selected to give the desired dynamic response. In that case, (2-59) will provide an indication of the increase in cancellation above that predicted in Section 2.5 and 2.6. Note that

γ_{max} is minimized by choosing p as close to k as possible, i.e., only adapting in the presence of interference. It remains to develop an equivalent expression to (2-59) when the source is extended, and to use these results to generate design guidelines for the implementation of the canceller structure.

2.8 Spatial Response of the LMS Canceller in the Presence of an Extended Source. Although the main thrust of this study was the analysis of the effectiveness of the canceller in rejecting an extended interference without considering the effect of the canceller on some plane wave signal of interest, it is clear that the detection of such a signal is the eventual goal. Appendix H therefore considers the spatial response of the canceller, that is, its response to a plane wave from some direction, ϕ_s, as a function of that direction. This response is just the power that would appear at the canceller output due to a plane wave signal at the angle ϕ_s. In the case of a uniformly distributed, spatially uncorrelated, plane wave source, this spatial response, $B_w(\phi_s)$, is developed in terms of the DPSS's and their eigenvalues and evaluated numerically on the computer. Figures 2-24 through 2-26 show the response of the canceller in the presence of such a source centered at 45° relative to broadside and with an angular extend of 20°. The interference to noise ratio is 40 dB, and the hydrophones are uniformly spaced 1/2 wavelength apart. The Figures show the results using 1, 4, and 8 references, respectively. The spatial response can be seen to include a notch in the direction of the interference, as one would expect. From the Figures 2-24 through 2-26 and those given in Appendix H, it can be seen that the notch broadens and deepens as references are added until there are 3-4 references, at which point additional references only

66
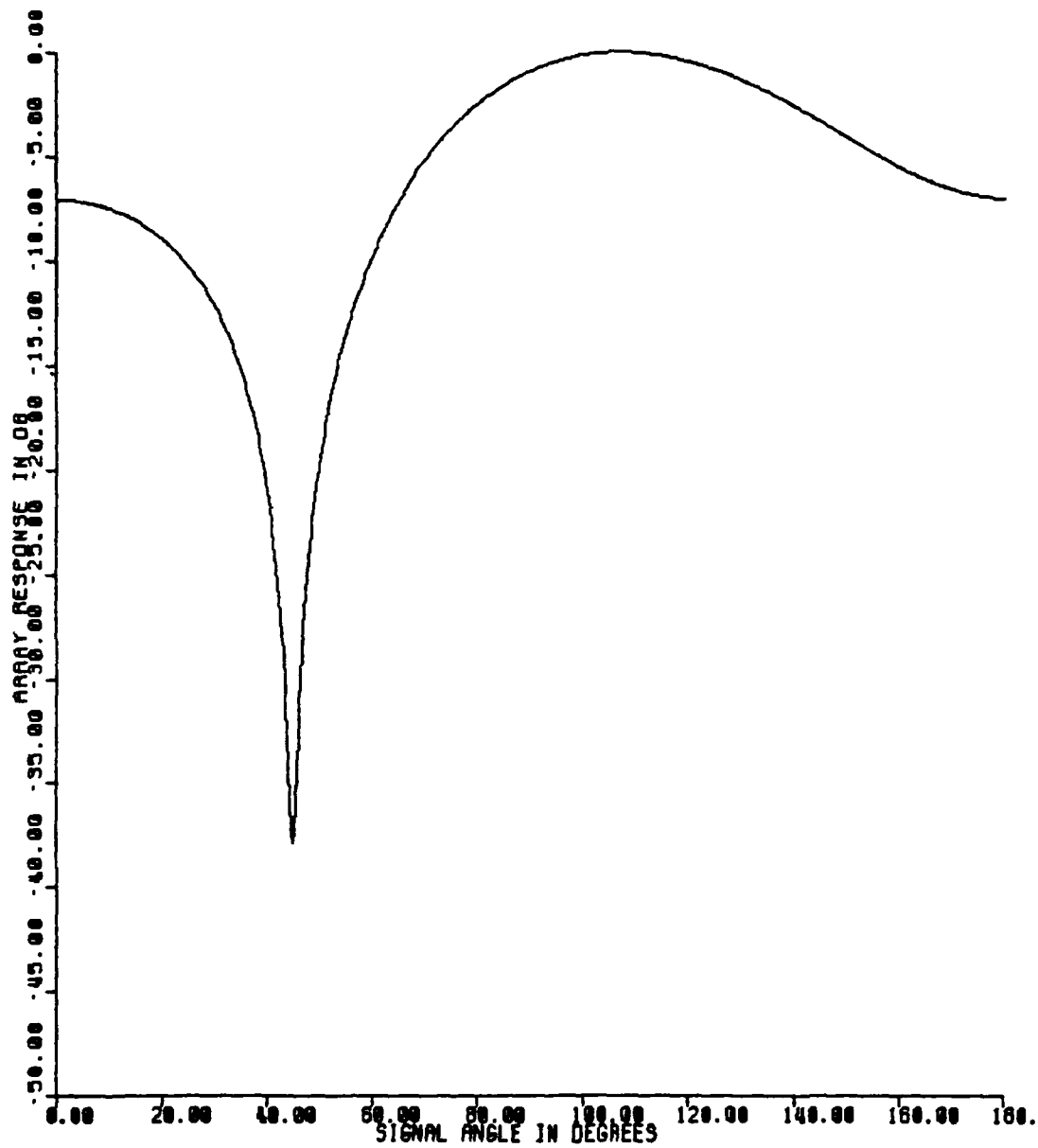
FIGURE 2-24: Spatial Response for 20° Uniform Extended Source at 45°

d/λ = .5, m=1, K=1, INR=40 dB
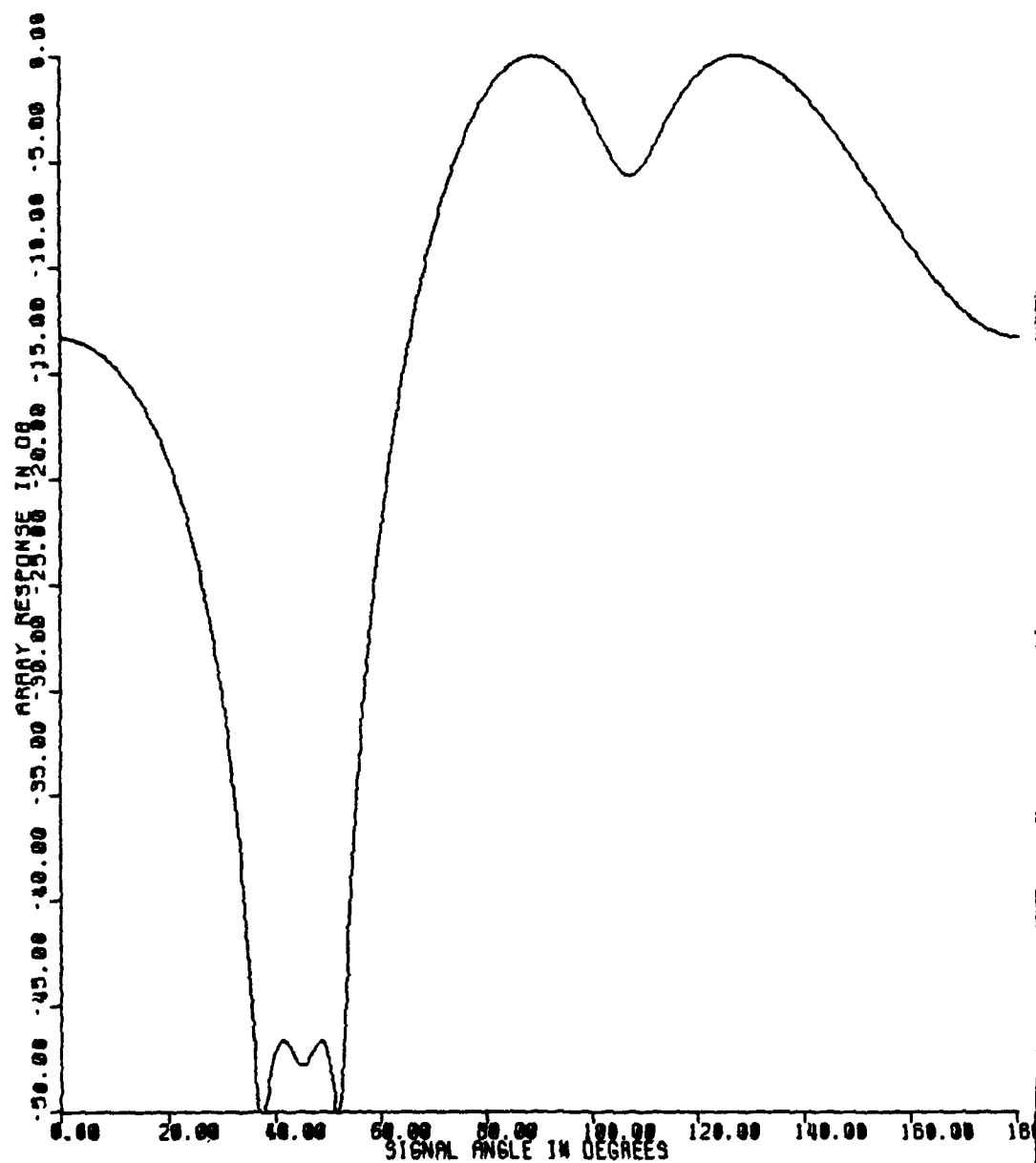
FIGURE 2-25: Spatial Response for 20° Uniform Extended Source at 45°
d/λ = .5, m=1, K=4, INR = 40 dB
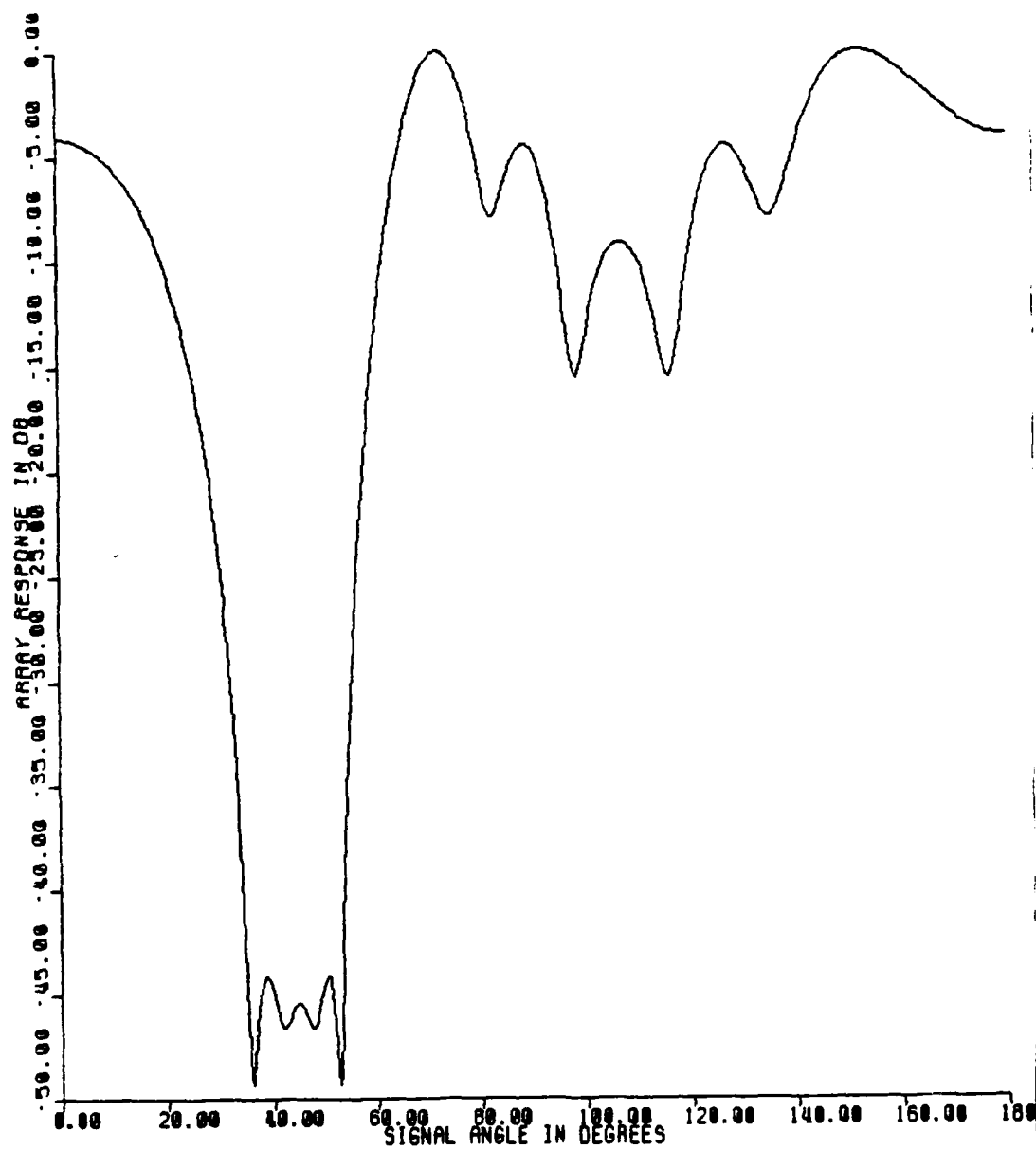
FIGURE 2-26: Spatial Response for 20° Uniform Extended Source at 45°

d/λ = .5, m=1, K=8, INR = 40 dB

69

sharpen the sides of the notch and improve the spatial response to signals in directions other than that of the interference. The results of Section 2.5 indicate that for narrow sources, more use of more than 3-4 hydrophones will not yield sufficient cancellation improvement to justify their cost. Therefore, the results of Appendix H suggest that the reason for adding more references may be to assure adequate signal response in some direction of interest.

It was shown in Section 2.5 that as the distance between the reference array and the primary increase, the cancellation of the interference decreased. Figures 2-27 and 2-28 show the spatial response of the canceller for the same source and an 8 element reference array as above, but with $m = 10$ and $m = 20$ (recall that the reference hydrophone spacing is d and the distance from the primary to the closest reference is md). It can be seen that the notch depth has decreased, indicating a degradation in the cancellation, and that there has been some degradation is the response pattern in directions other than that of the interference.

When interpretting these figures it should be kept in mind that the primary consists of a single omnidirectional hydrophone, rather than an array, as would be used in most sonar situations. As indicated in Appendix L, when a primary array is used, the responses like those of Figures 2-24 through 2-28 would be multiplied by the response pattern of the primary array. This would greatly attenuate (by the primary array sidelobe level) those regions outside the mainlobe of the primary array. Assuming, then, that the reverberation that limits the active detection performance arrives on or near the main lobe, the signal response in the
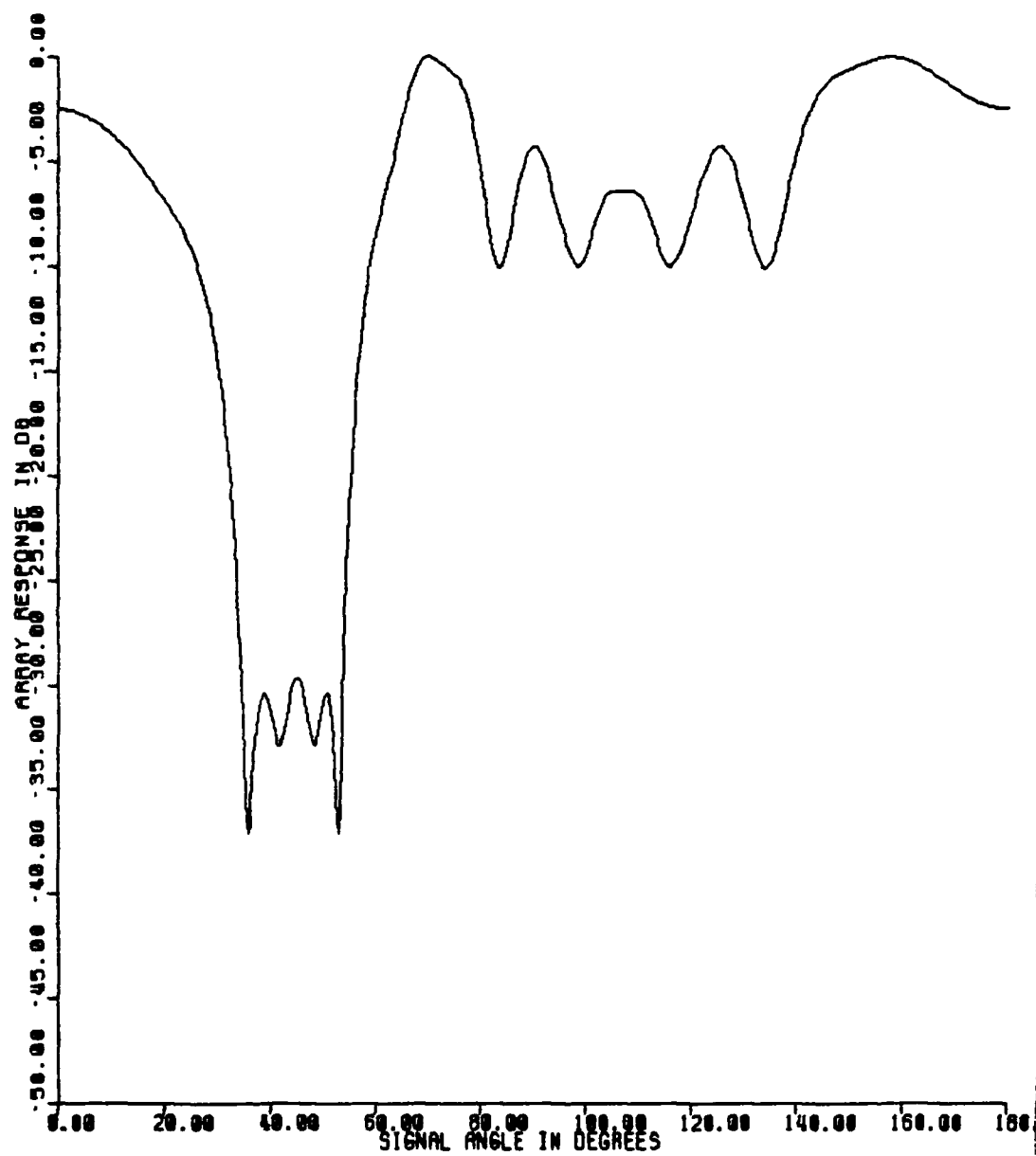
FIGURE 2-27: Spatial Response for 20° Uniform Extended Source at 45°

d/λ = .5, m=10, K=8, INR = 40 dB

71
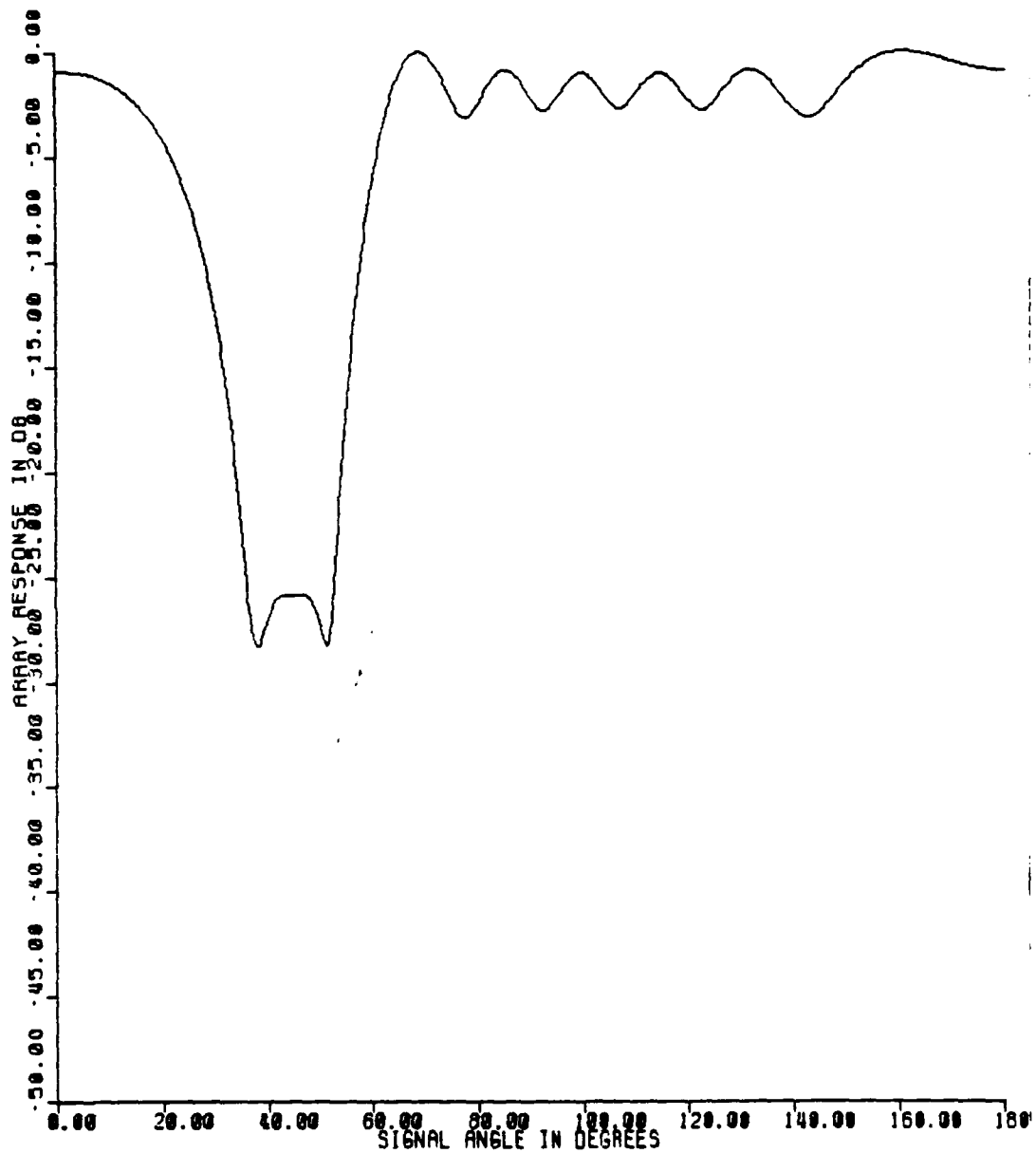
FIGURE 2-28: Spatial Response for 20° Uniform Extended Source at 45°
d/λ = .5, m=1, K=8, INR = 20 dB

72

vicinity of the notch is of primary interest. The reason for adding references would then be to increase the slope of the sides of the notch.

With this in mind, it can be seen that in Figures 2-27 and 2-28, increasing the distance between the references and primary did not significantly degrade the spatial response in the vicinity of the notch. It can be conjectured then that signal attenuation will not be a primary consideration in selecting the distance between the primary and references when the primary is a steered array and the interference is in the mainlobe.

As the interference-to-noise-ratio decreases, there is a reduction in the depth of the null at the location of the interference. Figure 2-29 shows the spatial response for the cases of Figure 2-26 ($m=1$, $K=8$, $\Phi=10°$) but the interference-to-noise ratio has been reduced to 30 dB. Figure 2-30 repeats the same case, but with an interference-to-noise ratio of 20 dB. It is interesting to note that the array response in directions other than the interference direction is affected very little by the change in interference-to-noise ratio.

A major task of the next phase of this study is the investigation of the effect of the canceller upon a plane wave signal, and the quantification of the effectiveness of the canceller in improving the detectability of such a signal. During the next phase, the above conjectures will be examined and quantified.
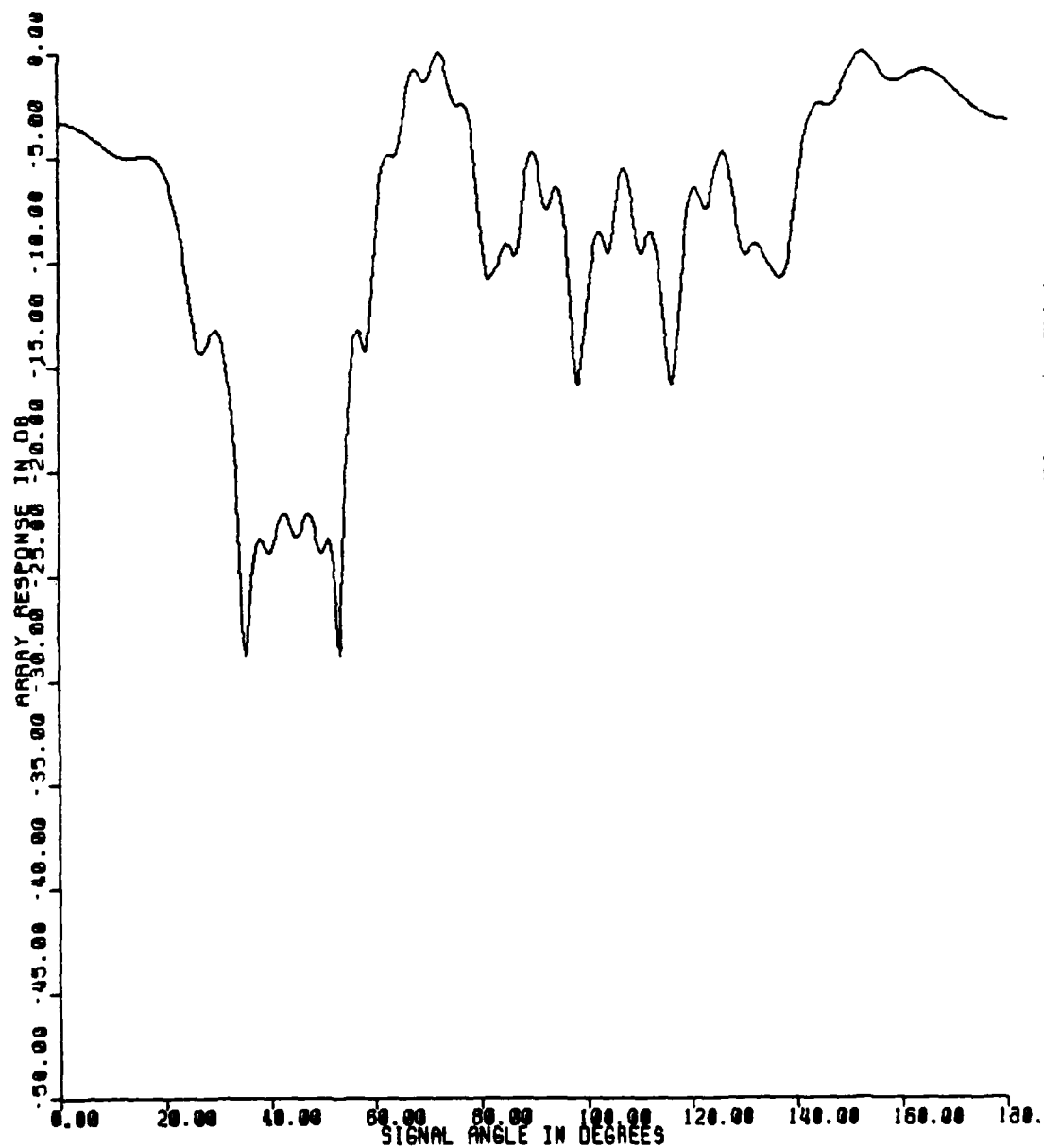
FIGURE 2-29: Spatial Response for 20° Uniform Extended source at 45°

d/λ = .5, m=20, K=8, INR = 40 dB
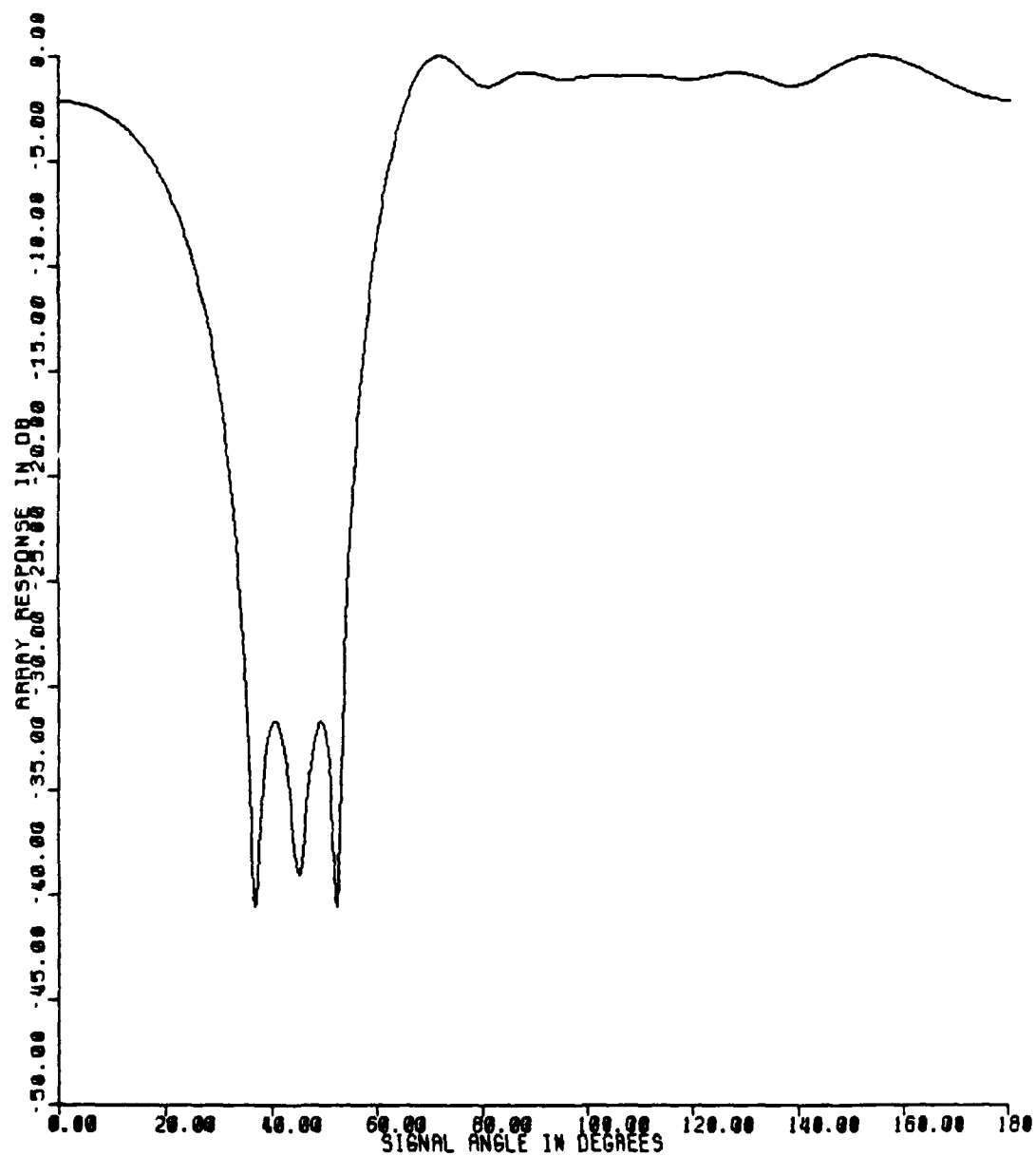
FIGURE 2-30: Spatial Response for Uniform Extended Source at 45°

d/λ = .5, m=1, K=8, INR = 30 dB

3.0 CONCLUSIONS AND RECOMMENDATIONS

3. CONCLUSIONS AND RECOMMENDATIONS

This study has considered the LMS adaptive cancellation of CZ surface reverberation using a bistatic approach, where passive hydrophones spatially separated from the transmit/receive array are used as references. This was done by modelling the surface reverberation as a narrow extended source that is spatially uncorrelated and uniformly distributed. The work to date has concentrated on the ability of the LMS structure to reject the reverberation in the absence of a plane wave signal of interest. It was shown that by a judicious choice of system parameters, such as hydrophone spacing and number of references, the reverberation can be cancelled arbitarily close to the ambient noise flow. Unlike the case of a point interference, however, if care is not taken in the placement of references, little or no cancellation may be possible regardless of the number of references. Through a combination of analytical and numerical techniques, the parametric sensitivities of the cancellation performance to source extent, hydrophone spacing, distance between references and primary array, and number of references has been characterized. These results comprise the basic tools for the design of a canceller for use in a given situation.

An important result was that for narrow extended sources, such as CZ reverberation, there is a law of diminishing returns with respect to the number of references to be employed. That is, beyond some number of references, say K_o, more references do not provide sufficient additional cancellation to justify the computational cost of including them. A design guideline for selection of the number of references was derived. It appears that for the cancellation of CZ surface reverberation in a sonar with a horizontal

beamwidth of less than 20°, at most 4-5 references are required. Of course, these references only supply adequate cancellation if the other design guidelines are met.

Since this phase of the study considered the behavior of the canceller in the absence of signal, the results presented here cannot be used to predict the improvement in the detection of a plane wave signal in the presence of the CZ reverberation. Some of the analysis of the response of the canceller to the signal has been initiated in the work reported on the spatial response of the canceller. In the next phase, this work will be continued, with the goal of deriving a detection performance measure, such as deflection, for the canceller structure. The effect of signal presence during adaptation (to "signal bias" problem) will also be investigated.

The work in this phase of the study has been based upon several theoretical models of the canceller structure and the CZ reberberation. During the next phase, computer simulations will be run to validate both the analysis and the mathametical models used. This will include development of a computer model for the extended source for use with existing programs for the multiple canceller structure. If suitable sea tapes can be obtained, actual CZ reverbation will be compared statistically to the theoretical models used here, and, if possible, run through the multiple canceller algorithm.
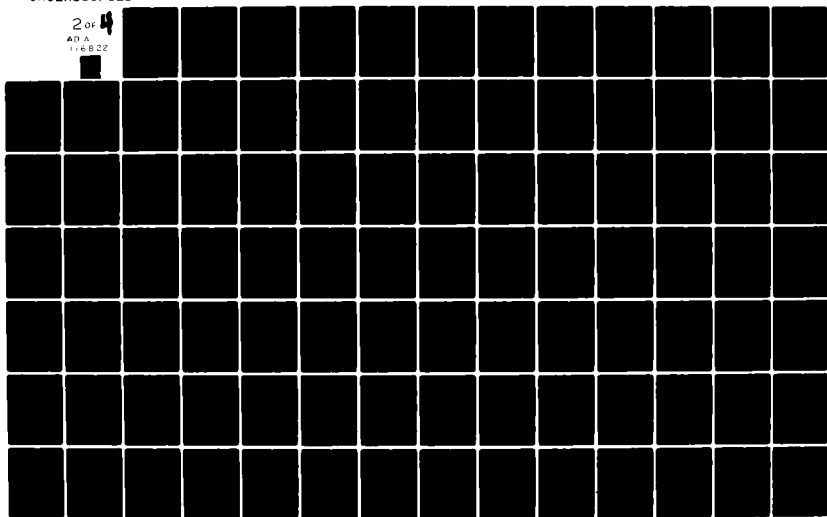
REFERENCES

REFERENCES

[1]   S.P. Applebaum, "Adaptive Arrays", Syracuse University Research
       Corporation Technical Report SURC TR-66-001, August 1966 (Revised
       March 1975)

[2]   B. Widrow et al, "Adaptive Noise Cancelling: Principles and Applications",
       Proc. I.E.E.E., Vol. 63, No. 12, Dec. 1973.

[3]   B. Widrow, "Adaptive Filters" in Aspects of Network and System Theory,
       R. Kalman and N. DeClarts Eds., New York: Rinehart and Winston,
       1971.

[4]   F.A. Reed and P.L. Feintuch, "A Comparison of LMS Adaptive Can-
       cellers Implemented in the Frequency Domain and the Time Domain,"
       I.E.E.E. Trans. on Circuits and Systems, Vol. CAS-28, No. 6,
       pp. 610-615, June 1981.

[5]   N.J. Bershad and P.L. Feintuch, "Analysis of the Frequency Domain
       Adaptive Filter," Proc. I.E.E.E, Vol. 67, pp 1658-1659, December 1979.

[6]   M. Dentino, J. McCool, and B. Widrow, "Adaptive Filtering in the Fre-
       quency Domain," Proc. I.E.E.E., Vol. 66, pp 1658-1659 December 1978.

[7]   B. Widrow, J. McCool, and M. Ball, "The Complex LMS Algorithm,"
       Naval Undersea Center Tech. Report NUC TN 1437, October 1974.

[8]   F.A. Reed, P.L. Feintuch, and N.J. Bershad, "Time Delay Estimation
       Using the LMS Adaptive Filter – Static Behavior," I.E.E.E. Trans. on
       Acoustics, Speech, and Signal Processing, Vol. ASSP-29, No. 3,
       pp 561-569, June 1981.

[9]   P.L. Feintuch, N.J. Bershad, and F.A. Reed, "Time Delay Estimation
       Using the LMS Adaptive Filter – Dynamic Behavior", I.E.E.E. Trans.on
       Acoustics, Speech, and Signal Processing", Vol. ASSP-29, No. 3,
       pp 571-576, June 1981.

[10]   H.L. Van Trees, _Detection, Estimation and Modulation Theory, Part III_,
        New York, John Wiley and Sons, 1971.

[11]   N.J. Bershad, P.L. Feintuch, F.A. Reed, and B. Fisher, "Tracking
        Characteristics of the LMS Adaptive Line Enhancer – Response to a
        Linear Chirp Signal in Noise," _I.E.E.E. Trans. on Acoustics, Speech
        and Signal Processing_. Vol. ASSP-28,, No. 5, pp 504-516, October 1980.

[12]   H. Widrow, "The Strong Szego Limit Theorem for Circular Arcs,"
        Indiana University Math. Journal, Vol. 21, No. 3, 1971.

[13]   D. Slepian, "Prolate Spheroidal Wave Functions, Fourier Analysis,
        and Uncertainty – V: The Discrete Case," _The Bell System Tech.
        Journal_, Vol. 57, No. 5, May-June 1978.

[14]   J.B. Thomas. _An Introduction to Statistical Communication Theory_,
        New York, John Wiley and Sons, 1969.

[15]   U. Grenander and G. Szego, _Toeplitz Forms and Their Applications_,
        Berkley and Los Angeles, University of California Press, 1958.

[16]   J. Lamperti, _Stochastic Processes_, New York, Springer-Verlag, 1977.

[17]   A.M. Yaglom, _An Introduction to the Theory of Stationary Random
        Functions_," New York, Dover Publications, Inc., 1962.

[18]   J.L. Doob, _Stochastic Processes_, New York, John Wiley and Sons, 1953.

[19]   M. Abramowitz and I.A. Stegun, eds. _Handbook of Mathamatical
        Functions_, National Bureau of Standards Publication, 1970.

APPENDIX A: DERIVATION OF THE FAR FIELD MODEL

APPENDIX A: DERIVATION OF THE FAR FIELD MODEL

Consider the array geometry shown in Figure A-1 located in a noise field consisting of an ambient noise background and a strong extended interference source. The array consists of K+1 acoustic hydrophones arranged as a horizontal line array. Of the K+1 hydrophones, K will be denoted reference hydrophones, as shown, and used to cancel in the LMS sense, the interference from the output of the primary hydrophone. The reference hydrophones are uniformly spaced d feet apart, while the primary hydrophone is located md ft from the nearest reference. The reference hydrophone outputs are denoted $e_k(t)$ for $k = 0, 1, ... K-1$, while the primary hydrophone output is $e_d(t)$.

It will be assumed in the development of the noise field model that the ambient noise produces zero mean, wide sense stationary noise at the output of each hydrophone with $n_k(t)$ the ambient noise at the output of the $k\underline{\text{th}}$ reference ($k = 0, 1, ... K-1$) and $n_d(t)$ the output of the primary. It is assumed that

$$E[n_k(t)n_l(t+\tau)] = R_n(\tau) \; \delta_{kl} \qquad \begin{array}{l} k = 0, 1, ...K-1 \\ l = 0, 1, ...K-1 \end{array} \qquad (A-1)$$

$$E[n_d(t)n_d(t+\tau)] = R_d(\tau) \qquad\qquad\qquad (A-2)$$

and

$$E[n_d(t)n_k(t+\tau)] = 0 \qquad\qquad k = 0, 1, ... K-1 \qquad (A-3)$$

A-1

REFERENCE
HYDROPHONES

PRIMARY
HYDROPHONE
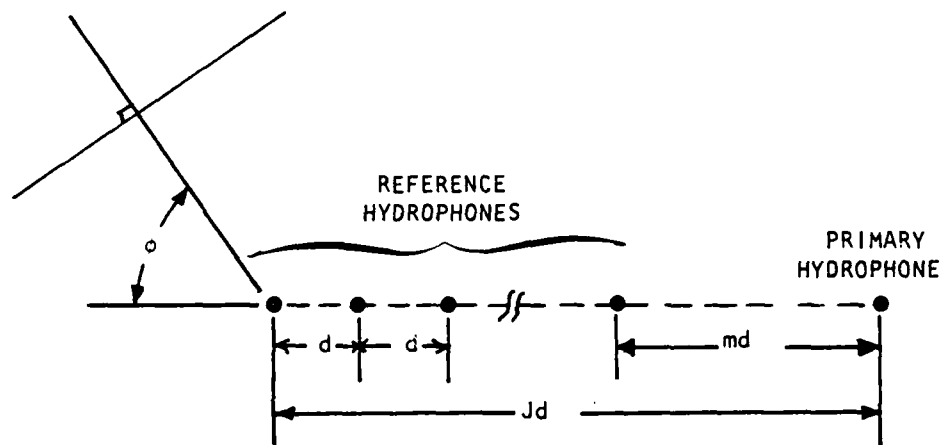
Figure A-1. Array Geometry for Far Field Model

where δ_{kl} is the Kronecker delta and $R_n(\tau)$ is the covariance function of the $N_d(t)$ and $R_d(\tau)$ is the covariance function of $n_d(t)$. That is, the ambient noise at the output of each hydrophone is uncorrelated with the ambient noise at the output of any other hydrophone. This assumption will be reasonable for realistic ambient noise fields if the hydrophone spacing is not much less than one half wavelength at the lowest frequency of interest.

Let the extended source be distributed in angle, ϕ, as shown in Figure A-1, and assume that the arrival from each angle is a plane wave across the length of the array. Let the arrival from the angle ϕ at reference hydrophone number zero, denoted $i(t, \phi)$, be a zero-mean, wide sense stationary random process with

$$E[i(t, \phi) \, i \, (t+\tau, \phi_2)] = R_I(\phi_1, \phi_2, \tau) \tag{A-4}$$

If the speed of sound in the water is given by c, then the propagation delay from reference number zero to a point kd feet along the line array for the arrival from angle ϕ is

$$\tau_k(\phi) = k \frac{d}{c} \cos \phi \tag{A-5}$$

Integrating over all ϕ to account for the entire extended source gives the hydrophone outputs as

$$e_k(t) = n_k(t) + \int_{-\pi}^{\pi} i \, (t - k\frac{d}{c} \cos \phi, \, \phi) \, d \, \phi, \quad k = 0,1, \ldots K-1 \tag{A-6}$$

and

$$e_d(t) = n_d(t) + \int_{-\pi}^{\pi} i \, (t - J \frac{d}{c} \cos \phi, \, \phi) \, d \, \phi \tag{A-7}$$

where

$$J = K + m - 1.$$

Assuming that the interference, $i \, (t, \phi)$, is uncorrelated with the ambient noise, that is,

$$E[i(t, \phi)n_k \, (t + \tau)] = 0 \qquad \forall \tau, \phi$$
$$k = 0, 1, \ldots K-1 \tag{A-8}$$

and

$$E[i(t, \phi)n_d \, (t + \tau)] = 0 \qquad \forall \tau, \phi \tag{A-9}$$

then the cross-covariance between the output of the $p\underline{th}$ and $q\underline{th}$ reference hydrophones is given by

$$R_e(p, q, \tau) = E[e_p(t)\, e_q(t + \tau)]$$

$$= R_n(\tau)\, \delta_{pq} + \int_{-\pi}^{\pi}\int_{-\pi}^{\pi} R_I\,[\,\phi_1,\,\phi_2, \tau + \frac{d}{c}\,(p\cos\phi_1 - q\cos\phi_2\,]\,d\phi_1 d\phi_2$$

$$(A-10)$$

Therefore, the cross-spectral density (CSD) between the outputs of the $p\underline{th}$ and $q\underline{th}$ hydrophones is

$$s_e(p, q, \omega) = \mathscr{F}[r_e(p, q, \tau)]$$

$$= \sigma_n^2(\omega)\delta_{pq} + \int_{-\pi}^{\pi}\int_{-\pi}^{\pi} S_I(\phi_1, \phi_2, \omega)\, e^{+j\frac{\omega d}{c}\,[p\cos\phi_1 - q\cos\phi_2]}\,d\phi_1 d\phi_2 \quad (A-11)$$

where

$$\mathscr{F}[x(\tau)] = \int_{-\infty}^{\infty} x(\tau)e^{-j\omega\tau}\,dt$$

$$(A-12)$$

$$\sigma^2(\omega) = \mathscr{F}[R_n(\tau)]$$

and

$$S_I(\omega, \phi_1, \phi_2) = \mathscr{F}[R_I(\tau, \phi_1, \phi_2)] \qquad (A-13)$$

is the spatial cross-covariance function of the source at frequency ω.

Similarly, it can be seen that

$$r_1(p, \tau) = E[e_d(t)e_p(t - \tau)] \qquad p = 0, 1, \ldots K-1$$

$$= \int_\pi^\pi \int_\pi^\pi R_I[\tau - \frac{d}{c}(J\cos\phi_1 - p\cos\phi_2)]d\phi_1 d\phi_2 \qquad (A-14)$$

$$s_1(p, \omega) = \mathscr{F}[r_1(p, \tau)]$$

$$= \int_{-\pi}^\pi \int_{-\pi}^\pi S_I(\phi_1, \phi_2, \omega)e^{-j\frac{\omega d}{c}[J\cos\phi_1 - p\cos\phi_2]}d\phi_1 d\phi_2 \qquad (A-15)$$

and

$$r_{11}(\tau) = E[e_d(t) e_d(t - \tau)]$$

$$= R_d(\tau) + \int_{-\pi}^\pi \int_{-\pi}^\pi R_I(\phi_1, \phi_2, \tau)d\phi_1 d\phi_2 \qquad (A-16)$$

$$S_{11}(\omega) = \mathscr{F}[r_{11}(\tau)]$$

$$\qquad (A-17)$$

$$= \sigma_d^2(\omega) + \int_{-\pi}^\pi \int_{-\pi}^\pi S_I(\phi_1, \phi_2, \omega) e^{-j\frac{\omega d}{c} J[\cos\phi_1 - \cos\phi_2]}d\phi_1 d\phi_2$$

where

$$\sigma_d^2(\omega) = \mathscr{F}[R_d(\tau)] \qquad (A-18)$$

Now, let $\underline{e}(t)$ be a random vector of the reference hydrophone outputs,

$$\underline{e}(t) = [e_0(t), e_1(t), \ldots e_{K-1}(t)]^T \qquad (A-19)$$

The cross-spectral density (CSD) matrix of the reference hydrophone outputs is

$$S_e(\omega) = \mathscr{F} \left| E[\underline{e}(t)\underline{e}^+(t)] \right|$$ (A-20)

$$= \left(s_e(p, q, \omega) \right) \quad \begin{array}{l} p = 0, 1, \ldots k\text{-}1 \\ q = 0, 1, \ldots k\text{-}1 \end{array}$$

The CSD vector between the reference hydrophone outputs and the primary hydrophone output is

$$\underline{s}_1(\omega) = \mathscr{F} \left| E[e_d(t)\underline{e}(t)] \right|$$

$$= [s_1(o, \omega), s_1(1, \omega), \ldots s_1(K\text{-}1, \omega)]^T$$ (A-21)

The power spectral density of the primary hydrophone output is then $S_{11}(\omega)$.

It will sometimes be convenient to explicitly represent the number of references, K, in the notation for the reference hydrophone CSD matrix and the CSD vector between references and primary. In these cases, $S_e(K, \omega)$ will be the reference hydrophone CSD with K references.

$$S_e(K, \omega) = S_e(\omega) \big|_{K \text{ references}}$$ (A-22)

and $\underline{s}_1(K, \omega)$ will be the CSD vector with K references

$$\underline{s}_1(K, \omega) = \underline{s}_1(\omega) \big|_{k \text{ references}}$$ (A-23)

A.1 Narrow Source Approximation

When the extended source is the surface reverberation from the convergence zone, the extent of the source will be much less than 2π radians. Suppose that the source is centered on an angle, ϕ_0, and is limited to the sector $[\phi_0 - \Phi, \phi_0 + \Phi]$, so

$$S_1(\omega, \phi_1, \phi_2) = 0 \qquad \begin{cases} \phi_1 \notin [\phi_0 - \Phi, \phi_0 + \Phi] \\[2ex] \phi_2 \notin [\phi_0 - \Phi, \phi_0 + \Phi] \end{cases} \qquad \text{(A-24)}$$

Then (A-11) can be written

$$s_e(p, q, \omega) = \sigma_n^2(\omega)\delta_{pq}$$

$$+ \int_{-\Phi}^{\Phi}\int_{-\Phi}^{\Phi} S_1(\phi_0+\phi_1, \phi_0+\phi_2,\omega)e^{+j\frac{\omega d}{c}\left[p\cos(\phi_0+\phi_1)-q\cos(\phi_0+\phi_2)\right]} d\phi_1 d\phi_2 \qquad \text{(A-25)}$$

If it is assumed that the source is narrow enough that

$$\sin \Phi \approx \Phi$$

and

$$\text{(A-26)}$$

$$\cos \Phi \approx 1$$

then

$$p\cos(\phi_0+\phi_1) - q\cos(\phi_0+\phi_2) \approx (p-q)\cos\phi_0 - (p\phi_1-q\phi_2)\sin\phi_0 \qquad \text{(A-27)}$$

Therefore

$$S_e(p, q, \omega) \approx \delta_n^2(\omega)\,\delta_{pq}$$

$$+ e^{+j\frac{\omega d}{c}(p-q)\cos\phi_0}\int_{-\Phi}^{\Phi}\int_{-\Phi}^{\Phi} S_I(\phi_0 + \phi_1,\ \phi_0 + \phi_2, \omega)\, e^{-j\frac{\omega d}{c}(p\phi_1 - q\phi_2)\sin\phi_0}\,d\phi_1 d\phi_2$$

(A-28)

It can be seen that under this assumption, there is a two-dimensional Fourier transform relationship between the hydrophone CSD and the source angular distribution. Similarly

$$s_1(p,\omega) \approx e^{-j\frac{\omega d}{c}(J-p)\cos\phi_0}\int_{-\Phi}^{\Phi}\int_{-\Phi}^{\Phi} S_I(\phi_0+\phi_1,\phi_0+\phi_2,\omega)\, e^{+j\frac{\omega d}{c}(J\phi_1 - p\phi_2)\sin\phi_0}\,d\phi_1 d\phi_2$$

(A-29)

and

$$S_{11}(\omega) \approx \sigma_d^2(\omega) + \int_{-\Phi}^{\Phi}\int_{-\Phi}^{\Phi} S_I(\phi_0 + \phi_1,\ \phi_0 + \phi_2,\ \omega)\, e^{j\frac{\omega d}{c}J(\phi_1 - \phi_2)\sin\phi_0}\,d\phi_1 d\phi_2$$

(A-30)

Using the notation given in (A-20) and (A-21), these expressions yield the following

$$S_e(\omega) = \sigma_n^2(\omega)\,I + G^+(\omega)\,S_{eo}(\omega)\,G(\omega)$$

(A-31)

where

$$S_{eo}(\omega) = \left(\int_{-\Phi}^{\Phi}\int_{-\Phi}^{\Phi} S_I(\phi_0+\phi_1,\phi_0+\phi_2,\omega)\, e^{+j\frac{\omega d}{c}(p\phi_1 - q\phi_2)\sin\phi_0}\,d\phi_1 d\phi_2\right)_{\substack{p = 0,\ 1,\ \ldots\ K-1 \\ q = 0,\ 1,\ \ldots\ K-1}}$$

(A-32)

and

$$G = \operatorname*{diag}_{p} \left(e^{-j\frac{\omega d}{c} p\cos\phi_0} \right) \tag{A-33}$$

Also

$$\underline{s}_1(\omega) = G e^{+ -j\frac{\omega d}{c} J\cos\phi_0} \underline{s}_0 \tag{A-34}$$

where the $p\underline{\text{th}}$ element of $\underline{s}_0$ is

$$s_0(p,\omega) = \int\!\!\int_{-\Phi -\Phi}^{\Phi\ \Phi} S_I(\phi_0+\phi_1, \phi_0+\phi_2, \omega) e^{j\frac{\omega d}{c}(J\phi_1 - p\phi_2)\sin\phi_0} d\phi_1 d\phi_2 \tag{A-35}$$

A.2 Spatially Uncorrelated, Narrow Source

It will be shown in Appendix B that for reverberation from the convergence zone, the extended source may be assumed to be spatially uncorrelated, that is,

$$S_I(\omega, \phi_1, \phi_2) = S_I(\phi_1, \omega)\, \delta(\phi_1 - \phi_2) \tag{A-36}$$

where $\delta(\phi)$ is the Dirac delta function. Under these assumptions, (A-28), (A-29), and (A-30) reduce to

$$s_e(p, q, \omega) = \sigma_n^2(\omega)\delta_{pq} + e^{-j\frac{\omega d}{c}(p-q)\cos\phi_0} \int_{-\Phi}^{\Phi} S_I(\phi_0+\phi, \omega) e^{+j\frac{\omega d}{c}(p-q)\phi\sin\phi_0} d\phi \tag{A-37}$$

$$s_1(p,\omega) = e^{-j\frac{\omega d}{c}(J-p)\cos\phi_0} \int_{-\Phi}^{\Phi} S_I(\phi_0+\phi, \omega) e^{+j\frac{\omega d}{c}(J-p)\phi\sin\phi_0} d\phi \tag{A-38}$$

and

$$S_{11}(\omega) = \sigma_d^2(\omega) + \int_{-\Phi}^{\Phi} S_I(\phi_0 +\phi, \omega) d\phi \tag{A-39}$$

For the spatially uncorrelated source, there is a simple Fourier transform relationship between the source distribution function, $S_I(\omega,\phi)$ and the CSD of the hydrophones.

Of particular interest will be the case when the source is not only narrow and spatially uncorrelated, but uniformly distributed on the sector $(\phi_0 - \Phi, \phi_0 + \Phi,)$

$$S_I(\omega, \phi) = \begin{cases} \sigma_I^2(\omega), & \phi \, \varepsilon \left[\phi_0 - \Phi, \phi_0 + \Phi\right] \\ 0, & \text{elsewhere} \end{cases} \tag{A-40}$$

Under these conditions, the integrals in (A-37), (A-38), and (A-39) can be evaluated, giving

$$s_e(p, q, \omega) = \sigma_n^2(\omega)\delta_{pq}$$

$$+ \sigma^2(\omega) \frac{\sin\left[(p-q)\frac{\omega d}{c}\Phi\sin\phi_0\right]}{\frac{1}{2}\left[(p-q)\frac{\omega d}{c}\sin\phi_0\right]} e^{j\frac{\omega d}{c}(p-q)\cos\phi_0} \tag{A-41}$$

$$s_0(p, \omega) = \sigma_I^2(\omega) \frac{\sin\left[(J-p)\frac{\omega d}{c}\Phi\sin\phi_0\right]}{\frac{1}{2}\left[(J-p)\frac{\omega d}{c}\sin\phi_0\right]} e^{-j\frac{\omega d}{c}(J-p)\cos\phi_0} \tag{A-42}$$

and

$$S_{11}(\omega) = \sigma_n^2(\omega) + 2\Phi\sigma_I^2(\omega) \tag{A-43}$$

Therefore, in the notation of (A-33) and (A-35),

$$S_{eo}(\omega) = \left(\sigma_I^2(\omega) \frac{\sin (p-q)\frac{\omega d}{c}\Phi\sin\phi_0}{\frac{1}{2}\left[(p-q)\frac{d}{c}\sin\phi_0\right]}\right)_{\substack{p = 0, 1, \ldots K-1 \\ q = 0, 1, \ldots K-1}} \tag{A-44}$$

A-10

and

$$s_0(p, \omega) = \sigma_I^2(\omega) \frac{\sin\left[(J-p)\frac{\omega d}{c}\Phi\sin\phi_0\right]}{\frac{1}{2}\left[(J-p)\frac{\omega d}{c}\sin\phi_0\right]}$$
(A-45)

APPENDIX B: APPLICATION OF THE FAR FIELD MODEL TO THE
SURFACE REVERBERATION FROM THE CONVERGENCE ZONE

APPENDIX B; APPLICATION OF THE FAR FIELD MODEL TO THE

SURFACE REVERBERATION FROM THE CONVERGENCE ZONE

B.1 Surface model with straight line propagation. Consider the geometry

shown in Figure B-1, in which the noise enamates from a sector of an annulus

on the ocean surface. The annulus is centered at the origin of the cylindrical

coordinate system, and has inside and outside radii R_I and R_o, respectively.

The sector is assumed to be of angular width $2\theta_1$ centered about an angle θ_o.

A hydrophone is located D feet below the origin and a second hydrophone d

feet away along the negative y axis, as shown. This can be viewed as a

model of the convergence zone surface reverberation, except that the propa-

gation paths are direct rather than along the usual refracted paths associated

with the convergence zone. In the following results, it will be shown that the

propagation paths from the source to the array do not affect the hydrophone

CSD under the plane wave and narrow source assumptions if the source is

spatially uncorrelated. The assumption is that the reverberating surface is

uncorrelated from point to point is commonly made (see, for example, Van

Trees[10]). The hydrophone below the origin represents the transmit/receive

array of the active sonar, and the other hydrophone is the reference. The

reverberation is limited to the angular sector, $\theta_o - \theta_1$ to $\theta_o + \theta_1$, by the

horizontal directivity of the transmitter.
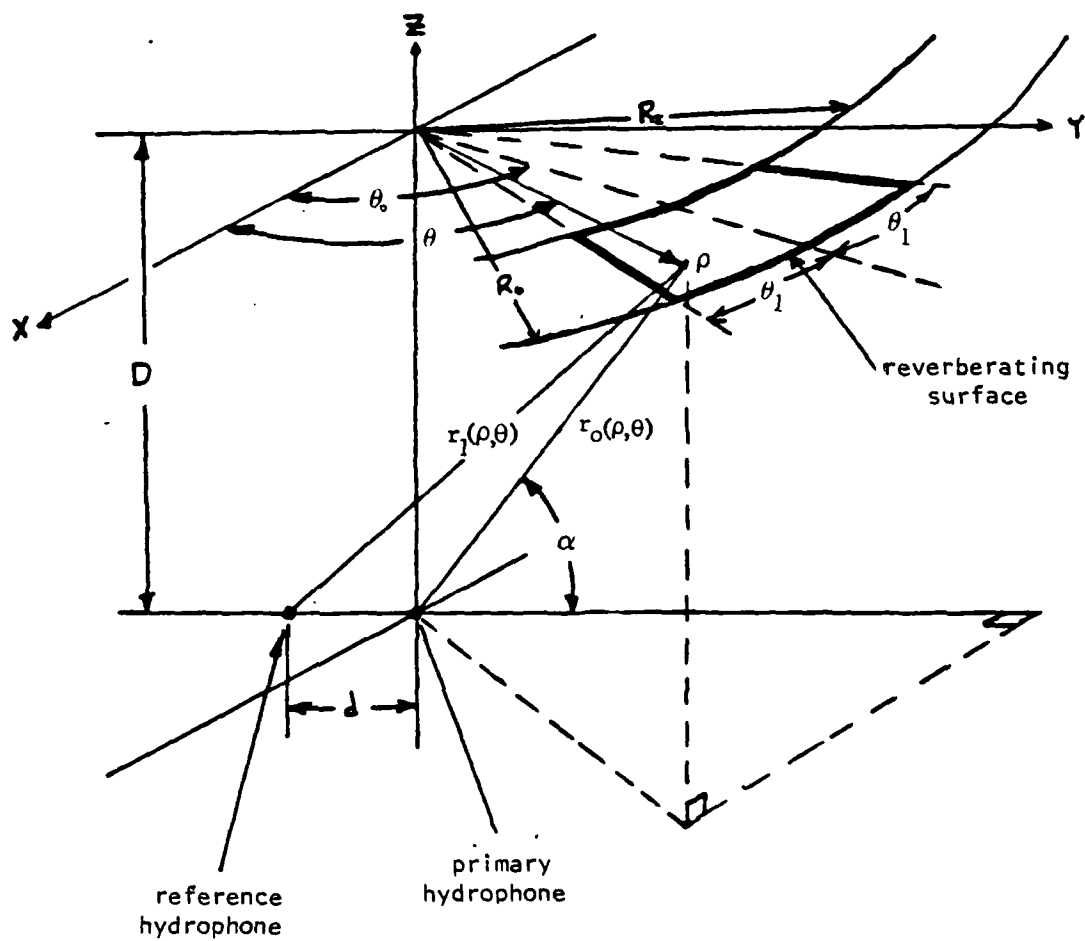
Figure B-1. Geometry for Surface Model with Straight Line Propagation

If the ambient noise is uncorrelated between the two hydrophones spaced d feet apart, the CSD of their outputs can be written as

$$s_e(d,\omega) = \sigma_n^2(\omega) \, \delta(d)$$

$$+ \int_{\theta_0 - \theta_1}^{\theta_0 + \theta_1} \int_{R_I}^{R_0} \int_{\theta_0 - \theta_1}^{\theta_0 + \theta_1} \int_{R_I}^{R_0} S_I(\rho_1, \rho_2, \theta_1, \theta_2, \omega) \qquad \text{(B-1)}$$

$$\cdot e^{+j \frac{\omega}{c} [r_0(\rho_1, \theta_1) - r_1(\rho_2, \theta_2)]} \rho_1 \rho_2 d\rho_2 d\theta_2 d\rho_1 d\theta_1$$

where

$$\sigma_n^2(\omega) = \textit{power spectral density of ambient noise}$$

$$S_I(\rho_1, \rho_2, \theta_1, \theta_2, \omega) = \textbf{CSD of noise radiated at } (\rho_1, \theta_1) \textbf{ and } (\rho_2, \theta_2)$$

$$r_0(\rho, \theta) = \textbf{range from point at } (\rho, \theta) \textbf{ to hydrophone zero}$$

$$r_1(\rho, \theta) = \textbf{range from point at } (\rho, \theta) \textbf{ to hydrophone one}$$

$$c = \textbf{speed of sound}$$

This result is just a straightforward extension of the model developed in Appendix A.

It is assumed that the source is spatially uncorrelated, i.e.,

$$S_I (\rho_1, \rho_2, \theta_1, \theta_2, \omega) = S_I (\rho_1, \theta_1, \omega) \delta (\rho_1 - \rho_2) \delta (\theta_1 - \theta_2) \qquad \text{(B-2)}$$

Then (B-1) reduces to

$$s_e(d, \omega) = \sigma_n^2(\omega) \delta (d)$$

$$+ \int_{\theta_0 - \theta_1}^{\theta_0 + \theta_1} \int_{R_1}^{R_0} S_I(\rho, \theta, \omega) e^{+j \frac{\omega}{c} [r_0(\rho, \theta) - r_1(\rho, \theta)]} \rho^2 d\rho d\theta \qquad \text{(B-3)}$$

Now, as in Appendix A, assume that the wavefront from each point on the annulus arrives at the hydrophones as a plane, and that the propagation distance can be approximated as the sum of the range from the point to hydrophone zero and the plane wave propagation delay. That is,

$$r_1(\rho, s) \approx r_0 (\rho, s) + d \cos \alpha \qquad \text{(B-4)}$$

where α is the angle the arrival direction makes with the axis of the two hydrophones. It can easily be shown that

$$\cos \alpha = \frac{\rho \cos \theta}{\sqrt{\rho^2 + D^2}} = \frac{1}{\sqrt{1 + \frac{D^2}{\rho^2}}} \cos \theta \qquad \text{(B-5)}$$

It is now assumed that $\rho \gg D$, which is certainly true for the convergence zone problem, so

$$\cos \alpha \approx \cos \theta \qquad \text{(B-6)}$$

and

$$s_e(d,\omega) = \sigma_n^2(\omega)\delta(d) + \int_{\theta_o - \theta_1}^{\theta_o + \theta_1} \int_{R_1}^{R_o} S_I(\rho,\theta,\omega)e^{+j\frac{\omega}{c}d\cos\theta}\rho^2 d\rho d\theta \tag{B-7}$$

or, making the change of variables $\theta' = \theta - \theta_o$,

$$s_e(d,\omega) = \sigma_n^2\delta(d) + \int_{-\theta_1}^{\theta_1} \int_{R_1}^{R_o} S_I(\rho,\theta'+\theta_o,\omega)e^{+j\frac{\omega d}{c}\cos(\theta'+\theta_o)}\rho^2 d\rho d\theta' \tag{B-8}$$

Note that $r_o(\rho,\theta)$, representing the long range propagation from the reverberating surface to the array, is not present in (B-8). Therefore, the use of straight line propagation paths instead of refracted convergence zone paths should have minimum effect upon the results, except as they produce different vertical arrival angles.

It is now assumed that θ_1 is small enough that $\cos\theta_1 \approx 1$, $\sin\theta_1 \approx \theta_1$, so

$$\cos(\theta' + \theta_o) = \cos\theta'\cos\theta_o - \sin\theta'\sin\theta_o \approx \cos\theta_o - \theta'\sin\theta_o \tag{B-9}$$

and

$$s_e(d,\omega) \approx \sigma_n^2(\omega)\delta(d)$$

$$\tag{B-10}$$

$$+ e^{j\frac{\omega d}{c}\cos\theta_o} \int_{-\theta_1}^{\theta_1} \int_{R_1}^{R_o} S_I(\rho,\theta,\omega)e^{-j\frac{\omega d}{c}\theta\sin\theta_o}\rho^2 d\rho d\theta$$

B-5

This has exactly the same form as equation (A-25) of Appendix A, which gave the CSD for a uniformly distributed, uncorrelated source in the far field model.

Next, it is assumed that the source CSD function, $S_I(\rho,\theta,\omega)$, is separable in ρ and θ, that is

$$S_I(\rho,\theta,\omega) = S_{Ir}(\rho,\omega) S_{Ia}(\theta,\omega) \qquad \text{(B-11)}$$

so that

$$s_e(d,\omega) = \sigma_n^{\,2}(\omega)\,\delta(d)$$

$$+ e^{j\frac{\omega d}{c}\cos\theta_o}\left[\int_{R_I}^{R_o} S_{Ir}(\rho,\omega)\rho^2 d\rho\right]\left[\int_{-\theta_1}^{\theta_1} S_{Ia}(\rho,\omega)e^{-j\frac{\omega d}{c}\theta\sin\theta_o}d\theta\right] \qquad \text{(B-12)}$$

Now, if the source CSD is assumed to be uniform in angle,

$$S_{Ia}(\theta,\omega) = \sigma_I^{\,2}(\omega) \qquad \text{(B-13)}$$

then

$$s_e(d,\omega) = \sigma_n^{\,2}(\omega)\,\delta(d)$$

$$\text{(B-14)}$$

$$+ \sigma_I^{\,2}(\omega)\,G_r(\omega)\,\frac{\sin\left[2\pi\theta_1\frac{d}{\lambda}\sin\theta_o\right]}{\pi\frac{d}{\lambda}\sin\theta_o}\,e^{j\frac{\omega d}{c}\cos\theta_o}$$

where

$$G_r(\omega) = \int_{R_I}^{R_o} S_{Ir}(\rho,\omega) \, \rho^2 dp \qquad (B-15)$$

If the pair of hydrophones on the x-axis is replaced by a line array of uniform spacing, d, then the CSD between the outputs of the pth and q^{th} hydrophones is

$$s_e(p,q,\omega) = \sigma_n^2(\omega) \, \delta_{pq} \qquad (B-16)$$

$$+ \, \sigma_I^2(\omega) \, G_r(\omega) \, \frac{\sin[\,2\pi\theta_1(p-q)\frac{d}{\lambda}\sin\theta_o\,]}{\pi\frac{d}{\lambda}\sin\theta_o} \, e^{\, j\frac{\omega d}{c}(p-q)\cos\theta_o}$$

where δ_{pq} is the Kronecker delta. Note that the plane wave assumption must be valid over the entire length of the array.

This has exactly the same form as (A-41), so that the far field model can be applied to this surface source under the above assumptions.

B.2 <u>Vertical arrival model</u>. Consider the spherical coordinate system shown in Figure B-2. As before the noise field is assumed to consist of spatially uncorrelated hydrophone noise plus an extended source. Here, the extended source is assumed to be distributed over a horizontal sector, $\theta_o - \theta_1 < \theta < \theta_o + \theta_1$ and a vertical angle, $\phi_o - \phi < \phi < \phi_o + \phi$, and

$$S_I(\theta_1,\theta_2,\phi_1,\phi_2,\omega) = \text{CSD between arrivals from angles } (\theta_1,\phi_1) \text{ and } (\theta_2,\phi_2)$$

$$r_i(\theta,\phi) = \text{propagation distance from source arriving at } (\theta,\phi) \text{ to}$$

$$\text{hydrophone i } (i = 0,1)$$
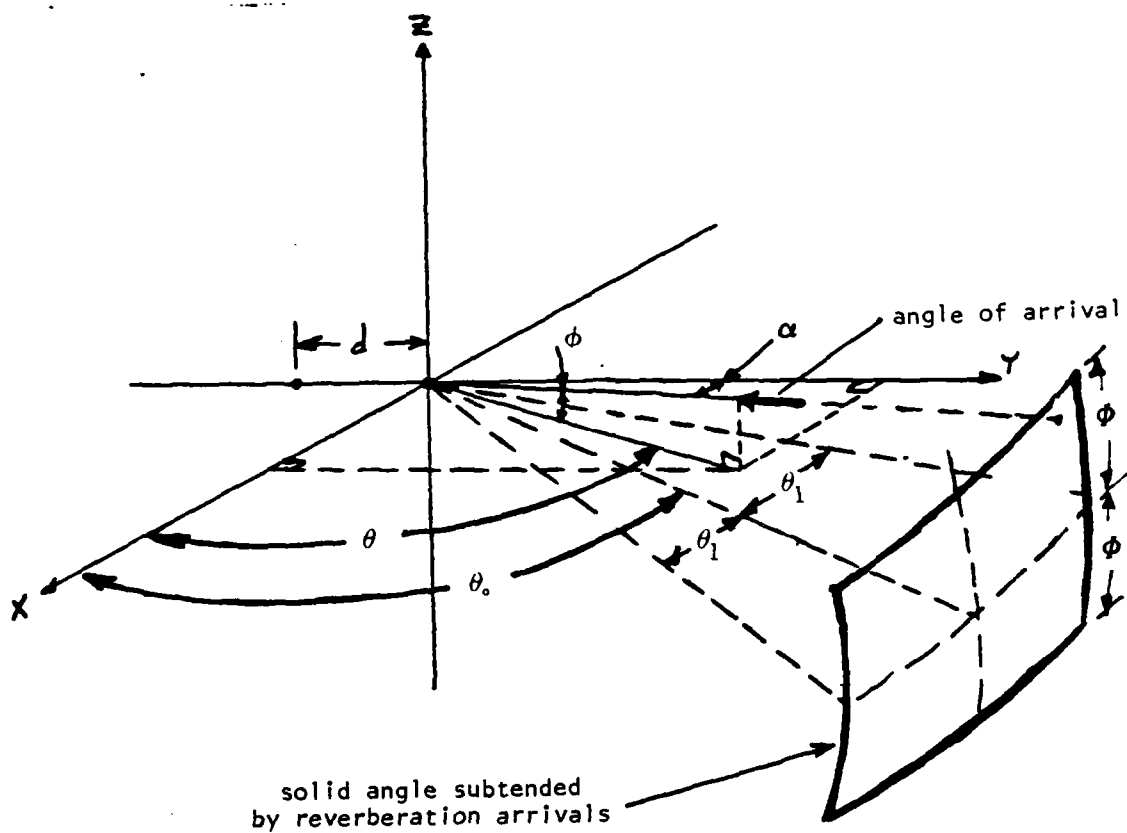
Figure B-2. Geometry for Vertical Arrival Model

It is assumed that the source is spatially uncorrelated,

$$S_I(\theta_1,\theta_2,\phi_1,\phi_2,\omega) = S_I(\theta_1,\phi_1,\omega) \; \delta \; (\theta_1-\theta_2) \; \delta \; (\phi_1-\phi_2) \qquad \text{(B-17)}$$

so that the CSD of the two hydrophone outputs is

$$s_e(d,\omega) = \sigma_n^{\;2} \; \delta \; (d)$$

$$\qquad\qquad\qquad\qquad\qquad\qquad\qquad\qquad\qquad\qquad\qquad\qquad\qquad \text{(B-18)}$$

$$+ \int_{\theta_o-\theta_1}^{\theta_o+\theta_1} \int_{\phi_o-\phi}^{\phi_o+\phi} S_I(\theta,\phi,\omega) \; e^{\;j\frac{\omega}{c}[r_o(\theta,\phi)-r_1(\theta,\phi)]} \sin^2\phi \, d\phi \, d\theta$$

As in case B.1 above, it is assumed that the wavefront from each point on the source is planar, and that

$$r_1(\theta,\phi) = r_o(\theta,\phi) + d \cos \alpha \qquad\qquad\qquad\qquad \text{(B-19)}$$

In this case, however,

$$\cos \alpha = \cos \theta \cos \phi \qquad\qquad\qquad\qquad\qquad\qquad \text{(B-20)}$$

so

$$s_e(d,\omega) = \sigma_n^{\;2}(\omega) \; \delta \; (d)$$

$$+ \int_{\theta_o-\theta_1}^{\theta_o+\theta_1} \int_{\phi_o-\phi}^{\phi_o+\phi} S_I(\theta,\phi,\omega) e^{\;j\frac{\omega d}{c} \cos \theta \cos \phi} \sin^2\phi \, d\phi \, d\theta \qquad \text{(B-21)}$$

Note that the kernel, $\exp\left[-j\frac{\omega d}{c}\cos\theta\cos\phi\right]$ depends upon both variables of integration and is not separable. Because of this, reduction of (B-21) to a line source requires that either $\cos\theta\approx 1$ or $\cos\phi = 1$. This means that $\max\left[\theta_0-\theta,\theta_0+\theta\right]$ or $\max\left[\phi_0-\phi,\phi_0+\phi\right]$, respectively, be small, which is a much stronger condition than in case B.1, which only required that ϕ be small.

It will be assumed that the vertical arrival angles, $\phi\in\left[\phi_0-\phi,\phi_0+\phi\right]$, are close enough to the horizontal that $\cos\phi\approx 1$ and $\sin\phi\approx\phi$, which means that the arrivals must be within approximately $\pm 10°$ of the horizontal. This is consistent with the arrival angles associated with the convergence zone in surface ship hull mounted sonars. Under this assumption

$$s_e(d,\omega)\approx\sigma_n^{\,2}(\omega)\,\delta(d) \tag{B-22}$$

$$+\int_{\theta_0-\theta_1}^{\theta_0+\theta_1}\int_{\phi_0-\phi}^{\phi_0+\phi} S_I(\theta,\phi,\omega)e^{\,j\frac{\omega d}{c}\cos\theta}\phi^2\,d\phi\,d\theta$$

$$=\sigma_n^{\,2}(\omega)\delta(d) \tag{B-23}$$

$$+\int_{-\theta_1}^{\theta_1}\int_{\phi_0-\phi}^{\phi_0+\phi} S_I(\theta+\theta_0,\phi+\phi_0,\omega)\,e^{\,j\frac{\omega d}{c}\cos(\theta+\theta_0)}\phi^2\,d\phi\,d\theta$$

Proceeding as in Case B.1, assume that θ_1 is small, so

$$\cos(\theta+\theta_0)\approx\cos\theta_0-\theta\sin\theta_0 \tag{B-24}$$

and assume that $S_I(\theta, \phi, \omega)$ is separable,

$$S_I(\theta, \phi, \omega) = S_{Ih}(\theta, \omega) \, S_{Iv}(\phi, \omega) \tag{B-25}$$

so

$$s_e(d, \omega) \approx \sigma_n^2(\omega) \, \delta(d)$$

$$+ \left[\int_{\phi_o - \phi}^{\phi_o + \phi} S_{Iv}(\phi, \omega) \phi^2 d\phi \right] \tag{B-26}$$

$$\left[e^{\, j \frac{\omega d}{c} \cos \theta_o} \int_{-\theta_1}^{\theta_1} S_{Ih}(\theta, \omega) \, e^{-j \frac{\omega d}{c} \theta \sin \theta_o} d\theta_o \right]$$

When the source CDS is assumed uniform in θ, this gives

$$s_e(d, \omega) \approx \sigma_n^2(\omega) \, \delta(d) \tag{B-27}$$

$$+ \sigma_I^2(\omega) \, G_\phi(\omega) \, \frac{\sin \left[2\pi \theta_1 \frac{d}{\lambda} \sin \theta_o \right]}{\pi \frac{d}{\lambda} \sin \theta_o} e^{\, j \frac{\omega d}{c} \cos \theta_o}$$

where

$$G_\phi(\omega) = \int_{\phi_o - \phi}^{\phi_o + \phi} S_I(\phi, \omega) \, \phi^2 \, d\phi \tag{B-28}$$

This has exactly the same form as (A-41) and as the CSD of the far field model with a uniform, uncorrelated source. As before, for a uniformly spaced line array along the y axis with element spacing d, the CSD between the outputs of the pth and q^{th} hydrophones is

$$s_e(p,q,\omega) \approx \sigma_n^{\,2}(\omega)\, \delta_{pq}$$

(B-29)

$$+\sigma_{I(\omega)}^{\,2} G_\phi(\omega)\, \frac{\sin\left[2\pi(p-q)\theta_1 \frac{d}{\lambda}\sin\theta_o\right]}{\pi(p-q)\,\frac{d}{\lambda}\sin\theta_o}\, e^{\;j\frac{\omega d}{c}(p-q)\cos\theta_o}$$

B.3 <u>Summary</u>. Two source models that can be used as approximate representations of surface reverberation from the convergence zone have been developed. Under very reasonable assumptions, it has been shown that these models produce a hydrophone output CSD of the same form as an uncorrelated source, which was considered in   The assumptions needed for use of the model are

(a) The wavefront emanating from each point on the reverberating surface can be regarded as planar across the array.

(b) The reverberation is confined to an azimuth angular sector of width $2\theta_1$, with θ_1 small enough that $\sin\theta_1 \approx \theta_1$ and $\cos\theta_1 \approx 1$. The transmitting sonar must therefore provide sufficient directivity to justify this assumption if the model is to be valid.

(c) The reverberation at each point on the surface is uncorrelated with that at any other.

(d) The spectral density of the reverberation over the two

dimensions is separable.

(e) The spectral density of the reverberation is uniform in azimuth.

In addition, the vertical arrival angle model requires that

(f) The vertical arrival angles be concentrated in a narrow sector

about the horizontal, say $-\Phi \leq \phi \leq \Phi$, such that $\sin \phi \approx \phi$,

$\cos \phi \approx 1$.

Under these assumptions, the results for an uncorrelated line source

can be directly applied to the study of the cancellation of convergence zone

surface reverberation. These results also suggest that the line source

model can be used to approximate other two dimensional sources of narrow

angular extent.

APPENDIX C: DERIVATION OF THE OPTIMAL CANCELLER
AND CANCELLER OUTPUT SPECTRUM

APPENDIX C; DERIVATION OF THE OPTIMAL CANCELLER AND CANCELLER OUTPUT SPECTRUM

Consider the multiple reference canceller configuration shown in Figure C-1, in which the output of K reference hydrophones, denoted $e_i(t)$ with $i = 0,1 \ldots K-1$ are to be used to cancel an interference from the output of a primary hydrophone, $e_d(t)$. In keeping with the discussion of Appendix A, the hydrophones outputs are assumed to be zero mean random processes, that are at least wide sense stationary. That is,

$$E[e_p(t) \, e_q(t+\tau)] = r(p,q,\tau) \qquad \begin{array}{l} p = 0,1,\ldots K-1 \\ q = 0,1,\ldots K-1 \end{array}$$

where $E[\cdot]$ denotes expectation. The filters are linear and time invariant with impulse responses $h_i(t)$ for $i=0,\ldots K-1$. The impulse responses are to be chosen to minimize the mean square value of the error output, $E[\varepsilon^2(t)]$. The derivation here closely follows that of reference [14]

From Figure C-1, it can be seen that

$$\varepsilon(t) = e_d(t) - \sum_{k=0}^{K-1} \int_{-\infty}^{\infty} h_k(\tau) \, e_k(t-\tau) \, d\tau \qquad (C-1)$$
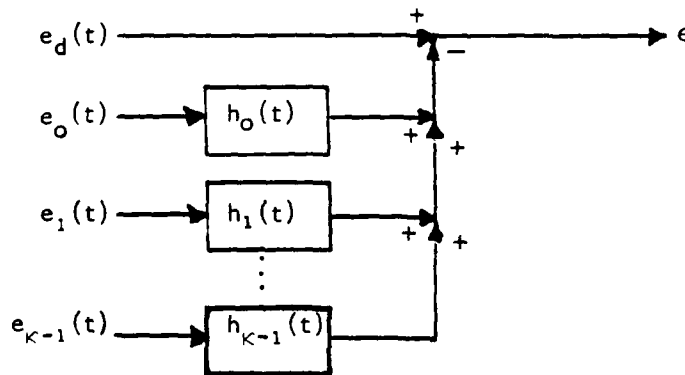
Figure C-1. Multiple Reference Canceller

so that

$$E[\varepsilon^2(t)] = r_{11}(0) - 2 \sum_{k=0}^{K-1} \int_{-\infty}^{\infty} h_k(\tau)\, r_1(k,\ \tau)\, d\tau$$

$$\text{(C-2)}$$

$$+ \sum_{K_1=0}^{K-1} \sum_{k_2=0}^{K-1} \int_{-\infty}^{\infty} \int_{-\infty}^{\infty} h_{k_1}(\tau)\, h_{k_2}(\rho)\, r_e(k_1, k_2, \tau-\rho)\, d\tau d\rho$$

with $r_e(p,q,\tau)$ the cross-correlation between $e_p(t)$ and $e_q(t)$, $r_1(p,\tau)$ the cross-correlation between $e_p(t)$ and $e_d(t)$, and $r_{11}(\tau)$ the covariance of $e_d(t)$.

Let the optimal impulse responses be denoted $h_k^o(t)$ for $i = 0, 1, \ldots K-1$, and let

$$h_k(t) = h_k^o(t) + \gamma_k\, \delta h_k(t) \qquad \text{(C-3)}$$

where $\delta h_k(t)$ is an arbitrary variation about $h_k^o(t)$ and γ_k a real constant. Substituting (C-3) in (C-2) gives the mean square error as

$$E[\varepsilon^2(t)] = J_o + 2 \sum_{k_1=0}^{K-1} \gamma_{k_1} \left[\sum_{k_2=0}^{K-1} \iint \delta h_k(\tau)\, h_{k_2}^o(\rho)\, r_1(k, \tau-\rho)\, d\tau d\rho \right.$$

$$\left. - \int \delta h_{k_1}(\tau)\, r_e(k_1, k_2, \tau)\, d\tau \right] - \sum_{k_1=0}^{K-1} \sum_{k_2=0}^{K-1} \gamma_{k_1} \gamma_{k_2}$$

$$\iint \delta h_{k_1}(\tau)\, \delta h_{k_2}(\rho)\, r_e(k_1, k_2, \tau-\rho)\, d\tau d\rho \qquad \text{(C-4)}$$

where

$$J_o = r_{11}(0) - 2 \sum_{k_1=0}^{K-1} \int h_{k_1}^o(\tau) \, r_1(k_1,\tau) \, d\tau$$

$$+ \sum_{k_1=0}^{K-1} \sum_{k_2=0}^{K-1} \iint h_{k_1}^o(\tau) \, h_{k_2}^o(\rho) \, r_e(k_1,k_2,\tau-\rho) \, d\tau d\rho \qquad \text{(C-5)}$$

is just the minimum mean square error. All integrals have upper and lower limits of ∞ and $-\infty$, respectively.

If a minimum exists, it will occur when

$$h_k(t) = h_k^o(t), \; k = 0, 1, \ldots K-1 \qquad \text{(C-6)}$$

A necessary condition for this minimum to occur is that

$$\frac{\partial}{\partial \gamma_k} \, E[\epsilon^2(t)] \Bigg|_{\substack{\gamma_0 = 0 \\ \vdots \\ \gamma_{K-1} = 0}} = 0, \; k = 0, 1, \ldots K-1 \qquad \text{(C-7)}$$

Using (3-4),

$$\frac{\partial}{\partial \gamma_n} E[\epsilon^2(t)] \Bigg|_{\substack{\gamma_0 = 0 \\ \vdots \\ \gamma_{K-1} = 0}} = 2\left[\sum_{i=0}^{K-1} \iint \delta h_n(\tau) \, h_i^o(\rho) \, r_e(n,i,\tau-\rho) \, d\tau d\rho \right.$$

$$\left. - \int \delta h_n(\tau) \, r_1(n,\tau) \, d\tau \right] \qquad \text{(C-8)}$$

For this to equal zero for arbitrary variation of $\delta h_n(t)$,

$$r_1(n,\tau) = \sum_{k=0}^{K-1} \int h_k^o(\rho) \, r_e(n,k,\tau-\rho) \, d\rho \qquad \text{(C-9)}$$

This must be satisfied for $n = 0, 1, \ldots K-1$. Recall from Section 2.1 that

$$S_{11}(\omega) = \mathscr{F}[r_{11}(\tau)]$$

$$s_1(p,\omega) = \mathscr{F}[r_1(p,\tau)]$$

$$S_e(p,q,\omega) = \mathscr{F}[r_e(p,q,\tau)]$$

where $\mathscr{F}[\cdot]$ denotes the Fourier transform with respect to τ, given by (A-12). Then taking the Fourier transform of (C-9) gives

$$s_1(n,\omega) = \sum_{k=0}^{K-1} H_k^o(\omega) \, S_e(n,k,\omega) \quad n = 0, 1, \ldots, K-1 \qquad \text{(C-10)}$$

where $H_k^o(\omega)$ is the transfer function of the kth optimal filter. Now, as in Appendix A, let

$$\underline{s}_1(\omega) = \left[s_1(0,\omega), \ s_1(1,\omega), \ \ldots \ s_1(K-1,\omega) \right]^T \qquad \text{(C-11)}$$

and

$$S_e(\omega) = (s_e(p,q,\omega)) \atop {p=0,1,\ldots K-1 \atop q=0,1,\ldots K-1} \qquad \text{(C-12)}$$

Then (C-10) can be written as

$$\underline{s}_1(\omega) = S_e(\omega) \ \underline{H}^o(\omega) \qquad \text{(C-13)}$$

where $\underline{H}^o(\omega)$ is a vector of the optimal transfer functions,

$$\underline{H}^o(\omega) = \left[H_0^o(\omega), \ H_1^o(\omega), \ \ldots, \ H_{K-1}^o(\omega) \right]^T \qquad \text{(C-14)}$$

Therefore,

$$\underline{H}^o(\omega) = S_e^{-1}(\omega) \ \underline{s}_1(\omega) \qquad \text{(C-15)}$$

Fourier transforming (C-3) to yield the spectrum of the irreducible error, termed the irreducible canceller output spectrum here, gives

$$E_k(\omega) = S_{11}(\omega) - 2 \sum_{k=0}^{K-1} H_k^{o*}(\omega) S_1(k,\omega)$$

$$+ \sum_{k_1=0}^{K-} \sum_{k_2=0}^{K-1} H_{k_1}^o(\omega) H_{k_2}^{o*}(\omega) s_e(k_1,k_2,\omega)$$

$$= S_{11}(\omega) - 2\underline{H}^{o*}(\omega) \underline{s}_1(\omega) + \underline{H}^{o*}(\omega) S_e(\omega) \underline{H}^{o*}(\omega) \qquad \text{(C-16)}$$

Substituting the optimal response from (C-13) gives the canceller output spectrum as

$$E_K(\omega) = S_{11}(\omega) - \underline{s}_1^+(\omega) S_e^{-1}(\omega) \underline{s}_1(\omega) \qquad \text{(C-17)}$$

Here, the subscript K in $E_K(\omega)$ indicates that K references have been used in the canceller.

It will be useful to express $E_K(\omega)$ as the ratio of determinants,

$$E_K(\omega) = \frac{\det[S_H(\omega)]}{\det[S_e(\omega)]} \qquad \text{(C-18)}$$

where $S_H(\omega)$ is a (K+1) x (K+1) matrix defined as

$$S_H(\omega) = \begin{bmatrix} S_e(\omega) & \underline{s}_1(\omega) \\ \underline{s}_1^+(\omega) & S_{11}(\omega) \end{bmatrix} \qquad \text{(C-19)}$$

This is easily shown using the following matrix identity.

Theorem: Determinant of a Bordered Matrix

Let the $(N+1) \times (N+1)$ square matrix, B, be defined as

$$B = \begin{bmatrix} A & \underline{x} \\ \underline{y}^+ & c \end{bmatrix} \tag{C-20}$$

where A is an arbitrary $N \times N$ matrix $\underline{x}$ is a N-dimensional column vector, $\underline{y}^+$ an N-dimensional row vector, and c a scalar. Then

$$\det[B] = c(\det[A]) - \underline{y}^+(\text{adj}[A]) \underline{x} \tag{C-21}$$

where $\det[\,\cdot\,]$ and $\text{adj}[\,\cdot\,]$ are the matrix determinant and adjoint, respectively.

Proof: Let

$$\underline{x} = \begin{bmatrix} x_1 \\ \vdots \\ x_n \end{bmatrix} \qquad \underline{y}^+ = [y_1^* \ \ldots \ y_n^*]$$

Using the Laplace expansion formula with the elements of the $N+1$ column of B as coefficients gives

$$\det[B] = \sum_{i=1}^{N+1} b_{i,N+1} (-1)^{i+N+1} \beta_{i,N+1} \tag{C-22}$$

with $b_{i,N+1}$ the ith element of the $(N+1)^{th}$ column and $\beta_{i,N+1}$ the minor of $b_{i,N+1}$. Note that

$$b_{N+1,N+1} = c \qquad \text{and} \qquad \beta_{N+1,N+1} = (A) \qquad\qquad (C\text{-}23)$$

Further,

$$b_{i,N+1} = X_i, \; 1 \le i \le N \qquad\qquad (C\text{-}24)$$

Now, the minor of $b_{i,N+1}$ for $1 \le i \le N$ is the determinant of the matrix obtained by deleting the i-th row and the $(N+1)^{th}$ column, denoted C_i. That is,

$$C_i = \begin{bmatrix} a_{11} & \cdots & a_{1,N} \\ \vdots & & \vdots \\ a_{i-1,1} & \cdots & a_{i-1,N} \\ a_{i+1,1} & \cdots & a_{i+1,N} \\ \vdots & & \vdots \\ a_{N,1} & \cdots & a_{N,N} \\ y_1^* & \cdots & y_N^* \end{bmatrix} \qquad\qquad (C\text{-}25)$$

where $a_{i,j}$ is the i,j^{th} element of A. To obtain $\beta_{i,N+1}$, reapply the Laplace expansion formula with the y_i^*'s as coefficients

$$\beta_{i,N+1} = \det[C_i] = \sum_j y_j^* (-1)^{j+N+1} \alpha_{i,j} \qquad\qquad (C\text{-}26)$$

with $\alpha_{i,j}$, determinant of the matrix remaining when the Nth row and j^{th} column of C_i are deleted. Inspection of (C-25), however, shows that $\alpha_{i,j}$ is exactly the minor of $a_{i,j}$ in the matrix A.

Therefore,

$$\det[B] = c(\det[A]) \sum_{i=1}^{N} X_i(-1)^{i+N+1} \sum_{j=1}^{N} y_j^*(-1)^{j+N+1} \alpha_{i,j}$$

$$= c(\det[A]) \sum_{i=1}^{N} \sum_{j=1}^{N} y_j^*(-1)^{i+j} \alpha_{i,j} X_i \qquad (C-27)$$

The quantity $(-1)^{i+j} \alpha_{i,j}$ is the cofactor of $a_{i,j}$ in the matrix A, denoted $A_{i,j}$.

Hence

$$\det[B] = c(\det[A]) - \underline{y}^{+} \begin{bmatrix} A_{11} & A_{12} & \cdots & A_{1N} \\ \cdot & \cdot & & \cdot \\ \cdot & \cdot & & \cdot \\ \cdot & \cdot & & \cdot \\ A_{N1} & A_{N2} & \cdots & A_{NN} \end{bmatrix} \underline{X} \qquad (C-28)$$

or

$$\det[B] = c(\det[A]) - \underline{y}^{*} (\mathrm{Adj}[A]) \underline{X} \qquad (C-29)$$

Using this theorem,

$$\det[S_H(\omega)] = S_{11}(\omega) \det[S_e(\omega)] - \underline{s}_1^{*}(\omega) \mathrm{Adj}[S_e(\omega)] \underline{s}_1(\omega) \qquad (C-30)$$

where Adj[A] in the adjoint matrix of A. Clearly then,

$$\frac{\det[S_H(\omega)]}{\det[S_e(\omega)]} = S_{11}(\omega) - \underline{s}_1^{+}(\omega) S_e^{-1}(\omega) \underline{s}_1(\omega) = E_K(\omega) \qquad (C-31)$$

In the special notation of (A-22) and (A-23)

C-9

$$E_K(\omega) = S_{11}(\omega) \underline{s}_1^+(K,\omega+) S_e^{-1}(K,\omega) \, \underline{s}_1(K,\omega) \qquad \text{(C-32)}$$

$$= \frac{\det\{S_H(K,\omega)\}}{\det\{S_e(K,\omega)\}}$$

where

$$S_H(K,\omega) = S_H(\omega)\Big|_{K \text{ references}} \qquad \text{(C-33)}$$

APPENDIX D: THE EQUIVALENCE OF EXTENDED SOURCE
CANCELLATION AND THE LINEAR PREDICTION OF A
BANDLIMITED TEMPORAL SEQUENCE

APPENDIX D: THE EQUIVALENCE OF EXTENDED SOURCE CANCELLATION AND THE LINEAR PREDICTION OF A BANDLIMITED TEMPORAL SEQUENCE

Consider K+1 hydrophones oriented as shown in Figure D-1, and let the output of the pth hydrophone be x_p (t), where the primary hydrophone from which the interference is to be cancelled, takes the $(J+1)^{th}$ position. Let the cross-correlation function between the pth and q^{th} hydrophone outputs be given by

$$R_{pq}(\omega) = E[n_p(t) \, n_q(t+\tau)] \tag{D-1}$$

and let the cross-spectral density between the pth and q^{th} outputs be

$$s_e(p,q,\omega) = \mathscr{F}[R_{pq}(t)] \tag{D-2}$$

where $\mathscr{F}[\cdot]$ denotes the Fourier transform with respect to the variable τ.

Now, denote

$$S_e(\omega) = (s_e(p,q,\omega)) \quad p = 0, \, 1, \ldots K-1$$
$$q = 0, \, 1, \ldots K-1 \tag{D-3}$$

$$\underline{s}_1(\omega) = [s_1(0,\omega), s_1(1,\omega), \ldots, s_1(K-1,\omega)]^T \tag{D-4}$$

It is assumed that the process is spatially as well as temporally stationary, so that

$$s_e(p,p+\Delta,\omega) = s_e(q,q+\Delta,\omega) \tag{D-5}$$
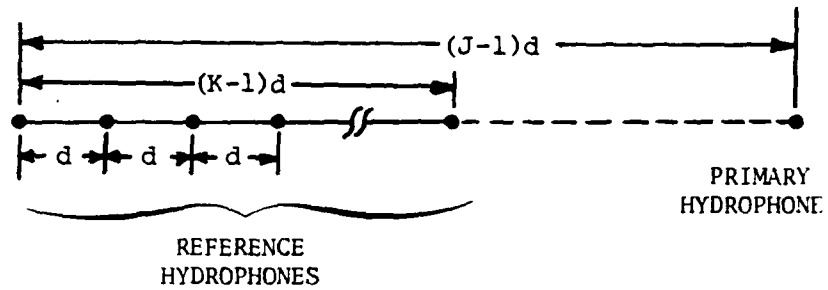
Figure D-1: Hydrophone Geometry for Spatial Cancellation

for any p and q. It is shown in Appendix C that the power spectral density of the canceller output for K references is

$$E_K(\omega) = S_{11}(\omega) - \underline{s}_1^+(\omega)\, S_e^{-1}(\omega)\underline{s}_1(\omega) \qquad\qquad (D-6)$$

Next, consider the temporal problem of predicting a stationary random sequence, m steps ahead. Let a continuous random process, $x(t)$, with correlation function $R_x(\tau)$ be sampled at a uniform rate of $1/T_s$ samples per second, so that the random sequence is $\left\{x(nT_s)\right\}_{n=..,-1,0,1,2,...}$. The correlation between the pth and q^{th} samples will be $R_x[(p-q)T_s]$. Given the finite past $\{x(-KT_s),...,x(-T_s)\}$, the goal is to predict in the minimum mean square error sense the value of the mth element of the sequence, $x(mT_s)$. It can easily be shown that the prediction error is

$$E(m) = R_x(0) - \underline{r}_{dx}\,T\, R_{xx}^{-1}\, \underline{r}_{dx} \qquad\qquad (D-7)$$

where

$$R_{xx} = (R_x[(p-q)T_s]), \quad p = -K,-K+1,...,-1$$
$$q = -K,-K+1,...,-1 \qquad\qquad (D-8)$$

$$= (R_x[(p-q)T_s]), \quad p = 0,1,...K-1$$
$$q = 0,1,...K-1$$

and

$$\underline{r}_{dx} = [R_x(m),\, R_x(m+1),\, ...\, R_x(m+K)]^T \qquad\qquad (D-9)$$

Comparing (D-6) and (D-7), it can be seen that the temporal linear prediction problem is equivalent to the spatial LMS cancellation at a single frequency. The temporal statistics, R_{xx}, $\underline{r}_{dx}$, and $R_x(o)$ correspond to $S_e(\omega)$, $\underline{s}_1(\omega)$, and $S_{11}(\omega)$ in the spatial case. It is convenient to note that in the spatial case, using the notation of Appendix A,

$$\underline{s}_1(p, \omega) = s_e(J-1, p, \omega) \tag{D-10}$$

and

$$S_{11}(\omega) = s_e(p, p, \omega), \text{ any } p \tag{D-11}$$

Therefore,

$$\underline{s}_1(\omega) = [s_e(J-1, 0, \omega), \ s_e(J-1, 1, \omega), \ \ldots, \ s_e(J-1, K-1, \omega)]^T \tag{D-12}$$

This makes the equivalence of $R_x[(p-q)T_s]$ and $S_e(p, q, \omega)$ clear.

The analogy can be extended one step further if the source is assumed to be a narrow plane wave source in the same plane as the array, distributed in angle ϕ, as shown in Figure D-2. Let the arrival from any angle, ϕ_1, be uncorrelated with arrivals for any angle, ϕ_2, if $\phi_1 \neq \phi_2$, and let the source be distributed in angle from $\phi_0 - \Phi$ to $\phi_0 + \Phi$ with angular density $S_I(\omega, \phi)$ in that interval. The source is assumed to be narrow if

$$\sin \Phi \simeq \Phi$$
$$\cos \Phi \simeq 1 \tag{D-10}$$

Also assume that ambient noise with spectral density, $\sigma_n^2(\omega)$ appears at the hydrophone outputs, and is uncorrelated from hydrophone to hydrophone. Then, from Appendix A,

$$s_e(p,q,\omega) \approx \sigma_n^2(\omega)\, \delta_{pq}$$

(D-11)

$$+ e^{-j\frac{\omega d}{c}(p-q)\cos\phi_0} \int_{-\phi}^{\phi} S_I(\phi+\phi_0,\omega) e^{+j\frac{\omega d}{c}(p-q)\phi\sin\phi_0}\, d\phi$$

This discussion will be facilitated by demonstrating that the value of the canceller output spectrum, $E_k(\omega)$, given by (D-6), is not affected by the factor $\exp\left[-j\frac{\omega d}{c}(p-q)\cos\phi_0\right]$ in the second term of (D-11). From equation (C-27)

$$E_K(\omega) = \frac{\det\,[S_H(K,\omega)]}{\det\,[S_e(K,\omega)]}$$

(D-12)

where

$$S_H(K,\omega) = \begin{bmatrix} S_e(K,\omega) & \underline{s}_1(K,\omega) \\ \underline{s}_1^+(K,\omega) & S_{11}(\omega) \end{bmatrix}$$

(D-13)

Given the hydrophone CSD of the form of (D-11), it is possible to write

$$S_H(K,\omega) = G_1^+(K)\, S_{Ho}(K,\omega)\, G_1(K)$$

(D-14)

$$S_e(K,\omega) = G^+(K)\, S_{eo}(K,\omega)\, G(K)$$

(D-15)

where

$$G(K) = \underset{p=0, 1, \ldots, K-1}{\text{diag}} \left[e^{+jp \frac{\omega d}{c} \cos \phi_o} \right] \tag{D-16}$$

$$G_1(K) = \begin{bmatrix} G(K) & 0 \\ \underline{0}^+ & e^{-jK\frac{\omega d}{c} \cos \phi_o} \end{bmatrix}$$

with $\underline{0}$ a K-dimensional vector of zeros and

$$S_{eo}(K,\omega) = (s_{eo}(p,q,\omega))_{\substack{p=0,1, \ldots K \\ q=0,1, \ldots K}} \tag{D-17}$$

with

$$s_{eo}(p,q,\omega) = \sigma_n^2(\omega) \, \delta_{pq} + \int_{-\phi}^{\phi} \sigma_I^2(\omega,\phi) e^{-j \phi(p-q) \frac{\omega d}{c} \sin \phi_o} d\phi \tag{D-18}$$

also

$$S_{Ho}(K,\omega) = \begin{bmatrix} S_{eo}(K,\omega) & \underline{s}_o(K,\omega) \\ \underline{s}_o^+(K,\omega) & S_{11}(K) \end{bmatrix} \tag{D-19}$$

where

$$\underline{s}_o(K,\omega) = [s_{eo}(o,m,\omega), \, s_{eo}(1,m,\omega), \, \ldots, \, s_{eo}(K-1,m,\omega)]^T \tag{D-20}$$

It can be seen that

$$\det [G(K)] = \prod_{p=0}^{K-1} e^{+ jp \frac{\omega d}{c} \cos \phi_0} = (\det [G^+(K)])^*$$ (D-21)

and

$$\det [G_1(K)] = e^{- jK \frac{\omega d}{c} \cos \phi_0} \det [G(K)] = (\det [G_1^+(K)])^*$$ (D-22)

Then using the fact that

$$\det [ABC] = \det [A] \det [B] \det [C]$$

(D-12), (D-14), (D-15), (D-17), and (D-18) give

$$E_K(\omega) = \frac{\det [S_{Ho}(K,\omega)]}{\det [S_{eo}(K,\omega)]}$$ (D-23)

Therefore, (D-11) can be replaced without loss of generality by

$$s_e(p,q,\omega) \approx \sigma_n^2(\omega) \delta_{pq}$$

(D-24)

$$+ \int_{-\phi}^{\phi} S_I(\phi+\phi_0,\omega) e^{j \frac{\omega d}{c} (p-q) \phi \sin \phi_0} \, d\phi$$

so that the CSD, $s_e(p,q,\omega)$, is the Fourier transform of the source density, $S_I(\phi+\phi_0,\omega)$.

In the temporal case, when uncorrelated noise with variance σ_n^2 is added to each time sample,

$$R_x[(p-q)T_s] = \sigma_n^2 \, \delta_{pq} + \int_{-\infty}^{\infty} S_{xx}(f)e^{j2\pi f(p-q)T_s}df, \quad f = \frac{\omega}{2\pi} \qquad (D\text{-}25)$$

where $S_{xx}(f)$ is the power spectral density of the process $x(t)$. If the process is bandlimited,

$$S_{xx}(f) = \begin{cases} S_{xx}(f+f_0), & f_0-B \le f \le f_0+B \\ 0 & , \text{ otherwise} \end{cases} \qquad (D\text{-}26)$$

Then (E-14) becomes

$$R_x(p-q)T_s] = \sigma_n^2 \, \delta_{pq} + \int_{-B}^{B} S_{xx}(f+f_0)e^{j2\pi f(p-q)T_s}df \qquad (D\text{-}27)$$

Comparing (D-24) and (D-27), it can be seen that the angular density of the extended source is analogous to the spectral density in the temporal case. Further the angular extent of the source, Φ, corresponds to the bandwidth of the temporal process, B, and the temporal sample interval, T_s, corresponds to the spatial sample interval

$$\gamma = \frac{\omega d}{2\pi c} \sin \phi_0 = \frac{d}{\lambda} \sin \phi$$

with λ the wavelength of the frequency, f.

Now, the samples of the random process, $x(t)$, comprise a random sequence $\{x_n\}$ $n = \ldots, -1, 0, 1, 2, \ldots$ with

$$x_n = x(nT_s) \qquad \text{(D-28)}$$

Define

$$R_k = E[x_n\, x_{n+k}] \qquad \text{(D-29)}$$

and note that

$$R_k = R_x[kT_s] \qquad \text{(D-30)}$$

The power spectral density of the sampled sequence, $\{x_n\}$, may be defined on $[-\pi, \pi)$ as

$$H_x(\alpha) = \sum_{k=-\infty}^{\infty} R_k e^{jk\alpha} \qquad \text{(D-31)}$$

where the inverse transform relationship is

$$R_k = \frac{1}{2\pi} \int_{-\pi}^{\pi} H_x(\alpha) e^{-jk\alpha}\, d\alpha \qquad \text{(D-32)}$$

Note that (D-27) can be rewritten as

$$R_x[(p-q)T_s] = \sigma_n^2\, \delta_{pq} + \int_{-2\pi B T_s}^{2\pi B T_s} S_{xx}\left(\frac{\alpha}{2\pi T_s} + f_0\right) e^{j(p-q)\alpha} \frac{d\alpha}{2\pi T_s} \qquad \text{(D-33)}$$

D-9

If it is assumed that $BT_s \leq 1/2$, then direct comparison of (D-32) and (D-33) shows that

$$H_x(\alpha) = \sigma_n^2$$

$$+ \frac{1}{T_s} S_{xx}\left(\frac{\alpha}{2\pi T_s} + f_0\right) \text{Rect}\left[\frac{\alpha}{2\pi B T_s}\right], \begin{cases} \alpha \varepsilon [-\pi, \pi) \\ BT_s \leq \frac{1}{2} \end{cases}$$

(D-34)

On the other hand, if $BT_s > 1/2$, the aliases of the sampled power spectral density must be considered, and $H_x(\alpha)$ must be replaced by $H_{fx}(\alpha)$ in (D-32) where

$$H_{fx}(\alpha) = \sigma_n^2 + \sum_{k=-\infty}^{\infty} H_x(\alpha+2\pi k)$$

(D-35)

$$= \sigma_n^2 + \sum_{k=-\infty}^{\infty} \frac{S_{xx}\left(\frac{\alpha+2\pi k}{2\pi T_s} + f_0\right)}{T_s} \text{Rect}\left[\frac{\alpha+2\pi k}{2\pi B T_s}\right], \quad \alpha \varepsilon [-\pi, \pi)$$

Now, consider the spatial cancellation problem starting with equation (D-24). Define the elements of the hydrophone cross-spectral density matrix as

$$S_k = \mathscr{F}\left\{E[e_n |t| e_{n+k}(t+\tau)]\right\}$$

(D-36)

Analogous to the power spectral density of the temporal process is the wave number-frequency spectrum (WNFS) of the hydrophone outputs, given by

$$H_e(\alpha, \omega) = \sum_{k=-\infty}^{\infty} S_k \, e^{jk\alpha} \qquad \alpha\epsilon[-\pi, \pi) \qquad (D-37)$$

with the inverse relationship

$$S_k = \frac{1}{2\pi} \int_{-\pi}^{\pi} H_e(\alpha, \omega) \, e^{-jk\alpha} \, d\alpha \qquad (D-38)$$

However, (D-24) gives S_k as

$$S_k = \sigma_n^2(\omega) \, \delta(k) + \int_{-\phi}^{\phi} S_I(\omega, \phi+\phi_o) e^{-j\phi k \frac{\omega d}{c} \sin \phi_o} \, d\phi \qquad (D-39)$$

Making the substitution

$$\alpha = \phi \, \frac{\omega d}{c} \sin \phi_o$$

$$\qquad (D-40)$$

$$d\alpha = \frac{\omega d}{c} \sin \phi_o \, d\phi$$

and letting

$$\gamma = \frac{1}{2\pi} \, \frac{\omega d}{c} \sin \phi_o = \frac{d}{\lambda} \sin \phi_o$$

D-11

gives

$$S_k = \sigma_n^2 (\omega) \, \delta(k) + \int_{-2\pi\gamma\phi}^{2\pi\gamma\phi} S_I \left(\omega, \frac{\alpha}{2\pi\gamma} + \phi_o\right) e^{-jk\alpha} \frac{d\alpha}{2\pi\gamma} \qquad \text{(D-41)}$$

Assume for the moment that $\gamma\phi \le 1/2$. Then comparing (D-41) with (D-36) shows that

$$H_e(\alpha, \omega) = \sigma_n^2(\omega) + \frac{S_I \left(\omega, \frac{\alpha}{2\pi\gamma} + \phi_o\right)}{\gamma} \, \text{Rect} \, [\alpha/2\pi\gamma\phi] \qquad \text{(D-42)}$$

where

$$\text{Rect} \, \left[\frac{x}{X}\right] = \begin{cases} 1, & |x| \le X \\ 0, & \text{otherwise} \end{cases}$$

Next, consider the case when $\gamma\phi > 1/2$, so that the noise field is under sampled spatially, and the portion of the spectrum extending beyond $[-\pi, \pi]$ will fold back into $[-\pi, \pi)$. Let $H_{fe}(\alpha, \omega)$ be the folded spectrum

$$H_{fe}(\alpha, \omega) = \sigma_n^2(\omega) + \sum_{k=-\infty}^{\infty} H_e(\alpha + 2\pi k, \omega), \quad \alpha \epsilon \, [-\pi, \pi] \qquad \text{(D-43)}$$

where $H_e(\alpha, \omega)$ is defined by (D-42).
Then

$$H_{fe}(\alpha, \omega) = \sigma_n^2(\omega) + \sum_{k=-\infty}^{\infty} S_I \left(\omega, \frac{\alpha + 2\pi k}{2\pi\gamma} + \phi_o\right) \frac{}{\gamma} \, \text{Rect} \left[\frac{\alpha + 2\pi k}{2\pi\gamma\phi}\right], \quad \alpha \epsilon [-\pi, \pi]$$

$$\text{(D-44)}$$

D.1. Results from linear prediction theory. The applicable results from linear prediction theory fall into two general categories. In the special case of m = 1, when the line array of references and the primary constitute a uniformly spaced line array, results depend upon the Toeplitz properties of the hydrophone cross-spectral density matrix. The second class of results which apply to m ≥ 1 are from the more general theory of stationary random functions. Most of the results to be presented concern the irreducible prediction error, which, for the temporal prediction problem, is the mean square error in predicting the desired number of steps ahead using the infinite past. If $E_K(m)$ denotes the error in predicting m steps ahead using K samples of the past, then

$$E_K(m) = \min_{a_{K-1},a_{K-2},\ldots,a_1,a_0} E\left| x(m) - \sum_{k=-K+1}^{0} a_k X(k) \right|^2 \qquad (D-45)$$

where $E(\cdot)$ denotes expectation. Then the irreducible prediction error is

$$E_\infty(m) = \lim_{K \to \infty} E_K(m) \qquad (D-46)$$

In the context of the cancellation of the extended source, the results apply at a single frequency, so the notation must be changed to $E_K(m,\omega)$ and $E_\infty(m,\omega)$. The parameter $E_K(m,\omega)$ is the spectral density of the canceller output at the frequency ω using K reference hydrophones and with the primary md feet from the nearest reference. The $E_\infty(m,\omega)$ is the limit on the single frequency canceller output spectrum as the array becomes infinitely long $(K \to \infty)$. This clearly conflicts with the assumption of a plane

wave source, which requires that wavefront curvature be negligible across the extent of the array. The irreducible error, $E_\infty(m,\omega)$, is therefore best interpreted as a lower bound on the canceller output spectrum in the spatial case. It should be noted that in numerical evaluations, given in Appendix K, the lower bound was approached quite rapidly as K increased, so that K may not have to be very large for $E_K(m,\omega)$ to be near $E_\infty(m,\omega)$.

A basic result from the theory of Toeplitz operators in the Szego Theorem [15], which relates the irreducible prediction error, $E_\infty(1)$, to the spectral density of the random sequence, $H_x(\omega)$.

Theorem 1: Let a zero mean stationary random sequence, $\{x(n)\}$, have correlation function

$$R_k = E[x(n)x(n+k)] \qquad (D-47)$$

and power spectral density

$$H_x(\alpha) = \sum_{k=-\infty}^{\infty} R_k e^{jk\alpha} \qquad (D-48)$$

Then

$$E_\infty(1) = \lim_{K \to \infty} E_K(1) = \exp\left[\frac{1}{2\pi} \int_{-\pi}^{\pi} \log H_x(\alpha) d\alpha \right] \qquad (D-49)$$

When $\log [H_x(\alpha)]$ is not inte grable on $[-\pi,\pi)$, the right hand side of (D-49) is replaced by zero. The theorem as given here is somewhat more restrictive

D-14

than given in [15] in that it assumes the existence of the spectral density,
$H_x(\alpha)$, rather than allowing for a spectral distribution that contains jumps
or that is not everywhere differentiable.

Note that under the last stipulation of the Theorem, any time log $[H_x(\alpha)]$
is not integrable, the irreducible prediction error is zero, so the process
can be predicted perfectly from the infinite past. Such a process is termed
a _singular_ stochastic process by Lamperti [16] or a _deterministic_ stochastic
process by Azego [15]. The condition under which the process is singular
which will be of interest here is as follows.

Theorem 2: A stationary random process is _singular_, i.e., it can be
predicted perfectly in the mean square sense from its infinite past, if

$$\int_{-\pi}^{\pi} \log H_x(\alpha)\, d\alpha = -\infty \qquad\qquad (D\text{-}50)$$

This will occur if $H_x(\alpha)$ is zero for any $\alpha\varepsilon[-\pi,\pi)$. Then any random
sequence whose spectrum is zero in some region on $[-\pi,\pi)$ will be singular.
Note that if $\sigma_n^2 \neq 0$ in (D-34), then the process is not singular, as would be
expected. In fact, the irreducible error will always be greater than σ_n^2,
except in the trivial case of $H_x(\alpha) = \sigma_n^2$.

Theorem 3: Let the stationary random process $x(n)$, have spectral density
of the form

$$H_x(\alpha) = \sigma_n^2 + H_{x0}(\alpha), \quad H_{x0}(\alpha) \neq 0 \qquad\qquad (D\text{-}51)$$

Then $E_\infty(1) \sim \sigma_n^2$. This can be seen by observing that

$$\exp\left[\frac{1}{2\pi}\int_{-\pi}^{\pi} \ln H_x(\alpha)d\alpha\right] = \exp\left[\frac{1}{2\pi}\int_{-\pi}^{\pi} \ln\left[\sigma_n^2 + H_{x0}(\alpha)\right]d\alpha\right]$$

$$= \exp\left[\ln\sigma_n^2 + \frac{1}{2\pi}\int_{-\pi}^{\pi} \ln\left[1 + \frac{H_{xo}(\alpha)}{\sigma_n^2}\right]d\alpha\right]$$

$$= \sigma_n^2 \exp\left[\frac{1}{2\pi}\int_{-\pi}^{\pi} \ln\left[1 + \frac{H_{xo}(\alpha)}{\sigma_n^2}\right]d\alpha\right] \geq \sigma_n^2$$

(D-52)

since the argument of the integral is always positive if $H_{x0}(\alpha) \neq 0$.

In terms of the cancellation of an extended source, Theorems 1 through 3 apply to the power spectrum of the canceller output, $E_\infty(1,\omega)$. As shown above, the wave number-frequency spectrum, $H_e(\alpha,\omega)$, is directly related to the angular distribution of a narrow extended plane wave source. These theorems therefore provide conditions on the source distribution under which complete cancellation is possible in the noise free ($\sigma_n^2(\omega) = 0$) case and indicate that cancellation to the noise floor is not possible in the presence of ambient noise.

Theorem 1a: Let $\mathscr{S}$ be an extended, uncorrelated, plane wave source as defined above, distributed in the same plane as the reference array and

primary of the geometry of Figure D-1. In the case whem $m = 1$, the wave number-frequency spectrum of the hydrophone outputs is

$$H_e(\alpha,\omega) = \sigma_n^2(\omega) + \sum_{k=-\infty}^{\infty} \frac{1}{\gamma} S_I\left(\frac{\alpha+2\pi k}{2\pi\gamma} + \phi_0,\omega\right) \text{Rect}\left[\frac{\alpha+2\pi k}{2\pi\gamma\phi}\right], \alpha\epsilon[-\pi,\pi) \quad (D-53)$$

Under the condition that $\gamma\phi \le 1/2$, this reduces to

$$H_e(\alpha,\omega) = \sigma_n^2(\omega) + \frac{1}{\gamma} S_I\left(\frac{\alpha}{2\pi\gamma} + \phi_0,\omega\right) \text{Rect}\left[\frac{\alpha}{2\pi\gamma\phi}\right] \quad (D-54)$$

Theorem 2a: Let $\sigma_n^2(\omega) = 0$ and assume that $\gamma\phi \le \frac{1}{2}$. Then the extended source gives

$$E_\infty(1,\omega) = 0 \quad (D-55)$$

Theorem 3a: Assume that $\sigma_n^2(\omega) \ne 0$. Then by Theorem 3, the extended source cannot be cancelled to the noise floor.

The results of Theorem 2 can easily be extended to $m > 1$ by observing the following.

Theorem 4: Let $E_\infty(m,\omega)$ be the irreducible error in predicting, in the minimum mean square sense, the stationary random sequence, $x(n)$, m steps ahead. If $E_\infty(1) = 0$, then

$$E_\infty(m) = 0 \quad m = 1,2,\ldots. \quad (D-56)$$

This can be proven by noting that, under the stationarity assumptions, $x(2)$ can be predicted perfectly using the infinite past, $\left\{ \ldots, x(0), x(1) \right\}$ if $E_\infty(1) = 0$. Given $\left\{ \ldots, x(-1), x(0) \right\}$, it is possible to predict $x(1)$ perfectly. Hence, $x(2)$ can be predicted using $\left\{ \ldots, x(-1), x(0) \right\}$ with zero mean square error, $E_\infty(2) = 0$. By induction, (D-56) is true.

This result means that in the noise free case, the canceller output power for an extended source tends asymptotically (in K) to zero, regardless of m, that is, regardless of the distance between the primary hydrophone and the reference array.

In the case when $E_\infty(1) = 0$, it is often possible to determine the asymptotic behavior of $E_K(1)$ for large K using the Strong Szego Limit Theorem for Circular Arcs[12]. Applied specifically to the problem being considered here, the Theorem is as follows:

Theorem 5: Let $x(n)$ be a stationary random sequence with spectral density $H_x(\alpha)$ and correlation R_k, $k = \ldots -1, 0, 1, \ldots$. Let $H_x(\alpha)$ be strictly positive on $-A \leq \alpha \leq A$ with $A < \pi$, and zero otherwise. Further let $dH_x(\alpha)/d\alpha$ satisfy a Lipschitz condition with exponent greater than $1/2$ on $-A \leq \alpha \leq A$. Then the minimum mean square error in predicting $x(n)$ given $\left\{ x(n-K), x(n-K+1), \ldots, x(n-1) \right\}$ using a linear combination of the observations is asymptotic in K to $L(K)$, where

$$L(K) = G \left[\sin \left(\frac{A}{2} \right) \right]^{2K+1} \tag{D-57}$$

and

$$G = \exp\left[\frac{1}{2\pi} \int_{-\pi}^{\pi} \log\left\{ H_X\left[2 \sin^{-1}(\sin \frac{A}{2}\cos \theta) \right] \right\} d\theta \right] \qquad \text{(D-58)}$$

The theorem requires a modification of the version presented in [12]. The modification is derived in the Supplement I to this Appendix.

Theorem 5 can be applied to the spatial cancellation problem by replacing $H_x(\alpha)$ with $H_e(\alpha,\omega)$ as given in Theorem 1a. Inspection of equation (D-42) shows that, due to the aliasing of the angular distribution of the source when $\gamma\phi \geq 1/2$, the Theorem only applies when $\gamma\phi < 1/2$.

Theorem 5a: Let $\gamma\phi < 1/2$, and let

$$H_e(\alpha,\omega) = \frac{1}{\gamma} S_I\left(\frac{\alpha}{2\pi\gamma} + \phi_0, \omega \right) \text{Rect}\left[\frac{\alpha}{2\pi\gamma\phi} \right] \qquad \text{(D-59)}$$

where $H_e(\alpha,\omega)$ is strictly positive on $-A \leq \alpha \leq A$, and where $\partial H_e(\alpha,\omega)/\partial\alpha$ satisfies a Lipschitz condition in α with exponent greater than 1/2 on that interval. Then the irreducible canceller output spectrum, $E_K(1,\omega)$, of an LMS canceller using a line array of K references spaced d feet apart to cancel the source from the output of a primary in the same line as the references and d feet away satisfies

$$E_K(1,\omega) \sim G(\omega) \left[\sin \pi\gamma\phi \right]^{2K+1} \qquad \text{(D-60)}$$

where $\sim$ denotes asymptotic in K and where $G(\omega)$ is given by

$$G(\omega) = \exp\left[\frac{1}{2\pi} \int_{-\pi}^{\pi} \left\{ \log H_e[2 \sin^{-1}(\sin(\pi\gamma\phi)\cos \theta), \omega] \right\} \right] d\theta \qquad \text{(D-61)}$$

From this Theorem, it can be seen that the canceller output spectrum, $E_K(1,\omega)$, goes exponentially to zero in K when $\gamma\Phi < 1/2$ in the ambient noise free case. Somewhat surprisingly, the rate does not depend upon the shape of the source angular distribution, but only upon $\gamma\Phi$. In evaluations of $E_K(1,\omega)$ given in Appendix K for uniform angular source, (d-47) appears to be a good approximation to $E_K(1,\omega)$, even for modest K.

Note that if ambient noise is present, so that

$$H_e(\alpha,\omega) = \sigma_n^2$$

$$+ \frac{1}{\gamma} S_n \left(\frac{\alpha}{2\pi\gamma} + \phi_0, \omega \right) \text{Rect}\left[\frac{\alpha}{2\pi\gamma\Phi} \right], \quad \alpha\varepsilon[-\pi,\pi] \tag{D-62}$$

Then the extent of $H_e(\alpha,\omega)$ is $[-\pi,\pi]$. This corresponds to $A = \pi$, which violates the conditions of Theorem 5. (With noise present, (D-62) may also violate the Lipschitz condition). However, Theorem 3a has already shown that $E_k(1,\omega)$ approaches a positive floor as $K \to \infty$.

In the extended source cancellation problem, the noise free case is of somewhat limited interest. It would be desirable to characterize $E_\infty(m,\omega)$ for $m > 1$ in the noise present case, which would provide a lower bound on cancellation as the reference array is moved farther from the primary. This can be done using some results from the general theory of stationary random processes which do not depend upon the Toeplitz properties of the covariance matrix.

In the noise present temporal case, it can be seen that

$$\int_{-\pi}^{\pi} \log \, [H_x(\alpha)] d\alpha > -\infty \tag{D-63}$$

so that the process, $x(n)$, is not singular. If the spectral distribution of the process, say $\widetilde{H}_x(\alpha)$, does not contain any jumps and is differentiable everywhere, then $x(n)$ is a <u>regular</u> random sequence, [17] and

$$\widetilde{H}_x(\mu) = \int_{-\pi}^{\pi} H_x(\alpha) d\alpha \tag{D-64}$$

A regular random sequence has a moving average representation

$$x(n) = \sum_{k=0}^{\infty} c_k \, \xi(n-k) \tag{D-65}$$

where $\xi(n)$ is a sequence of uncorrelated random variables. It can readily be shown that the minimum mean square error predictor of $x(m)$ given $\left\{ x(n) \right\}_{n \leq 0}$ is[16]

$$\hat{x}(m) = \sum_{k=m}^{\infty} c_k \, \xi(m-k) \tag{D-66}$$

so that the prediction error is

$$E_\infty(m) = \sum_{k=0}^{m-1} |c_k|^2 \qquad (D-67)$$

Therefore, if the c_k's in (D-67) can be found, the irreducible prediction error for m steps ahead is known.

The restriction of the process to the class of regular random processes will not limit the usefulness of these results in the extended source problem. As an aside, however, this restriction need not be made at all. As long as the process is non-singular,

$$\int_{-\pi}^{\pi} \ln H_x(\alpha)d\alpha > -\infty \qquad (D-68)$$

then it has a unique decomposition,

$$x(n) = u(n) + v(n) \qquad (D-69)$$

where u(n) is regular, v(n) is singular, and u is orthogonal to v. Since v(n) is singular, it can be predicted perfectly given the infinite past, and need not be considered in determination of the minimum prediction error for x(n). As a regular process, u(n) has the moving average representation,

$$u(n) = \sum_{k=0}^{\infty} d_k \, \xi(n-k) \qquad (D-70)$$

where $\xi(n)$ is an uncorrelated random sequence. The irreducible m step ahead prediction error for $u(n)$ (hence, for $v(n)$, taking into account the singularity of $v(n)$) is then

$$E_\infty(m) = \sum_{k=0}^{m-1} |d_k|^2 \qquad\qquad (D-71)$$

These results are rigorously derived in Lamperti [16] or Doob [18].

Even without finding the c_k's of the moving average representation (D-65) provides a useful result for the cancellation of a narrow extended source. By (D-67), the minimum canceller output power in the noise present case, $E_\infty(m,\omega)$, is a non-decreasing sequence in m. The cancellation floor therefore cannot become smaller as the reference array is moved away from the primary.

The c_k's in the moving average representation of a regular process can be found using a factorization of the spectral density $H_x(\alpha)$, given by the following theorem from Doob[18].

Theorem 6: Let $\{x(n)\}$ be a stationary, zero mean regular random sequence with spectral density, $H_x(\alpha)$. Then the coefficients of the moving average representation are uniquely determined by the following

$$c_o = \exp\left\{\frac{1}{2\pi} \int_{-\pi}^{\pi} \log H_x(\alpha)\, d\alpha\right\} \qquad\qquad (D-72)$$

$$E_\infty(m,\omega) = \lim_{K \to \infty} E_K(m,\omega) \qquad (D\text{-}75)$$

Then

$$E_\infty(m,\omega) = \sum_{\kappa=0}^{m-1} |c_k(\omega)|^2 \qquad (D\text{-}76)$$

where the $c_k(\omega)$ satisfy the equations

$$c_0(\omega) = \exp\left\{\frac{1}{2\pi} \int_{-\pi}^{\pi} \log H_e(\alpha,\omega)\, d\alpha\right\} \qquad (D\text{-}77)$$

and

$$\sum_{n=0}^{\infty} c_n^*(\omega)\, Z^n = \exp\left\{\frac{b_0(\omega)}{2} + \sum_{n=1}^{\infty} b_n(\omega)\, Z^n\right\} \qquad (D\text{-}78)$$

where

$$b_n(\omega) = \frac{1}{2\pi} \int_{-\pi}^{\pi} \log[H_e(\alpha,\omega)]\, e^{-jn\alpha} d\alpha \qquad (D\text{-}79)$$

specifically, from Supplement II,

$$c_1^*(\omega) = b_1(\omega)\, c_0(\omega) \qquad (D\text{-}80)$$

$$c_2^*(\omega) = \left[b_1^2(\omega) + b_2(\omega)\right] c_0(\omega) \qquad (D\text{-}81)$$

$$\sum_{n=0}^{\infty} c_n^* z^n = \exp\left\{\frac{b_0}{2} + \sum_{n=1}^{\infty} b_n z^n\right\} \qquad \text{(D-73)}$$

where

$$b_n = \frac{1}{2\pi} \int_{-\pi}^{\pi} \log[H_x(\alpha)] e^{-jn\alpha} d\alpha \qquad \text{(D-74)}$$

By expanding the right hand side of (D-73) in a power series, or by differentiating (D-73) and letting $z \to 0$, it is possible to obtain explicit expressions for the c_k's, and hence, for

$$E_\infty(m) = \sum_{k=0}^{m-1} |c_k|^2$$

However, the expressions resulting from this procedure are quite complicated. Supplement II to this Appendix derives expressions for c_0, c_1, c_2, c_3, c_4, and c_5 as a function of the b_k's defined by (D-74), which allows evaluation of $E_\infty(n)$ for $m = 1$ through $m = 5$.

As before, the temporal linear prediction results given here can be applied to spatial LMS cancellation by replacing $H_x(\alpha)$ by $H_e(\alpha, \omega)$ given in Theorem 1a. This yeilds the following result;

Theorem 7: Let $E_K(m, \omega)$ be the output spectrum of an LMS spatial canceller as defined above, and let $H_e(\alpha, \omega)$ be defined as in Theorem 1a. Denote

$$c_3^*(\omega) = \left[b_1^{\,3}(\omega) + 3b_1(\omega)\, b_2(\omega) + b_3(\omega) \right] c_0(\omega) \qquad \text{D-82)}$$

$$c_4^*(\omega) = \left[b_1^{\,4}(\omega) + 6b_1^{\,2}(\omega)\, b_2(\omega) + 4b_1(\omega)\, b_3(\omega) \right. \qquad \text{(D-83)}$$

$$\left. + 3b_2^{\,2}(\omega) + b_4(\omega) \right] c_0(\omega)$$

$$c_5^*(\omega) = \left[b_1^{\,5}(\omega) + 10b_1^{\,3}(\omega) + 10b_1^{\,2}(\omega)\, b_3(\omega) \right.$$

$$\left. +15b_1(\omega)\, b_2^{\,2}(\omega) + 10b_2(\omega)\, b_5(\omega) + 5b_1(\omega)\, b_4(\omega) \right. \qquad \text{(D-84)}$$

$$\left. +b_5(\omega) \right] c_0(\omega)$$

Supplement I: Strong Szego Limit For Circular Arcs. The Strong Szero
Limit Theorem for Circular Arcs is given in [12] as follows;

Theorem 8: Let f be a function satifying f (θ) = f (2π - θ) which is
supported on a closed arc α ≤ θ ≤2π - α and which when restricted to that
arc is positive and satisfies a Lipschitz condition with an exponent greater
than 1/2. Let $D_k[f]$ be the Toeplitz determinant

$$D_K[f] = \det \left(\frac{1}{2\pi} \int_0^{2\pi} e^{j(p-q)\theta} f(\theta)\, d\theta \right)_{\substack{p=0,1,\ldots K-1 \\ q=0,1,\ldots K-1}} \qquad \text{(D-85)}$$

Then as K→∞ , one has the asymptotic formula

$$D_K[f] \sim 2^{1/12}\, e^{3\xi'(-1)} \left(\sin \frac{\alpha}{2} \right)^{-\frac{1}{4}} E[F]^2\, K^{-\frac{1}{4}} G[F]^K \left(\cos \frac{\alpha}{2} \right)^{K^2} \qquad \text{(D-86)}$$

where if

$$\log f(\theta) = \sum_{k=\infty}^{\infty} f_k e^{jk\theta} \qquad (D-87)$$

one defines

$$F[f] = \exp(f_0) \qquad (D-88)$$

$$G[f] = \exp \frac{1}{4} \sum_{k=1}^{\infty} k f_k f_{-k} \qquad (D-89)$$

and

$$F(\theta) = f\left(2 \cos^{-1}\left(\cos \frac{\alpha}{2} \cos \theta\right)\right) \qquad (D-90)$$

Here, $\zeta'(x)$ is the derivative of the Riemann zeta function. [19] The proof of this Theorem is given in [12].

Theorem 5 requires the limit of the Toeplitz determinant when the function f satisfies all the conditions of Theeorem 8, but is supported on the closed arc $-\beta \leq \theta \leq \beta$. In this case, a Corollary to the Theorem may be stated as follows;

Corollary 1; Let f be a function satisfying all conditions of Theorem 8, except that its region of support is the closed arc $-\beta \leq \theta \leq \beta$. Then the Toeplitz determinant,

$$D_n[f] = \det \left(\frac{1}{2\pi} \int_{\pi}^{\pi} e^{j(p-q)\theta} f(\theta)d\theta \right)_{\substack{p=0,1,\ldots K-1 \\ q=0,1,\ldots K-1}} \tag{D-91}$$

has the asymptotic formula as $K \to \infty$

$$D_k[f] \sim 2^{1/12} e^{3\S'(-1)} \left(\cos \frac{\beta}{2} \right)^{-1/4} E[F]^2 K^{-\frac{1}{4}} G[F]^K \left(\sin \frac{\beta}{2} \right)^{K^2} \tag{D-92}$$

where G and E are as defined in Theorem 8 but

$$F[\theta] = f \left(2 \sin^{-1} \left(\sin \frac{\beta}{2} \cos \theta \right) \right) \tag{D-93}$$

Proof: Consider

$$\frac{1}{2\pi} \int_{-\pi}^{\pi} e^{jn\theta} f(\theta)d\theta \tag{D-91}$$

where f has support on $[-\beta, \beta]$. With the substitution $\theta = \phi - \pi$,

$$\frac{1}{2\pi} \int_{-\pi}^{\pi} e^{jn\theta} f(\theta)d\theta = \frac{1}{2\pi} \int_{0}^{2\pi} e^{jn(\phi-\pi)} f(\phi-\pi)d\phi \tag{D-92}$$

$$= (-1)^n \frac{1}{2\pi} \int_{0}^{2\pi} e^{jn\phi} g(\phi)d\phi$$

with $g(\phi) = f(\phi - \pi)$. Note that g has support on $[\pi - \beta, \pi + \beta]$, and letting $\alpha = \pi - \beta$, g has support on $[\alpha, 2\pi - \alpha]$. Thus if f meets all the other requirements of Theorem 1 on $[-\beta, \beta]$, then g satisfies the conditions of Theorem 1.

In order to relate

$$\det\left((-1)^{p-q} \frac{1}{2\pi} \int_0^{2\pi} e^{j(p-q)\phi} g(\phi)d\phi \right)_{\substack{p=0,1,\ldots K-1 \\ q=0,1,\ldots K-1}} \tag{D-93}$$

to

$$\det\left(\frac{1}{2\pi} \int_0^{2\pi} e^{j(p-1)\phi} g(\phi)d\phi \right)_{\substack{p=0,1,\ldots K-1 \\ q=0,1,\ldots K-1}}$$

the following theorem may be used.

Theorem 9: Let two square matrices, A and B be defined by

$$A = \left(a(p,q) \right)_{\substack{p=0,1,\ldots K-1 \\ q=0,1,\ldots K-1}}$$

and

$$B = \left((-1)^{p-q} a(p-q) \right)_{\substack{p=0,1,\ldots K-1 \\ p=0,1,\ldots K-1}}$$

Then $\det(A) = \det(B)$

Proof: Let M be a diagonal matrix

$$M = \operatorname*{diag}_{p=0,1,\ldots K-1} \left((-1)^p \right) \tag{D-94}$$

and note that

$$M^{-1} = \operatorname*{diag}_{p=0,1,\ldots K-1} \left((-1)^{-p} \right) = M \tag{D-95}$$

Now, the matrix B can be written in terms of A as

$$B = MAM^{-1} = MAM \tag{D-96}$$

Therefore

$$\det[B] = \det[MAM] = \det^2[M] \det[A] \tag{D-97}$$

$$= \det[A]$$

Using this theorem,

$$\det \left(\frac{1}{2\pi} \int_{\pi}^{\pi} e^{j(p-q)\theta} f(\theta) d\theta \right)_{\substack{p=2,1,\ldots K-1 \\ q=0,1,\ldots K-1}}$$

$$= \det \left((-1)^{p-q} \int_0^{2\pi} e^{j(p-q)\phi} g(\phi) d\phi \right)_{\substack{p=0,1,\ldots K-1 \\ q=0,1,\ldots K-1}} \tag{D-98}$$

$$= \det \left(\frac{1}{2\pi} \int_0^{2\pi} e^{j(p-q)\phi} g(\phi) d\phi \right)_{\substack{p=0,1,\ldots K-1 \\ q=0,1,\ldots K-1}}$$

where $g(\phi) = f(\phi - \pi)$ is supported for $\phi \varepsilon [\alpha, \ 2\pi - \alpha]$ with $\alpha = \pi - \beta$. Further, g meets all the requirements of Theorem 8, so that limit of the Toeplitz determinant, (D-91), can be found. The result is that

$$D_K[f] \sim 2^{\frac{1}{12}} e^{3 \zeta'(-1)} \left(\sin \frac{\pi-\beta}{2}\right)^{-\frac{1}{4}} E[F]^2 K^{-\frac{1}{4}} G[F]^K \left(\cos \frac{\pi-\beta}{2}\right)^{K^2} \quad \text{(D-99)}$$

$$= 2^{\frac{1}{12}} e^{3 \zeta'(-1)} \left(\cos \frac{\beta}{2}\right)^{-\frac{1}{4}} E[F]^2 K^{-\frac{1}{4}} G[F]^K \left(\sin \frac{\beta}{2}\right)^{K^2}$$

where if

$$\log g(\phi) = \sum_{k=\infty}^{\infty} g_k \, e^{jk\phi} \quad \text{(D-100)}$$

define

$$G[g] = \exp [g_0]. \quad \text{(D-101)}$$

and

$$E[g] = \exp \frac{1}{4} \sum_{k=1}^{\infty} k g_k \, g_{-k} \quad \text{(D-102)}$$

Further

$$F(\phi) = g \left(2 \cos^{-1}\left(\cos \frac{\pi-\beta}{2} \ \cos \phi\right)\right) \quad \text{(D-103)}$$

$$= g \left(2 \cos^{-1}\left(\sin \frac{\beta}{2} \cos \phi\right)\right)$$

but

$$g(\phi) = f(\pi - \phi)$$

so

$$g\left(2 \cos^{-1}\left(\sin \frac{\beta}{2} \cos \phi\right)\right) = f\left(\pi - 2 \cos^{-1}\left(\sin \frac{\beta}{2} \cos \phi\right)\right) \quad \text{(D-104)}$$

Let the argument of f in (A-23) be x, so

$$x = \pi - 2 \cos^{-1}\left(\sin \frac{\beta}{2} \cos \phi\right)$$

or

$$\cos \frac{x - \pi}{2} = \sin \frac{\beta}{2} \cos \phi \quad \text{(D-105)}$$

so that

$$x = 2 \sin^{-1}\left(\sin \frac{\beta}{2} \cos \phi\right) \quad \text{(D-106)}$$

and

$$F(\phi) = g\left(2 \sin^{-1}\left(\sin \frac{\beta}{2} \cos \phi\right)\right) \quad \text{(D-107)}$$

This Theorem allows the determination of the asymptote of the ratio of Toeplitz determinants as follows:

Corollary 2: Let f be a function satisfying the conditions of Corollary 1, and let $D_K[f]$ be the Toeplitz determinant

$$D_K[f] = \det \left(\frac{1}{2\pi} \int_{-\pi}^{\pi} e^{j(p-q)\theta} f(\theta) \, d\theta \right)_{\substack{p=0,1,\ldots K-1 \\ q=0,1,\ldots K-1}} \qquad \text{(D-108)}$$

Then as $K \to \infty$, the ratio $D_{K+1}[f]/D_K[f]$ has the asymptotic formula

$$\frac{D_{K+1}[f]}{D_K[f]} \sim G[F] \left(\sin \frac{\beta}{2} \right) \left(\sin \frac{\beta}{2} \right)^{2K} \qquad \text{(D-109)}$$

with G and F as defined in Corollary 1.

Proof: By Collary 1,

$$\frac{D_{K+1}[f]}{D_K[f]} \sim \frac{2^{\frac{1}{12}} e^{3\zeta'(-1)} \left(\cos \frac{\beta}{2} \right)^{-\frac{1}{4}} E[F]^2 (K+1)^{-\frac{1}{4}} G[F]^{K+1} \left(\sin \frac{\beta}{2} \right)^{K^2+2K+1}}{2^{\frac{1}{12}} e^{3\zeta'(-1)} \left(\cos \frac{\beta}{2} \right)^{-\frac{1}{4}} E[F]^2 K^{-1/4} G[F]^K \left(\sin \frac{\beta}{2} \right)^{K^2}}$$

$$= \left(\frac{K+1}{K} \right)^{-1/4} G[F] \left(\sin \frac{\beta}{2} \right)^{2K+1} \qquad \text{(D-110)}$$

$$\sim G[F] \left(\sin \right) \frac{\beta}{2} \left(\sin \frac{\beta}{2} \right)^{2K}$$

Supplement II: Evaluation of Irreducible Prediction Error for Specific

Values of m

From equation (D-78),

$$\sum_{n=0}^{\infty} c_n^* Z^n = \exp\left\{\frac{b_0}{2} + \sum_{n=1}^{\infty} b_n Z^n\right\} \tag{D-111}$$

Let

$$C(Z) = \sum_{n=0}^{\infty} c_n^* Z^n \tag{D-112}$$

$$B(Z) = \frac{b_0}{2} + \sum_{n=1}^{\infty} b_n Z^n \tag{D-113}$$

Now, denote

$$C^{(m)}(Z) = \frac{d^m C(Z)}{dZ^m} \ , \ \ B^{(m)}(Z) = \frac{d^m B(Z)}{dZ^m} \tag{D-114}$$

and note that for $m > 0$,

$$C^{(m)}(0) = m! \ c_m^* \ , \ B^{(m)}(0) = m! b_m \tag{D-115}$$

Using (D-111), and dropping the arguments, Z, for convenience

$$C^{(1)} = \exp[B] \, B^{(1)} \tag{D-116}$$

$$C^{(2)} = \exp[B] \left\{ B^{(1)^2} + B^{(2)} \right\} \tag{D-117}$$

$$C^{(3)} = \exp[B] \, B^{(1)} \left\{ B^{(1)^2} + B^{(2)} \right\}$$

$$+ \exp[B] \left\{ 2B^{(1)} \, B^{(2)} + B^{(3)} \right\}$$

$$= \exp[B] \left\{ B^{(1)^3} + 3B^{(1)} \, B^{(2)} + B^{(3)} \right\} \tag{D-118}$$

$$C^{(4)} = \exp[B] \, B^{(1)} \left\{ B^{(1)^3} + 3B^{(1)} \, B^{(2)} + B^{(3)} \right\}$$

$$+ \exp[B] \left\{ 3B^{(1)^2} \, B^{(2)} + 3B^{(2)^2} + 3B^{(1)} \, B^{(3)} + B^{(4)} \right\}$$

$$= \exp[B] \left\{ B^{(1)^4} + 6B^{(1)^2} \, B^{(2)} + 4B^{(1)} \, B^{(3)} \right. \tag{D-119}$$

$$\left. + 3B^{(2)^2} + B^{(4)} \right\}$$

$$C^{(5)} = \exp[B] \left\{ B^{(1)^5} + 10B^{(1)^4} \, B^{(2)} + 10B^{(1)^2} \, B^{(3)} \right. \tag{D-120}$$

$$\left. + 15B^{(1)} \, B^{(2)^2} + 10B^{(2)} \, B^{(3)} + 5B^{(1)} \, B^{(4)} + B^{(5)} \right\}$$

Therefore, setting Z = 0 and using (B-5) and (B-6),

$$c_m^* = \sum_{k=1}^{m} \binom{m-1}{k-1} \, c_{m-k}^* \, b_k \tag{D-121}$$

where, from (D-117)

$$c_0^* = \exp (b_0/2) \qquad\qquad (D-122)$$

Some specific c_m^*'s are then

$$c_1^* = c_0^* b_1 = b_1 \exp (b_0/2) \qquad\qquad (D-123)$$

$$c_2^* = c_1^* b_1 + c_0^* b_2$$

$$= \left(c_0^* b_1^2 + c_0^* g_2 \right) = [b_1^2 + b_2] \exp [b_0/2] \qquad\qquad (D-124)$$

$$c_3^* = c_2^* b_1 + 2c_1^* b_2 + c_0^* b_3$$

$$= [b_1^2 + b_2] b_1 c_0^* + 2 b_1 b_2 c_0^* + c_0^* b_3 \qquad\qquad (D-125)$$

$$= [b_1^3 + 3b_1 b_2 + b_3] \exp (b_0/2)$$

$$c_4^* = c_3^* b_1 + 3c_2^* b_2 + 3 c_1^* b_3 + c_0^* b_4$$

$$= [b_1^3 + 3b_1 b_2 + {}^* b_3] b_1 C_0^* + 3b_2 [b_1^2 + b_2] c_0^2$$

$$+ 3 b_1 b_3 c_0^* + c_0^* b_4 \qquad\qquad (D-126)$$

$$= [b_1^4 + 6b_1^2 b_2 + 4b_1 b_3 + 3b_2^2 + b_4] \exp [b_0/2]$$

$$c_5^* = c_4^* b_1 + 4c_3^* b_2 + 6\,c_2^* b_3 + 4c_1^* b_4 + c_0^* b_5$$

$$= b_1\,[b_1^4 + 6b_1^2\,b_2 + 4b_1 b_3 + 3b_2^2 + b_4]\,c_0^*$$

$$+ 4b_2\,[b_1^3 + 3b_1\,b_2 + b_2]\,c_0^* + 6b_3\,[b_1^2 + b_2]\,c_0^*$$

$$+ 4b_4\,b_1\,c_0^* + b_5\,c_0^*$$

$$= [b_1^5 + 10b_1^3\,b_2 + 10b_1^2\,b_3 + 15b_1\,b_2^2 + 10b_2\,b_3 + 5b_1\,b_4$$

$$+ b_5]\,\exp\,[b_0/2] \tag{D-127}$$

From (D-76)

$$E_\infty(m,\omega) = \sum_{k=0}^{m-1}\ |c_k|^2 \tag{D-128}$$

APPENDIX E: CANCELLER PERFORMANCE IN TERMS OF
DISCRETE PROLATE SPHEROIDAL SEQUENCES

APPENDIX E: CANCELLER PERFORMANCE IN TERMS OF DISCRETE PROLATE SPHEROIDAL SEQUENCES

The power spectral density of the optimal canceller output, from equation (G-17) of Appendix C is given by

$$E_K(\omega) = S_{11}(\omega) - \underline{s}_1^+(\omega) S_e^{-1}(\omega) \underline{s}_1(\omega) \tag{E-1}$$

with

$S_{11}(\omega) =$ PSD of the primary

$S_e(\omega) =$ CSD matrix of the reference hydrophone outputs

$\underline{s}_1(\omega) =$ CSD vector between the primary and reference hydrophone outputs

For the far field extended source described in Appendix A, assuming a uniformly distributed, narrow, spatially uncorrelated source, the statistics of the hydrophone outputs are

$$S_{11}(\omega) = 2\Phi\sigma_I^2(\omega) + \sigma_n^2 \tag{E-2}$$

$$\underline{s}_1 = \sigma_I^2(\omega) e^{-j\frac{\omega d}{c} J \cos\phi_0} G^+ \underline{s}_0 \tag{E-3}$$

where $\tag{E-4}$

$$\underline{s}_0 = [s_0(o,\omega), s_0(1,\omega), \ldots s_0(K-1,\omega)]^T$$

$$s_0(p,\omega) = \frac{\sin\left[(J-p)\frac{\omega d}{c}\Phi \sin\phi_0\right]}{\left[\frac{1}{2}(J-p)\frac{\omega d}{c}\sin\phi_0\right]} \tag{E-5}$$

and

$$S_e = \sigma_n^2(\omega)I + \sigma_I^2(\omega)G^+ S_{eo(\underline{\omega})}G \qquad \text{(E-6)}$$

where

$$S_{eo}(\omega) = \left(\frac{\sin\left[(p-q)\ \frac{\omega d}{c}\ \Phi \sin\ \phi_o\right]}{\frac{1}{2}\left[(p-q)\ \frac{\omega d}{c} \sin\ \phi_o\right]} \right) \qquad \begin{array}{l} p = 0,1,\ldots K-1 \\ q = 0,1,\ldots K-1 \end{array} \qquad \text{(E-7)}$$

and

$$G = \operatorname*{diag}_{p}\left[e^{-j\ \frac{\omega d}{c}\ p\ \cos\ \phi_o}\right] \qquad \text{(E-8)}$$

The inverse, $S_{eo}^{-1}(\omega)$, can be obtained in terms of the eigenvalues and eigenvectors of $S_{eo}(\omega)$, which can be defined in terms of the Discrete Prolate Spheriodal Sequences (DPSS) as discussed in Slepian [13]. Note that (E-7) can be written

$$S_{eo}(\omega) = \frac{1}{\gamma}\left(\frac{\sin\ [2\pi W(p-q)]}{\pi\ (p-q)}\right) \qquad \begin{array}{l} p = 0,1,\ldots,K-1 \\ q = 0,1,\ldots,K-1 \end{array} \qquad \text{(E-9)}$$

with

$$\gamma = \frac{d}{\lambda}\ \sin\ \phi_o$$

$$W = \Phi\gamma$$

λ = wavelength at frequency ω

Now, the DPSS satisfy

$$\sum_{m=0}^{K-1} \frac{\sin[2\pi(n-m)W]}{\pi(n-m)} \, V_m^{(k)}(K,W) = \lambda_k(K,W) V_n^{(k)}(K,W) \qquad \text{(E-10)}$$

for $k=0,1,\ldots K-1$, where $\left\{ V_n^{(k)}(K,W) \right\}_{n=0,\pm 1,\pm 2\ldots}$ is the $k\underline{\text{th}}$ DPSS and where $\lambda_k(K,W)$ is the associated eigenvalue. Equation (E-10) for $k=0,1,\ldots K-1$ can be written in vector form as

$$\underline{s}_n^+ \, \underline{V}_k(K,W) = \lambda_k(K,W) \, V_n^{(k)}(K,W) \qquad \text{(E-11)}$$

where

$$\underline{s}_n = \left[s_n(o), \, s_n(1), \, \ldots \, s_n(k-1) \right]^T \qquad \text{(E-12)}$$

$$s_n(q) = \frac{\sin\left[2\pi(n-q)W \right]}{\pi(n-q)} \qquad \text{(E-13)}$$

and

$$\underline{V}_k(K,W) = \left[V_o^{(k)}(K,W), \, \ldots, \, V_{k-1}^{(k)}(K,W) \right]^T \qquad \text{(E-14)}$$

Therefore

$$
\begin{bmatrix} \underline{s}_o^+ \\ \\ \underline{s}_1^+ \\ \cdot \\ \cdot \\ \cdot \\ \underline{s}_{k-1}^+ \end{bmatrix} \underline{V}_k(K,W) = \lambda_k(K,W) \begin{bmatrix} V_o^{(k)}(K,W) \\ \\ V_1^{(k)}(K,W) \\ \cdot \\ \cdot \\ \cdot \\ V_{k-1}^{(k)}(K,W) \end{bmatrix} \qquad k=0,1,\ldots K-1 \qquad (E\text{-}15)
$$

Comparing (E-15) with (E-7), it can be seen that

$$
S_{eo}(\omega) = \frac{1}{\gamma} \begin{bmatrix} \underline{s}_o^+(\omega) \\ \\ \underline{s}_1^+(\omega) \\ \cdot \\ \cdot \\ \cdot \\ \underline{s}_K^+(\omega)_{-1} \end{bmatrix} \qquad \text{if } W = \gamma \Phi \qquad (E\text{-}16)
$$

with $\gamma = fd/c \sin \Phi_o$ and $\omega = 2\pi f$. Therefore, multiplying both sides of (E-15) by $1/\gamma$ gives

$$
S_{eo}\underline{V}_k\left(K,\gamma\Phi\right) = \frac{1}{\gamma} \lambda_k\left(K,\gamma\Phi\right) \underline{V}_k\left(K,\gamma\Phi\right) \qquad (E\text{-}17)
$$

In this form, it can clearly be seen that the set of eigenvectors $\left\{ \underline{V}_k(K,W) \right\}$, k=0,1, ..., K-1, of $S_{eo}(\omega)$ are the $\underline{V}_k(K,W)$ given by (E-14) with associated eigenvalues $[\frac{1}{\gamma} \lambda_k (K,W)]$. Noting that G is diagonal and that $G^{-1} = G^+$, it can be seen that

$$[G^+ S_{eo} G] \; G^+ \underline{V}_k(K,W) = \lambda_k(K,W) \; G^+ \underline{V}_k(K,W) \tag{E-18}$$

so that the $G^+ S_{eo} G$ has the same eigenvalues as S_{eo}, but its eigenvectors are $\left\{ G^+ \underline{V}_k (K,W) \right\}_{k=0,1,\ldots K-1}$. Consequently, S_e has the same eigenvectors, but its eigenvalues, $\left\{ \Gamma_k (K,W) \right\}_{k=0,1,\ldots K-1}$ are

$$\Gamma_k (K,W) = \sigma_n^2 + \frac{\sigma_I^2}{\gamma} \lambda_k (K,W) \tag{E-19}$$

Therefore,

$$S_e^{-1} = \sum_{k-o}^{K-1} \Gamma_k^{-1}(K,W) \; G^+ \underline{V}_k(K,W) \underline{V}_k^+(K,W) G \tag{E-20}$$

and

$$\underline{s}_1^+ S_e^{-1} \underline{s}_1 = \sum_{k-0}^{K-1} \Gamma_k^{-1}(K,W) \left| \underline{s}_1^+ G^+ \underline{V}_k(K,W) \right|^2 \tag{E-21}$$

Using (E-3) gives

$$\underline{s}_1^+ G^+ \underline{V}_k(K,W) = \sigma_I^2 \underline{s}_o^+ GG^+ \underline{V}_k e^{+j \frac{\omega d}{c} J \cos \phi_o} = \sigma_I^2 \underline{s}_o^+ \underline{V}_k(K,W) e^{+j \frac{\omega d}{c} J \cos \phi_o}$$

$$\tag{E-22}$$

but

$$\underline{s}_o^+ \underline{V}_k(K,W) = \sum_{m=0}^{K-1} \frac{\sin[2\pi (J-m)\gamma \phi]}{\frac{1}{2}[(J-m)2\pi\gamma]} V_m^{(k)}(K,W)$$

$$= \frac{1}{\gamma} \sum_{m=0}^{K-1} \frac{\sin[2\pi(J-m)W]}{\pi(J-m)} V_m^{(k)}(K,W) = \frac{1}{\gamma} \lambda_k(K,W) V_J^{(k)}(K,W) \quad (E-23)$$

by applying (E-10) again. Substituting this in (E-21) yields

$$\underline{s}_1^+ S_e^{-1} \underline{s}_1 = \sum_{k=0}^{K-1} \left[\frac{\sigma_I^4 \lambda_k^2(K,W)}{\gamma^2 \sigma_n^2 + \gamma \sigma_I^2 \lambda_k(K,W)} \right] |V_J^{(k)}(K,W)|^2$$

Therefore

$$E = \sigma_n^2 + \sigma_I^2 \left\{ 2\Phi - \frac{1}{\gamma} \sum_{k=0}^{K-1} \left[\frac{2\Phi \sigma_I^2 \lambda_k^2(K,W)}{2W\sigma_n^2 + 2\Phi \sigma_I^2 \lambda_k(K,W)} \right] |V_J^{(k)}(K,W)|^2 \right\} \quad (E-24)$$

For the moment, suppose that the noise field is totally due to the extended source, $\sigma_n^2 = o$, so

$$E = \sigma_I^2 \left[2\Phi - \frac{1}{\gamma} \sum_{k=0}^{K-1} \lambda_k(K,W) |V_J^{(k)}(K,W)|^2 \right] \quad (E-25)$$

A good check on this result is to let $J = J_o$ for some $0 \leqslant J_o < K - 1$, so that one reference is coincident with the primary hydrophone. This should give perfect cancellation. In that case

$$\sum_{k=0}^{K-1} \lambda_k(K,W) V_{J_o}^{(k)}(K,W) V_{J_o}^{(k)}(K,W)$$

$$= \sum_{k=0}^{K-1} \sum_{\ell=0}^{K-1} \frac{\sin[2\pi(J_o - \ell)W]}{\pi(J_o - \ell)} V_\ell^{(k)}(K,W) V_{J_o}^{(k)}(K,W)$$

$$= \sum_{\ell=0}^{K-1} \frac{\sin[2\pi(J_o - \ell)W]}{\pi(J_o - \ell)} \sum_{k=0}^{K-1} V_\ell^{(k)}(K,W) V_{J_o}^{(k)}(K,W) \qquad \text{(E-26)}$$

But the DPSS are orthogonal when index limited to $[0,K-1]$

$$\sum_{k=0}^{K-1} V_\ell^{(k)}(K,W) V_{J_o}^{(k)}(K,W) = \delta_{\ell J_o} \qquad \text{(E-27)}$$

so

$$\sum_{k=0}^{K-1} \lambda_k(K,W) V_{J_o}^{(k)}(K,W) V_{J_o}^{(k)}(K,W) = 2W = \frac{2\gamma\Phi}{\pi} \qquad \text{(E-28)}$$

Substituting this in (E-26) gives $E = 0$ indicating perfect cancellation of the source as it should when a reference is coincident with the primary.

APPENDIX F: RESULTS FOR THE UNIFORMLY DISTRIBUTED
FAR FIELD MODEL BASED ON TOEPLITZ PROPERTIES OF THE
HYDROPHONE CSD

APPENDIX F: RESULTS FOR THE UNIFORMLY DISTRIBUTED FAR FIELD MODEL BASED UPON TOEPLITZ PROPERTIES OF THE HYDROPHONE CSD

When the extended source is narrow in the sense of (A-24) and spatially uncorrelated, substitution of (D-53) into (D-49) yields the irreducible canceller output spectrum, $E_\infty(1,\omega)$ as

$$E_\infty(1,\omega) = \exp\left[\frac{1}{2\pi} \int_{-\pi}^{\pi} \ln\left[H_{fe}(\alpha,\omega)\right] d\omega\right.$$

$$= \exp\left[\frac{1}{2\pi} \int_{-\pi}^{\pi} \ln\left[\sigma_n^2(\omega) + \sum_{k=-\infty}^{\infty} \frac{S_I\left(\omega, \frac{\alpha+2\pi k}{2n\gamma} + \phi_0\right)}{\gamma} \text{Rect}\left[\frac{\alpha+2\pi k}{2\pi\gamma\phi}\right]\right]\right] d\alpha$$

$$= \sigma_n^2(\omega)\left\{\exp\frac{1}{2\pi}\int_{-\pi}^{\pi} \ln\left[1 + \frac{1}{\sigma_n^2(\omega)\,\gamma} \sum_{k=-\infty}^{\infty} S_I\left(\omega, \frac{\alpha+2\pi k}{2\pi\gamma} + \phi_0\right)\right.\right.$$

$$\left.\left.\text{Rect}\left[\frac{\alpha+2\pi k}{2\pi\gamma\phi}\right]\right] d\alpha\right\}$$

$$= \sigma_n^2(\omega)\exp\left\{\gamma\int_{-1/2\gamma}^{1/2\gamma} \ln\left[1 + \frac{1}{\sigma_n^2(\omega)\,\gamma} \sum_{k=-\infty}^{\infty} S_I\left(\omega, \phi + \frac{k}{\gamma} + \phi_0\right)\right.\right.$$

$$\left.\left.\text{Rect}\left[\frac{\phi + k/\gamma}{\phi}\right]\right] d\phi\right\} \tag{F-1}$$

When $\gamma\phi \leq \frac{1}{2}$, using (D-54), this reduces to

$$E_\infty(1,\omega) = \sigma_n^2(\omega)\exp\left\{\gamma\int_{-\phi}^{\phi} \ln\left[1 + \frac{1}{\gamma\sigma_n^2(\omega)} S_I(\omega, \phi + \phi_0)\right] d\phi\right\} \tag{F-2}$$

In the case when extended source is uniformly distributed on $[\Phi_o - \Phi, \Phi_o + \Phi]$, as in (A-40), then (F-1) and (F-2) can be evaluated in closed form. Since the uniform source distribution is a reasonable representation for a number of sonar problems, this result is quite important. Let

$$S_I(\phi,\omega) = \begin{cases} \sigma_I^2(\omega) & , \quad \phi\varepsilon[\Phi_o - \Phi, \ \Phi_o + \Phi] \\ 0 & , \quad \text{otherwise} \end{cases}$$

and define an integer, n, such that

$$\frac{n}{2} < \gamma\Phi < \frac{n+1}{2} \tag{F-3}$$

The positive alias in $H_{f_e}(\alpha,\omega)$ as defined by (F-1) centered at k/γ extends from $(k/\gamma) - \Phi$ to $(k/\gamma) + \Phi$, so if

$$\frac{k}{\gamma} - \Phi \le -\frac{1}{2\gamma} \tag{F-4}$$

the kth positive alias extends through the interval of integration, $\left[\frac{-1}{2\gamma}, \frac{1}{2\gamma}\right]$. If (F-4) is met, the kth negative alias also extends through the interval of integration. Let k_o be the number of aliases extending completely through $\left[\frac{-1}{2\gamma}, \frac{1}{2\gamma}\right]$. Using the above, $k_o = \lfloor \gamma\Phi - 1/2 \rfloor$ where $\lfloor X \rfloor$ is the largest integer $\le X$. The next, $(k_o + 1)^{th}$, alias extends from $(k_o+1)/\gamma - \Phi$ to $(k_o + 1)/\gamma + \Phi$

First, consider n (in (F-3)) even, so that

$$k_o = \left\lfloor \gamma\Phi - \frac{1}{2} \right\rfloor = \frac{n}{2} - 1 \tag{F-5}$$

Therefore

$$\frac{(k_o + 1)}{\gamma} - \Phi = \frac{n}{2\gamma} - \Phi \leq 0 \qquad\qquad (F\text{-}6)$$

since, by (3-98)

$$\gamma\Phi \geq \frac{n}{2}$$

Hence, the $(k_o + 1^{th})$ positive alias extends from $\frac{n}{2\gamma} - \Phi$ to $\frac{1}{2\gamma}$, while the negative alias extends from $\frac{-1}{2\gamma}$ to $-\frac{n}{2\gamma} + \Phi$, overlapping as shown in Figure F-1.
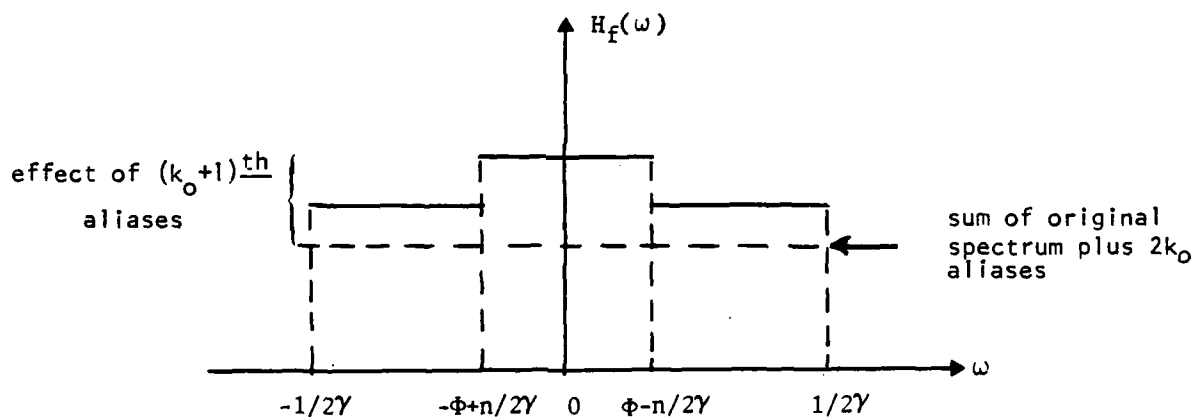
Figure F-1. Folded Spectral Density for Uniform Source, n even

Using this, there are $2k_o$ aliases (k_o positive plus k_o negative) extending through $[-1/2\gamma, 1/2\gamma]$ plus the primary spectrum and the sum of the $(k_o+1)^{th}$ aliases. Hence, in (F-1)

$$\sum_{k=-\infty}^{\infty} \sigma_I^2 \left(\omega, \phi + \frac{k}{\gamma} + \phi_0\right) \text{Rect} \left[\frac{\phi + k/\gamma}{\phi}\right]$$

$$\tag{F-7}$$

$$= \sigma_I^2(\omega) \left\{(2k_0 + 2) + \text{Rect}\left[\frac{\phi}{\frac{n}{2\gamma} - \phi}\right]\right\}$$

$$= \sigma_I^2(\omega) \left\{n + \text{Rect}\left[\frac{\phi}{\frac{n}{2\gamma} - \phi}\right]\right\}$$

Substituting this in (F-1) gives

$$\exp\left[\frac{1}{2\pi} \int_{-\pi}^{\pi} \ln\left[H_f(x)\right] dx\right]$$

$$= \sigma_n^2(\omega) \exp\left[\gamma \int_{\frac{-1}{2\gamma}}^{\frac{1}{2\gamma}} \ln\left[1 + \frac{\sigma_I^2(\omega)}{\sigma_n^2(\omega)\gamma}\left\{n + \text{Rect}\left[\frac{\phi}{\frac{n}{2} - \phi}\right]\right\}\right] d\phi\right]$$

$$= \sigma_n^2(\omega) \exp\left[\gamma \int_{\frac{-1}{2\gamma}}^{\frac{1}{2\gamma}} \ln\left[1 + \frac{n\sigma_I^2(\omega)}{\sigma_n^2(\omega)\gamma}\right] d\phi + \gamma \int_{\frac{n}{2\gamma} - \phi}^{-\frac{n}{2\gamma} + \phi} \ln\left[1 + \frac{\sigma_I^2(\omega)/\sigma_n^2(\omega)\gamma}{1 + \left[\frac{n\sigma_I^2(\omega)}{\sigma_n^2(\omega)\gamma}\right]}\right] d\phi\right]$$

F-4

$$= \left[\sigma_n^2(\omega) + \frac{n\sigma_I^2(\omega)}{\gamma} \right] \left[1 + \frac{\sigma_s^2(\omega)}{\sigma_n^2(\omega)\,\gamma + n\sigma_I^2(\omega)} \right]^{2\gamma\phi - n}$$

$$= \frac{\sigma_I^2(\omega)}{\gamma} \left[n + \frac{\gamma\sigma_n^2(\omega)}{\sigma_I^2(\omega)} \right] \left[1 + \left(n + \frac{\gamma\sigma_n^2(\omega)}{\sigma_I^2(\omega)} \right)^{-1} \right]^{2\gamma\phi - n} \tag{F-8}$$

Now define $W = \gamma\phi$ and note from (A-41) that the power from the extended source is $2\phi\,\sigma_I^2(\omega)$.

Then

$$E_\infty(1,\omega) = \frac{2\phi\,\sigma_I^2(\omega)}{2W} \, S \left[1 + \frac{1}{S} \right]^{2\gamma\phi - n} \tag{F-9}$$

where

$$S = n + \frac{2W\,\sigma_n^2(\omega)}{2\phi\,\sigma_I^2(\omega)} \tag{F-10}$$

This result is identical to that obtained by Slepian for the temporal linear prediction of a perfectly bandlimited random process in uncorrelated noise. However, Slepian considered the problem in terms of the Discrete Prolate Spheroidal Sequences (DPSS). The DPSS and their eigenvalues are associated with the hydrophone CSD matrix produced by the uniform source. This results depended upon the asymptotic evaluation of several complex integrals and did not demonstrate the effect of aliasing of the wave number-frequency spectrum, $H_e(\alpha,\omega)$, on the linear prediction error.

If n is odd then

$$k_o = \left\lfloor \gamma\phi - \frac{1}{2} \right\rfloor = \frac{n-1}{2} \qquad (F-11)$$

and the $(k_o+1)^{th}$ positive alias extends from $(k_o+1)/\gamma - \phi$ to $(k_o+1)/\gamma + \phi$, where

$$\frac{(k_o+1)}{\gamma} - \phi = \frac{n+1}{2\gamma} - \phi > 0 \qquad (F-12)$$

since $\gamma\phi \leq \frac{n+1}{2}$. Then the $(k_o+1)^{th}$ aliases do not overlap, as shown in Figure 3-2. Therefore, by the same argument used the even case,
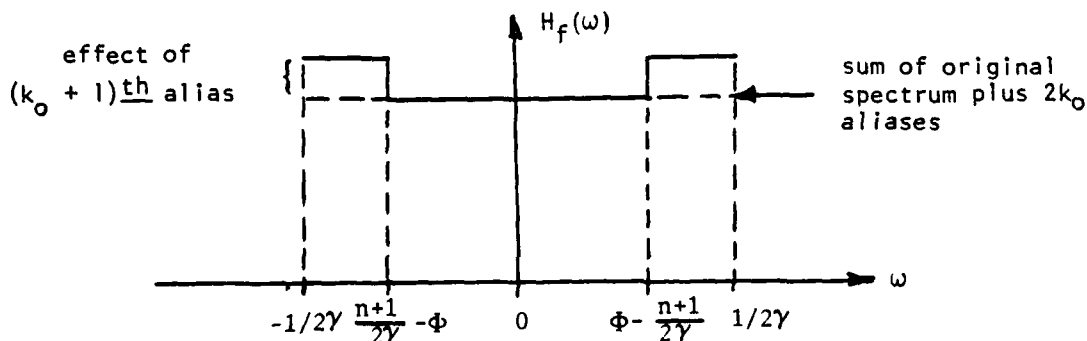
Figure F-2. Folded Spectral Density for Uniform Source; n odd

F.1 Interference Only Case

As mentioned above, the case where the noise field consists of only a narrow extended source with no ambient background does not occur in sonar. However, consideration of the ambient noise free, $\sigma_n^2(\omega) = 0$, case yields insight into the behavior of the LMS optimal canceller in the field produced by an extended source. Consider the irreducible canceller output spectrum, $E_\infty(1,\omega)$ when

$$\sigma_n^2(\omega) = 0$$

It is easily shown that (F-9) reduces to

$$E_\infty(1,\omega) \Bigg|_{\sigma_n^2(\omega) = 0} = \frac{2\Phi \; \sigma_I^2(\omega)}{2W} \; n \; \left(1 + \frac{1}{n}\right)^{2W-n} \qquad (\text{F-16})$$

with n defined as the integer such that

$$\frac{n}{2} < \gamma \, \Phi < \frac{n+1}{2} \qquad (\text{F-17})$$

Therefore, if $\gamma\Phi < \frac{1}{2}$, so that n=0,

$$E_\infty(1,\omega) \Bigg|_{\sigma_n^2(\omega) = 0} = 0, \qquad \gamma\Phi < \frac{1}{2} \qquad (\text{F-18})$$

and the extended source can be cancelled completely, at least asymptotically in K, the number of references. On the other hand, if $\gamma\Phi \geqslant 1/2$, $E_k(1,\omega)$ approaches some positive value as K becomes large. The significance of this

$$\sum_{k=-\infty}^{\infty} \sigma_I^2(\omega, \phi + \frac{k}{\gamma} + \phi_0) \text{ Rect}\left|\frac{\phi + k/\gamma}{\Phi}\right| =$$

$$\sigma_I^2(\omega) \left\{ (2k_0 + 1) + \text{Rect}\left[\frac{\phi - \alpha}{\frac{1}{2}(\Phi - \frac{n}{2\gamma})}\right] + \text{Rect}\left[\frac{\phi + \alpha}{\frac{1}{2}(\Phi - \frac{n}{2\gamma})}\right] \right\}$$

$$= \sigma_I^2(\omega) \left\{ n + \text{Rect}\left[\frac{\phi - \alpha}{\frac{1}{2}(\Phi - \frac{n}{2\gamma})}\right] + \text{Rect}\left[\frac{\phi + \alpha}{\frac{1}{2}(\Phi - \frac{n}{2\gamma})}\right] \right\} \qquad \text{(F-13)}$$

where

$$\alpha = \frac{\frac{3}{2}n + 1}{2\gamma} - \frac{3}{2}\Phi \qquad \text{(F-14)}$$

Integrating this as in F-8 gives

$$\exp\left[\frac{1}{2\pi}\int_{-\pi}^{\pi} \ell n \, H_f(x)dx\right] = \sigma_n^2(\omega) \left\{ \gamma \int_{-\frac{1}{2\gamma}}^{\frac{1}{2\gamma}} \ell n\left[1 + \frac{n\sigma_I^2(\omega)}{\sigma_n^2(\omega)\gamma}\right] d\phi \right.$$

$$+\gamma \int_{-\frac{1}{2\gamma}}^{\frac{n+1}{2\gamma} - \Phi} \ell n\left[1 + \frac{\sigma_I^2(\omega)/\sigma_n^2(\omega)\gamma}{1 + \left[\frac{n\sigma_I^2(\omega)}{\sigma_n^2(\omega)\gamma}\right]}\right] d\phi + \gamma \int_{\Phi - \frac{n+1}{2\gamma}}^{\frac{1}{2\gamma}} \ell n\left[1 + \frac{\sigma_I^2(\omega)/\sigma_n^2(\omega)\gamma}{1 + \left[\frac{n\sigma_I^2(\omega)}{\sigma_n^2(\omega)}\right]}\right] d\phi$$

$$= \left[\sigma_n^2(\omega) + \frac{n\sigma_I^2(\omega)}{\gamma}\right] \left[1 + \frac{\sigma_I^2(\omega)}{\sigma_n^2(\omega)\gamma + n\sigma_I^2(\omega)}\right]^{\gamma\Phi - \frac{n}{2}} \left[1 + \frac{\sigma_I^2(\omega)}{\sigma_n^2(\omega)\gamma + n\sigma_I^2(\omega)}\right]^{\gamma\Phi - \frac{n}{2}}$$

$$\text{(F-15)}$$

which is the same as (F-8). Therefore, n odd yields the same result.

fact can be appreciated by observing Figure F-3, which shows $E_\infty(1,\omega)$ as a
function of $\gamma\phi$ for $\gamma\phi \gtrsim 1/2$. Clearly, when $\gamma\phi > 1/2$ the cancellation of the
extended source is extremely limited. The condition $\gamma\phi < 1/2$ is therefore a
spatial Nyquist condition, with

$$\gamma = \frac{d}{\lambda} \sin \phi_0$$

the spatial sample interval, and ϕ, the source extent, analogous to bandwidth
in the temporal case. This result should be no surprise given the equiva-
lence of the temporal linear prediction problem and the spatial cancellation
problem developed in Appendix D.
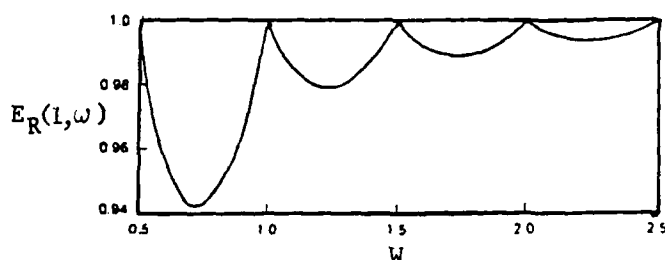
Figure F-3. Irreducible Canceller Output Power
vs. W for Uniform Extended Source
in Noise Free Case

Using the Strong Szego Limit Theorem for Circular Arcs [12], as discussed
in Appendix D, it is possible to determine the asymptote in K of $E_K(1, \omega)$
for the uniform, narrow, spatially uncorrelated source. For this source in
the noise free case the hydrophone CSD is, from Appendix A.

$$S_{k(\omega)} = s_e(p, p+k, \omega)$$

$$= \sigma_I^2(\omega) \frac{\sin[2\pi(p,q)W]}{\pi(p-q)\gamma} \tag{F-19}$$
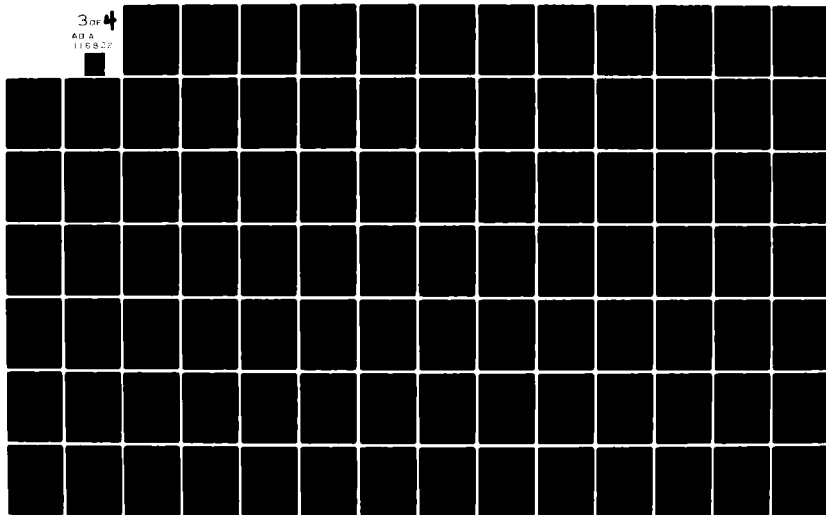
But from (D-38)

$$S_k(\omega) = \frac{1}{2\pi} \int_{-\pi}^{\pi} H_e(\alpha, \omega) e^{jk\alpha} d\alpha$$

so if $\gamma\Phi < \pi$, choosing

$$H_e(\alpha, \omega) = \frac{\sigma_I^2(\omega)}{\gamma} \text{Rect}\left[\frac{\alpha}{4\pi\omega}\right], \quad \alpha\epsilon[-\pi, \pi] \tag{F-20}$$

where

$$\text{Rect}\left[\frac{t}{T}\right] = \begin{cases} 1, \ t\epsilon\left[\frac{T}{2}, \frac{T}{2}\right] \\ 0, \ elsewhere \end{cases}$$

yields the correct $S_k(\omega)$. This function, $H_e(\alpha, \omega)$ satisfies the conditions of the Strong Szego Limit Theorem, stated as Theorem 5a in Appendix D, so that

$$E_k(1, \omega) \sim G(\omega)\left[\sin \pi\gamma\Phi\right]^{2K+1} \tag{F-21}$$

where $\sim$ denotes asymptotic in K and, from (D-58),

$$G(\omega) = \exp\left[\frac{1}{2\pi}\int_{-\pi}^{\pi} \log\left[\frac{\sigma_I^2(\omega)}{\gamma} \text{Rect}\left\{\frac{\hat{2}\sin^{-1}[\sin(\pi W)\cos\theta]}{4\pi W}\right\}\right] d\theta\right.$$

$$\tag{F-22}$$

where

$$\text{Rect} \left\{ \frac{2 \sin^{-1}[\sin(\pi W) \cos \theta]}{4\pi W} \right\} = \begin{cases} 1, & |2\sin^{-1}[\sin(\pi W)\cos \theta]| \leq 2\pi W \\ 0, & \text{otherwise} \end{cases} \qquad \text{(F-23)}$$
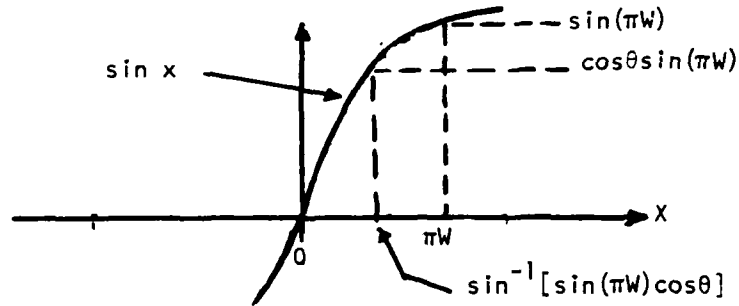
Figure F-4. Relationship Between πW
and $\sin^{-1}[\sin(\pi W) \cos \theta]$

But from Figure F-4, it can be seen that

$$\sin^{-1}[\sin(\pi W) \cos \theta] \leq |\pi W|, \quad \text{all } \theta \epsilon(-\pi, \pi)$$

or

$$2\sin^{-1}[\sin(\pi W) \cos \theta] \leq |2\pi W|, \text{ all } \theta \epsilon[-\pi, \pi)$$

which implies that

$$G(\omega) = \exp \left[\frac{1}{2\pi} \int_{-\pi}^{\pi} \log \frac{\sigma_I^2(\omega)}{\gamma} \, d\theta \right] = \frac{\sigma_I^2(\omega)}{\gamma} \qquad \text{(F-24)}$$

so that

$$E_K(1,\omega) \sim \frac{\sigma_I^2(\omega)}{\gamma} \left[\sin \pi W \right]^{2K+1} \qquad \text{(F-25)}$$

Thus for large K, the canceller output spectrum goes to zero exponentially in K, with the rate dependent upon $\sin(\pi W)$.

F.2 Interference Plus Noise Case

When ambient noise is present, the change in the irreducible canceller output spectrum, $E_\infty(1,\omega)$, as W transitions from $W < \frac{1}{2}$ to $W \geq \frac{1}{2}$ is not quite as dramatic, but still supports the notion of $W = \frac{1}{2}$ as a spatial Nyquist criterion, particularly at high interference to noise ratios. Figures F-5, F-6, F-7, and F-8 show

$$E_R(1,\omega) = \frac{E_\infty(1,\omega)}{2\Phi\sigma_I^2(\omega)} \qquad (F-26)$$

as a function of W for interference to noise ratios of 40, 30, 20, and 10 dB, respectively. The interference to noise ratio is defined as

$$INR = \frac{2\Phi\sigma_I^2(\omega)}{\sigma_n^2(\omega)} \qquad (F-27)$$

When noise is present it can be seen that it may be necessary to choose W significantly less than 1/2 to achieve acceptable cancellation, even with a larte number of reference hydrophones. Of course, from Appendix D, the extended source cannot be cancelled to the noise floor when $\sigma_n^2(\omega) \neq 0$.

For high interference-to-noise ratio, $2\Phi\sigma_I^2(\omega)/\sigma_n^2(\omega) >> 1$, so that in (F-10) for $n \geq 1$

$$S \approx n \qquad (F-28)$$

and (F-9) is approximately

$$E_\infty(1,\omega) \approx \frac{2\Phi\sigma_I^2(\omega)}{2\omega} \, n \left(1 + \frac{1}{n}\right)^{2\omega - n} \qquad (F-29)$$
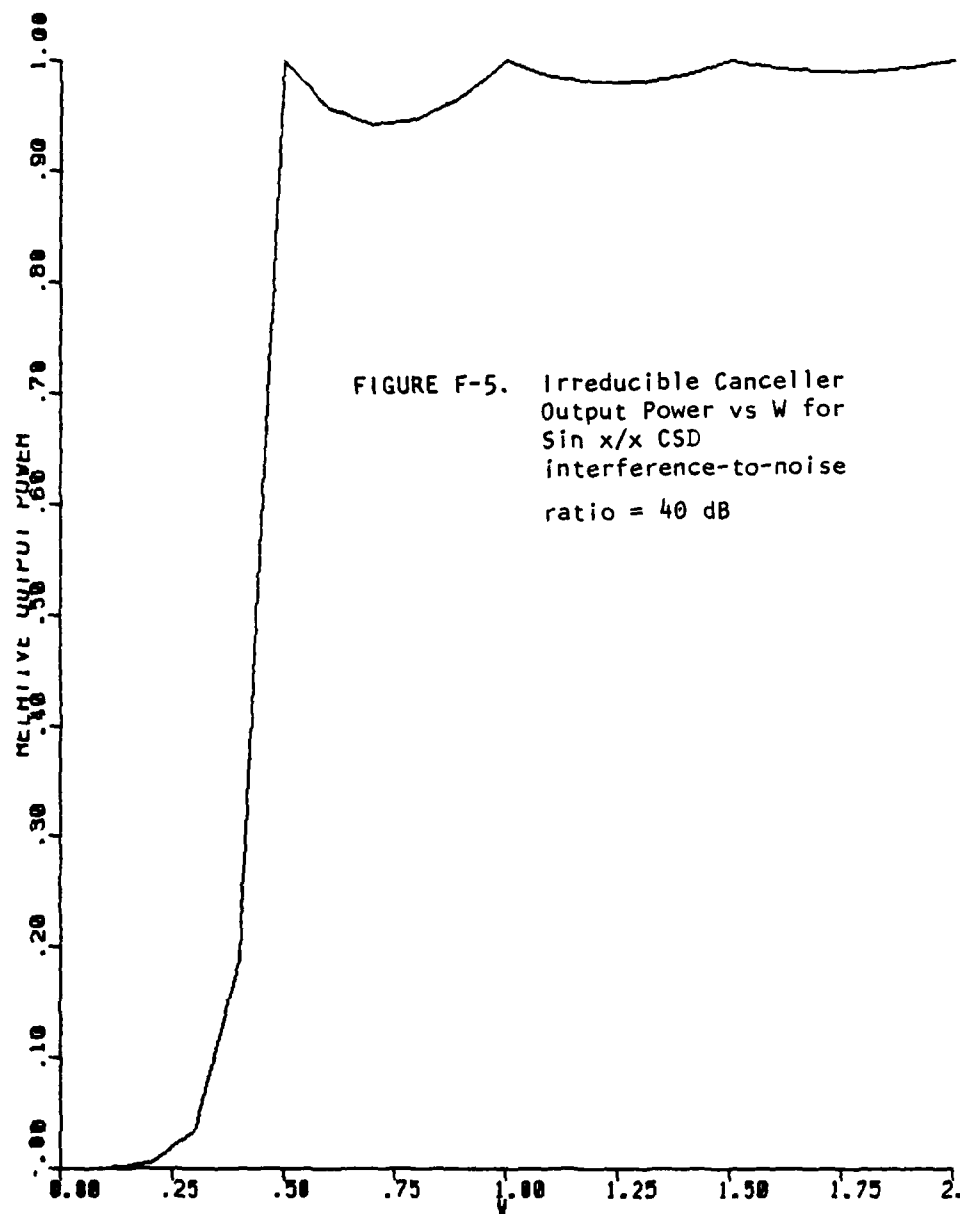
FIGURE F-5. Irreducible Canceller Output Power vs W for Sin x/x CSD interference-to-noise

ratio = 40 dB
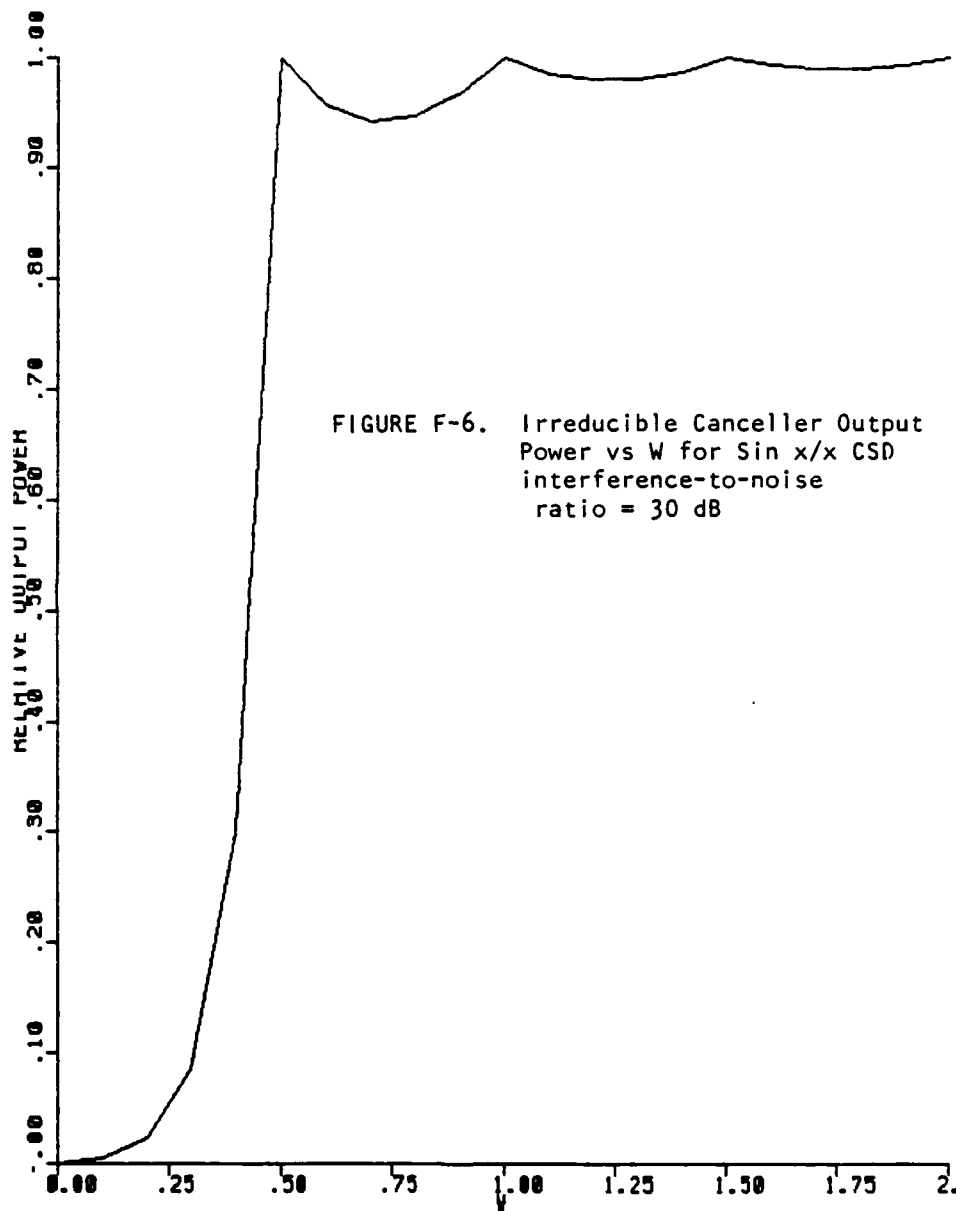
FIGURE F-6.   Irreducible Canceller Output Power vs W for Sin x/x CSD interference-to-noise ratio = 30 dB
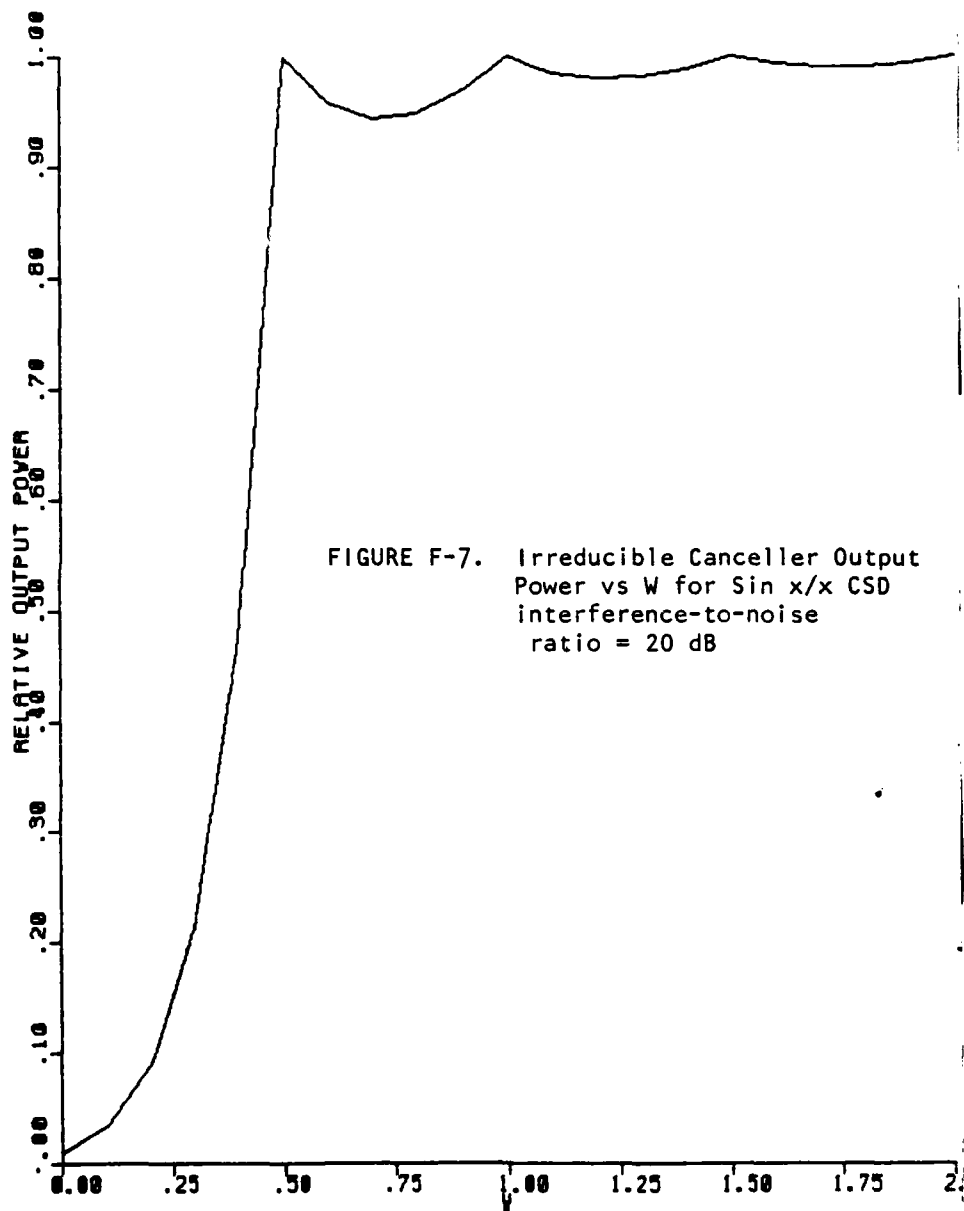
FIGURE F-7.   Irreducible Canceller Output
Power vs W for Sin x/x CSD
interference-to-noise
ratio = 20 dB

FIGURE F-8. Irreducible Canceller Output
Power vs W for Sin x/x CSD
interference-to-noise
ratio = 10 dB
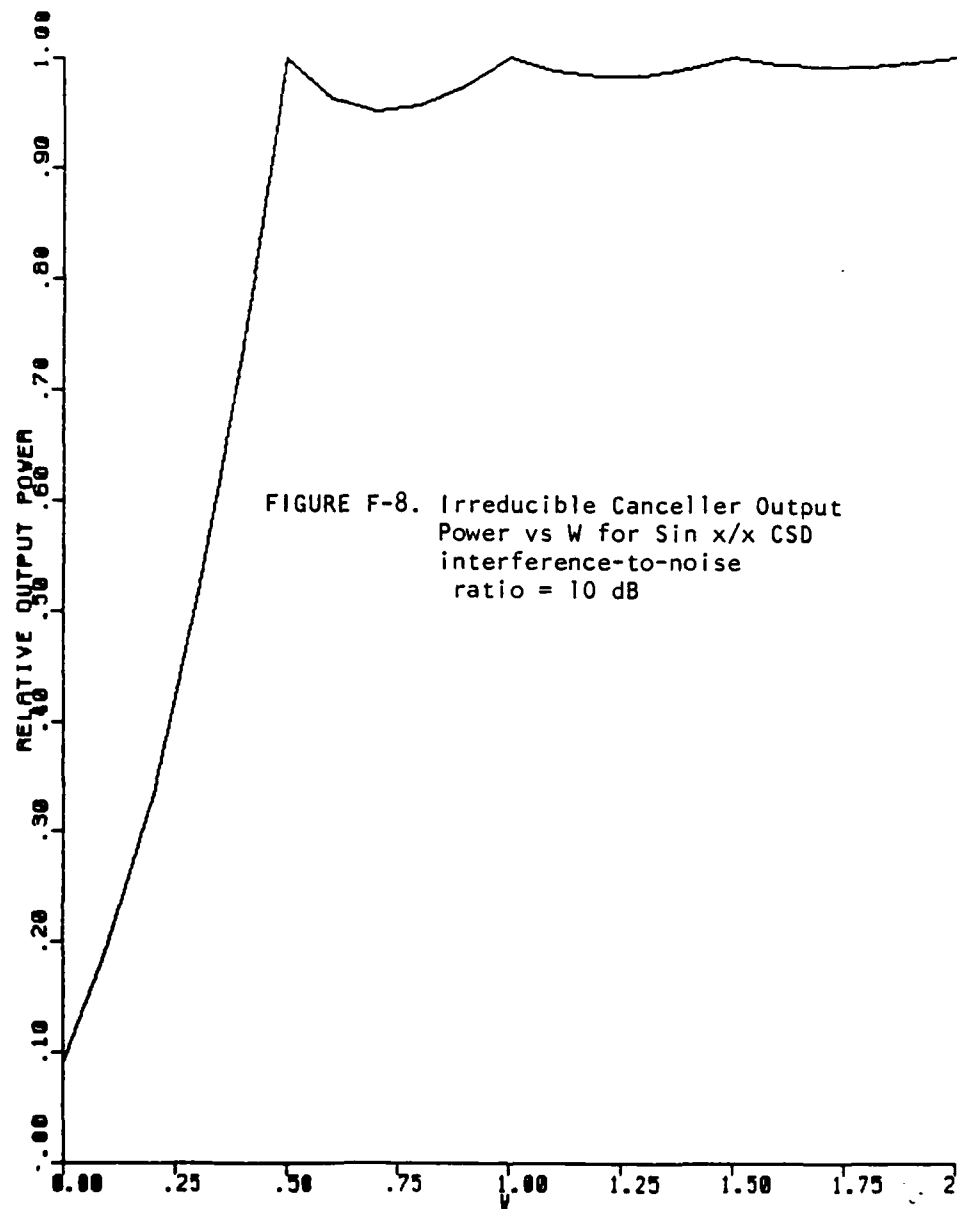
Hence, for high INR and $\gamma \Phi \geq 1/2$ ($n \geq 1$), the interference plus noise case reduces approximately to the noise free case.

APPENDIX G: CANCELLATION OF A SOURCE PRODUCING AN
EXPONENTIAL HYDROPHONE CROSS-SPECTRAL DENSITY MATRIX

APPENDIX G: CANCELLATION OF A SOURCE PRODUCING AN EXPONENTIAL HYDROPHONE CROSS-SPECTRAL DENSITY MATRIX
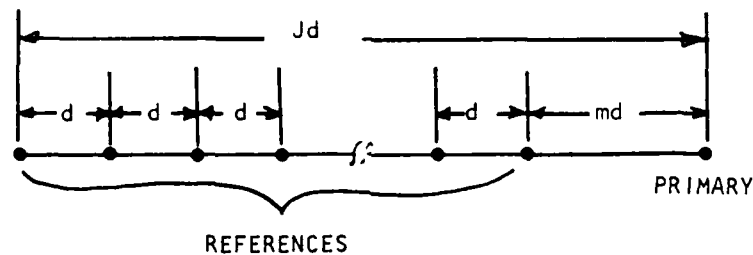
Figure G-1: Array Geometry for Cancellation

Consider a line array of K reference sensors used to cancel, in the minimum mean square sense, an interference from the output of a primary hydrophone which lies along the same line as the references. Let the references be spaced d feet apart, and let the space between the nearest reference and the primary be md feet, as shown in Figure G-1. Suppose that the ambient noise field produces zero mean noise with spectral density, $\sigma_n^2(\omega)$, at the hydrophones, uncorrelated from hydrophone to hydrophone. In addition, the noise field contains an extended interference which produces zero mean noise at each hydrophone with the cross-spectral density between hydrophones spaced kd apart given by

$$\sigma_I^2(\omega)e^{-B(\omega)|k|d} \tag{G-1}$$

Then the cross-spectral density (CSD) between the pth and q^{th} hyrdophone outputs is

$$s_e(p,q,\omega) = \sigma_n^2(\omega)\delta_{pq} + \sigma_I^2(\omega)e^{-B(\omega)|p-q|d} \tag{G-2}$$

while the CSD between the pth reference and the primary is

$$s_e(p,J,\omega) = \sigma_I^2(\omega)e^{-B(\omega)|p-J|d} \qquad (G-3)$$

Appendix C developed the power spectral density of the minimum mean square canceller using K references as

$$E_K(\omega) = \frac{\det [S_H(K,\omega)]}{\det [S_e(K,\omega)]} \qquad (G-4)$$

where

$$S_e(K,\omega) = \left(s_e(p,q)\right)_{\substack{p=0,1,\ldots K-1 \\ p=0,1,\ldots K-1}} \qquad (G-5)$$

and

$$S_H(K,\omega) = \begin{bmatrix} S_e(K,\omega) & \underline{s}_1(K,\omega) \\ & \\ \underline{s}_1^+(K,\omega) & S_{11}(\omega) \end{bmatrix} \qquad (G-6)$$

with

$$\underline{s}_1(K,\omega) = [s_e(o,J,\omega), s_e(1,J,\omega),\ldots, s_e(K-1,J,\omega)]^T \qquad (G-7)$$

$$S_{11}(\omega) = \sigma_n^2(\omega) + \sigma_I^2(\omega) \qquad (G-8)$$

For the model being considered here, it can be seen that

$$S_e(K,\omega) = \sigma_I^2(\omega) \begin{bmatrix} \beta+\rho^0 & \rho^1 & \rho^2 & \rho^{K-2} & \rho^{K-1} \\[6pt] \rho^1 & \beta+\rho^0 & \rho^1 & \rho^{K-3} & \rho^{K-2} \\[6pt] \rho^2 & \rho^1 & \beta+\rho^0 & \rho^{K-4} & \rho^{K-3} \\[12pt] & & & \beta+\rho_o & \rho^1 \\[6pt] \rho^{K-1} & \rho^{K-2} & \rho^{K-3} & \rho^1 & \beta+\rho^0 \end{bmatrix} \qquad \text{(G-9)}$$

with

$$\beta = \sigma_n^2/\sigma_I^2$$

$$\rho = e^{-Bd}$$

and

$$S_H(K,\omega) = \sigma_I^2(\omega) \left[\left[\frac{1}{\sigma_I^2(\omega)} S_e(K,\omega) \right] \begin{matrix} \rho^{m+K-1} \\ \rho^{m+K-2} \\ \cdot \\ \cdot \\ \cdot \\ \rho^m \end{matrix} \atop \begin{matrix} \rho^{m+K-1} & \rho^{m+K-2} & \ldots & \rho^m & \beta+\rho^0 \end{matrix} \right] \qquad \text{(G-10)}$$

G.1 Special Case: m = 1

In the special case where m = 1, both $S_e(K,\omega)$ and $S_H(K,\omega)$ are Toeplitz matrices. This allows use of the results of Szego[15], as discussed in Appendix D, to determine the irreducible canceller output power for the LMS canceller with a source producing an exponential CSD. It will be convenient in this Appendix to explicitly indicate the value of m in the notation for the canceller output power, so let

$$E_K(m,\omega) = E_K(\omega) \Big|_{md} = \text{distance between reference array and primary}$$

From Appendix D, let

$$S_k = S_e(p,p+k,\omega) \qquad \text{any } p$$

so that

$$S_{eo}(K,\omega) = \begin{bmatrix} S_0 & S_1 & S_2 & \cdots & S_{k-1} \\ S_{-1} & S_0 & S_1 & \cdots & S_{k-2} \\ \vdots & \vdots & & & \vdots \\ \vdots & \vdots & & & \vdots \\ S_{-k} & S_{-k+1} & \cdots & & S_0 \end{bmatrix}$$

Then from Appendix D, the irreducible canceller output power at frequency ω is

$$E_\infty(1,\omega) = \lim_{K \to \infty} E_K(1,\omega)$$

$$= \exp\left(\frac{1}{2\pi} \int_{-\pi}^{\pi} \ln H_e(\alpha,\omega)d\alpha\right)$$

where

$$H_e(\alpha,\omega) = \sum_{k=-\infty}^{\infty} S_k e^{jk\alpha}$$

In the special case of an exponential CSD, (G-2),

$$S_k = \beta\delta(k) + \rho^{|k|}$$

with

$$\delta(k) = \begin{cases} 1, & k=0 \\ \\ 0, & \text{otherwise} \end{cases}$$

then

$$\det\,[S_H(K,\omega)] = [\sigma_I^{\,2}(\omega)]^{K+1}\det\,[S_e(K+1,\omega)],$$

$$\det\,[S_e(K,\omega)] = [\sigma_I^{\,2}(\omega)]^K\,\det\,[S_e(K,\omega)];$$

and

$$H_e(\alpha,\omega) = \beta + \sum_{k=-\infty}^{\infty} \rho^{|k|}e^{jk\alpha}$$

$$= \beta + \frac{1-\rho^2}{1-2\,\rho\cos\,\alpha+\rho^2} \qquad\qquad\text{(G-14)}$$

$$= \frac{\beta(1+\rho^2) + (1-\rho^2) - 2\beta\rho\cos\alpha}{1-2\rho\cos\alpha+\rho^2}$$

therefore

$$\ln H_e(\alpha,\omega) = -\ln(1+\rho^2) - \ln(1 - \frac{2\rho}{1+\rho^2} \cos \alpha)$$

$$+ \ln [\beta(1+\rho^2) + (1-\rho^2)] + \ln (1 - \frac{2 \beta\rho}{\beta(1+\rho^2) + (1-\rho^2)} \cos\alpha)$$

(G-15)

Fortunately,

$$\int_{-\pi}^{\pi} \ln [1-A\cos \alpha] d\alpha = 2\pi\ln \left[\frac{1+ \sqrt{1-A^2}}{2}\right]$$

(G-16)

so

$$\frac{1}{2\pi} \int_{-\pi}^{\pi} \ln [1 - \frac{2\rho}{1+\rho^2} \cos\alpha] d\alpha = \ln \left[\frac{1 + \sqrt{1-\left(\frac{2\rho}{1+\rho^2}\right)^2}}{2}\right]$$

(G-17)

and

$$\frac{1}{2\pi} \int_{-\pi}^{\pi} \ln \left[1 - \frac{2\beta\rho}{\beta(1+\rho^2) + (1-\rho^2)} \cos \alpha\right] d\alpha = \ln\left[\frac{1 + \sqrt{1 - \left(\frac{2\beta\rho}{\beta(1+\rho^2) + (1-\rho^2)}\right)^2}}{2}\right]$$

(G-18)

Then

$$\frac{1}{2\pi} \int_{-\pi}^{\pi} \ln H(\alpha)d\alpha = -\ln(1+\rho^2) - \ln\left[\frac{1 + \sqrt{1 - \left(\frac{2\rho}{1+\rho 2}\right)^2}}{2}\right]$$

$$+ \ln\left[\beta(1+\rho^2) + (1-\rho^2)\right] + \ln\left[\frac{1 + \sqrt{1 - \left(\frac{2\beta\rho}{(1+\rho^2) + (1-\rho^2)}\right)^2}}{2}\right]$$

$$= -\ln\left[\frac{(1+\rho^2) + \sqrt{(1+\rho^2)^2 - (2\rho)^2}}{2}\right]$$

$$+ \ln\left[\frac{\beta(1+\rho^2) + (1-\rho^2) + \sqrt{[\beta(1+\rho^2) + (1-\rho^2)]^2 - (2\beta\rho)^2}}{2}\right]$$

$$= \ln\left[\frac{\beta(1+\rho^2) + (1-\rho^2) + \sqrt{[\beta(1+\rho^2) + (1-\rho^2)]^2 - (2\beta\rho)^2}}{2}\right] \qquad \text{(G-19)}$$

Therefore

$$E_\infty(1,\omega) = \frac{[\sigma_I^2(\omega)]^{K+1} \det[S_e(K+1,\omega)]}{[\sigma_I^2(\omega)]^K \det[S_e(K,\omega)]}$$

$$= \sigma_I^2(\omega)\exp\left[\frac{1}{2\pi}\int_{-\pi}^{\pi}\ln H_e(\alpha,\omega)d\alpha\right]$$

$$= \sigma_I^2(\omega)\frac{\beta(1+\rho^2) + (1-\rho^2) + \sqrt{[\beta(1+\rho^2) + (1-\rho^2)]^2 - (\beta\rho)^2}}{2}$$

$$\qquad \text{(G-20)}$$

Now as $\rho \to o$ (for example, as the hydrophones move farther apart, $d \to \infty$),

$$\lim_{\rho \to o} E_\infty(1,\omega) = \sigma_I^2(\omega) \frac{\beta+1 + \sqrt{(\beta+1)^2}}{2} = \sigma_I^2(\omega) + \sigma_n^2(\omega) \qquad (G-21)$$

which shows that there is no cancellation, as would be expected. On the other hand, as $\rho \to 1$, the references become coincident with the primary and

$$\lim_{\rho \to 1} E_\infty(1,\omega) = \sigma_n^2(\omega) \qquad (G-22)$$

which indicates perfect cancellation.

Next, consider $\beta \to o$, indicating the noise free (interference only) case. Then

$$\lim_{\beta \to o} E_\infty(1,\omega) = \sigma_I^2(\omega) (1 - \rho^2) \qquad (G-23)$$

Therefore, even in the absence of a noise floor, the interference is not cancelled completely. This is a significant difference between the exponential cross-spectral density and the sin x/x CSD considered in Appendix F.

G.2 General Case; m>1

Return to equation (G-10), and observe that if the Kth column of $S_H(K,\omega)$ is multiplied by ρ^m and subtracted from the last column (which does not change the determinant), it becomes

$$\sigma_I^2(\omega) \begin{bmatrix} \begin{bmatrix} & & & \\ & & \frac{S_e(K,\omega)}{\sigma_I^2(\omega)} & \\ & & & \\ \rho^{m+K-1} & \cdots & \rho^m & \end{bmatrix} \begin{matrix} o \\ o \\ \vdots \\ \vdots \\ o \\ -\beta\rho^m \\ \beta+\rho^o-\rho^{2m} \end{matrix} \end{bmatrix} \qquad \text{(G-24)}$$

Repeating this on the Kth row and the last row gives

$$\sigma_I^2(\omega) \begin{bmatrix} \begin{bmatrix} & & & \\ & & \frac{S_e(K,\omega)}{\sigma_I^2(\omega)} & \\ & & & \\ o \; o & \cdots & o \; -\beta\rho^m & \end{bmatrix} \begin{matrix} o \\ o \\ \vdots \\ \vdots \\ o \\ -\beta\rho^m \\ (\beta + \rho^o - \rho^{2m} + \beta\rho^{2m}) \end{matrix} \end{bmatrix} \qquad \text{(G-25)}$$

Under these operations, the determinant is unchanged, so det $[S_H(K,\omega)]$ is equal to the determinant of (G-25), which is easily shown to be

$$\det[S_H(K,\omega)] = [\sigma_I^2(\omega)] \; [\beta(1+\rho^{2m}) + (1-\rho^{2m})] \; \det[S_e(K,\omega)]$$

$$- [\sigma_I^2(\omega)]^2 \; \beta^2 \; \rho^{2m} \; \det[S_e(K-1,\omega)] \qquad \text{(G-26)}$$

then

$$E_K(m,\omega) = \frac{\det [S_H(K,\omega)]}{\det [S_e(K,\omega)]}$$

$$= \sigma_I^2(\omega)[\beta(1+\rho^{2m}) + (1-\rho^{2m})] \; [\sigma_I^2(\omega)]^2 \beta^2 \rho^{2m} \; \frac{\det [S_e(K-1,\omega)]}{\det [S_e(K,\omega)]}$$

$$\text{(G-27)}$$

The limit of the ratio of determinants, using (G-12) and (G-14) is

$$\lim_{K \to \infty} \frac{\det\ [S_e(K-1,\omega)]}{\det\ [S_e(K,\omega)]} = [\sigma_I^2(\omega)]^{-1} \exp\left[-\frac{1}{2\pi}\int_{-\pi}^{\pi} \ln\ H_e(\alpha,\omega)d\alpha\right]$$

$$= [\sigma_I^2(\omega)]^{-1}\left[\frac{\beta(1+\rho^2) + (1-\rho^2) + \sqrt{[\beta(1+\rho^2) + (1-\rho^2)]^2 - (2\beta\rho)^2}}{2}\right]^{-1} \tag{G-28}$$

Therefore

$$E_\infty(m,\omega) = \sigma_I^2(\omega)\left\{[\beta(1+\rho^{2m}) + (1-\rho^{2m})]\right.$$

$$\left. - \frac{2\beta^2\rho^{2m}}{\beta(1+\rho^2) + (1-\rho^2) + \sqrt{[\beta(1+\rho^2) + (1-\rho^2)]^2 - (2\beta\rho)^2}}\right\} \tag{G-29}$$

When m = 1, this reduces to (20), as it should.

Now, when $\rho \to o$, this goes to

$$\lim_{\rho \to o} E_\infty(m,\omega) = \sigma_I^2(\omega)\ [\beta+1] = \sigma_I^2(\omega) + \sigma_n^2(\omega) \tag{G-30}$$

again indicating no cancellation, as would be expected. When $\rho \to 1$,

$$\lim_{\rho \to 1} E_\infty(m,\omega) = \sigma_n^2(\omega) \tag{G-31}$$

which shows that the interference is completely cancelled when one of the references is coincident with the primary. Finally, when $\beta \to o$, the noise free case,

$$\lim_{\beta \to o} E_\infty(m,\omega) = \sigma_I^2(\omega)[1-\rho^{2m}] \tag{G-32}$$

The fact that the canceller output power has the lower bound $(1-\rho^{2m})$ $\sigma_I^2(\omega)$ in the noise free case can be explained in terms of the special nature of the exponential CSD. The sequence of reference hydrophone outputs at a single frequency can be shown to be a first order Markov sequence. As a result, in the noise free case, the optimal canceller uses only the output of the reference closest to the primary and achieves the bound $(1-\rho^{2m})$ $\sigma_I^2(\omega)$ with that single reference. Adding further references does not reduce the canceller output power.

The amount of cancellation achieved by the canceller is best characterized by the minimum relative canceller output power, given by

$$E_R(m,\omega) = \frac{E_\infty(m,\omega)}{\sigma_I^2(\omega) + \sigma_n^2(\omega)} \qquad (G-33)$$

where $\sigma_I^2(\omega) + \sigma_n^2(\omega)$ is the output power of the primary hydrophone without cancellation. Noting that

$$\sigma_I^2(\omega) + \sigma_n^2(\omega) = \sigma_I^2(\omega)\,(1 + \beta)$$

gives

$$E_R(m,\omega) = \frac{1}{1+\beta}\left\{ [\beta(1+\rho^{2m}) + (1-\rho^{2m})] - \right.$$

$$\left. - \frac{2\beta^2\rho^{2m}}{\beta(1+\rho^2) + (1-\rho^2) + \sqrt{[\beta(1+\rho^2) + (1-\rho^2)]^2 - (2\beta\rho)^2}} \right\} \qquad (G-34)$$

Figures G-2 through G-6 plot the minimum relative error given by (34) as a function of ρ for values of 10 log $(1/\beta)$ of 50, 40, 30, 20, and 10 dB respectively. It can be seen that cancellation to near the noise floor, $\sigma_n^2(\omega)$, requires that the primary and references be very highly correlated. This is again due to the Markov nature of the hydrophone outputs under the exponential CSD. At high interference to noise ratio, the optimal canceller uses only the reference closest to the primary and the output power is proportional to $(1-\rho^{2m})$. Additional references have no effect, so the canceller depends completely on the proximity of the closest reference to the primary to achieve cancellation. Hence, ρ must be very close to unity to produce cancellation to near the noise floor. Again the curves in Figures 2 through 6 approach $\beta/(1+\beta) = \sigma_n^2(\omega)/(\sigma_I^2(\omega)+\sigma_n^2(\omega))$ as $\rho \to 1$ because the model maintains the ambient noise as uncorrelated from hydrophone to hydrophone, regardless of ρ.

G.3 Comparison With Results for Sin X/X Cross-Spectral Density

Appendix F considered the line array structure of Figure G-1 with an extended source producing the hydrophone CSD,

$$s_e(p,q,\omega) = \sigma_n^2(\omega)\,\delta_{pq} + \sigma_I^2(\omega)\,\frac{\sin[(p-q)\,\frac{\omega d}{c}\,\phi\,\sin\,\phi_o]}{\frac{1}{2}[(p-q)\,\frac{\omega d}{c}\,\sin\,\phi_o]} \qquad (G-35)$$

This represents a uniform source with angular extent $\pm\phi$ about the angle ϕ_o, in the same plane as the line array. For convenience, let

$$\gamma = \frac{d}{\gamma}\,\sin\,\phi_o \qquad (G-36)$$

and

$$W = \phi\gamma \qquad (G-37)$$

FIGURE G-2. Minimum Canceller
Output Power vs ρ
for various m

interference-to-noise ratio= 50 dB

FIGURE G-3. Minimum Canceller Output Power vs ρ for various m

interference-to-noise ratio = 40 dB

G-14

Figure G-4. Minimum Canceller
Output Power vs ρ
for various m
interference-to-noise ratio = 30 dB

G-15

FIGURE G-5. Minimum Canceller Output Power vs ρ for various m

interference-to-noise ratio = 20 dB

FIGURE G-6. Minimum Canceller
Output Power vs ρ
for various m

interference-to-noise ratio = 10 dB

so that G-35 can be written

$$s_e(p,q,\omega) = \sigma_n^2(\omega)\, \delta_{pq} + \sigma_I^2(\omega)\, \frac{\sin\,[2\pi\,(p-q)W]}{\pi(p-q)\gamma} \qquad (G\text{-}38)$$

The minimum canceller output spectrum for this CSD has been determined explicitly only for the case m = 1. In the noise free case, using the results of Widom [12], it has been shown that in the absence of ambient noise, $\sigma_n^2(\omega) = 0$, the canceller output spectrum, $E_K(1,\omega)$, approaches zero exponentially with the number of references, K, if W < 1/2. Then the minimum canceller output spectrum is

$$E_\infty(1,\omega) = 0; \quad \sigma_n^2(\omega) = 0, \ W < 1/2 \qquad (G\text{-}39)$$

Note that $W = \gamma\phi$ is analogous to the product $B(\omega)d$ in the exponential case. The result given in (G-39) is a significant difference between the sin x/x CSD and the exponential, which gave

$$E_\infty(1,\omega) = \sigma_I^2(\omega)\,(1-\rho^2)\ ;\ \sigma_n^2(\omega) = 0 \qquad (G\text{-}40)$$

regardless of $B(\omega)d$. This difference is due to the Markov property underlying the exponential CSD.

In the noise free case, $\sigma_n^2(\omega) = 0$, when $\frac{n}{2} \le W \le \frac{n+1}{2}$ for n = 1, 2. ..., the minimum canceller output spectrum is given by

$$E_\infty(1,\omega) = 2\phi\,\phi_I^2(\omega)\, n(1+\tfrac{1}{n})^{2W-n} \qquad (G\text{-}41)$$

The primary hydrophone output spectrum without cancellation is $2\Phi\sigma_s^2(\omega)$ so that the relative canceller output power for the sin x/x CSD is

$$E_R(1,\omega) = n(1 + \frac{1}{n})^{2W-n} \tag{G-42}$$

This is plotted in Figure G-7 for n=1 through n=5, and shows that cancellation is severely limited if $W \geq 1/2$. This sampling criterion in the noise free case does not have an analog in the case of the exponential CSD. On the other hand, when $B(\omega)d > 1/2$, analogous to $W > 1/2$, then $\rho < .606$ and the cancellation for the exponential CSD is

$$E_R(1,\omega) \geq (1-\rho^2) = .632$$

so that significant cancellation is not achieved in the exponential case either. The degradation is much more graceful in the exponential case, however.
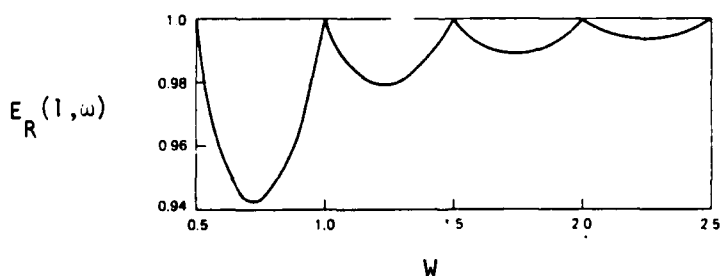
Figure G-7. Minimum Canceller Output Power
vs. W. for Sin x/x CSD, m = 1
Interference-to-Noise Ratio = +∞

Of course, the case when noise is present is of much greater interest. It is shown in Appendix F that for m=1, with noise present the CSD given in (G-38) yields

$$E_{\infty}(1,\omega) = \frac{2\Phi \sigma_I^2(\omega)}{2W} \, S(1 + \frac{1}{S})^{2W-n} \tag{G-43}$$

for

$$\frac{n}{2} < W < \frac{n+1}{2} \, , \; n = 0, 1, 2 \ldots \tag{G-44}$$

and

$$S = n + \frac{2W \, \sigma_n^2(\omega)}{2\Phi \sigma_I^2(\omega)} \tag{G-45}$$

For high interference to noise ratio, $2\Phi \sigma_I^2(\omega)/\sigma_n^2(\omega) \gg 1$,

$$S \approx n, \quad n = 1, 2, \ldots$$

so that for $n > 1$, this reduces approximately to the noise free case, (G-42). For $W < 1/2$

$$E_{\infty}(1,\omega) = \sigma_n^2(\omega) \left(1 + \frac{2\Phi \sigma_I^2(\omega)}{2W\sigma_n^2(\omega)} \right)^{2W} \, , \; W < 1/2 \tag{G-46}$$

When $W = 0$,

$$E_{\infty}(1,\omega) = \sigma_n^2(\omega) \tag{G-47}$$

indicating cancellation to the ambient noise floor, and when W = 1/2

$$E_R(1,\omega) = \sigma_n^2(\omega) + 2\Phi\ \sigma_I^2(\omega) \qquad\qquad (G\text{-}48)$$

so that no cancellation occurs.

It appears that the parameter $B(\omega)d$ in the exponential case and $W = \dfrac{d}{\lambda}\ \Phi\ \sin\ \phi_0$ in the sin x/x case play a similar role, relating the distance between hydrophones (spatial sampling interval) to the source extent (Φ) or the CSD bandwidth, $B(\omega)$. Therefore, in order to compare the behavior of the optimal canceller with the two CSD's the irreducible relative canceller output power, $E_R(1,\omega)$ was computed as a function of $B(\omega)d$ and W, respectively, using (G-34) and (G-43). Figures G-8 through G-11 show $E_R(1,\omega)$ for the exponential CSD for interference to noise ratios of 40 dB, 30 dB, 20 dB, and 10 dB for $B(\omega)d$ varying between 0.0 and 2.0. Figures F-5 through F-8 show $E_R(1,\omega)$ for the sin x/x CSD for the same range of INR with W varying from 0.0 to 2.0. The following observations may be made regarding the figures, letting $W = B(\omega)d$ for convenience;

  (a) If $W \geq 1/2$ in the sin x/x case, virtually no cancellation is achievable, as already observed.   No such sampling criterion is apparent for the exponential case, but cancellation is still severely limited for $B(\omega)d \geq 1/2$. Either CSD requires a value of W much smaller than 1/2 if the canceller is to produce cancellation in the 10 to 40 dB range.

  (b) The optimal canceller produces better results for the exponential CSD for W larger than approximately 0.4. However, in the important region of small W, producing more than 10 dB of

FIGURE G-8. Minimum Canceller Output Power
vs W = B(ω)d for Exponential
CSD, m=1

interference-to-noise ratio = 40 dB

FIGURE G-9. Minimum Canceller Output
Power vs W=B(ω)d for
Exponential CSD, m=1

interference-to-noise ratio = 30 dB

FIGURE G-10. Minimum Canceller Output Power
vs W=B(ω)d for Exponential CSD,
m=1

INTERFERENCE-TO-NOISE RATIO = 20 dB

FIGURE G-11. Minimum Canceller Output Power
vs W=B(ω)d for Exponential CSD
m=1

interference-to-noise ratio = 10 dB
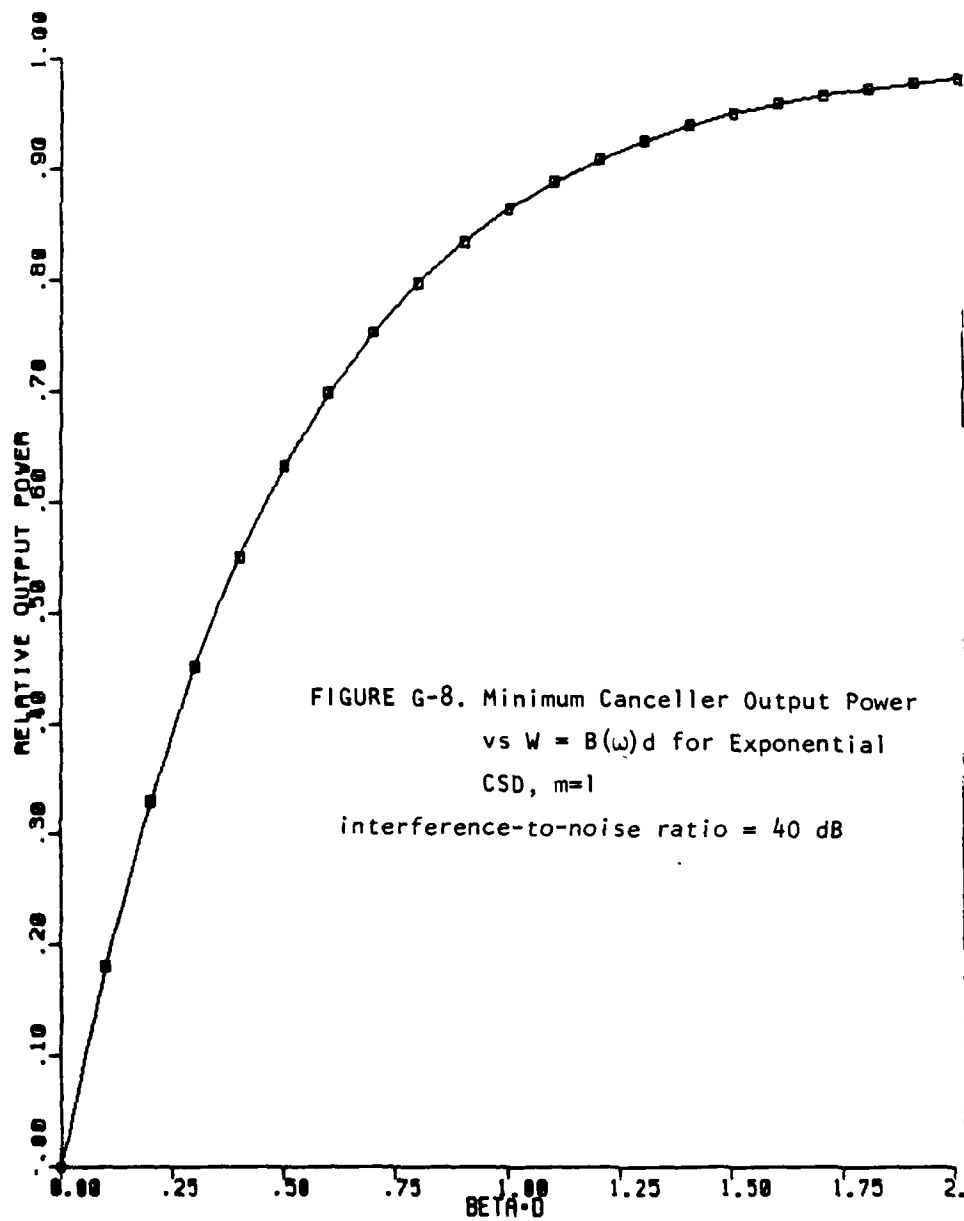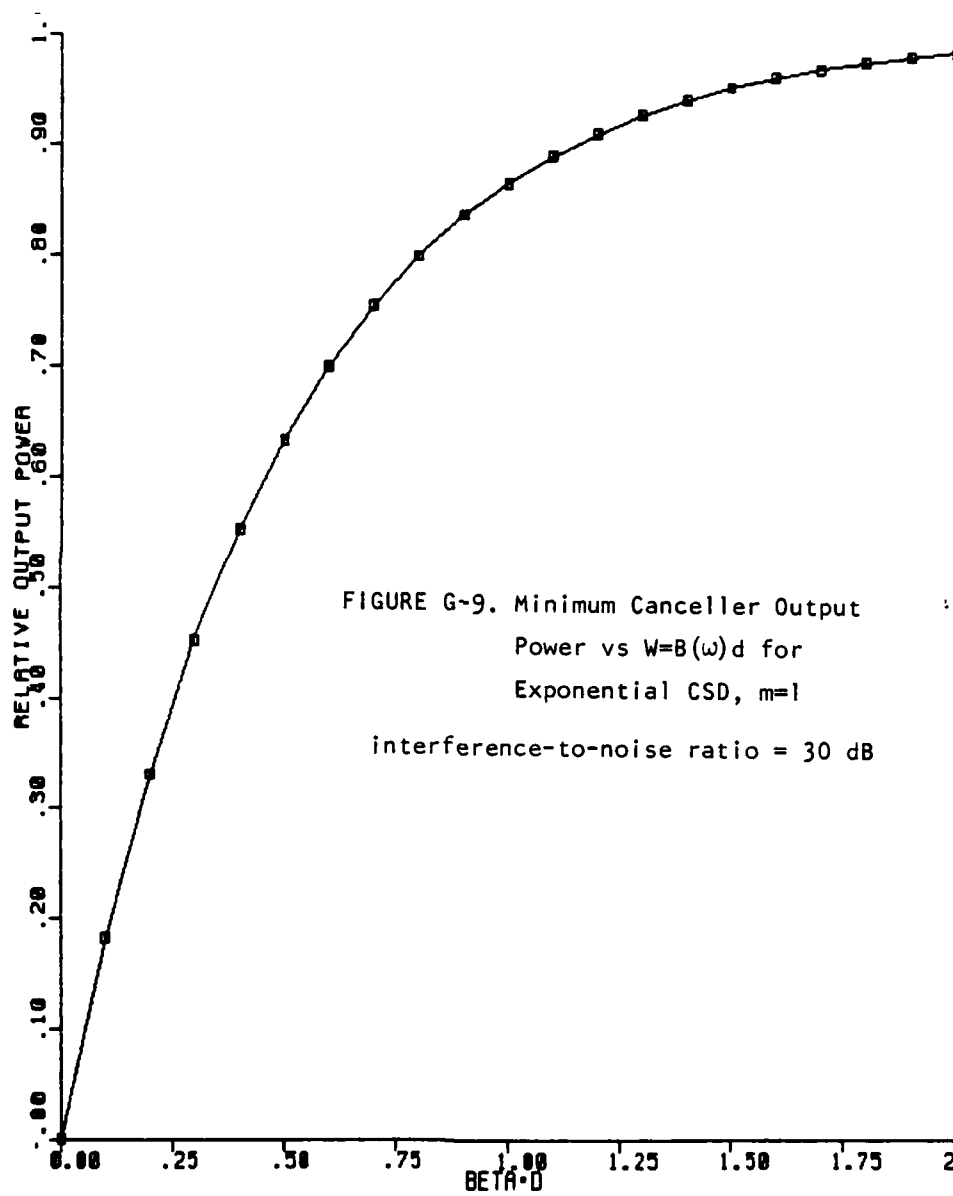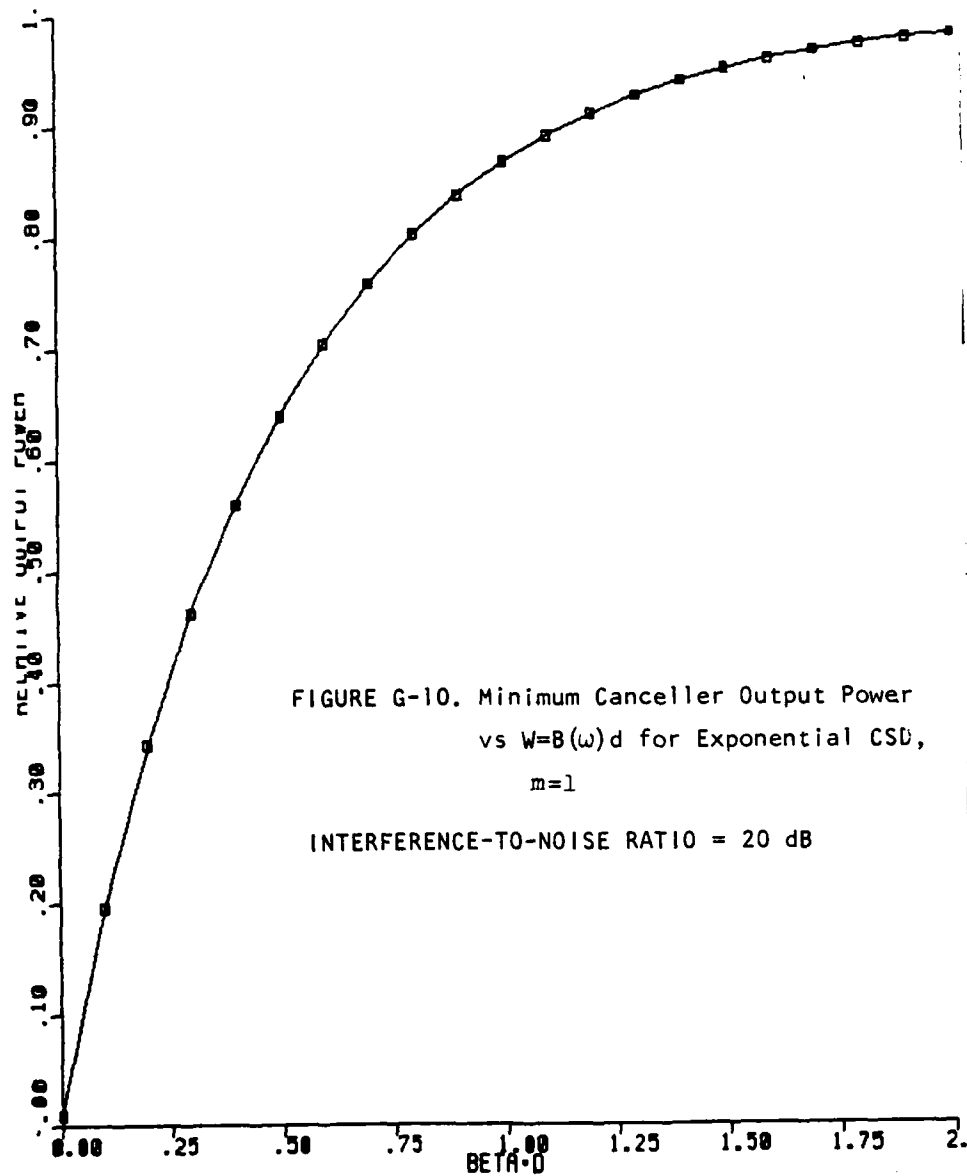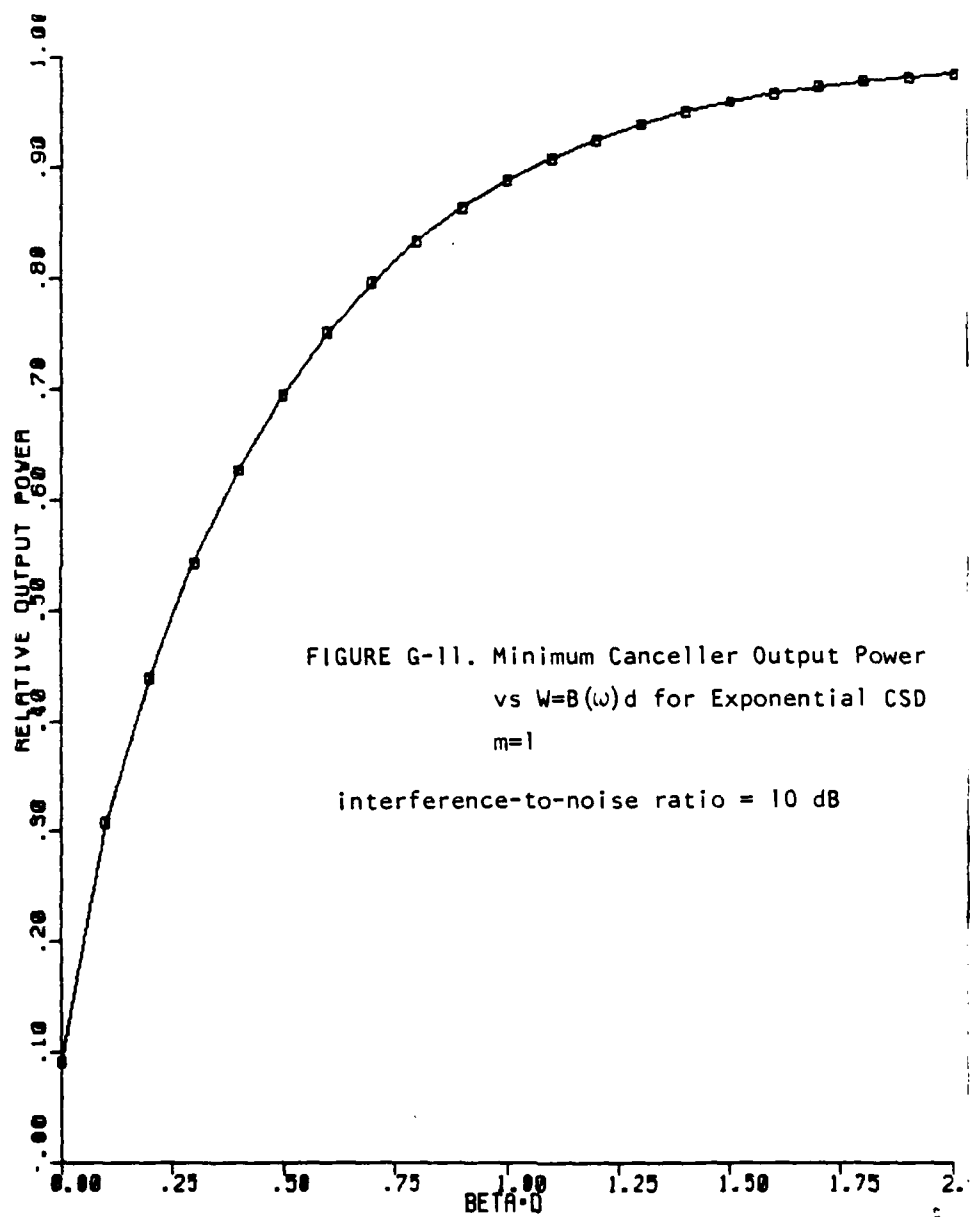
cancellation, the canceller is better able to reject the sin x/x

source. This is due to the Markov property of the exponential

source, as discussed above.

G.4 Conclusions

The minimum canceller output power has been obtained at a single

frequency, ω, for a source producing an exponential CSD along the line

array of references. In the case of m=1, where results exist for the sin x/x

CSD, the exponential CSD produces significantly different results than the

sin x/x case, as noted in (a) and (b) above. The differences between the

two reflect a Markov property inherent in the double exponential CSD. It is

likely that the differences also result from the fact that the sin x/x CSD is

produced by an angle limited source, while the exponential case results

from a source distributed on $(-\pi, \pi)$. Like the sin x/x CSD, the source

producing the exponential CSD cannot be cancelled to an ambient noise

floor for m=1. Further, the minimum canceller output power is shown to

increase with m, just as the numerical results indicated for the sin x/x.

However, the parametric behavior of the canceller with the two CDS's

differs sufficiently that the exponential case cannot be used to predict the

canceller performance with the sin x/x CSD.

APPENDIX H: SPATIAL RESPONSE OF THE LMS CANCELLER
IN THE PRESENCE OF AN EXTENDED SOURCE

APPENDIX H – SPATIAL RESPONSE OF THE LMS CANCELLER IN THE PRESENCE OF AN EXTENDED SOURCE

Although the primary emphasis of this study has been on the cancellation of an extended interference, without regard for the effect of the cancellation process on a signal of interest, the eventual application of the canceller will involve detection of a plane wave signal that is masked by the interference. This Appendix therefore considers the plane wave response of the cancelled output as a function of the angle of a plane wave signal. In other words, given a primary hydrophone with unit weighting and K reference hydrophones with the frequency domain LMS weighting

$$-S_e^{-1}(\omega) \, \underline{s}_1(\omega) \tag{H-1}$$

what is the spatial response, or beam pattern, of the canceller output.

The spatial response at frequency, ω, of an array of K+1 hydrophones with arbitrary weighting

$$\underline{W}(\omega) = [W_0(\omega), \, W_2(\omega), \, \ldots \, W_k(\omega)]^T \tag{H-2}$$

with $W_k(\omega)$ the weight applied to hydrophone k at frequency ω is given by

$$B_\omega(\phi_s) = \left| \underline{W}^+(\omega) \, \underline{d} \right|^2 \tag{H-3}$$

where

$$d = \left[e^{j \frac{\omega}{c} \tau_0}, \, e^{j \frac{\omega}{c} \tau_1}, \, \ldots, \, e^{j \frac{\omega}{c} \tau_{k-1}} \right]^T \tag{H-4}$$

and

τ_k = propagation delay to the kth hydrophone.

For the spatial cancellation problem with the array geometry of Figure H-1,

$$\tau_k = \begin{cases} \dfrac{d}{c} \ k \ \cos\phi_s & k=0, \ 1, \ \dots \ K-1 \\[2em] \dfrac{d}{c} \ J \ \cos\phi_s & k=K \end{cases} \tag{H-5}$$

that is, the Kth hydrophone (the primary) takes the Jth position. By the first paragraph in this section,

$$\underline{W}(\omega) = \begin{bmatrix} -S_e^{-1}(\omega) \ \underline{s}_1(\omega) \\[1em] 1 \end{bmatrix} \tag{H-6}$$

The vector, $\underline{d}$, can be written as

$$\underline{d} = \begin{bmatrix} \underline{d}_0 \\[1em] e^{j \frac{\omega d}{c} J \cos\phi_s} \end{bmatrix} \tag{H-7}$$

where

$$\underline{d}_0 = \begin{bmatrix} 1, \ e^{j \frac{\omega d}{c} \cos\phi_s}, \ \dots, \ e^{j \frac{\omega d}{c} (K-1) \cos\phi_s} \end{bmatrix}^T \tag{H-8}$$

Then (H-3) yields

$$B_w(\phi_s) = \left| e^{j \frac{\omega d}{c} J \cos \phi_s} - \underline{s}_1^+(\omega) \, S_e^{-1}(\omega) \, \underline{d}_0 \right|^2 \qquad \text{(H-9)}$$

Now, assume that the extended source is the uniformly distributed, uncorrelated, narrow source defined in Appendix A, satisfying (A-26), (A-36), and (A-40). It is shown in Appendix E that for this source, $S_e^{-1}(\omega)$ can be written in terms of its eigenvalues and eigenvectors as

$$S_e^{-1}(\omega) = \sum_{k=0}^{K-1} \left\{ \left[\frac{\gamma}{\gamma \sigma_n^2 + \sigma_I^2 \, \lambda_k(K,W)} \right] G^+ \, \underline{V}_k(K,W) \, \underline{V}_k^+(K,W) G \right\} \qquad \text{(H-10)}$$

where $\gamma = d/\lambda \, \sin\phi_0$ and

$$\underline{V}_k(K,W) = [V_0^{(k)}(K,W), \, V_1^{(k)}(K,W), \, \ldots, \, V_{K-1}^{(k)}(K,W)]^T, \qquad \text{(H-11)}$$

$\{V_m^{(k)}(K,W)\}_{m=0, \, 1, \, \ldots K-1}$ is the kth Discrete Prolate Spheroidal Sequence (DPSS) index limited to [0, K-1], and $\lambda_k(k,w)$ is the associated eigenvalue. Also

$$G = \operatorname*{diag}_{p=0, \, 1, \, \ldots \, K-1} \left[e^{-j \frac{\omega d}{c} p \cos\phi_0} \right] \qquad \text{(H-12)}$$

Using (H-10) gives

$$\underline{s}_1^+(\omega)\, S_e^{-1}(\omega)\, \underline{d} = \sum_{k=0}^{K-1} \left[\frac{\gamma}{\gamma\sigma_n^2(\omega) + \sigma_I^2(\omega)\lambda_k(K,\omega)} \right] [\underline{s}_1^+(\omega)\, G^+\underline{V}_k(K,\omega)]$$

$$\cdot\, [\underline{V}_k^+(K,\omega)\, G\, \underline{d}]$$

$$= \sum_{k=0}^{K-1} \left[\frac{\sigma_I^2(\omega)\, \lambda_k(K,\omega)}{\gamma\sigma_n^2(\omega) + \sigma_I^2(\omega)\lambda_k(K,\omega)} \right] V_J^{(k)}(K,\omega)\, e^{j\frac{\omega d}{c}J\cos\phi_0}$$

$$\cdot\, [\underline{V}_k^+(K,\omega)\, G\, \underline{d}] \qquad\qquad (H-13)$$

using (E-18) and (E-19) from Appendix E. Note that

$$\underline{V}_k^+(K,\omega)\, G\, \underline{d} = \sum_{m=0}^{K-1} V_m^{(k)}(K,\omega)\, e^{j\frac{\omega d}{c}m\,(\cos\phi_s - \cos\phi_0)} \qquad (H-14)$$

is just a Fourier transform of the DPSS.

Using expressions (H-13) and (H-14), the spatial response of the canceller in the presence of a uniform extended source has been evaluated for various values of source extent, 2ϕ, source angular position, ϕ_0, and interference to noise ratio, INR. Figures H-1 through H-8 show the spatial response when m=1, so that the reference array plus primary comprises a uniform array, with the following parameters:

$d/\lambda = 0.5$

$INR = 40$ dB

2ς = interference source extent = $20°$

ϕ_0 = interference angle = $45°$

The figures show the response for the number of references, K, equal
to 1, 2, ..., 8 respectively. In Figure H-1, with only one reference, the
array response only has a single null which is steered to the center of the
interference source. As more references are added (in Figures H-2
through H-8), the notch in the spatial response at $45°$ broadens to approx-
imately $20°$ wide, the extent of the source. For K < 7, this broadening
of the notch is accompanied by a considerable attenuation of the response
in other directions. For example, with K=2, there is a 15 dB attenuation
at endfire ($\phi = 0°$), even though the interference is $45°$ away. Gradually,
as more references are added, the notch sharpens, becoming more nearly
rectangular, and the attenuation at other angles away from the interference
decreases to a more acceptable value.

Note that once K=3 or 4, additional references do not appear to deepen
the notch very much, suggesting that further interference cancellation will
not be substantial. For the parameters given above,

$$W = \varsigma \frac{d}{\lambda} \sin \phi_0 = .062$$

Figure K-21, which shows the canceller output spectrum as a function of
K for $\omega = .06$ and INR=40 dB, verifies that little further cancellation occurs
beyond K=3. Therefore, Figures H-1 through H-8 indicate that the reason
for adding references may be to assure adequate signal response in some
direction other than the interference arrival angles. For example, in Fig-
ure H-3, with K=3, a signal arriving at $60°$, $15°$ away from the interference,
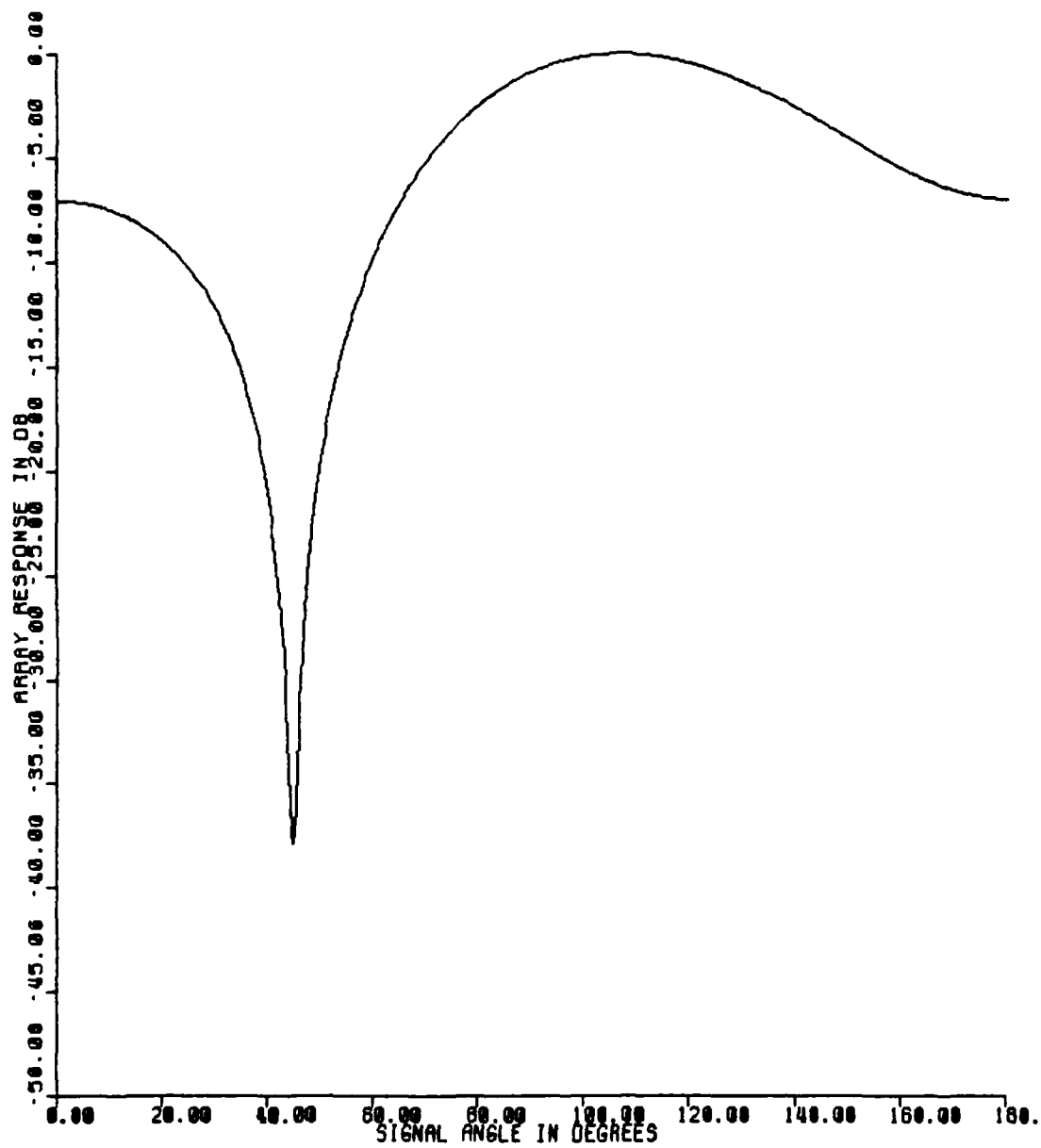
FIGURE H-1. Spatial Response for 20° Uniform Extended Source at 45°

d/λ = .5, m=1, K=1, INR=40 dB
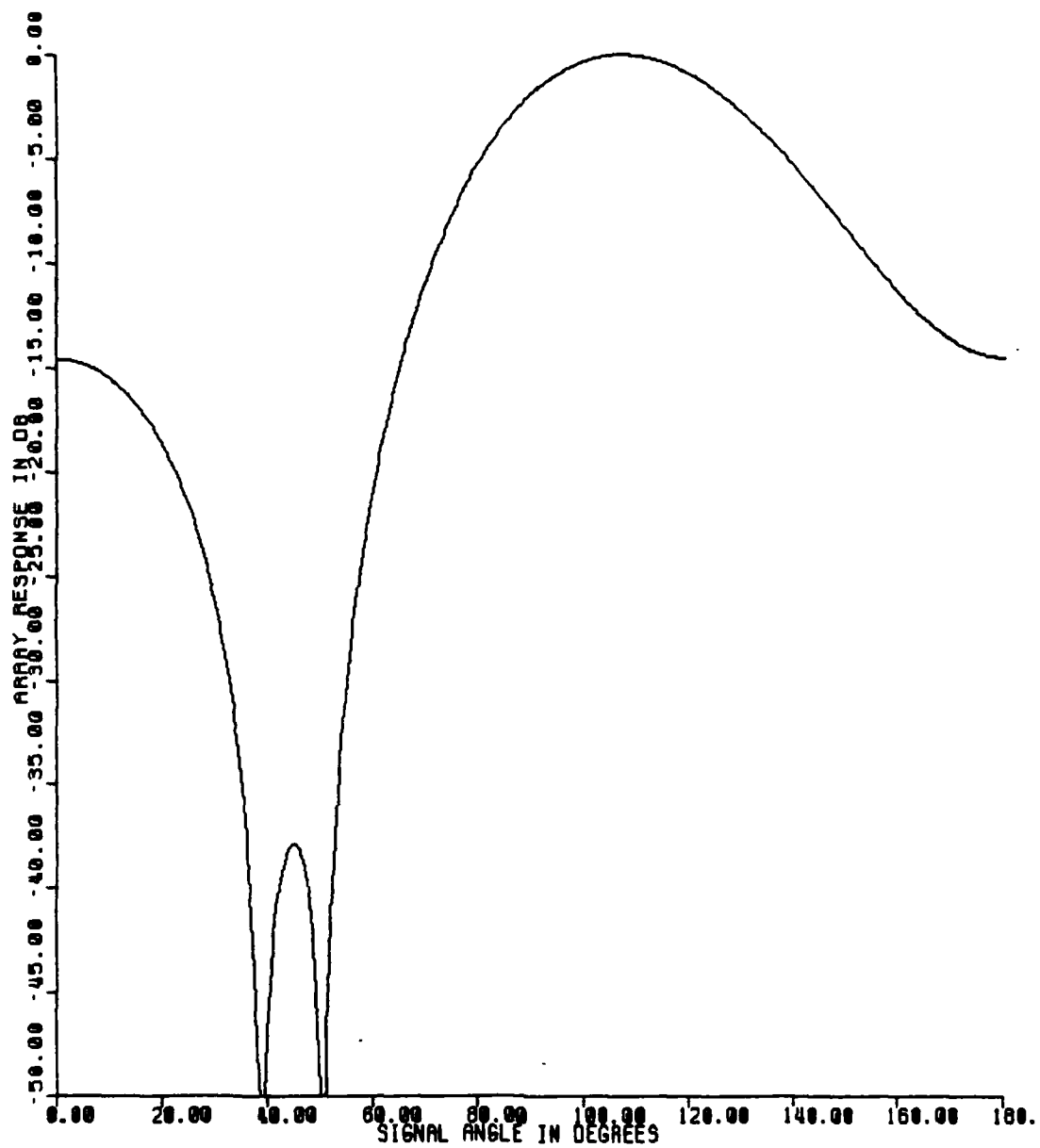
FIGURE H-2. Spatial Response for 20° Uniform Extended Source at 45°

d/λ = .5, m=1, K=2, INR = 40 dB
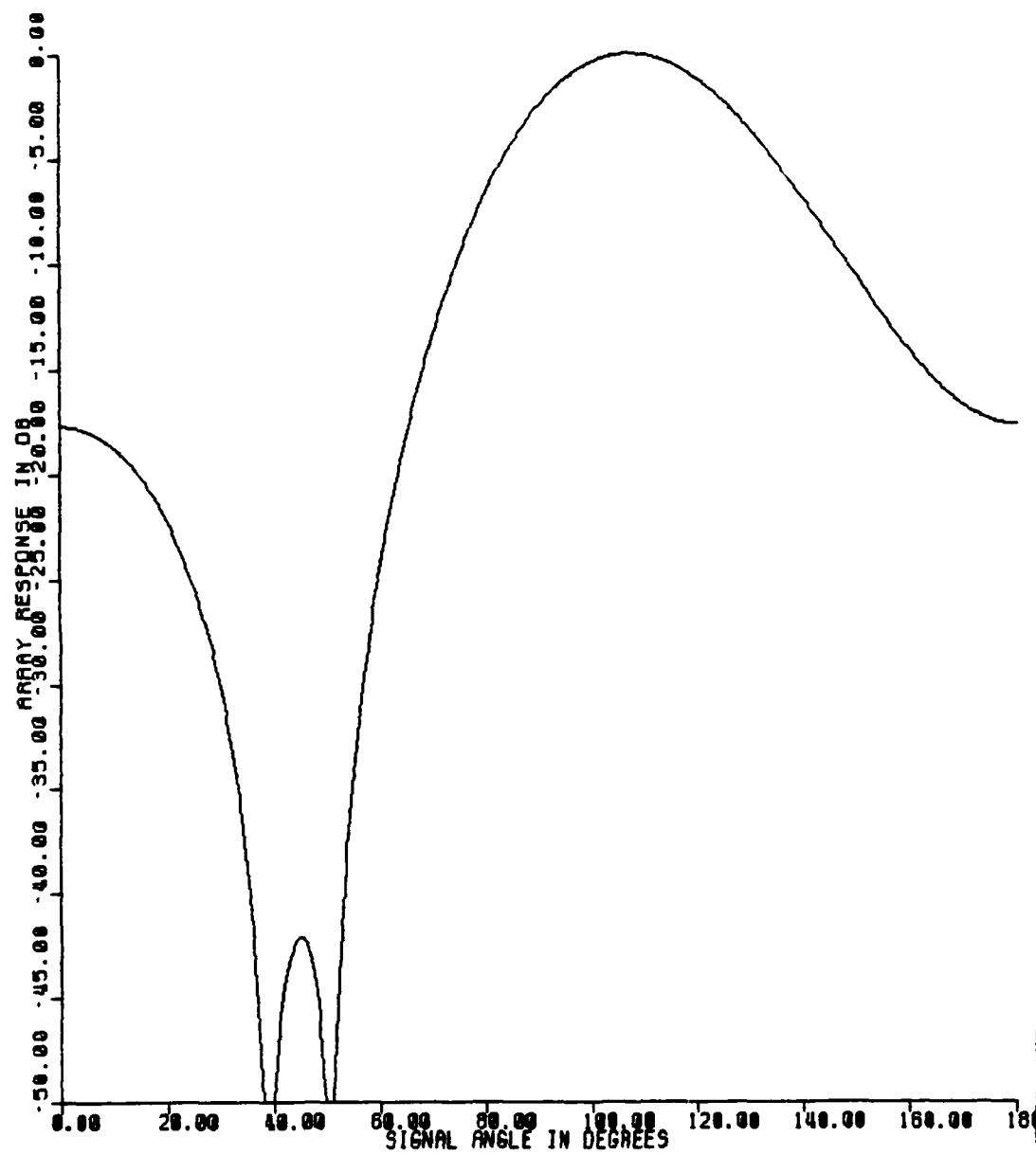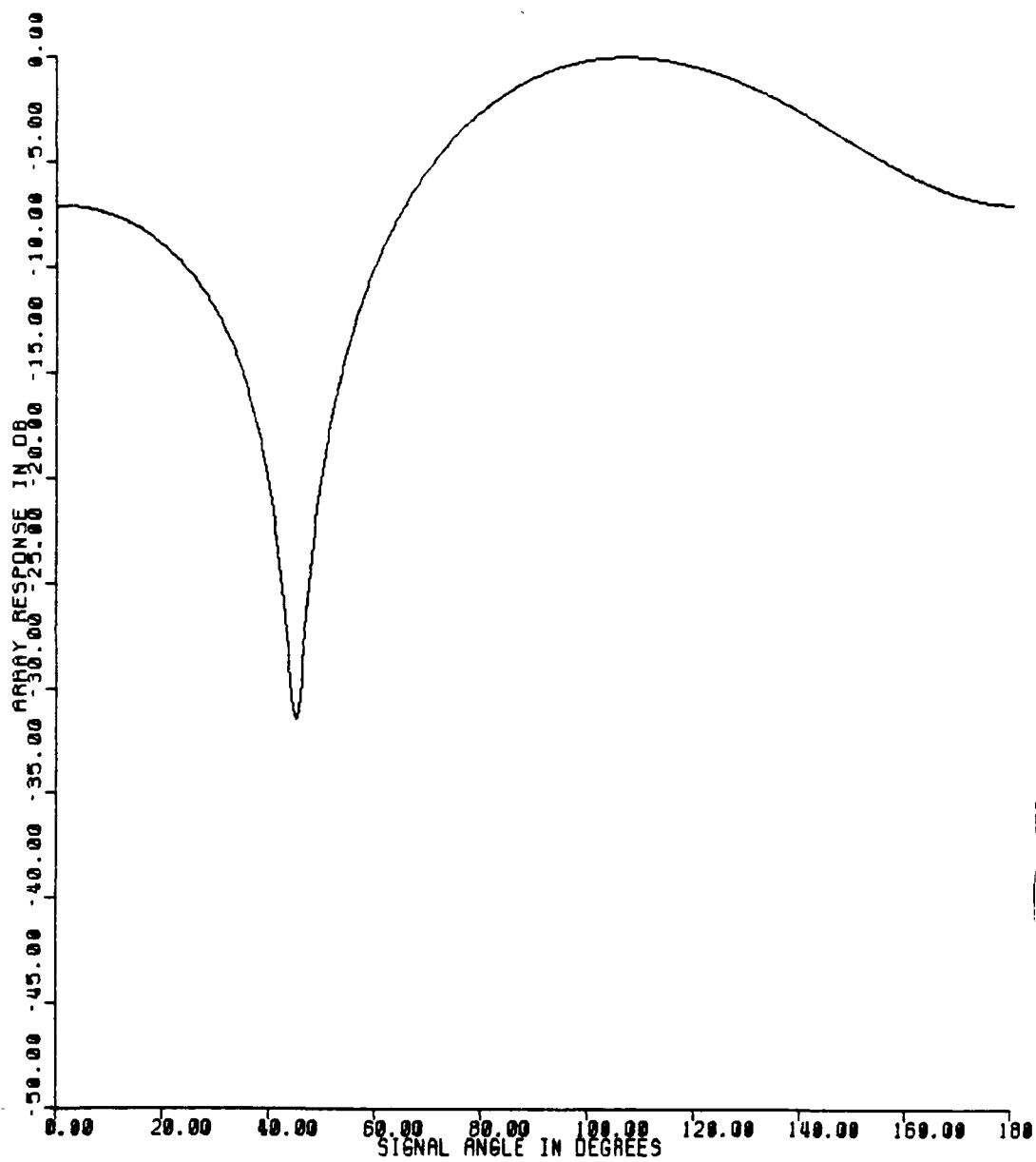
FIGURE H-3. Spatial Response for 20° Uniform Extended Source at 45°

d/λ = .5, m=1, K=3, INR = 40 dB
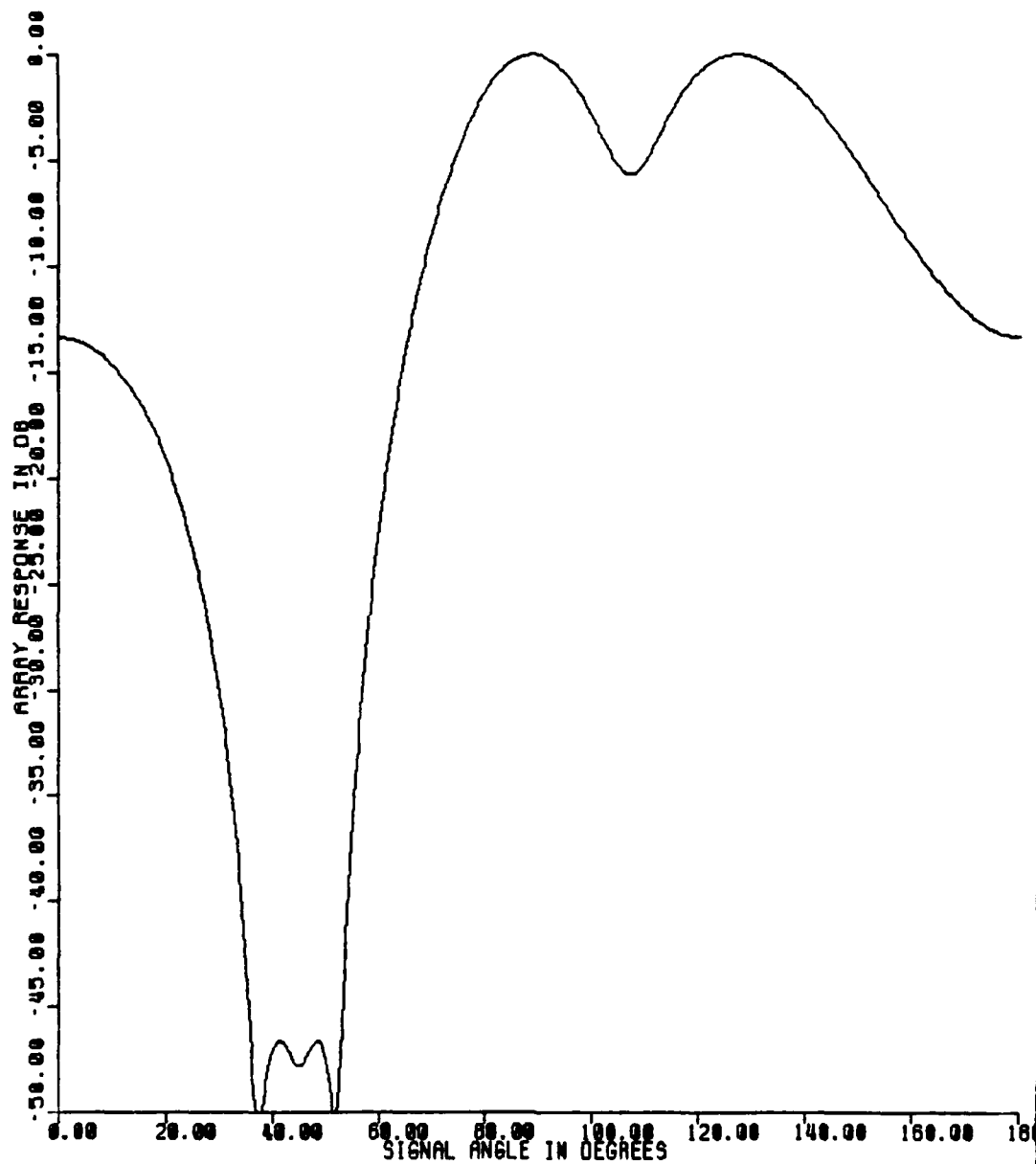
FIGURE H-4. Spatial Response for 20° Uniform Extended Source at 45°

d/λ = .5, m=1, K=4, INR = 40 dB
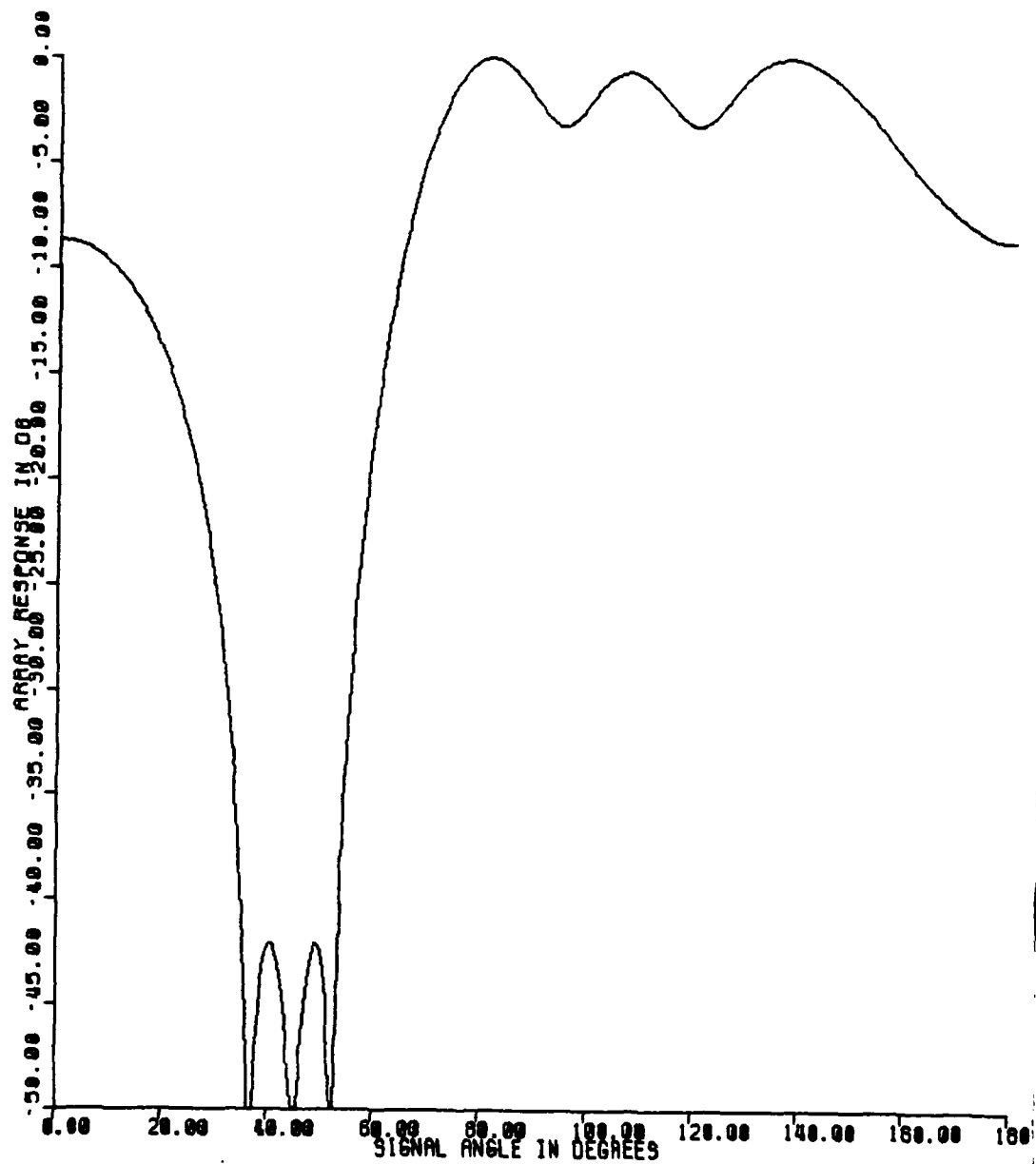
FIGURE H-5. Spatial Response for 20° Uniform Extended Source at 45°

d/λ = .5, m=1, K=5, INR = 40 dB
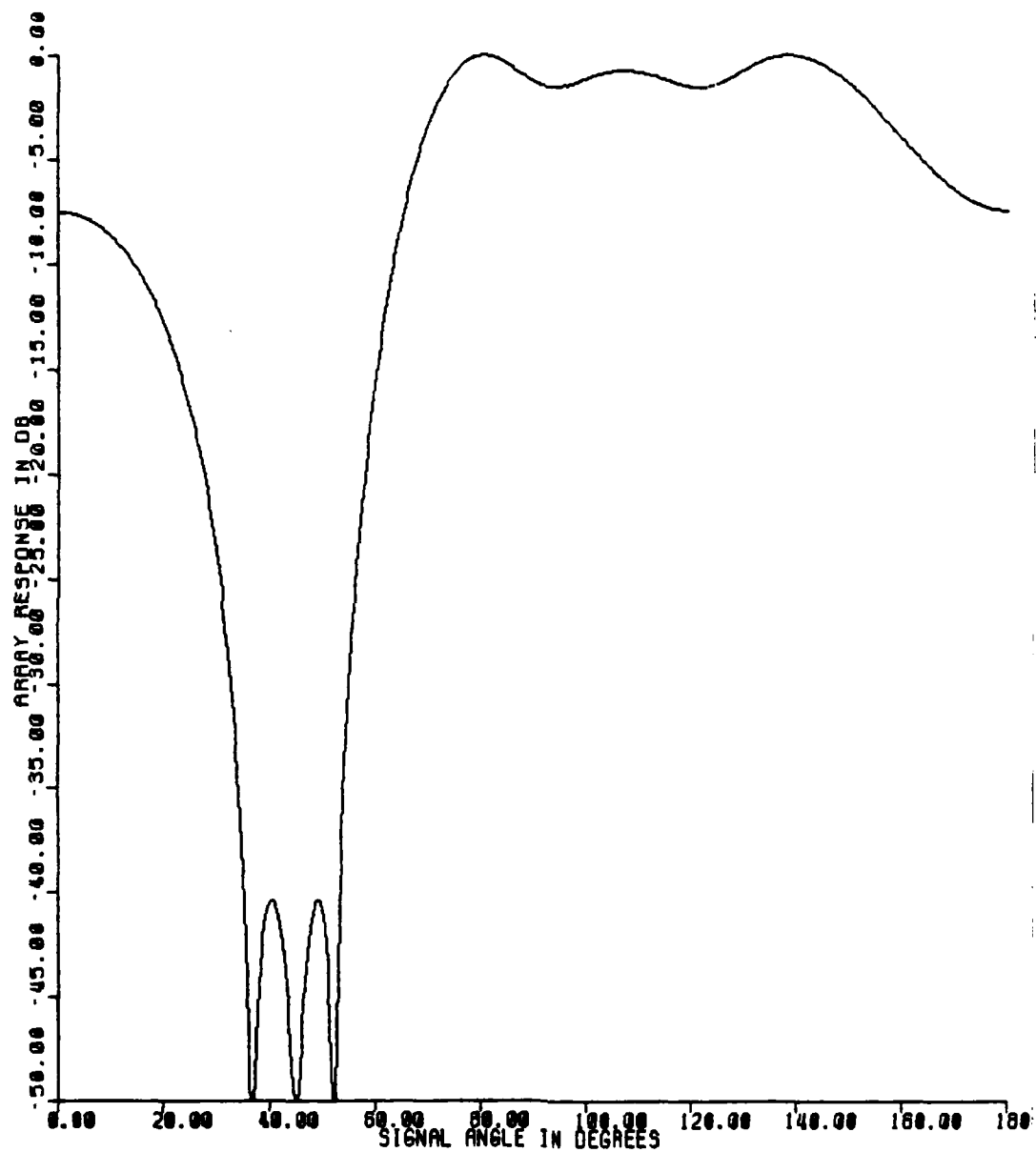
FIGURE H-6. Spatial Response for 20° Uniform Extended Source at 45°
d/λ = .5, m=1, K=6, INR = 40 dB

H-11
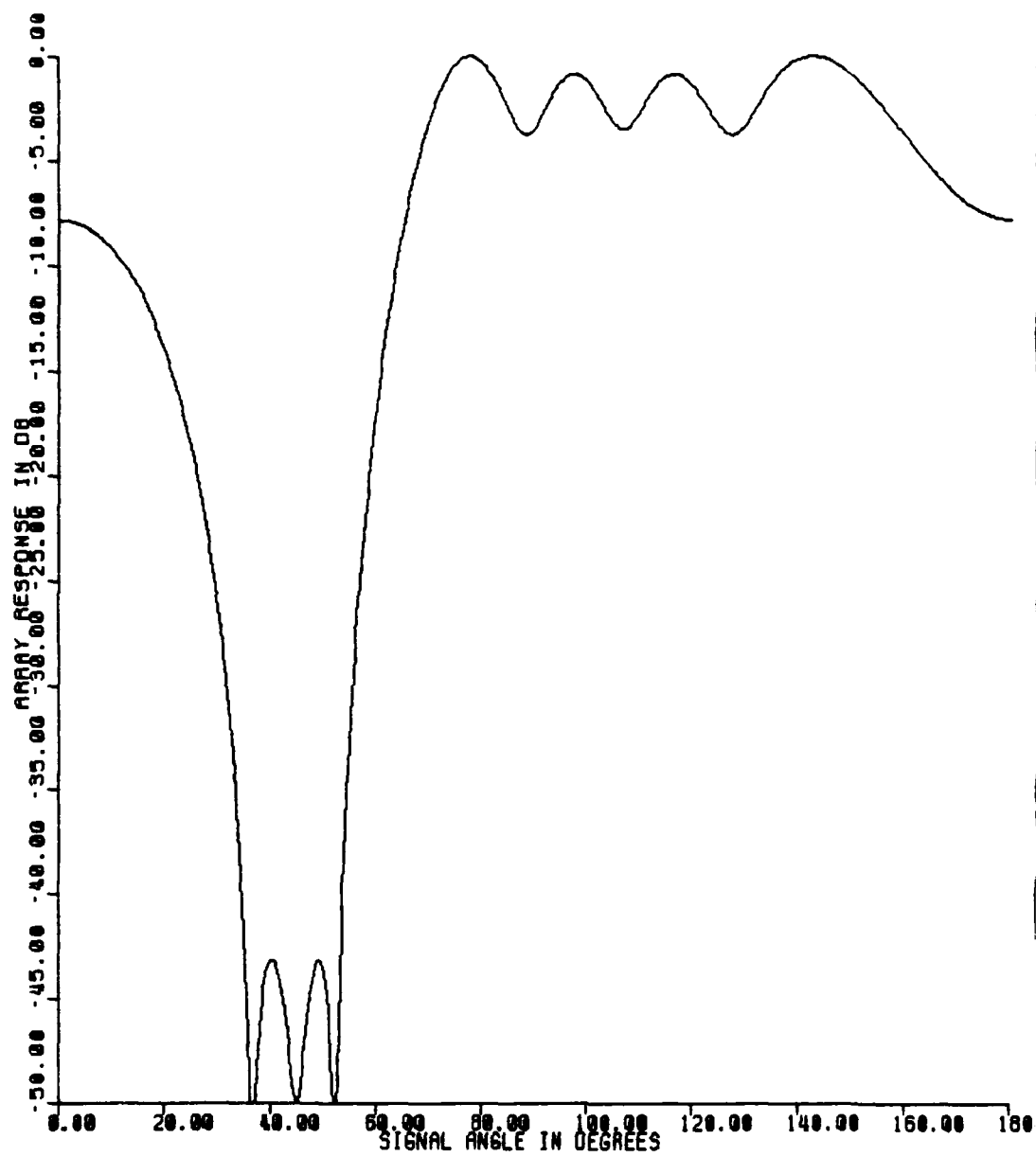
FIGURE H-7. Spatial Response for 20° Uniform Extended Source at 45°
d/λ = .5, m=1, K=7, INR = 40 DB
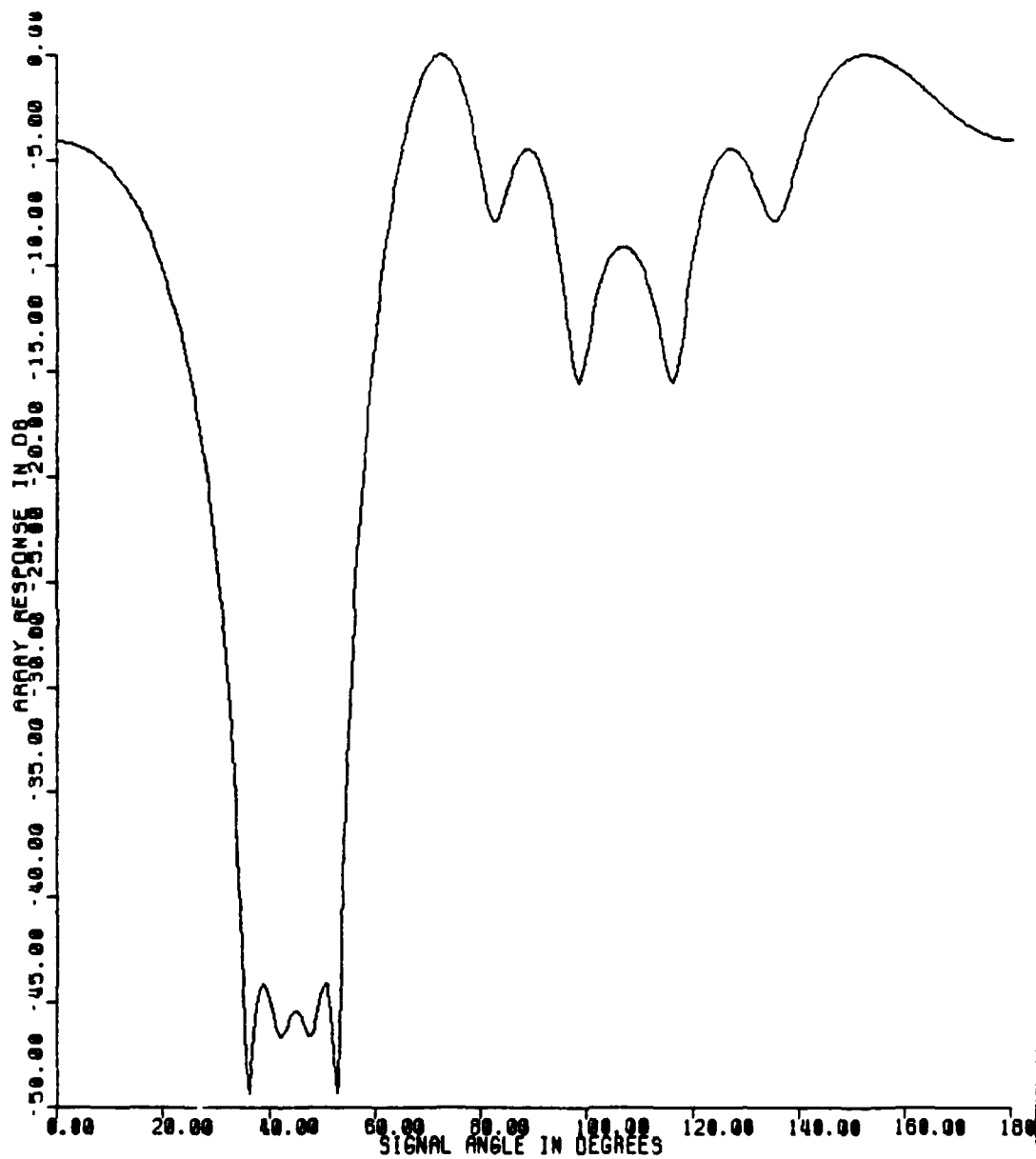
FIGURE H-8. Spatial Response for 20° Uniform Extended Source at 45°

d/λ = .5, m=1, K=8, INR = 40 dB

suffers 25 dB of attenuation, while when K=8 in Figure H-8, the signal attenuation is only 12 dB.

When interpretting these figures it should be kept in mind that the primary consists of a single omnidirectional hydrophone, rather than an array, as would be used in most sonar situations. As indicated in Appendix L, when a primary array is used, the responses like those of Figures H-1 through H-6 would be multiplied by the response pattern of the primary array. This would greatly attenuate (by the primary array sidelobe level) those regions outside the mainlobe of the primary array. Assuming, then, that the reverberation that limits the active detection performance arrives on or near the main lobe, the signal response in the vicinity of the notch is of primary interest. The reason for adding references would then be to increase the slope of the sides of the notch.

It is observed in Appendix K that as the primary is moved farther from the references, the cancellation of the extended source degrades. Figures H-9, H-10, and H-11, which show the spatial response for the same case as H-1 through H-8 but with m=5, 10, and 20, respectively confirm this. The depth of the notch is 40 dB, 32 dB, and 23 dB for m=5, 10 and 20, respectively while m=1 gives a notch approximately 47 dB deep. In addition to the reduction in cancellation as in increases, Figures H-9 through H-11 show that there is a degradation in the array response to signals arriving from directions other than the angular
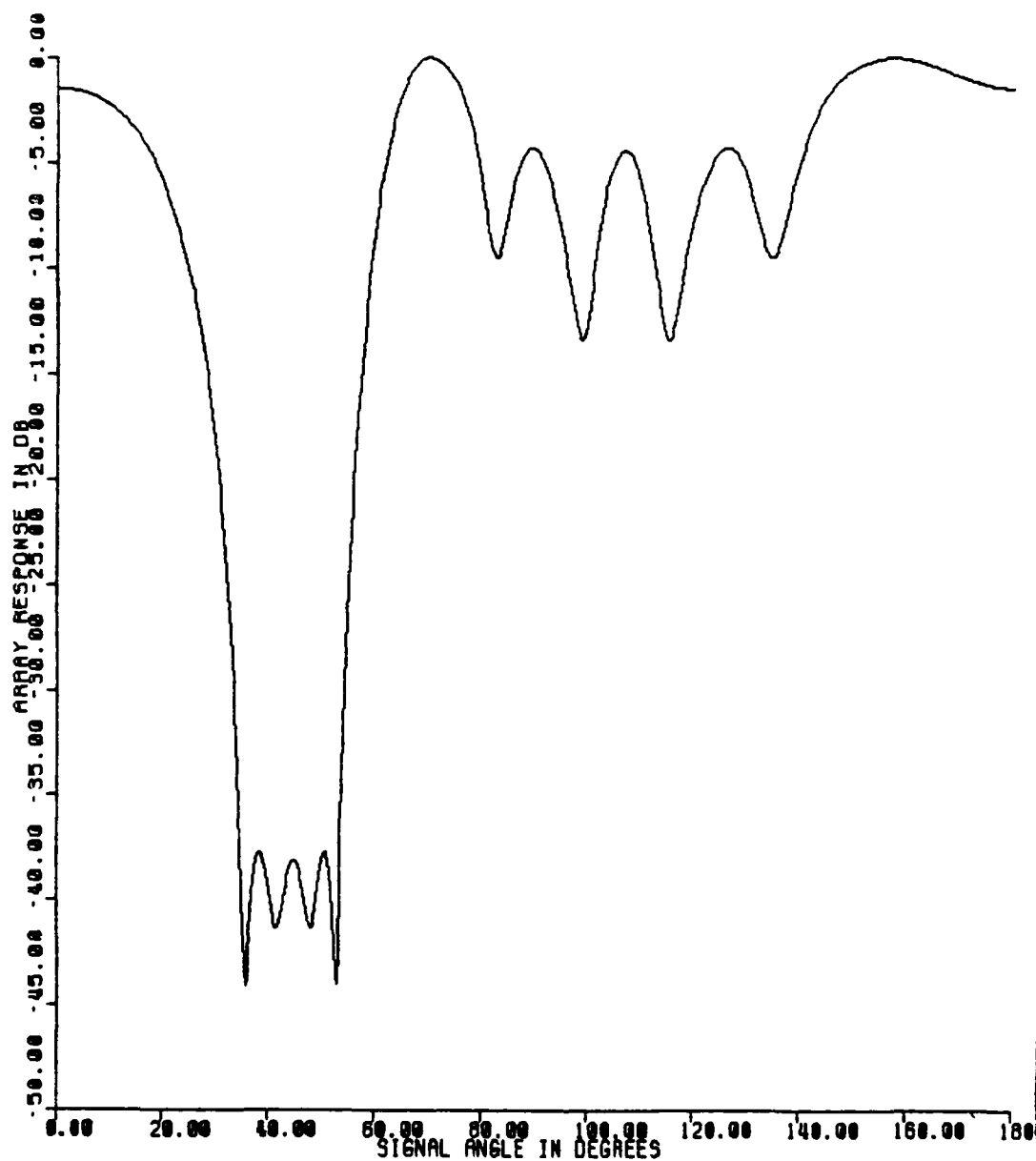
FIGURE H-9. Spatial Response for 20° Uniform Extended Source at 45°

d/λ = .5, m=5, K=8, INR = 40 DB
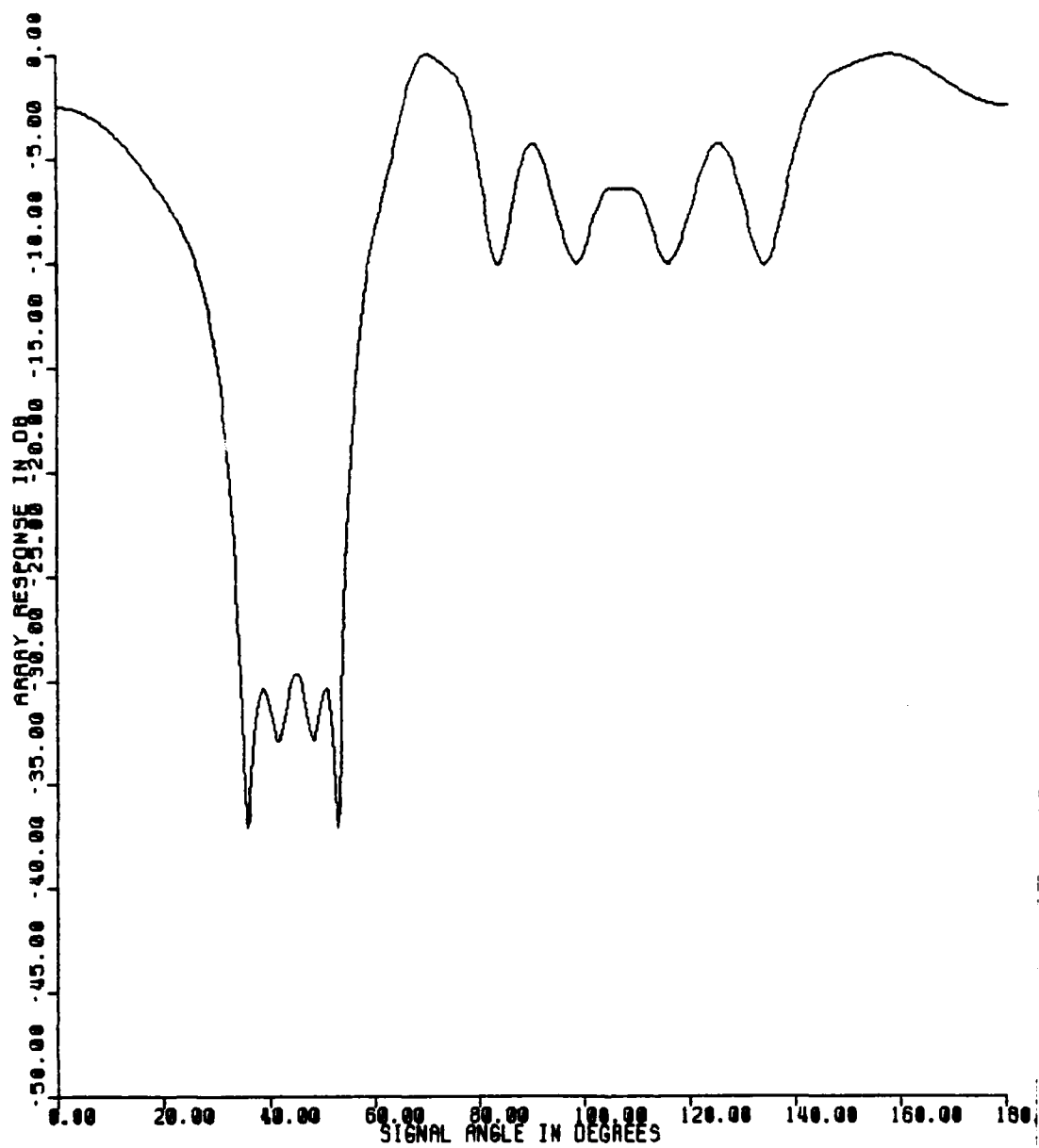
FIGURE H-10. Spatial Response for 20° Uniform Extended Source at 45°

d/λ = .5, m=10, K=8, INR = 40 dB
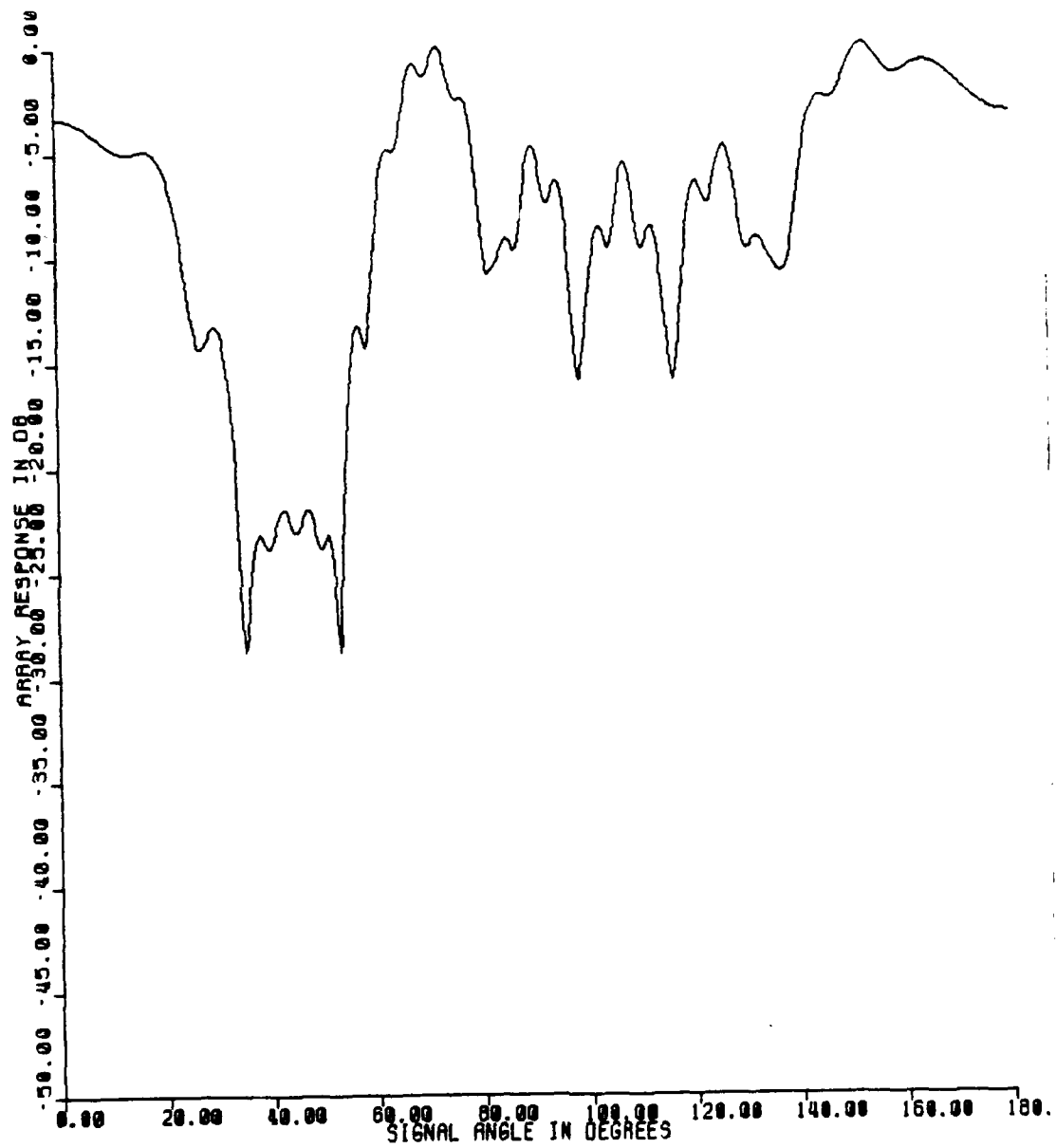
FIGURE H-11. Spatial Response for 20° Uniform Extended source at 45°

d/λ = .5, m=20, K=8, INR = 40 dB
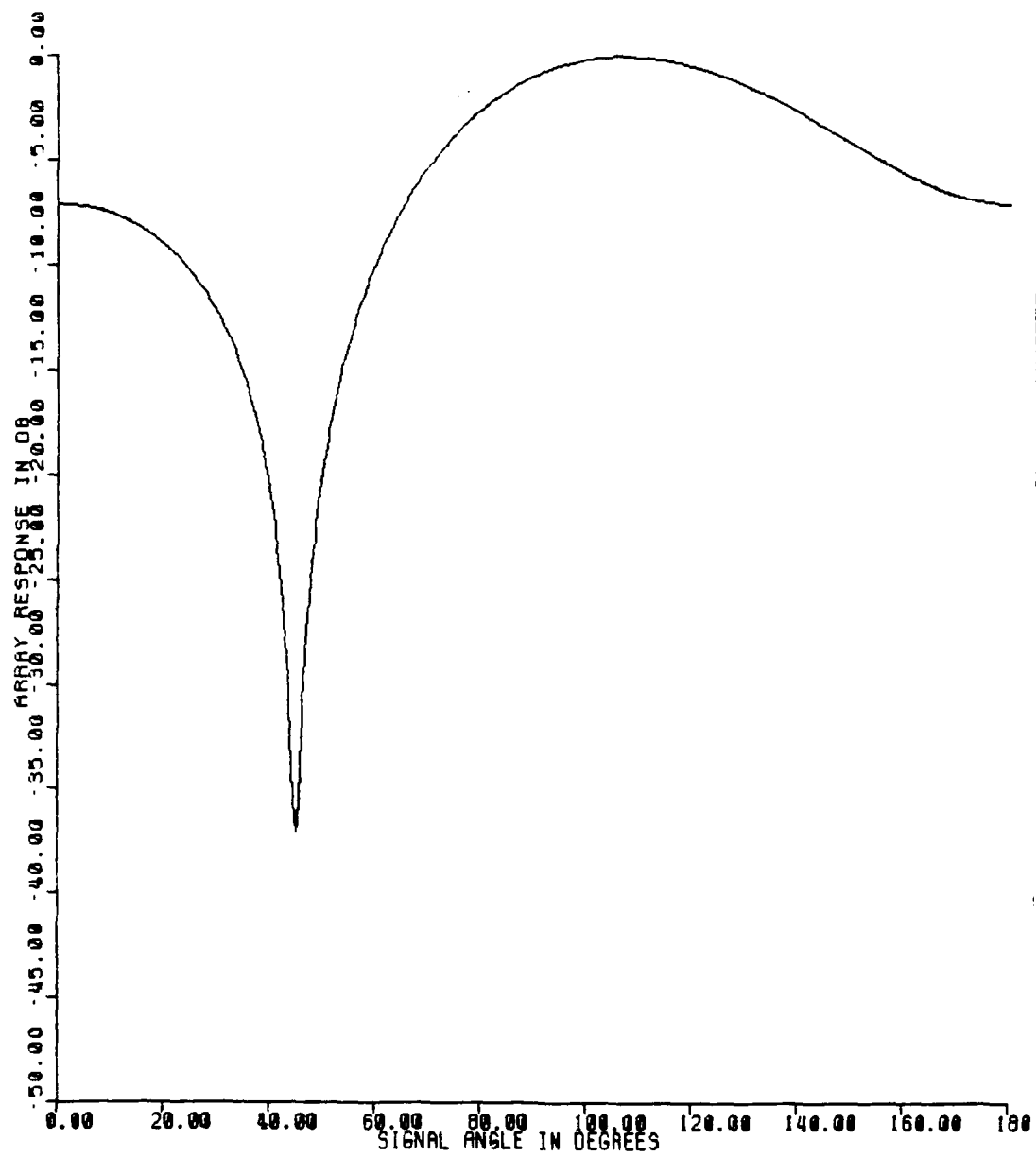
FIGURE H-12. Spatial Response for 20° Uniform Extended Source at 45°

d/λ = .5, m=1, K=1, INR = 30 dB

H-18
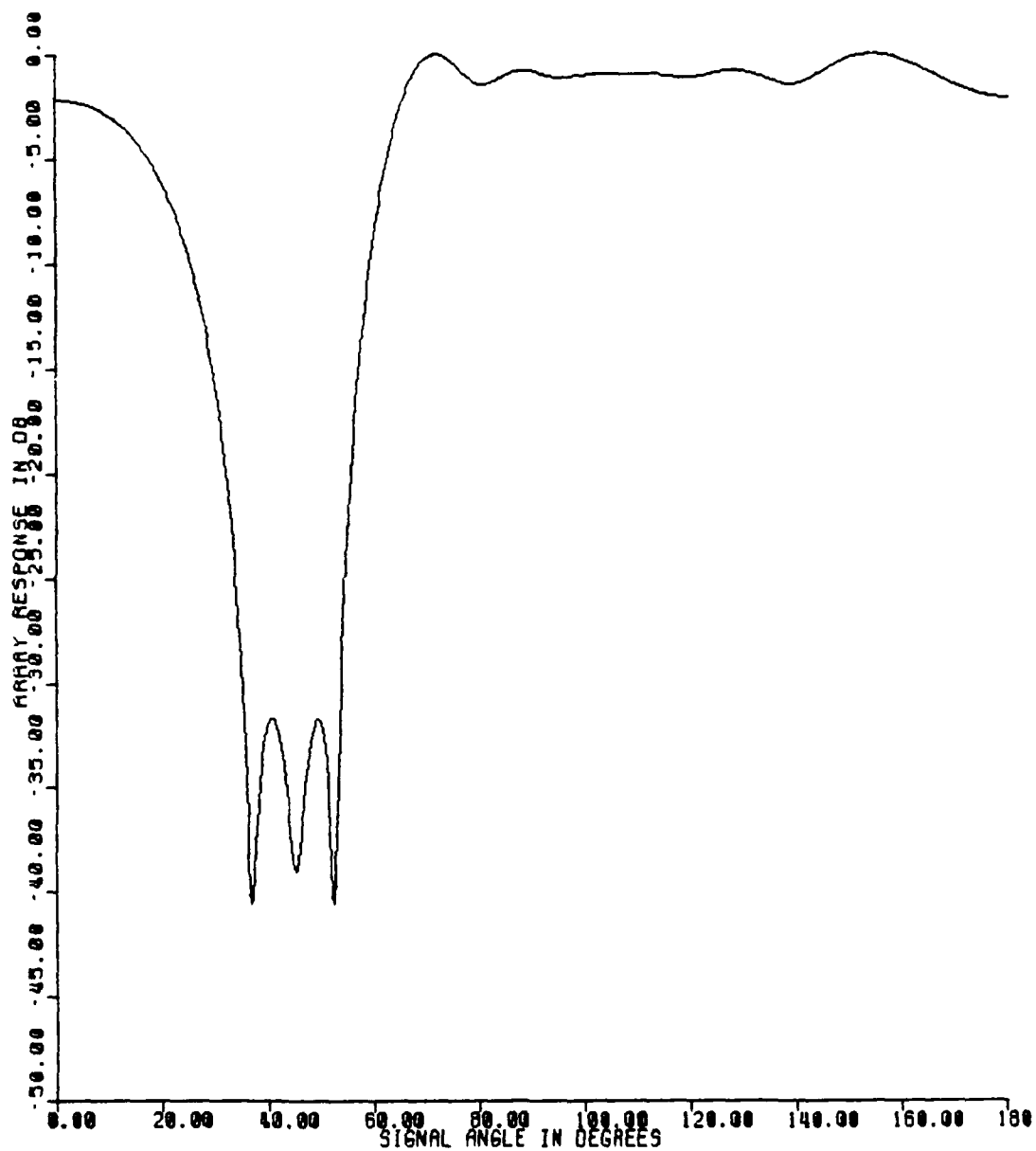
FIGURE H-13. Spatial Response for Uniform Extended Source at 45°

d/λ = .5, m=1, K=8, INR = 30 dB

FIGURE H-14. Spatial Response for 20° Uniform Extended Source at 45°

d/λ = .5, m=1, K=1, INR = 20 dB
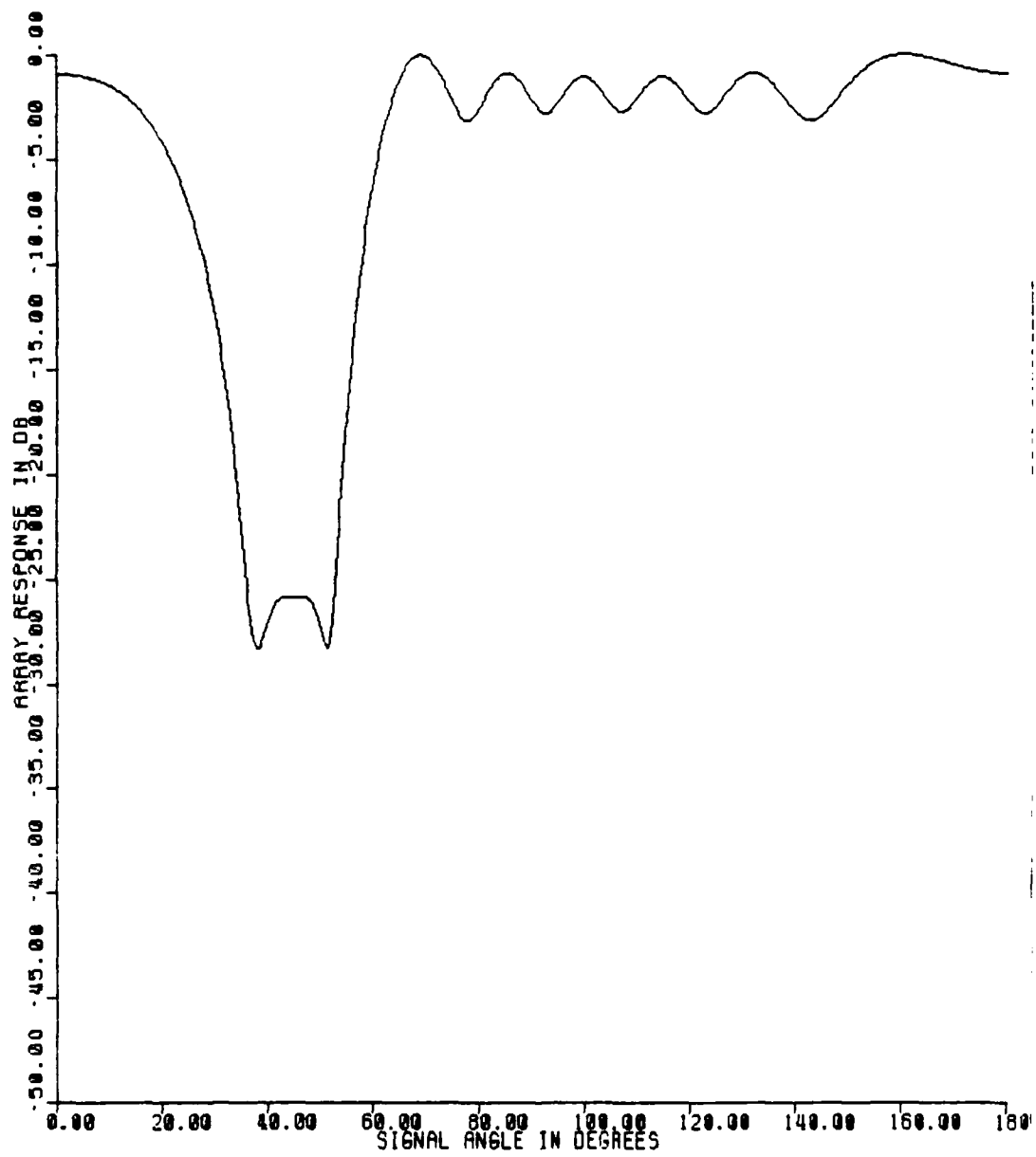
FIGURE H-15. Spatial Response for 20° Uniform Extended Source at 45°
d/λ = .5, m=1, K=8, INR = 20 dB

APPENDIX I: USE OF THE OUTPUT OF A STEERED
LINE ARRAY AS THE PRIMARY

APPENDIX I – USE OF THE OUTPUT OF A STEERED LINE ARRAY AS THE PRIMARY

In most situations, the primary input to the optimal canceller is not the output of a single omnidirectional hydrophone, but that of an array of hydrophones steered in some direction of interest. The directional response of the array will reduce the effect of reverberation arriving outside the mainlobe by an amount equal to the sidelobe level, but reverberation arriving in the mainlobe will remain unattenuated at the beam output. Further, situations occur in the sonar environment in which reverberation arriving in the sidelobes has sufficient power to prevent detection of a much weaker signal in the mainlobe.

This Appendix considers the case when the primary input to the canceller is the output of a line array of hydrophones, colinear with the reference array as shown in Figure I-1, and steered in a direction ϕ_d, as shown. Let the N hydrophones in the primary array be uniformly spaced d_p feet apart, and let the distance between the primary and the reference array be Ld feet, as shown in Figure I-1. The plane wave assumption made in Appendix A is assumed to be valid over both the reference and primary arrays.

The outputs of the N hydrophones in the primary array are denoted $y_n(t)$ for n=0, 1, ... N-1. A beamformer steered in the direction ϕ_d computes its output as

$$z(t) = \sum_{n=0}^{N-1} a_n \, y_n \left(t - (N-n-1) \frac{d_p}{c} \cos \phi_d \right) \tag{I-1}$$

Further, the $\eta_n(t)$ are uncorrelated with the ambient noise components of the reference hydrophone outputs,

$$E\left[\eta_n(t)\, n_k(t+\tau)\right] = 0, \begin{cases} n=0,\ 1,\ \ldots\ N-1 \\ k=0,\ 1,\ \ldots\ K-1 \end{cases} \tag{I-4}$$

Since $z(t)$ replaces $e_d(t)$ as the primary input to the canceller structure, (A-14) becomes

$$r_1(k,\ \tau) = E[z(t)\, e_k(t+\tau)]$$

$$= E\left\{\left[\sum_{n=0}^{N=1} a_n\, \eta_n\, \left(t-(N-n-1)\,\frac{d_p}{c}\cos\phi_d\right)\right.\right.$$

$$+ \sum_{n=0}^{N-1} a_n \int_{-\pi}^{\pi} i\{t - [(L+K-1)\,\frac{d}{c} + nd_p]\cos\phi_1 - (N-n-1)\,\frac{d_p}{c}\cos\phi_d, \phi_1\}d\phi_1\Bigg]$$

$$\left.\cdot\left[n_k(t+\tau) + \int_{-\pi}^{\pi} i\,(t+\tau-k\,\frac{d}{c}\cos\phi_2,\ \phi_2)\ d\phi_2\right]\right\}$$

$$= \sum_{n=0}^{N-1} a_n \int_{-\pi}^{\pi} \int_{-\pi}^{\pi} R_I\,\{\tau + \frac{d_p}{c}\,[(N-1)\cos\phi_d$$

$$+ n\,(\cos\phi_1 - \cos\phi_2)] + \frac{d}{c}\,[L+K-1]\cos\phi_1 - \frac{d}{c}\,k\cos\phi_2,\ \phi_1,\ \phi_2\}\ d\phi_1 d\phi_2 \tag{I-5}$$

Therefore (A-15) is replaced by

$$s_1(k, \omega) = \mathcal{F}[r_1(k,\tau)]$$

$$= \sum_{n=0}^{N-1} a_n \int_{-\pi}^{\pi} \int_{-\pi}^{\pi} S_I(\phi_1, \phi_2, \omega) \exp\{-j \frac{\omega}{c} [(L\_K-1) \, d \cos \phi_1$$

$$- kd \cos \phi_2 + (N-1)\phi d_p \cos \phi_d$$

$$+ nd_p (\cos \phi_1 - \cos \phi_d)]\} \, d\phi_1 \, d\phi_2$$

$$= \int_{-\pi}^{\pi} \int_{-\pi}^{\pi} S_I(\phi_1, \phi_2, \omega) \left[\sum_{n=0}^{N-1} a_n \exp\{-j \frac{\omega}{c}\right.$$

$$\left. \cdot [nd_p(\cos \phi_1 - \cos \phi_d)]\} \right] \exp\{-j \frac{\omega}{c} [(L+K-1)d \cos \phi_1$$

$$- kd \cos \phi_2 + (N-1) \, d_p \cos \phi_d\} \, d\phi_1 \, d\phi_2 \qquad (I-6)$$

The bracketted term is just the response of the primary array, steered in
direction ϕ_d, to a plane wave from direction, ϕ_1. Denote

$$B(\theta) = \sum_{n=0}^{N-1} a_n \, e^{-j \frac{\omega d_p}{c} n \theta} \qquad (I-7)$$
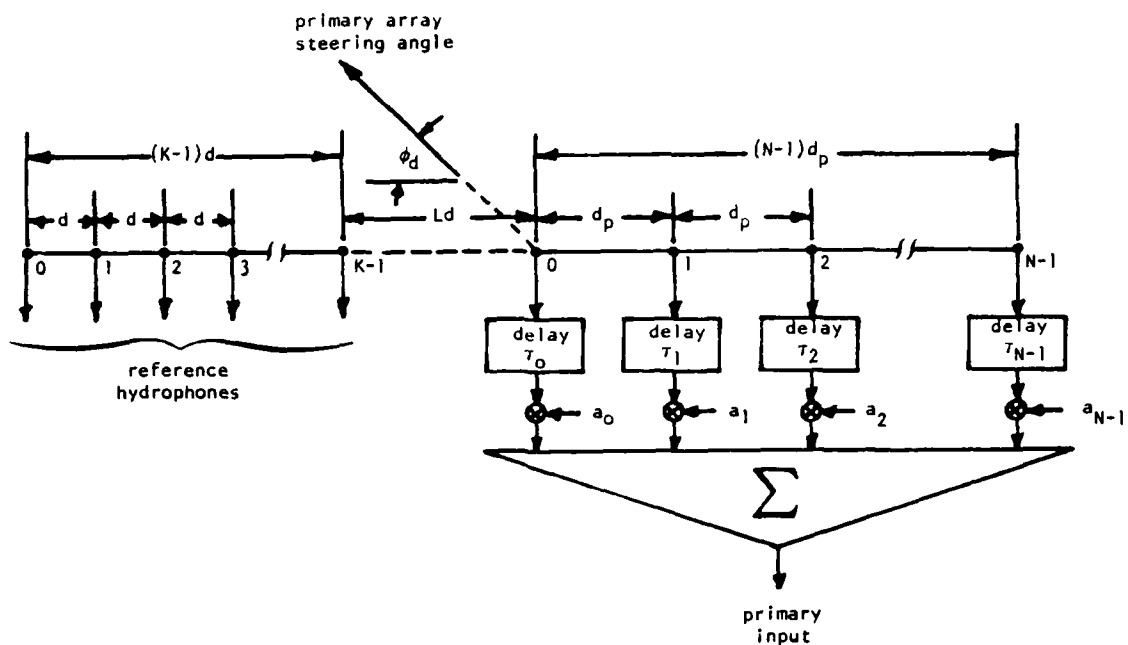
Figure I-1.   Use of a Line Array as the Primary Input

where the a_n are real shading coefficients.   This beamformer output

replaces $e_d(t)$ as the primary input to the canceller.   Extending equations

(A-6) and (A-7) to the primary array gives the hydrophone outputs as

$$y_n(t) = \eta_n(t) + \int_{-\pi}^{\pi} i \left[t - \frac{1}{c}\left[(L+K-1)d + nd_p\right]\cos\phi\right]d\phi \qquad (I-2)$$

where $\eta_n(t)$ is the ambient noise component of the output of primary hydro-

phone n.   As before, the $\eta_n(t)$ are assumed to be zero mean, stationary

random processes with

$$E\left[\eta_n(t)\,\eta_m(t+\tau)\right] = R_n(\tau)\,\delta_{nm}, \begin{cases} n=0, \ 1, \ \dots \ N-1 \\ m=0, \ 1, \ \dots \ N-1 \end{cases} \qquad (I-3)$$

so that

$$s_1 (k,\omega) = \int_{-\pi}^{\pi} \int_{-\pi}^{\pi} S_I(\phi_1, \phi_2, \omega) B(\cos \phi_1 - \cos \phi_d)$$

$$\exp \{-j \frac{\omega}{c} [(L+K-1)d \cos \phi_1 - kd \cos \phi_2\} d\phi_1 d\phi_2$$

$$\cdot \exp \{-j \frac{\omega}{c} (N-1)d_p \cos \phi_d\} \qquad (I-8)$$

Comparison of this result with (A-15) shows that the case with a primary array can be treated by placing a single primary hydrophone a distance Ld from the nearest reference hydrophone if the hydrophone has the directional response

$$H(\phi) = B(\cos \phi - \cos \phi_d) \exp \{-j \frac{\omega}{c} (N-1)d_p \cos \phi_d\} \qquad (I-9)$$

This equivalent model is illustrated in Figure I-2.

Similarly, it can be seen that (A-16) becomes

$$r_{11}(\tau) = E[z(t) z(t+\tau)] = \sum_{n=0}^{N-1} a_n^2 R_n(\tau)$$

$$+ \sum_{n=0}^{N-1} \sum_{m=0}^{N-1} a_n a_m \int_{-\pi}^{\pi} \int_{-\pi}^{\pi} R_I \{\tau - \frac{d_p}{c} n (\cos \phi_1 - \cos \phi_d)$$

$$+ \frac{d_p}{c} m (\cos \phi_2 - \cos \phi_d), \phi_1, \phi_2\} d\phi_1 d\phi_2 \qquad (I-10)$$

$$= \left[\sum_{n=0}^{N=1} a_n \right] \sigma_n^2(\omega) + \int_{-\pi}^{\pi} \int_{-\pi}^{\pi} S_I(\phi_1, \phi_2, \omega) B (\cos \phi_1 - \cos \phi_d)$$

$$B^*(\cos \phi_d - \cos \phi_d) \ d\phi_1 d\phi_2 \qquad (I-11)$$

This result shows that in the equivalent model of Figure I-2, the spectral density of the ambient noise component of the primary hydrophone output must be

$$\sigma_z^2(\omega) = \left[\sum_{n=0}^{N-1} a_n^2 \right] \sigma_n^2(\omega) \qquad (I-12)$$

Next, consider this model in the special cases discussed in Appdenix A.1. Under the narrow source approximation,

$$s_1(k, \omega) = \int_{-\phi}^{\phi} \int_{-\phi}^{\phi} S_I(\phi_0 + \phi_1, \phi_0 + \phi_2, \omega) B (\cos (\phi_0 + \phi_1) - \cos \phi_d)$$

$$\exp \{-j \frac{\omega}{c} [(L+K-1) \ d \cos (\phi_0 + \phi_2)\} \ d\phi_1 d\phi_2$$

$$\exp \{-j \frac{\omega}{c} (N-1) \ d_p \cos \phi_d \}$$

$$\approx e^{-j \frac{\omega d}{c} (K\_L-1-k) \cos \phi_0} \int_{-\phi}^{\phi} \int_{-\phi}^{\phi} S_I (\phi_0 + \phi_1, \phi_0 + \phi_2, \omega)$$

$$[B (\cos(\phi_0 + \phi_1) - \cos \phi_d) \exp \{-j \frac{\omega}{c} (N-1) \ d_p \cos \phi_d \}]$$

$$\cdot \exp \{j \frac{\omega d}{c} [(K+L-1) \phi_1 - k\phi_2] \sin \phi_0\} \ d\phi_1 d\phi_2 \qquad (I-13)$$
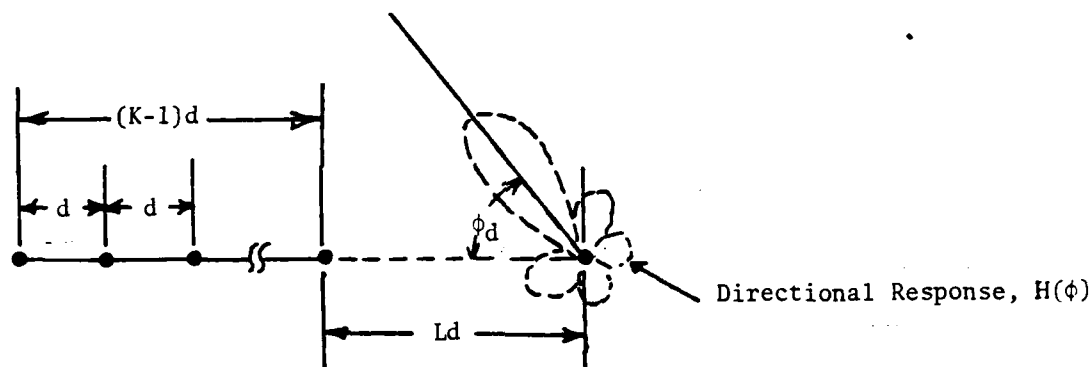
Figure I-2.   Equivalent Model for Primary Hydrophone Array

and (A-17) is replaced by

$$S_{11}(\omega) = \left[\sum_{n=0}^{N-1} a_n\right] \sigma_n^{\,2}(\omega) + \int_{-\pi}^{\pi} \int_{-\pi}^{\pi} S_I(\phi_1,\ \phi_2,\ \omega)$$

$$\left[\sum_{n=0}^{N-1} a_n\ \exp\{-j\ \frac{\omega d_p}{c}\,n(\cos\ \phi_1 - \cos\ \phi_d)\}\right]$$

$$\left[\sum_{m=0}^{N-1} a_m\ \exp\ \{j\ \frac{\omega d_p}{c}\,n(\cos\ \phi_2 - \cos\ \phi_d)\}\right]\,d\phi_1 d\phi_2$$

and

$$S_{11}(\omega) \simeq \sigma_z^2(\omega) + \int_{-\phi}^{\phi} \int_{-\phi}^{\phi} S_I(\phi_0 + \phi_1, \ \phi_0 + \phi_2, \ \omega)$$

$$B \ [\cos(\phi_0 + \phi_1) - \cos \phi_d] \ B^*[\cos(\phi_0 + \phi_2) - \cos \phi_d] \ d\phi_1 d\phi_2$$

$$(I-14)$$

Equations (I-13) and (I-14) correspond to (A-27) and (A-28), respectively.

When the source is additionally assumed to be spatially uncorrelated (I-13) and (I-14) further simplify to

$$s_1(k, \omega) \simeq e^{-j \frac{\omega d}{c} (K+L-1-k) \cos \phi_0} \int_{-\phi}^{\phi} S_I(\phi_0 + \phi, \ \omega)$$

$$[B \ (\cos(\phi_0 + \phi) - \cos \phi_d) \ \exp \ \{-j \frac{\omega d_p}{c} (N-1) \cos \phi_d\}]$$

$$\exp \ \{-j \frac{\omega d}{c} (K+L-1-k)\phi \ \sin \ \phi_0 \ d\phi \} \qquad (I-15)$$

and

$$S_{11}(\omega) \simeq \sigma_z^2(\omega) + \int_{-\phi}^{\phi} S_1(\phi_0 + \phi, \ \omega) |B \ [\cos(\phi_0 + \phi) - \cos \phi_d]|^2 \ d\phi$$

$$(I-16)$$

In Appendix A.2, the case when the extended source is uniformly distributed was considered. Under this assumption, the CSD, $s_1(k, \omega)$, and the PSD, $S_{11}(\omega)$ assumed the simple forms given by (A-40) and (A-41). When an array is used at the primary input and the source is uniform as defined in (A-38), (I-13) and (I-16) become

$$s_1(k, \omega) \approx e^{-j \frac{\omega d}{c} (K+L-1-k) \cos \phi_0} \int_{-\Phi}^{\Phi} \sigma_I^2(\omega)$$

$$[B (\cos(\phi_0 + \phi) - \cos \phi_d) \exp \{-j \frac{\omega d_p}{c} (N-1) \cos \phi_d]$$

$$\exp \{-j \frac{\omega d}{c} (K+L-1-k) \phi \sin \phi_0 \} d\phi \qquad (I-17)$$

and

$$S_{11}(\omega) \approx \sigma_z^2(\omega) + \int_{-\Phi}^{\Phi} \sigma_I^2(\omega) \, |B \, [\cos(\phi_0 + \phi) - \cos \phi_d]|^2 \, d\phi \qquad (I-18)$$

Hence $s_1(k,\omega)$ does not reduce to the sin x/x form given in (A-40) unless $B [\cos(\phi_0 + \phi) - \cos \phi_d]$ is constant for $\phi \epsilon [-\Phi, \Phi]$. That is, the form of (A-40) only occurs if the directional response of the primary array is constant, or at least nearly constant, over the extent of the interference source.

APPENDIX J: THE USE OF AN ADAPTIVE LMS CANCELLER IN THE
NON-STATIONARY REVERBERATION ENVIRONMENT

APPENDIX J – THE USE OF AN ADAPTIVE LMS CANCELLER IN THE NON-STATIONARY REVERBERATION ENVIRONMENT

In practice, the second order statistics of the reverberation are not known, and the canceller is implemented using a multiple LMS adaptive canceller structure as discussed in the Introduction. However, most of the work in this report has considered the performance of an optimal (in the least mean square sense) canceller with stationary extended source. Since the LMS adaptive filter converges in the mean to the discrete Wiener filter, the performance of the optimal filter can be regarded as representative of that of the adaptive canceller if algorithm noise, sampling, and finite filter length effects are negligible. The assumption of stationarity is necessary for the formulation of the problem in terms of the Wiener (LMS optimal) filter.

In a passive sonar environment, the assumption of stationarity on the canceller inputs reasonably models most sonar problems. On the other hand, the active sonar environment, taken as a whole, is markedly non-stationary. A transmission cycle will consist of a transmission, followed by periods in which reverberation from various sources (surface, bottom, convergence zone, etc.) dominates the noise field. Between reverberation periods, the ambient noise will be the primary limitation on sonar performance. It is therefore necessary to consider the effects of this non-stationary noise field on the performance of the adaptive canceller and any modifications to its structure necessary to accommodate this environment.

The canceller structure being discussed here is directed specifically toward suppression of surface reverberation from the convergence zone. If the filter is adapting during periods which the noise is due to the

ambient field or to reverberation from other sources, then the filter weights may not be reflective of the convergence zone reverberation. In order to allow detection of targets appearing during the onset of surface reverberation during any given transmission cycle, the canceller must have acquired enough information about the reverberation statistics during the preceding cycles, and retained enough of that information between the reverberation periods.

It is well known[11] that the LMS adaptive algorithm adapts much more rapidly in an environment producing correlation between its inputs (such as reverberation from any source) than to one producing uncorrelated inputs (such as ambient noise field would). That is, the filter "learns" the correlation properties of an input rapidly in comparison to the way it "forgets" those properties once the correlation disappears. Therefore, in order to maintain the properties of the convergence zone reverberation in the filter weights, it is first essential that all other forms of reverberation be excluded from the adaptation process. Because of the long range to the convergence zone, this can be done by freezing the adaptive weights following transmission until all other forms of reverberation have died out, then starting the adaptation process. Since the two way propagation time to the convergence zone is so long, the adaptation could be started some fixed time interval after transmission.

The question then arises as to the effect of the periods in which only ambient noise is present on the filter weights. This can be analyzed for a single reference structure using a simplified, approximate model, as follows. The LMS algorithm for real weights is given by [3]

$$\underline{W}(N+1) = [I - \mu \underline{X}(n)\underline{X}^T(n)] \underline{W}(n) + \mu d(n) \underline{X}(n) \qquad (J-1)$$

J-2

where

$\underline{W}(n)$ = weight vector at time n

$\underline{X}(n)$ = reference hydrophone output data vector

$= [x(n), x(n-1),...x(n-M)]^T$

$d(n)$ = primary hydrophone output sequence

μ = adaptation constant

Using the assumption that the present weight vector is uncorrelated with the present data vector and averaging (J-1) yields a difference equation for the mean weights,

$$\underline{E}[W(n+1)] = [I - \mu R_{xx}(n)] \, E \, [\underline{W}(n)] + \mu \underline{R}_{dx}(n) \qquad (J-2)$$

where

$$R_{xx}(n) = E \, [\underline{X}(n)\underline{X}^T(n)]$$

$$\underline{R}_{dx}(n) = E \, [d(n) \, X(n)]$$

If $R_{xx}(n)$ and $R_{dx}(n)$ are independent of the n, then

$$\lim_{n \to \infty} E[W(n)] = R_{xx}^{-1} \underline{R}_{dx} \qquad (J-3)$$

which is the discrete Wiener filter as indicated above.

Now, assume that a pulse is transmitted starting every T seconds, and that the weights are frozen during the period $nT + T_w$, that is, for the T_w seconds following the start of each transmission as shown in Figure J-1. This presumably excludes all reverberation except for
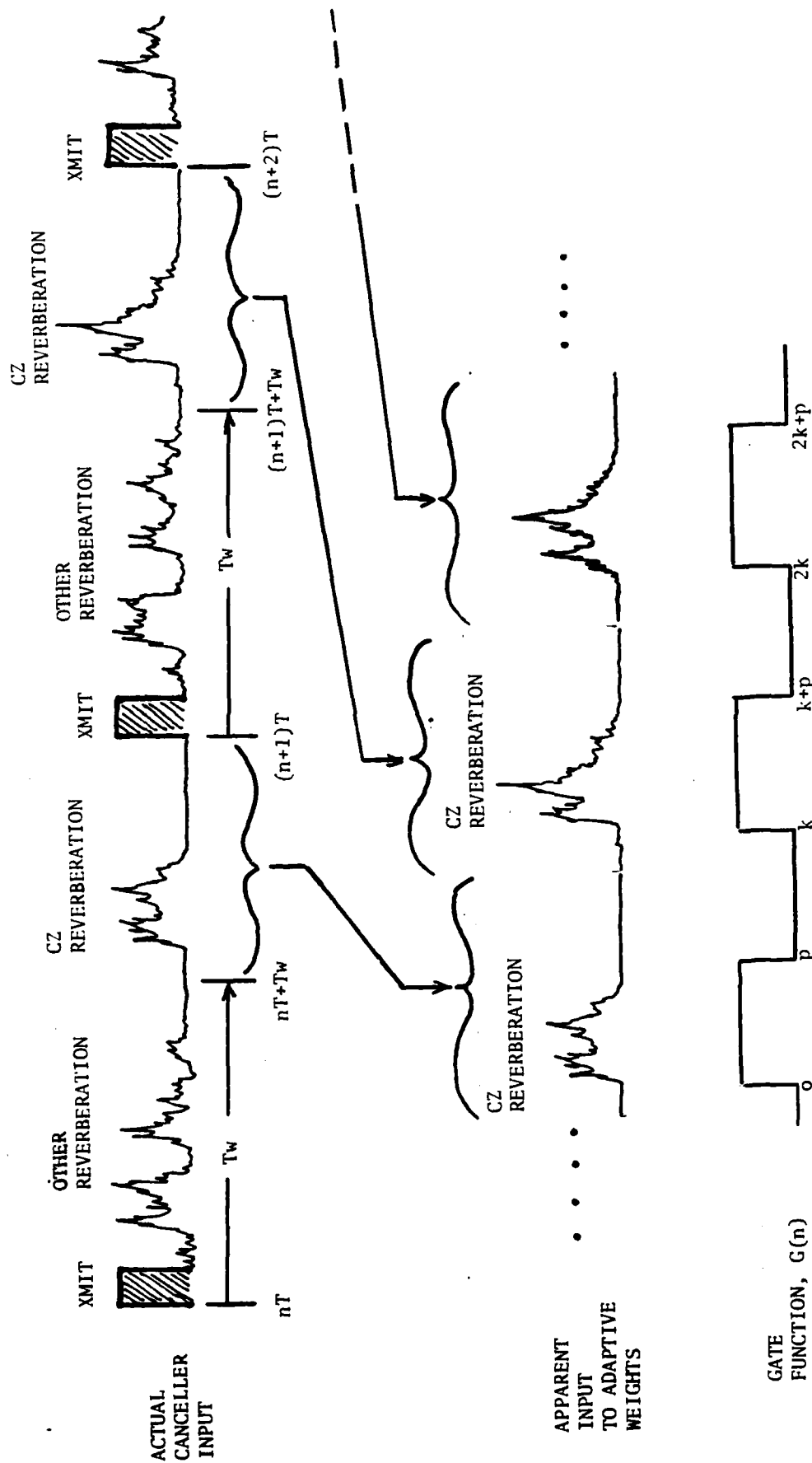
Figure J-1: Effective Input to Adaptive Weights Due to Freezing the Weights for a Time Tw After Onset of Transmission

J-4

convergence zone from the filter surface reverberation during adaptation. From the point of view of the adaptive weights, then, the input consists of the intervals $[nT + T_w, (n+1)T]$ for $n = 1, 2, \ldots$ concatenated together as shown in Figure J-1 to form a continuous input sequence. Suppose that this concatenated input is sampled every T seconds to produce the inputs $x(n)$ and $d(n)$.

First, consider the primary input to the canceller. Let the gate function, $G(n)$, shown in Figure J-1 characterize the period during which the reverberation is present. Let $d_o(n)$ be the portion of the desired input due to ambient noise and let $r_d(n)$ be the reverberation as seen by the primary. Then

$$d(n) = d_o(n) + G(n)r_d(n) \qquad (J-4)$$

Similarly, let $x_o(n)$ be the ambient noise at the reference input and $r_x(n)$ be the reverberation as seen by the reference. It is now assumed that the gate function seen by the reference is just a delayed version of $G(n)$, i.e.,

$$x(n) = x_o(n) + G(n-\Delta)\, r_x(n) \qquad (J-5)$$

with Δ an integer. Then

$$\underline{X}(n) = \underline{X}_o(n) + H_G(n-\Delta)\underline{r}_x(n) \qquad (J-6)$$

where

$$\underline{X}_o = [x_o(n), x_o(n-1), \ldots x_o(n-M)]^T \qquad (J-7)$$

$$\underline{r}_x(n) = [r_x(n), r_x(n-1), \ldots, r_x(n-M)]^T \qquad (J-8)$$

and

$$H_G(n-\Delta) = \text{diag} \, [G(n-m-\Delta)] \qquad\qquad (J-9)$$
$$m = 0,1, \ldots M$$

Consequently

$$R_{xx}(n) = P_n I + H_G(n-\Delta) R_{RR} \, H_G^+ \, (n-\Delta) \qquad\qquad (J-10)$$

and

$$\underline{R}_{dx}(n) = H_G(n-\Delta) R_{dx} \, G(n-\Delta) \qquad\qquad (J-11)$$

where it has been assumed that the ambient noise is uncorrelated in time with power, P_n, and is also uncorrelated between hydrophones. R_{RR} is the reverberation return covariance matrix, and R_{dx} the reverberation return cross-correlation vector. Note that the reverberation has been assumed stationary during the period when $G(n)$ is unity.

Now, consider $H_G(n-\Delta)$ for $o \leq n < k$ as shown in Figure J-1. $H_G(n-\Delta)$ is an identity matrix if

$$o \leq n - m - \Delta \leq p \qquad\qquad (J-12)$$

for $m = 0, 1, \ldots M$, hence if $M + \Delta \leq n \leq p + \Delta$

$$H_G(n-\Delta) = I, \begin{cases} n < k \\ M + \Delta \leq n \leq p + \Delta \end{cases} \qquad\qquad (J-13)$$

Thus, for p-M iterations of the filter during the first p iterations, $H_G(n-\Delta) = I$. Similarly, for $o \leq n \leq k$,

$$H_G(n-\Delta) = \underline{0} \qquad\qquad (J-14)$$

if $p < n-m-\Delta < k$ for $m = 0, 1, \ldots M$. This occurs if $p+M+\Delta < n < k+\Delta$, so that $H_G(n-\Delta) = 0$ for $k-p-M-2$ iterations during the $k-p$ iterations from $n = p+1$ to $n = k-1$. These arguments can easily be extended to the successive transmission cycles.

It now is assumed that the length of the filter, M, is much less than the reverberation duration, p, and the duration of the reverberation-free period, $k-p$. Then "most of the time", $\underline{G}(n-\Delta)$ will be either I or O, and it seems reasonable that the short periods when this is not true will not significantly affect the filter response. Then, approximately

$$H_G(n-\Delta) = G(n)I \qquad (J-15)$$

and

$$R_{xx}(n) = P_oI + G(n) R_{RR} \qquad (J-16)$$

$$\underline{R}_{dx}(n) = G(n) \, G(n-\Delta) \, R_{dx} \qquad (J-17)$$

If it is additionally assumed that the duration of the reverberation, p, is long in comparison with the inter-hydrophone delay, Δ, then (J-11) can be approximately written

$$\underline{R}_{dx}(n) = G(n) \, R_{dx} \qquad (J-18)$$

without significantly affecting the results.

Using equations (J-16) and (J-18) in (J-2) yeilds

$$E[W(n+1)] = \{I(1-\mu P_n) - \mu G(n)R_{RR}\} \quad E[W(n)] + \mu G(n)R_{dx} \qquad (J-19)$$

Since R_{RR} is a positive definite symmetric real matrix, it can always be written as normal form as

$$R_{RR} = P^T \Lambda P = P^{-1} \Lambda P \qquad (J\text{-}20)$$

where P is an ortho normal matrix consisting of the eigenvectors of R_{RR}, and $\Lambda = \text{Diag} [\lambda_1, \lambda_2, \ldots \lambda_M)$

$$= \text{eigenvalues of } R_{RR}$$

Hence (J-19) can be written as

$$E[W(n+1)] = \{I(1-\mu P_n) + \mu P^T G(n)\Lambda P\} E[W(n)] + \mu G(n)R_{dx} \qquad (J\text{-}21)$$

Multiplying (J-21) from the left by P and letting $Q(n) = P E[\underline{W}(n)]$ yields

$$Q(n+1) = \{(1-\mu P_n)I - \mu G(n)\Lambda\} Q(n) + \mu G(n)PR_{dx} \qquad (J\text{-}22)$$

Since the matrices inside the brackets are diagonal, each component of Q(n) can be solved for separately

$$Q_i(n+1) = 1 - \mu[P_N + G(n)\lambda_i]\} Q_i(n) + \mu G(n)(PR_{dx})_i \qquad (J\text{-}23)$$

The above is a piece-wise constant parameter linear system with on-off input and on-off system parameters. Then (J-23) can be contrasted with the approach in [11] where the eigenvalues are constant but the eigenvectors are not. Here the eigenvalues of (J-19) (not the eigenvectors) are the functions of time. Thus transforming to the eigenvectors of the data covariance matrix allows closed form solution for the mean weights.

Now (J-23) can be solved in a piece-wise manner as follows. Letting $(PR_{dx})_i = \alpha_i$, during the time $0 \leq n \leq p$ (reverberation return is present)

$$Q_i(n) = Q_i(o) \, g_i^n \; + \; \mu\alpha_i \sum_{m=1}^{n} g_i^{n-m}$$

where

$$g_i = 1 - \mu(P_n + \lambda_i) \tag{J-24}$$

g_i^n is the discrete time impulse response of the system described by (J-23) when $G(n) = 1$. The sum can be written in closed form so that

$$Q_i(n) = Q_i(o) \, g_i^n \; + \; \mu\alpha_i \left(\frac{1 - g_i^n}{1 - g_i} \right), \quad 0 \leq n \leq p \tag{J-25}$$

Assume, for simplicity that $Q_i(o) = 0$ all i. Then, for $p \leq n \leq k$, $G(n) = o$ and

$$Q_i(n) = Q_i(p) \, b^{n-p}, \quad b = 1 - \mu P_n. \tag{J-26}$$

That is, when the reverberation disappears, the driving function of (J-19) is zero.

The system decays from its value when the input disappears with impulse response b^n. After one complete period $(n=k)$,

$$Q_i(k) = Q_i(p) \, b^{k-p} = \mu\alpha_i \left(\frac{1 - g_i^p}{1 - g_i} \right) b^{k-p} \tag{J-27}$$

If one repeats the same arguments during the successive periods of $G(n)$, the following solution results

$$Q_i[mk+p] = \frac{\mu\alpha_i(1-g_i^{p})}{1-g_i} \sum_{r=0}^{m} [g_i^{p} g^{k-p}]^r \qquad (J-28)$$

$$Q_i[(m+1)k] = b^{k-p} Q_i[mk+p]$$

at the switching times. In between switching times, for $mk+p < n < (m+1)k$

$$Q_i(n) = b^{n-(mk+p)} Q_i[mk+p] \qquad (J-29)$$

and for $mk < n < mk + p$

$$Q_i(n) = g_i^{n-mk} Q_i(mk) + \mu\alpha_i \frac{[i-g_i^{n-mk}]}{1-g_i} \qquad (J-30)$$

Equations (J-29) and (J-30) have simple physical interpretations. Equation (J-29) implies that, between switching times when no input is applied, the system decays with a rate b from its value when the input was last applied, while (J-30) implies that the system response consists of (a) a transient response term $g_i^{n-mk} Q_i(mk)$ due to the initial condition ($Q_i(mk)$) when the input is turned on, with decay rate g_i, and (b) a response to the input $\mu\alpha_i$ with the step response of first order system with time constant g_i, $(1-g_i^{n-mk})/(1-g_i)$.

As the number of iterations increases, the $Q_i(n)$ becomes periodic with

$$\lim_{m \to \infty} Q_i(n) = b^{n-(mk+p)} Q_i(mk+p) \qquad mk+p \leq n \leq (m+1)k \quad (J-31)$$

$$\lim_{m \to \infty} Q_i(n) = \frac{\mu \alpha_i}{1-g_i} \left\{ \frac{g_i^{n-mk}(1-g_i^p)g^{k-p}}{1-g_i^p b^{k-p}} + (1-g_i^{n-mk}) \right\} mk \leq n \leq mk+p \quad (J-32)$$

As a check, letting $m \to \infty$ in (J-28) and $n=mk+p$ in (J-32) yields equality. Also, letting $n=(m+1)$ and $m \to \infty$, (J-31) and (J-28) yield agreement. Also

$$\lim_{m \to \infty} Q_i(n) = \frac{\mu \alpha_i}{1-g_i}, \quad p = k \text{ (no dead time)}$$

$$\lim_{m \to \infty} Q_i(n) = 0 \quad , \quad p = o \text{ (no input)} \qquad (J-33)$$

This result is analogous to the response of an RC filter to a periodic rectangular pulse train as shown in Figure J-2. There is an initial transient buildup that tries approach a steady value that would occur with no pulsing. Because of the pulsing, a decay is superimposed upon this transient. If the response, when the pulse is on, is large in comparison to the response when the pulse is off, the steady state value is quickly achieved. If the reverse is true, then the weights do not change significantly. Two factors contribute to the response; the percentage of time in each mode (duty cycle) and the rapidity of the response in each mode. Now the rapidity of the response in each mode is given by g_i and b with

$$g_i = 1 - \mu(P_n + \lambda_i) < 1 - \mu P_n = b \qquad (J-34)$$
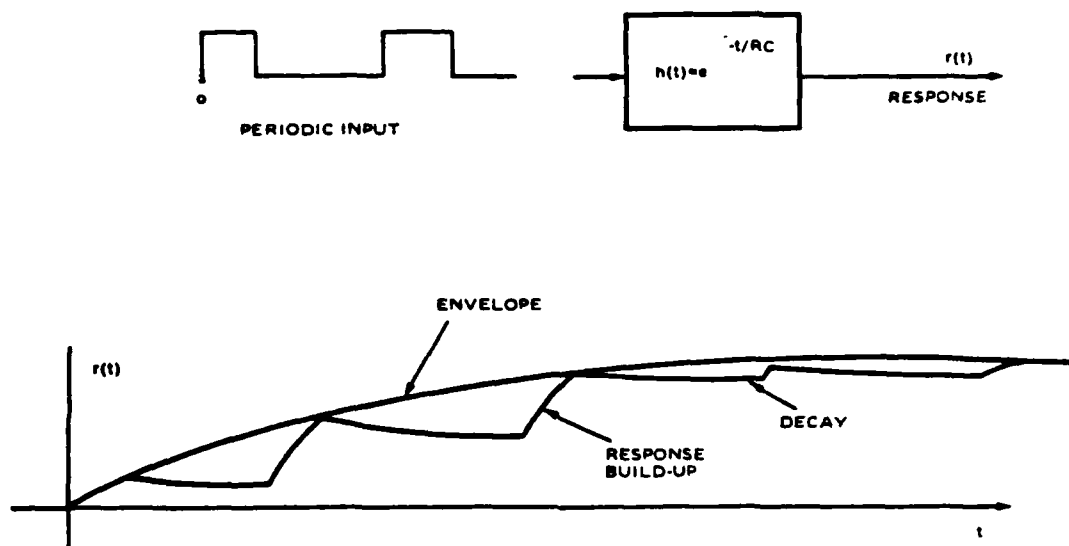
Figure J-2. Weight Response Analogy to RC Filter Response

Using (J-28), as $m \to \infty$,

$$Q_i[mk+p] = \frac{\mu\alpha_i \ (1-g_i^p)}{(1-g_i) \ (1-g_i^p b^{k-p})} \qquad (J-35)$$

Equation (J-35) can be viewed as consisting of three factors,

steady-state response with no pulsing $= \dfrac{\mu\alpha_i}{1-g_i}$ \qquad (See Eq. (J-33))

transient response during one pulse $= 1-g_i^p$

long term transient response $= (1-g_i^p b^{k-p})^{-1}$

Imbedded in the last factor is the time constant to achieve a periodic steady-state. From (J-28), the factor in the sum can be written as follows:

$$\left(g_i^{\,p}\, b^{k-p}\right)^m = \left(g_i^{\,p/k}\, b^{1-\frac{p}{k}}\right)^{km} \tag{J-36}$$

However, km = total no. of algorithm iterations (ignoring relatively few iterations during one period for large k). Hence, the factor $g_i^{\,p/k}\, b^{1-p/k}$ is the effective time constant of the pulsed system. Now

$$g_i^{\,p/k}\, b^{1-p/k} = \left[\frac{1-\mu(P_n+\lambda_i)}{1-\mu P_n}\right]^{\frac{p}{k}} \;(1-\mu P_n)$$

$$= \left[1 - \frac{\mu\lambda_i}{1-\mu P_n}\right]^{\frac{p}{k}} \;(1-\mu P_n) \tag{J-37}$$

But p/k is the duty cycle. If $\mu P_n \ll 1$ and $\mu\lambda_i \ll 1$, all i, then

$$g_i^{\,p/k}\, b^{1-p/k} \approx (1-\mu \tfrac{p}{k}\, \lambda_i)\,(1-\mu P_n) \approx 1 - \mu(P_n + \lambda_i \tfrac{p}{k}) \tag{J-38}$$

Hence the response of the pulsed system is determined by the product of μ and the sum of the noise power plus the eigenvalue times the duty cycle (sort of the time average eigenvalue). This result is very physically satisfying.

Alternatively, in equation (J-37), the factor $(1-g_i^{\,p})/(1-g_i^{\,p}\, b^{k-p})$ can be viewed as the steady-state amplitude loss.

One may now transform back to the original coordinate system to obtain the behavior of $\underline{E}[W(n)]$. Assuming steady-state periodic behavior and using equations (J-31) and (J-32), for $mk+p < n < (m+1)k$

$$\lim_{n \to \infty} E[\underline{W}(n)] = b^{n-(mk+p)} E[\underline{W}(mk+p)]$$

$$= b^{n-(mk+p)} \mu P^T \operatorname*{Diag}_{\substack{i=0,1,\ldots \\ M-1}} \left[\frac{1-g_i^p}{1-g_i} \frac{1}{1-g_i^p b^{k-p}} \right] P\underline{R}_{dx} \qquad (J-39)$$

and for $mk \leq n \leq mk+p$

$$\lim_{n \to \infty} E[W(n)] = \mu P^T \operatorname{Diag} \left[\left\{ \frac{1-g_i^p}{1-g_i} \frac{g_i^{n-mk}}{1-g_i^p b^{k-p}} b^{k-p} + \frac{1-g_i^{n-mk}}{1-g_i} \right\} \right] P\underline{R}_{dx} \qquad (J-40)$$

It is clear from equations (J-39) and (J-40) that the mean weights are time varying, even in steady-state. The mean weights are periodic, however, to determine the difference between the mean weight and the Wiener weights requires specific knowledge of P. Note, as a check, for $p=k$, (J-40) becomes

$$\lim_{n \to \infty} E[\underline{W}(n)] = \mu P^T \operatorname{Diag} \left[\frac{1}{1-g_i} \right] P\underline{R}_{dx}$$

$$= \mu P^T \operatorname{Diag} \left[\frac{1}{\mu(\lambda_i + P_n)} \right] P\underline{R}_{dx}$$

$$= R_{xx}^{-1} R_{dx} = \text{Wiener weights} \qquad (J-41)$$

J-14

Of primary interest are the weights during the time the reverberation is present, given by (J-39). Note that $(1-g_i) = 1 - [1-\mu(P_n+\lambda_i)] = \mu(P_n+\lambda_i)$, so (J-39) can be written

$$\lim_{n\to\infty} E[\underline{W}(n)] = P^T \operatorname*{diag}_i \left[\frac{1-g_i^p}{1-g_i^p \, b^{k-p}} \, g_i^{n-mk} \, b^{k-p} + (1-g_i^{n-mk}) \right]$$

$$\operatorname*{diag}_i \left[\frac{1}{P_n+\lambda_i} \right] P\underline{R}_{dx}$$

$$= P^T \, [P_n + \Lambda]^{-1} \, P\underline{R}_{dx}$$

$$+ P^T \operatorname*{diag}_i \left[g_i^{n-mk} \right] \operatorname*{diag}_i \left[\frac{1-b^{1-p}}{1-g_i^p \, b^{k-p}} \right] P[P_n + \Lambda]^{-1} \, P\underline{R}_{dx}$$

$$= \tilde{R}_{xx}^{-1} \, \underline{R}_{dx} - (1-b^{k-p}) \, P^T \, D_1^{n-mk} \, D_2 \, P(R_{xx}^{-1} \, \tilde{\underline{R}}_{dx}) \quad \text{(J-42)}$$

where

$$D_1 = \operatorname*{diag}_i \, [g_i] = \operatorname*{diag}_i \, [1-\mu(P_n+\lambda_i)] \quad \text{(J-43)}$$

and

$$D_2 = \operatorname*{diag}_i \left[\frac{1}{1-g_i^p \, b^{k-p}} \right]$$

$$= \operatorname*{diag}_i \left[\frac{1}{1-[1-\mu(P_n+\lambda_i)]^p \, [1-\mu P_n]^{k-p}} \right] \quad \text{(J-44)}$$

where $\tilde{R}_{xx}$ is the reference covariance that would occur if the reverberation were always present.

Then the first term is just the Wiener weights that would occur if the reverberation were always present, while the second term is a time varying deviation of the weights due to the pulsed nature of the reverberation. Note that since m simply defines the particular transmit cycle in which n lies, (J-42) can be rewritten

$$\lim_{n \to \infty} E[\underline{W}(n)] = \tilde{R}_{xx}^{-1}\underline{R}_{dx} + (1-b^{k-p})P^T D_1^{n'} D_2 P(\tilde{R}_{xx}^{-1}\underline{R}_{dx}) \qquad (J-45)$$

with n´ the time since the onset of reverberation in the current cycle. At the beginning of the reverberation (n´=0)

$$\lim_{n \to \infty} E[\underline{W}(n)] = \tilde{R}_{xx}^{-1}\underline{R}_{dx} + (1-b^{k-p})P^T D_2 P(\tilde{R}_{xx}^{-1}\underline{R}_{dx}) \qquad (J-46)$$

while at the end of the reverberation (n´=p)

$$\lim_{n \to \infty} E[\underline{W}(n)] = \tilde{R}_{xx}^{-1}\underline{R}_{dx} + (1-b^{k-p})P^T D_1^P D_1 P(\tilde{R}_{xx}^{-1}\underline{R}_{dx}) \qquad (J-47)$$

The conditions under which the weights converge to $\tilde{R}_{xx}^{-1}\underline{R}_{dx}$ are that either

$$(1-b^{k-p}) = 0 \Rightarrow k = p \qquad (J=48)$$

or

$$D_1^{n'} D_2 = 0 \qquad (J-49)$$

But

$$D_1^{n'} D_2 = \underset{i}{\text{diag}} \left[\frac{\left[1 - \mu [P_n + \lambda_i] \right]^{n'}}{1 - \left[1 - \mu [P_n + \lambda_i] \right]^{P} \left[1 - \mu P_n \right]^{k-p}} \right] \qquad (J\text{-}50)$$

For a filter with acceptable algorithm noise, $[P_n + \lambda_i] \ll 1$, so

$$D_1^{n'} D_2 > 0 \qquad (J\text{-}51)$$

Hence the Wiener weights, $\tilde{R}_{xx} R_{dx}$, are not reached in steady state unless p=k, so that the reverberation is always present. This means that the canceller performance is degraded fromthat which would be achieved if reverberation were alwyas present at the filter input. The degradation will depend upon the factor $(1 - b^{k-p})$ and upon the time varying maxtrix, $D_1^{n'} D_2$, given by (J-50).

Of most interest here is the mean square error of the adaptive canceller, which represents the power in the output. This is given by

$$E[E^2(n)] = E[d(n) - \underline{W}^T(n) \, \underline{X}(n)]^2$$

$$= E[d^2(n)] - 2E[\underline{W}^T(n) \, d(n) \, \underline{X}(n)]$$

$$+ E[\underline{W}^T(n) \, \underline{X}^T(n) \, \underline{W}(n)] \qquad (J\text{-}52)$$

J-17

Just as in the derivation of the mean weights, (J-2), it is quite common to assume that the weights are uncorrelated with the present data, so that

$$E_{\underline{W}(n)}[E^2(n)] = E[d^2(n)] - 2\underline{W}(n)\,\underline{R}_{dx}(n) + \underline{W}^T(n)\,R_{xx}(n)\,\underline{W}(n) \quad (J-53)$$

where $E_{\underline{W}(n)}$ denotes the expectation conditioned on $\underline{W}(n)$. In the actual adaptive implementation, the weights are random variable which can be written as

$$\underline{W}(n) = E[\underline{W}(n)] + \underline{Q}_W(n) \quad (J-54)$$

with $\underline{Q}_W(n)$ the zero mean, fluctuating part of $\underline{W}(n)$. Ignoring these fluctuations is equivalent to neglecting algorithm noise, which reduces (J-53) to

$$E[E^2(n)] = E[d^2(n)] - 2E[\underline{W}(n)]\,\underline{R}_{dx}(n)$$
$$+ E[\underline{W}^T(n)]\,R_{xx}(n)\,E[\underline{W}(n)] \quad (J-55)$$

If the reverberation were always present, then the inputs are stationary, and ( ) yields the Wiener solution in steady state,

$$\lim_{n \to \infty} E[E^2(n)] = \tilde{R}_{dd} - \underline{\tilde{R}}_{dx}^T\,\tilde{R}_{xx}^{-1}\,\underline{\tilde{R}}_{dx} \quad (J-56)$$

with $\tilde{R}_{dd} = E[d^2(n)]$ under the condition that the reverberation is always present. However in the actual case, it has been shown above that the mean weights are periodic as $n \to \infty$, and are given by equation (J-42).

This can be rewritten

$$\lim_{n \to \infty} E[W(n)] = [I-A] \, \tilde{R}_{xx}^{-1} \, \tilde{R}_{dx} \qquad (J-57)$$

where

$$A = (1-b^{k-p})P^T \, D_1^{n-mk} \, D_2 P \qquad (J-58)$$

The matrix, A, displays the time varying nature of the man weights. Note that when k=p, so that reverberation is on all the time, A=0, and equation (J-57) reduces to (J-56). On the other hand, if p=o, so that reverberation is always present, A=I, and the mean weights are zero, as they should be in an uncorrelated environment. Substituting (J-57) into (J-55) under the condition that the reverberation is present gives

$$\lim_{n \to \infty} [E^2(n)] = \tilde{R}_{dd} - \tilde{R}_{dx}^T \, \tilde{R}_{xx}^{-1} \, \tilde{R}_{dx} + \tilde{R}_{dx}^T \, \tilde{R}_{xx}^{-1} \, A\tilde{R}_{xx} \, A\tilde{R}_{xx}^{-1} \, \tilde{R}_{dx} \quad (J-59)$$

The first two terms are just the mean square error that would be achieved if the reverberation were always present, from (J-56), while the second term is the increase due to the "pulsed" character of the inputs.

Now, denote the second term in (J-59) as γ and use (J-58 to write

$$\gamma = (1-b^{k-p})^2 \, \tilde{R}_{dx}^T \, P^T \, D_1^{2(n-mk)} \, D_2^2 \, (Pn+\Lambda)^{-1} \, P \, \tilde{R}_{dx} \qquad (J-60$$

Let α_i be the $i\underline{th}$ element of $P\tilde{R}_{dx}$, which is the projection of $\tilde{R}_{dx}$ on the $i\underline{th}$ eigenvector. Then (J-60) becomes

J-19

$$\gamma = (1-b^{k-p})^2 \sum_{i=0}^{K-1} \frac{\alpha_i^2 D_{1i}^{2(n-mk)} D_{2i}^2}{P_n + \lambda_i} \tag{J-61}$$

where D_{1i} and D_{2i} are the $i\underline{th}$ diagonal components of D_1 and D_2, respectively, and where λ_i is the $i\underline{th}$ eigenvalue of $\tilde{R}_{xx}$. This can be written as

$$\gamma = (1-b^{k-p})^2 \sum_{i=0}^{K-1} \frac{\alpha_i^2 [1-\mu(P_n+\lambda_i)]^{2(n-mk)}}{(P_n+\lambda_i)[1-(1-\mu(P_n-\lambda_i))^P (1-\mu P_n)^{k-p}]^2} \tag{J-62}$$

In order to evaluate the increase in he canceller output power due to the "pulsed" character of the reverberation, it is necessary to know the eigenvalues of $\tilde{R}_{xx}$ and the projections of $\tilde{R}_{dx}$ on the eigenvectors of $\tilde{R}_{xx}$. Further, the increase in output power can be seen to depend upon μ, but this dependence is quite complex, as (J-62) shows.

J.1 Special Case - Narrowband Interference

Suppose that the interference consists of a single frequency sine wave of frequency, ωo, and that the array has the geometry of Figure A-1. Then

$$\tilde{R}_{xx} = (\frac{P_I}{2} \underline{d} \ \underline{d}^+ + \underline{d}* \ \underline{d}^T) \tag{J-63}$$

where

$$[I, e^{-j\omega_o(\Delta t)}, e^{-j\omega_o 2(\Delta t)}, \ldots\ldots e^{-j\omega_o(K-1)(\Delta t)}]^T \tag{J-64}$$

where $\underline{d}^+ \underline{d} = K$, and for simplicity $\underline{d}^T \underline{d} = 0$. Also

Δt = spacing between filter taps

and

$$\underline{\tilde{R}}_{dx} = \frac{P_I}{2} \; (e^{-j\omega_o \Delta} \; \underline{d} + e^{j\omega_o \Delta} \; \underline{d}*) \tag{J-65}$$

This special case gives

$$\lambda_1 = K \, P_I$$

$$\lambda_2 = \lambda_3 = \ldots \approx \lambda_K = 0 \tag{J-66}$$

$$P = [(\underline{d} + \underline{d}*), \; \underline{a}*, \; \underline{a}_2^*, \; \ldots \; \underline{a}_{K-2}^*]^T \tag{J-67}$$

where the $\underline{a}_i$ are any set of orthonormal vectors or thogonal to $\underline{d} + \underline{d}*$.
Then

$$a_i = \begin{cases} \sqrt{\frac{K}{2}} P_I \, \cos \, \omega_o \Delta, & i = 1 \\ 0, & \text{otherwise} \end{cases} \tag{5-68}$$

Substituting (J-68) into (J-62) gives

$$\gamma = \frac{[1 - (1-\mu P_n)^{k-p}]^2 \, MP_I^2 \, [1 - \mu(P_n + MP_I)]^{2(n-mk)}}{(P_n + MP_I) \, [1 - (1-\mu(P_n + MP_I))^P \, (1-\mu P_n)^{k-p}]} \tag{J-69}$$

The increase in the output power will be largest when the reverberation

first begins, n=mk, so

$$\gamma_{max} = \frac{MP_I[1 - (1-\mu P_n)^{k-p}]^2}{(P_n+MP_I)\ [1 - (1-\mu(P_n+MP_I))^P\ (1-\mu P_n)^{k-p}]}\ \cos^2\ (\omega_o\Delta/2)$$

$$\simeq \frac{[1 - (1-\mu P_n)^{k-p}]^2}{[1 - (1-\mu MP_I)^P\ (1-\mu P_n)^{k-p}]}\ \cos^2\ (\omega_o\Delta/2)$$

APPENDIX K: NUMERICAL EVALUATIONS OF THE LMS
CANCELLER PERFORMANCE WITH A UNIFORMLY DISTRIBUTED,
SPATIALLY UNCORRELATED NARROW SOURCE

APPENDIX K — NUMERICAL EVALUATIONS OF THE LMS CANCELLER PERFORMANCE WITH A UNIFORMLY DISTRIBUTED, SPATIALLY UNCORRELATED NARROW SOURCE

Using the results of Appendix E, the canceller output spectrum for K reference hydrophones, $E_k(\omega)$, can be evaluated on the computer. Similarly, using the results of Appendix H, the spatial response of the optimal canceller can be determined. Evaluation of (E-20) for $E_k(\omega)$ and (H-13) for the spatial response, $B_W(\phi_s)$, requires determination of the DPSS, $\{V_J^{(k)}\}_{k=0, 1, \ldots K-1}$ for $J \geq K$, and the associated eigenvalues, $\lambda_k(K,W)$. The DPSS, $\{V_n^{(k)}(K,W)\}_{k=0, 1, \ldots K-1}$ for $0 \leq n \leq K-1$ are computed by numerically solving the eigenvalue problem

$$S(K, \omega) \; \underline{V}_k(K,W) = \lambda_k(K,W) \; \underline{V}_k(K,W) \tag{K-1}$$

where

$$S(K,\omega) = \left(\frac{\sin \; (2\pi W(p-q))}{\pi(p-q)} \right)_{\substack{p=0, \; 1, \; \ldots \; K-1 \\ q=0, \; 1, \; \ldots \; K-1}} \tag{K-2}$$

The resulting $\underline{V}_k(K,W)$ are given by

$$\underline{V}_k(K,W) = [V_0^{(k)}(K,W), \; V_1^{(k)}(K,W), \; \ldots, \; V_{K-1}^{(k)}(K,W)]^T$$

and the $\lambda_k(K,W)$ are the desired eigenvalues. The $V_j^{(k)}(K,W)$ for $J \geq K$ can then be determined by evaluating equation (E-10),

$$\sum_{m=0}^{K-1} \frac{\sin \; [2\pi W(n-m)]}{\pi(n-m)} \; V_m^{(k)}(K,W) = \lambda_k(K,W) \; V_n^{(k)}(K,W) \tag{K-4}$$

In the development of the narrow source model in Appendix A, it was assumed that Φ was sufficiently that

$$\sin\ \Phi \simeq \Phi$$
$$\cos\ \Phi \simeq 1 \tag{K-5}$$

where

$$W = \Phi \frac{d}{\lambda} \sin \phi_o \tag{K-6}$$

This restriction will be interpreted as requiring that $\Phi < .2$ radians (approximately $11.5°$), mainly to assure that $\cos \Phi \simeq 1$. Therefore

$$W \leq .2 \frac{d}{\lambda} \sin \phi_0 < .2 \frac{d}{\lambda} \tag{K-7}$$

Usually in array designs,

$$.5 \leq \frac{d}{\lambda} \leq 1 \tag{K-8}$$

If $d/\lambda < .5$, the ambient noise components of the hydrophone outputs will be correlated, limiting their usefulness for increasing array gain. If the upper limit is exceeded, then the array response will include grating lobes. These considerations suggest that the main interest will be in values of $W < .2$. Certainly, given the sampling criterion, $W \leq .5$, developed in Appendix F, values of $W \geq .5$ will be of no practical interest. Several cases with $W > .5$ will be shown, however, to illustrate the importance of the sampling criterion.

The plots of the numerical results included here are summarized in Table K-1. Each plot shows the canceller output spectrum, $E_k^{(W)}$, at a single frequency, W, as a function of the number of reference hydrophones used in the canceller for a particular value of W. The results are given for a range of values of the parameter m, where the reference array is a distance, md, from the primary hydrophone. To determine the cancellation for a particular case of interest, the hydrophone spacing is computed in wavelengths for the frequency of interest, ω. Since cancellation will improve as W decreases, the largest value of ϕ_0 (the angle to the interference, always $\leq \pi/2$) should be used to compute (K-6), so that the resulting cancellation performance will be an lower bound on achievable cancellation. The distance from the primary to the references is then determined in units of d to provide the parameter, m.

Figures K-1 through K-5 were plotted using values of W that violate the sampling criterion, W > 1/2, to further illustrate just how limited cancellation is if this condition is not met. These curves clearly support Figure F-3, which showed the irreducible canceller output spectrum, $E_\infty(1,\omega)$ for the case m=1. Since it was also shown in Appendix D that

$$E_k(m,\omega) > E_k(1,\omega), m > 1 \qquad (K-9)$$

it would be expected that cancellation is also severely limited for m > 1 when W > .5.

The remaining Figures illustrate the properties of the canceller structure derived in the preceding sections. In the presence of noise, cancellation to the noise floor is never achieved, as predicted, and in fact

Table K-1. Parameter Values for Numerical Results in
Figures K-1 through K-62

W	INR			
	∞	40 dB	30 dB	20 dB
1.25	K-1	-	-	-
1.0	K-2	-	-	-
.75	K-3	-	-	-
.6	K-4	-	-	-
.5	K-5	-	-	-
.4	-	K-6	K-7	K-8
.3	-	K-9	K-10	K-11
.2	-	K-12	K-13	K-14
.1	-	K-15	K-16	K-17
.08	-	K-18	K-19	K-20
.06	-	K-21	K-22	K-23
.04	-	K-24	K-25	K-26
.02	-	K-27	K-28	K-29
.01	-	K-30	K-31	K-32
.008	-	K-33	K-34	K-35
.006	-	K-36	K-37	K-38
.004	-	K-39	K-40	K-41
.002	-	K-42	K-43	K-44
.001	-	K-45	K-46	K-47
.0008	-	K-48	K-49	K-50
.0006	-	K-51	K-52	K-53
.0004	-	K-54	K-55	K-56
.0002	-	K-57	K-58	K-59
.0001	-	K-60	K-61	K-62

the output spectrum can be significantly above the noise floor. Appendix D derived the cancellation floor, $E_\infty(1,\omega)$, for the m=1 case with W<1/2 as

$$E(1,\omega) = 2\Phi\sigma_I^2(\omega)(INR)^{-1} \left[1 + \frac{INR}{2W}\right]^{2W} \tag{K-10}$$

where $2\Phi\sigma_I^2(\omega)$ is the interference power received at any of the hydrophones and where INR is the interference to ambient noise ratio,

$$INR = \frac{2\Phi\sigma_I^2(\omega)}{\sigma_n^2(\omega)} \tag{K-11}$$

The power at the primary output without use of the canceller is $2\Phi\sigma_I^2(\omega) + \sigma_n^2(\omega)$, so that the maximum achievable cancellation, $C_\infty(1,\omega)$, is

$$C_\infty(1,\omega) = \frac{E_\infty(1,\omega)}{2\Phi\sigma_I^2(\omega) + \sigma_n^2(\omega)} = \frac{1}{1 + INR} \left[1 + \frac{INR}{2W}\right]^{2W} \tag{K-12}$$

This has been computed and shown on Figures K-6 through K-62.

Figures K-6 through K-62 clearly illustrate the diminishing returns in cancellation performance as references are added. If the cancellation floor is significantly below the uncancelled primary output, that is, if

$$E_\infty(\omega)\Big|_{m=1} = E_\infty(1,\omega) \ll 2\Phi\sigma_I^2(\omega) + \sigma_n^2(\omega) \tag{K-13}$$

then the performance improves dramatically with the first few references. However, the figures show a well defined transition point in K beyond which the additional interference rejection afforded by adding another
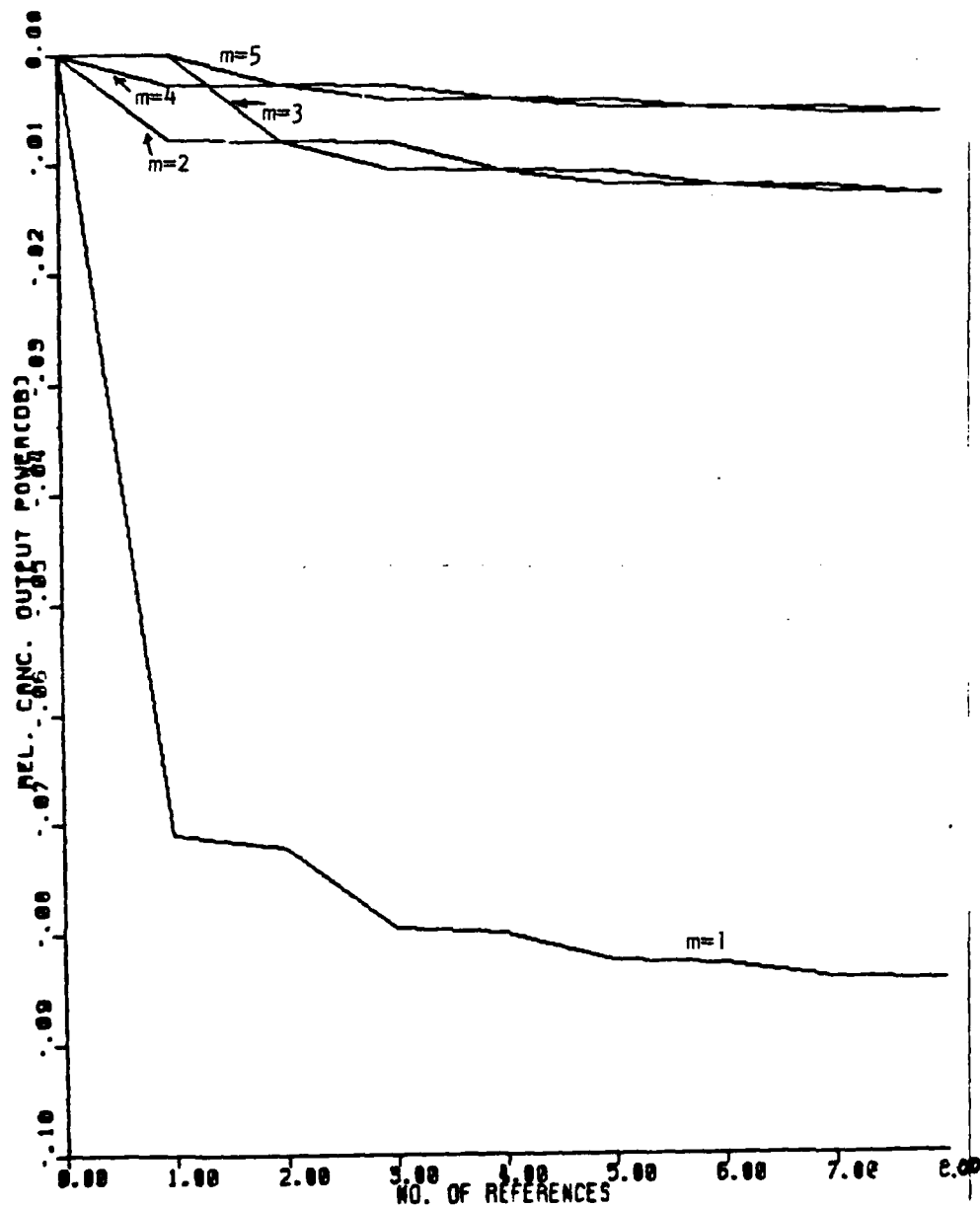
Figure K-1; Canceller Output Power
vs. No. of References when Sampling
Criterion is Exceeded
No Ambient Noise
W=1.25
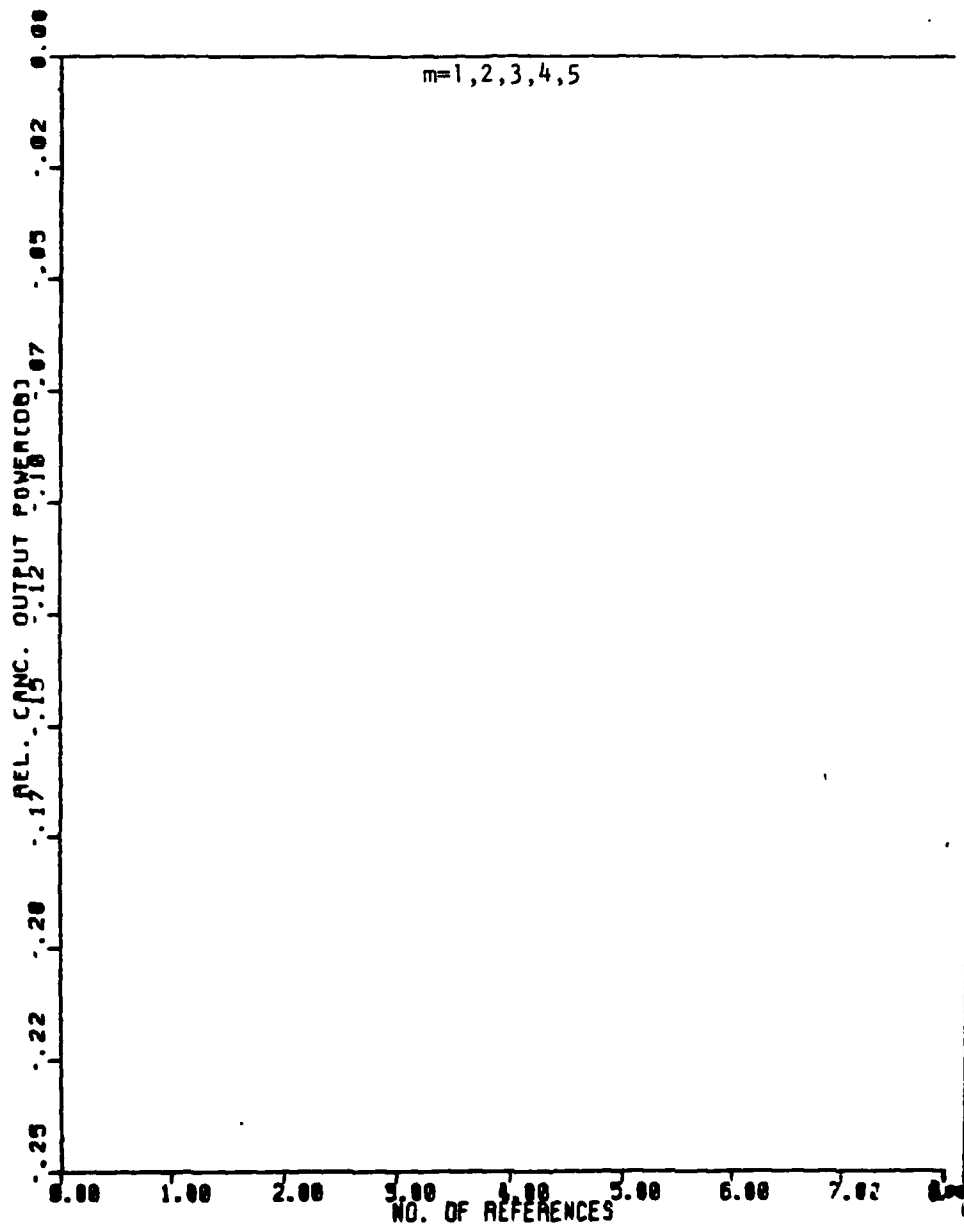
Figure K-2; Canceller Output Power
vs. No. of References when Sampling
Criterion is Exceeded
No Ambient Noise
W=1.0
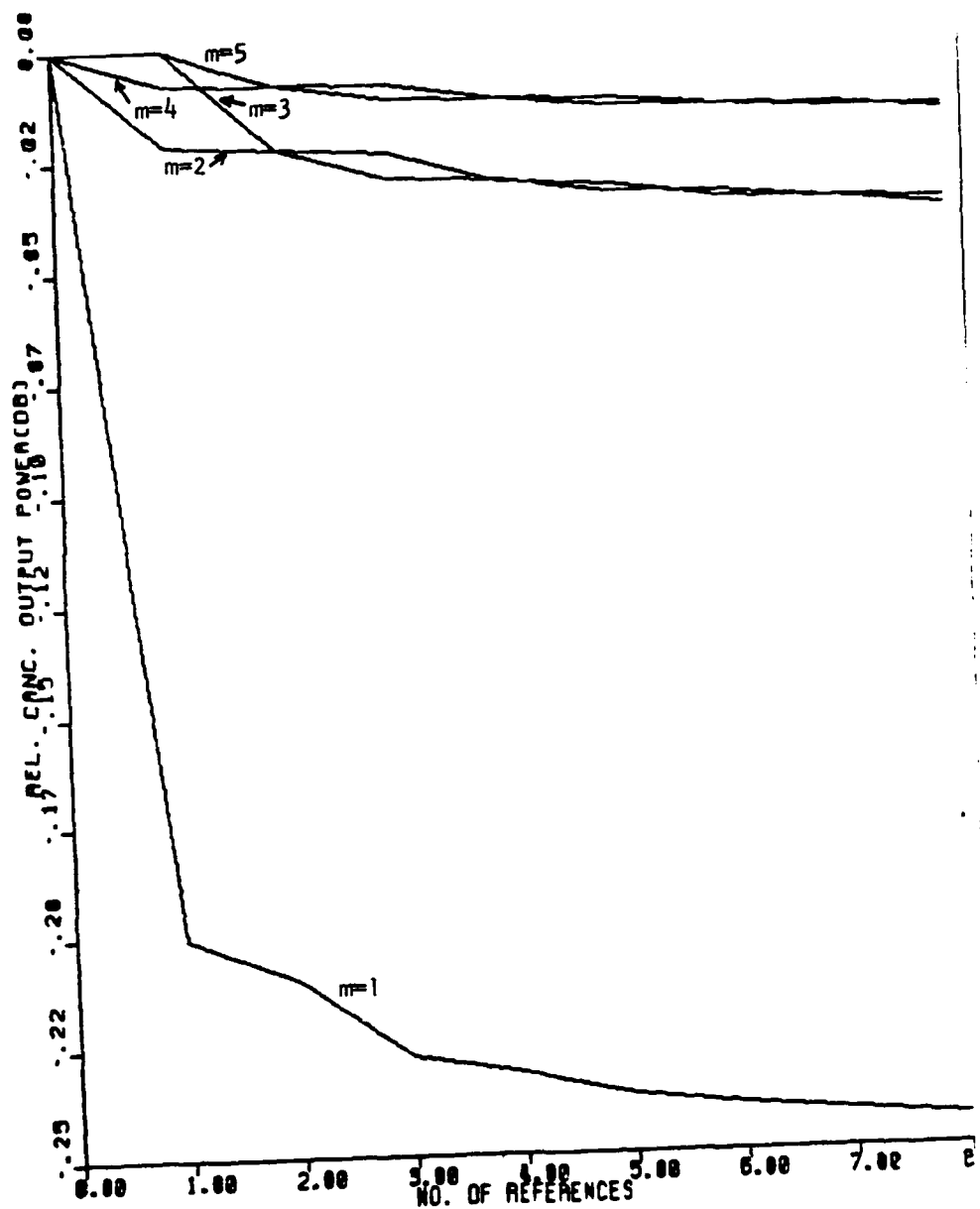
Figure K-3; Canceller Output Power
vs. No. of References when Sampling
Criterion is Exceeded
No Ambient Noise
W=.75

K-8
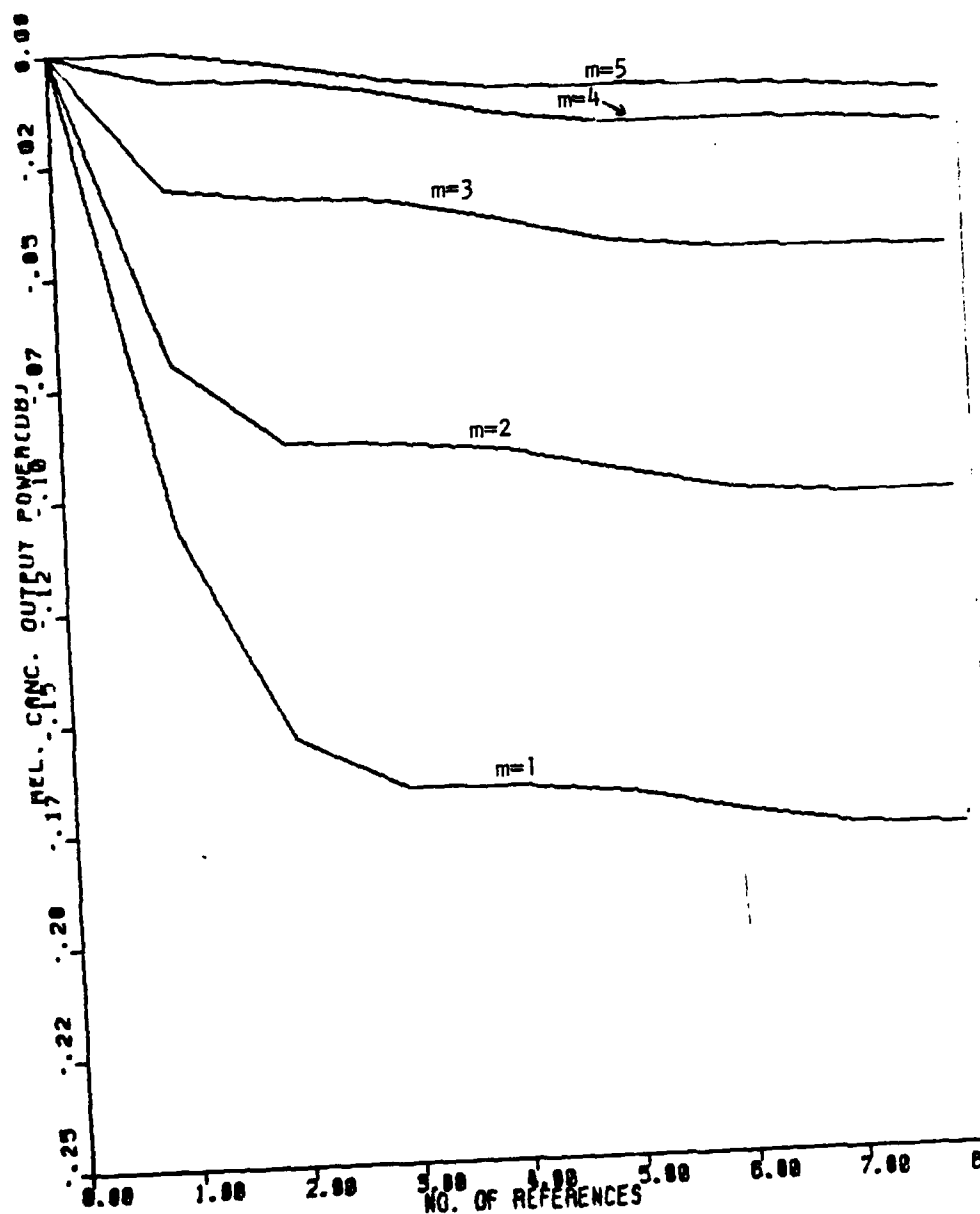
Figure K-4; Canceller Output Power
vs. No. of References when Sampling
Criterion is Exceeded
No Ambient Noise
W=.6
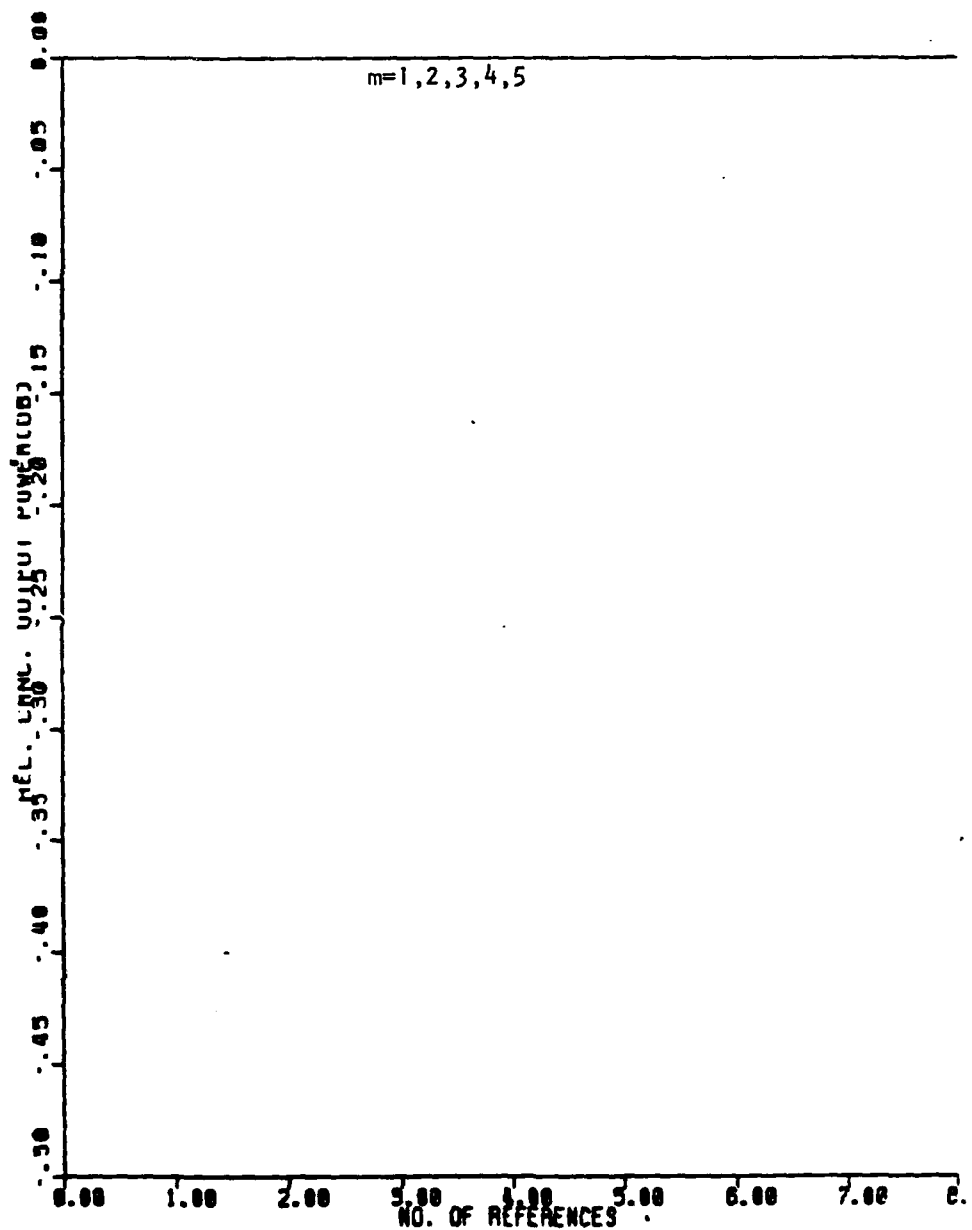
Figure K-5; Canceller Output Power
vs. No. of References when Sampling
Criterion is Exceeded
No Ambient Noise
W=.5

FIGURE K-6

W = .4
INR = 40 dB

K-11
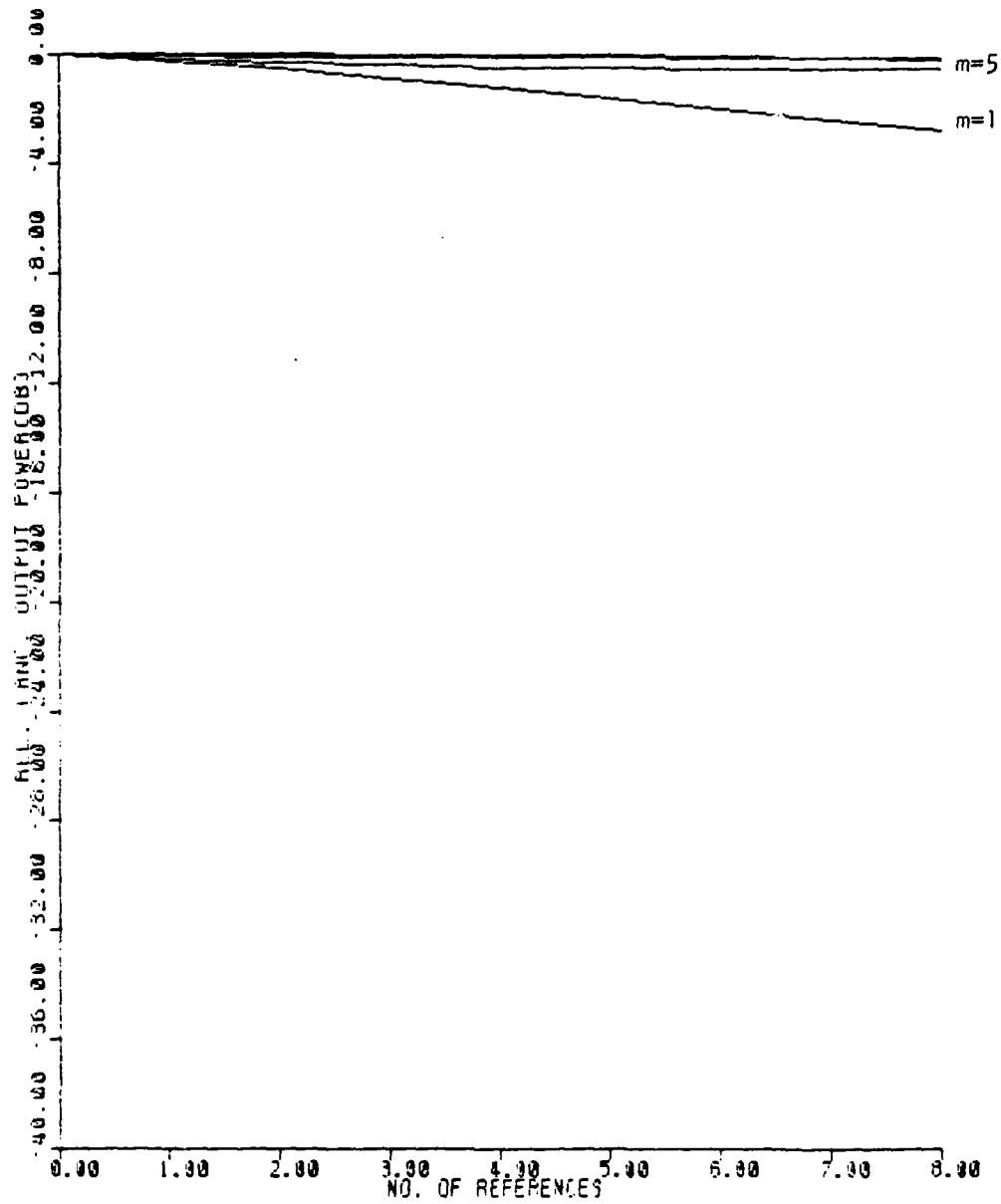
FIGURE K-7

W = .4
INR = 30 dB
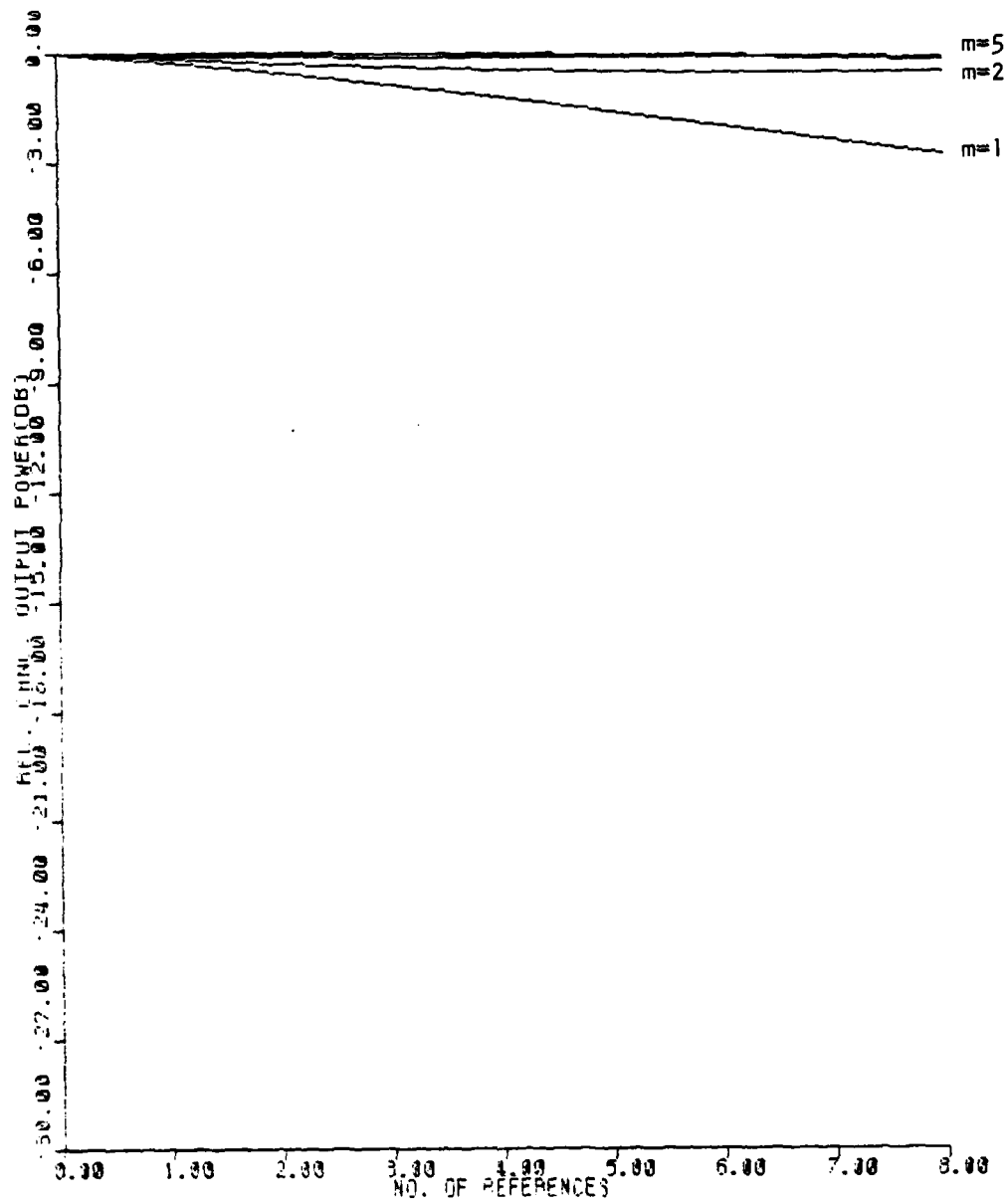
FIGURE K-8

W = .4
INR = 20 dB

K-13
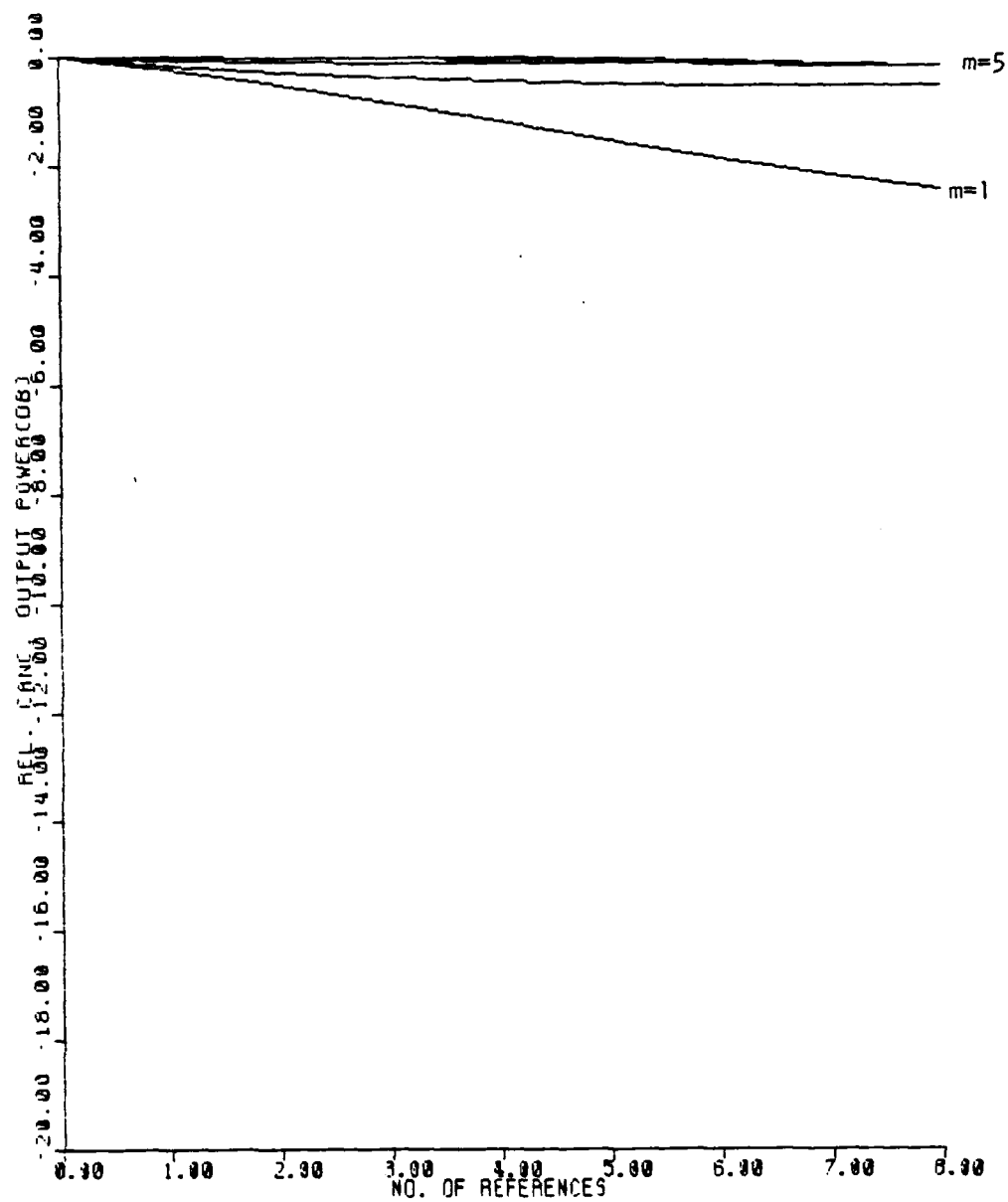
FIGURE K-9

W = .3
INR = 40 dB
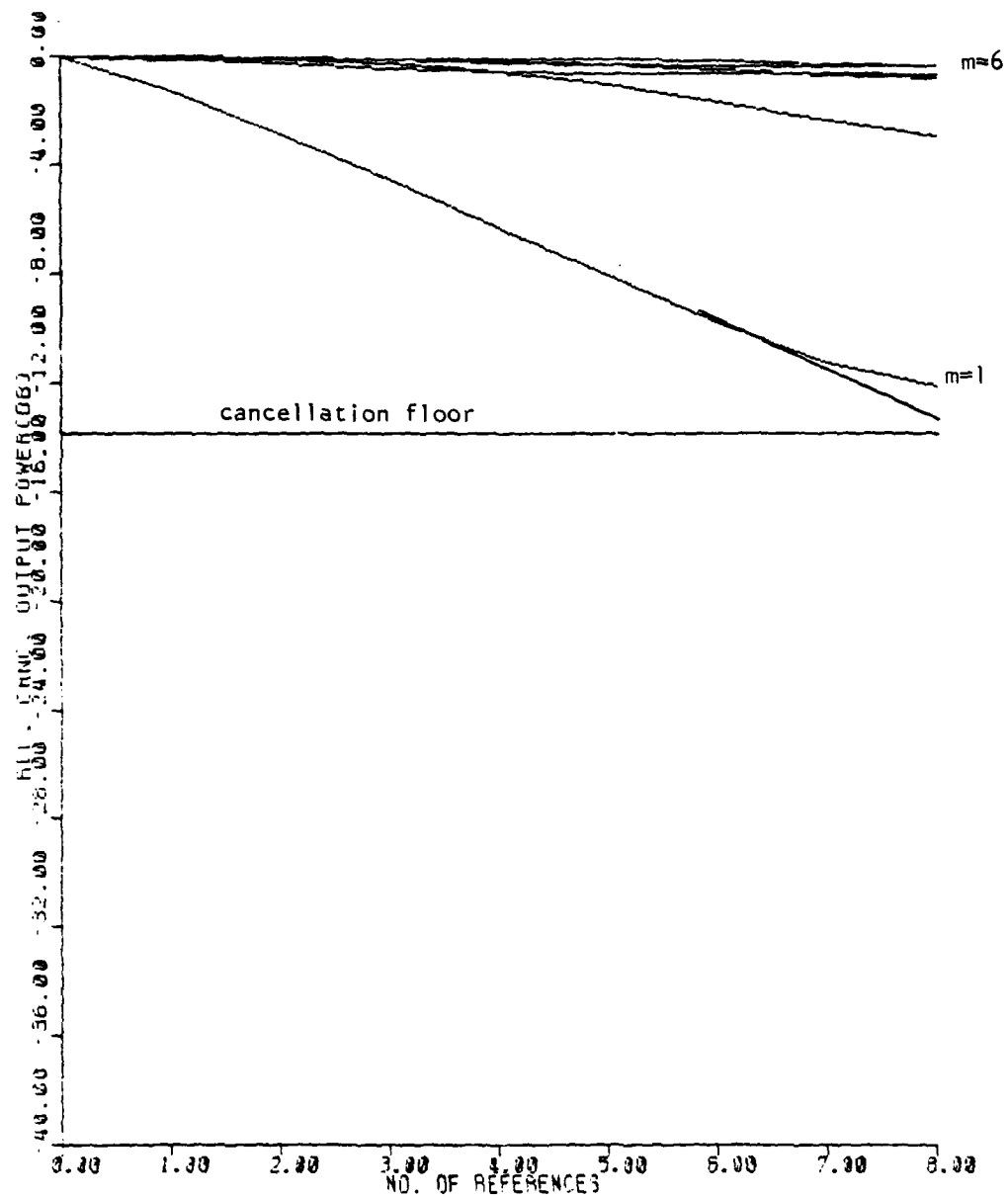
FIGURE K-10

W = .3
INR = 30 dB

FIGURE K-15

$W = 10^{-1}$

INR = 40 dB

cancellation floor

asymptote

m=5

m=3

m=1

NO. OF REFERENCES
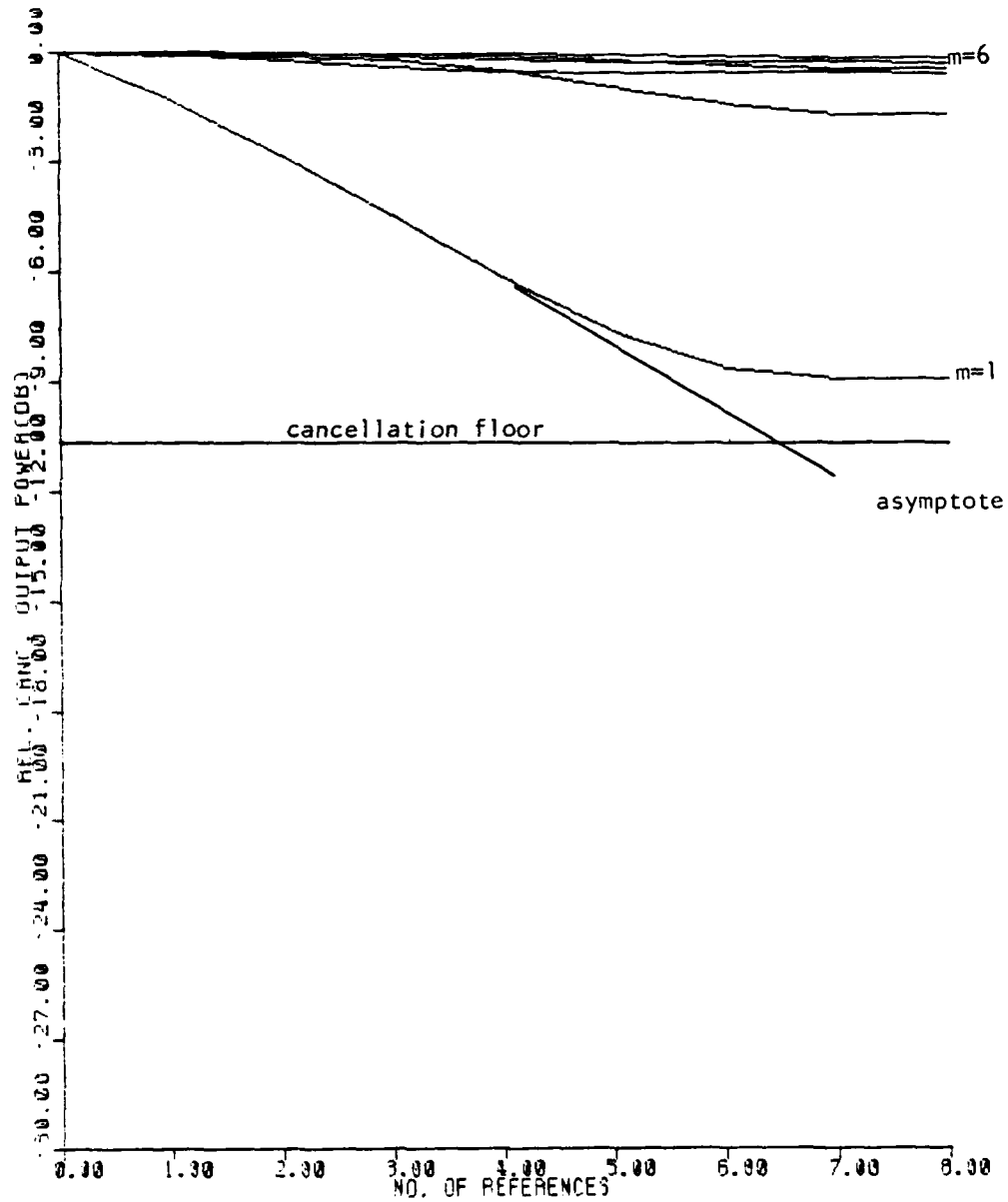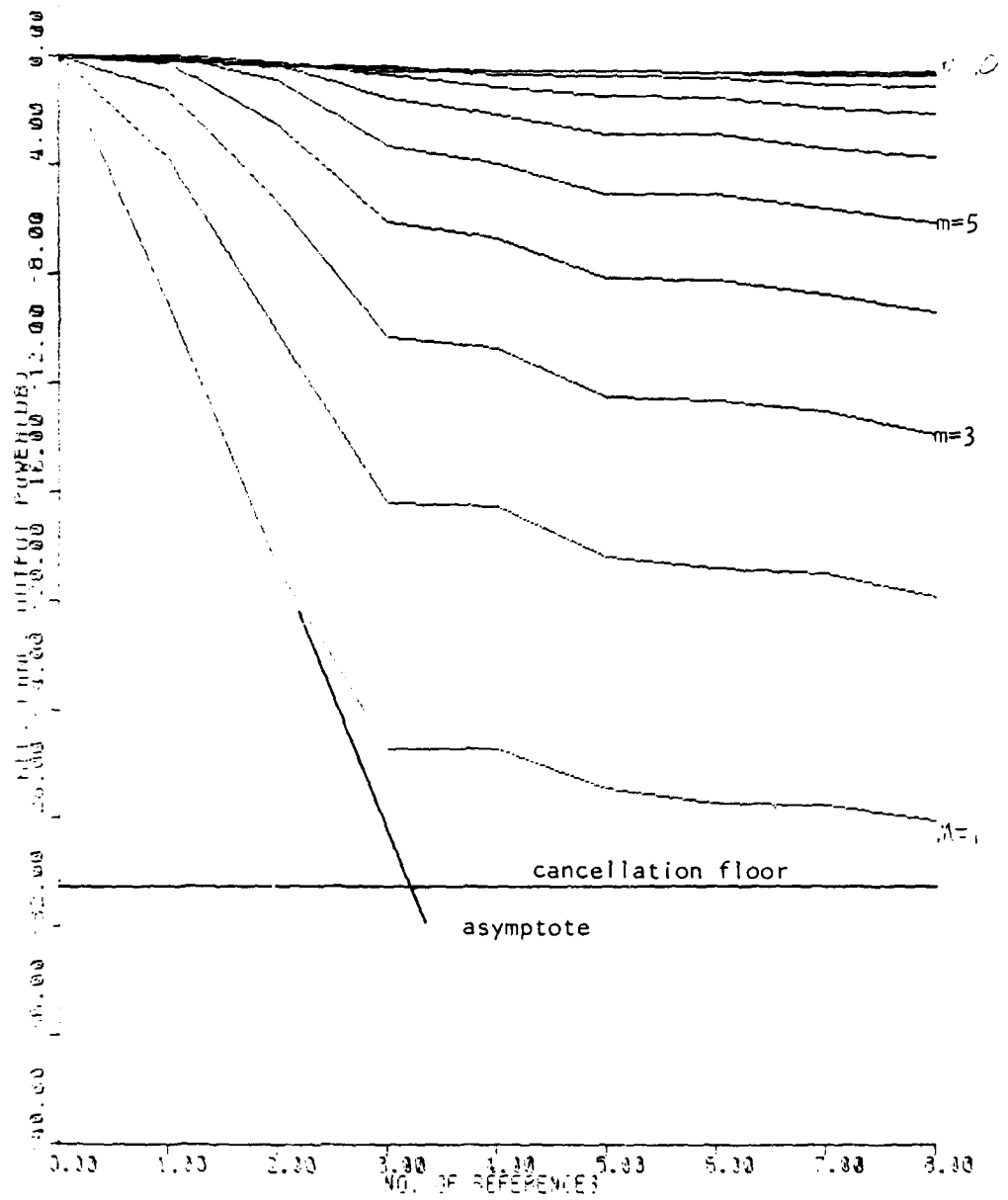
FIGURE K-11

W = .3
INR = 20 dB
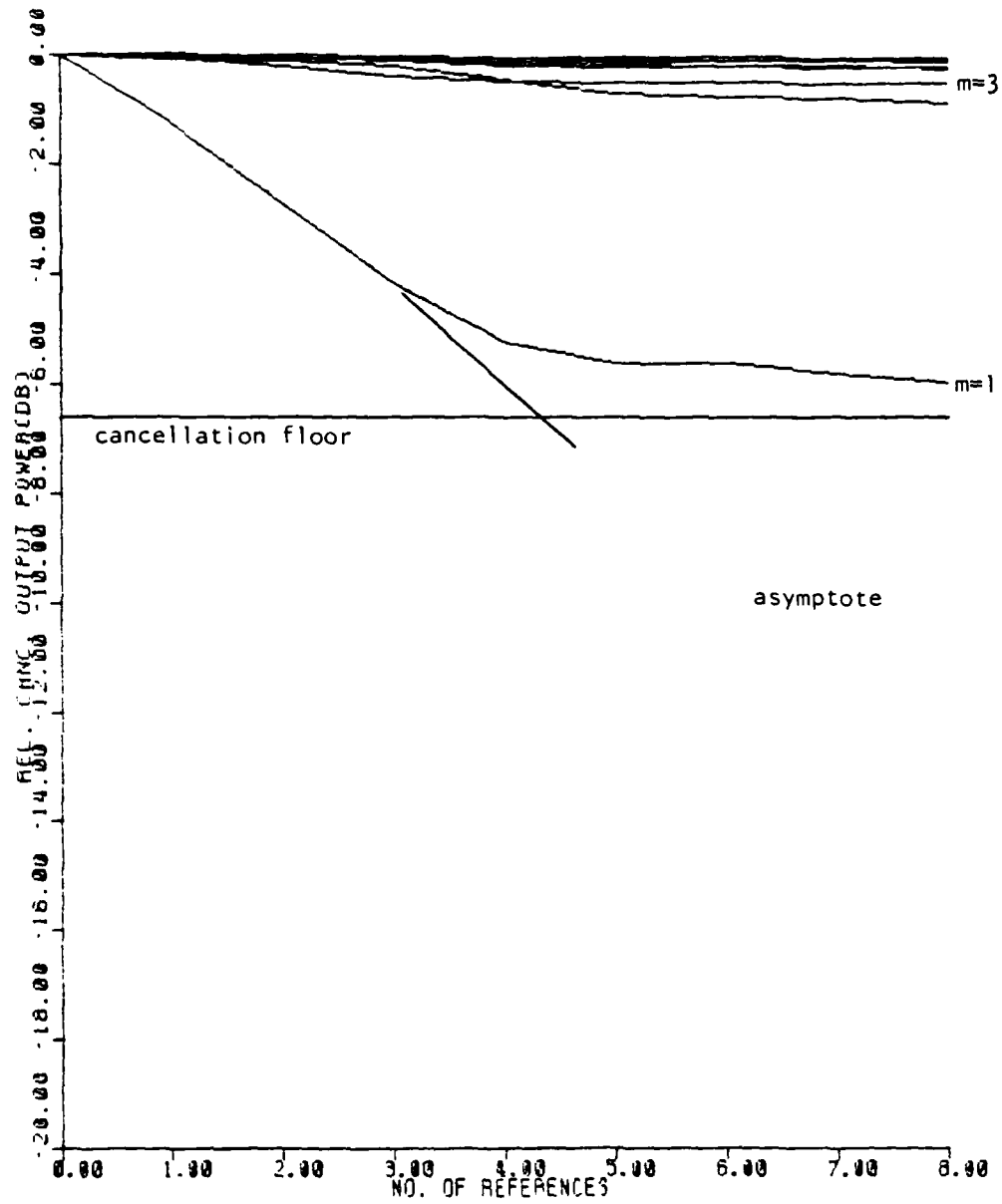
FIGURE K-12

W = .2
INR = 40 dB
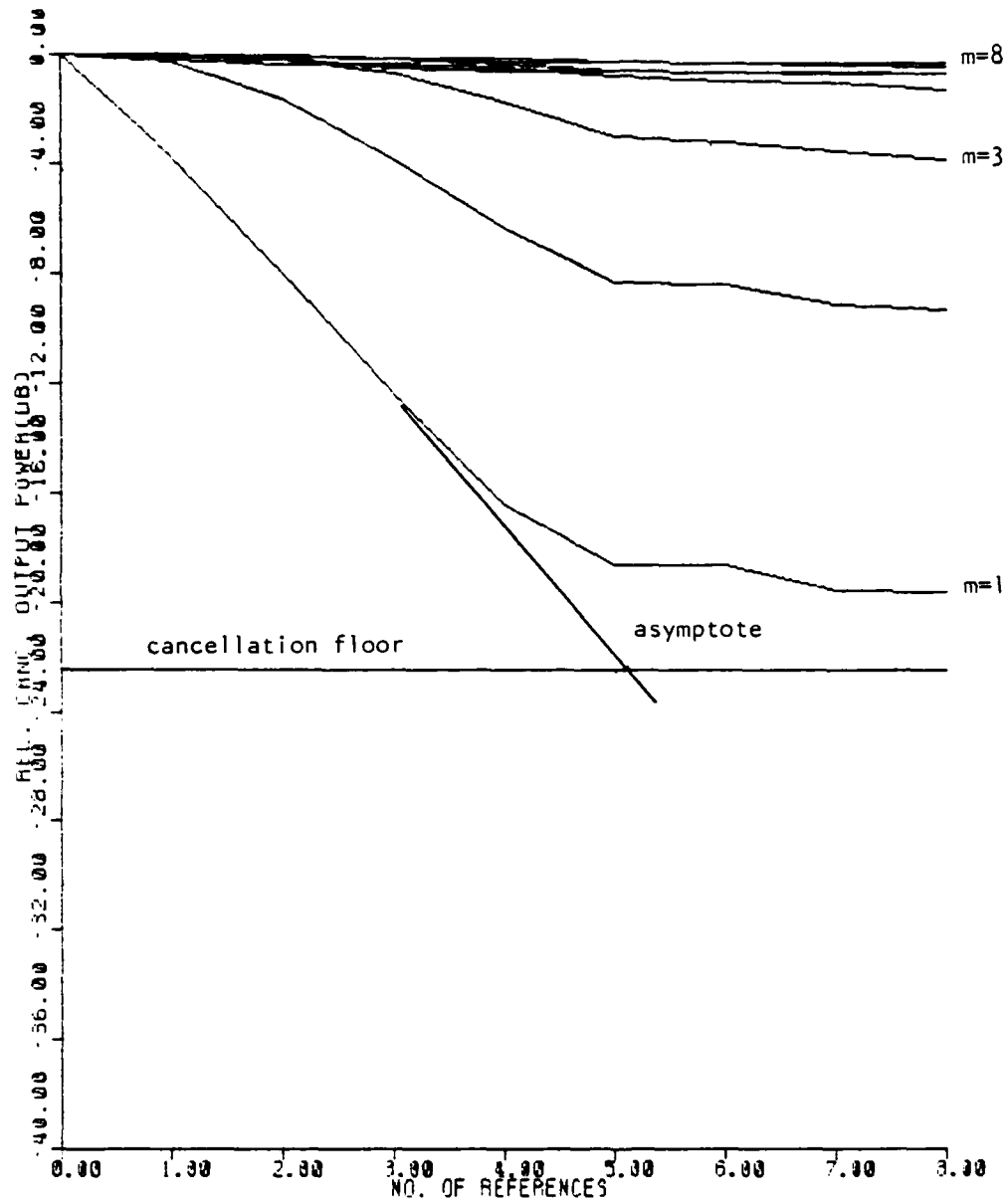
FIGURE K-13

W = .2
INR = 30 dB
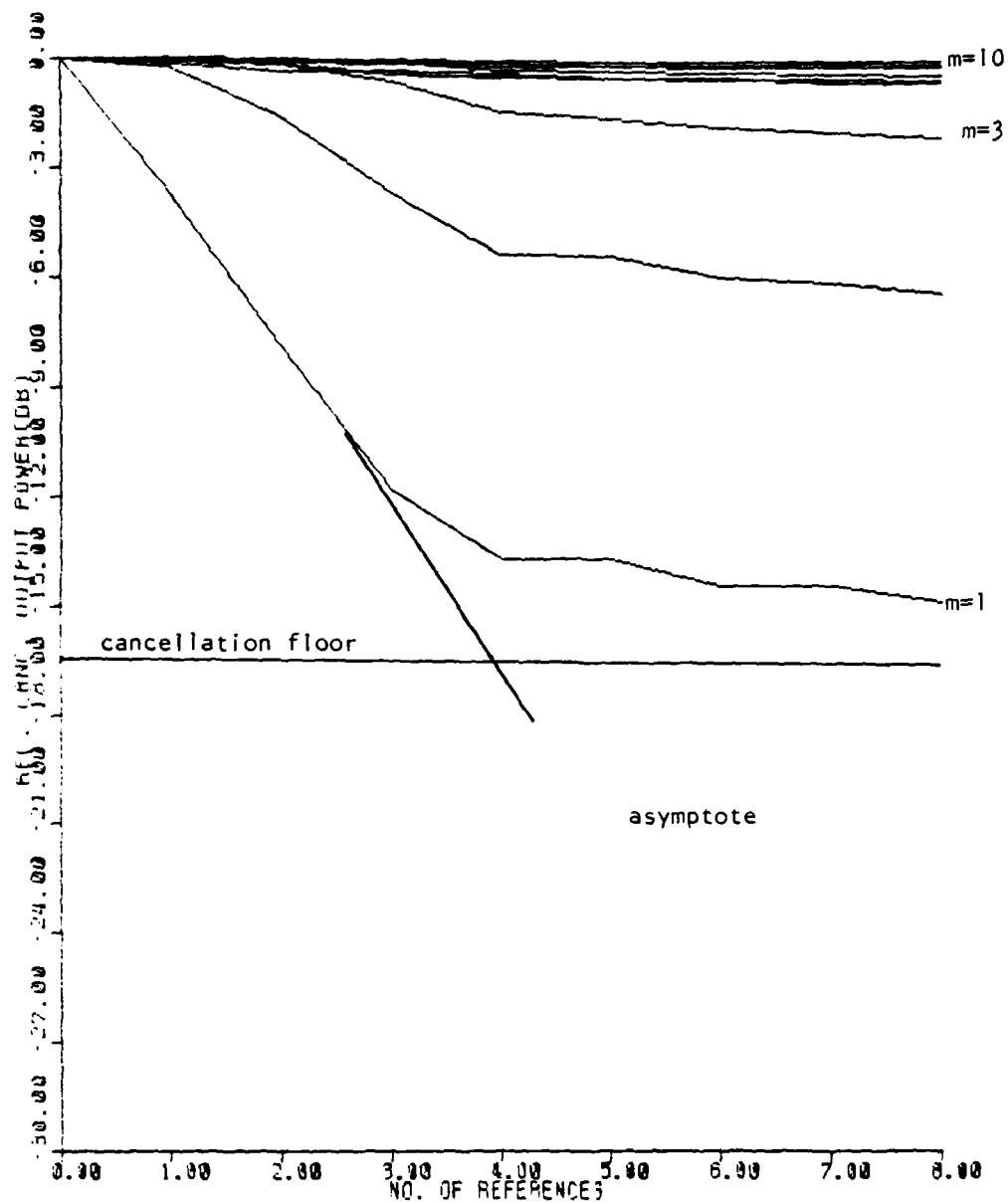
FIGURE K-14

$$W = 2 \times 10^{-1}$$
$$INR = 20 \text{ dB}$$
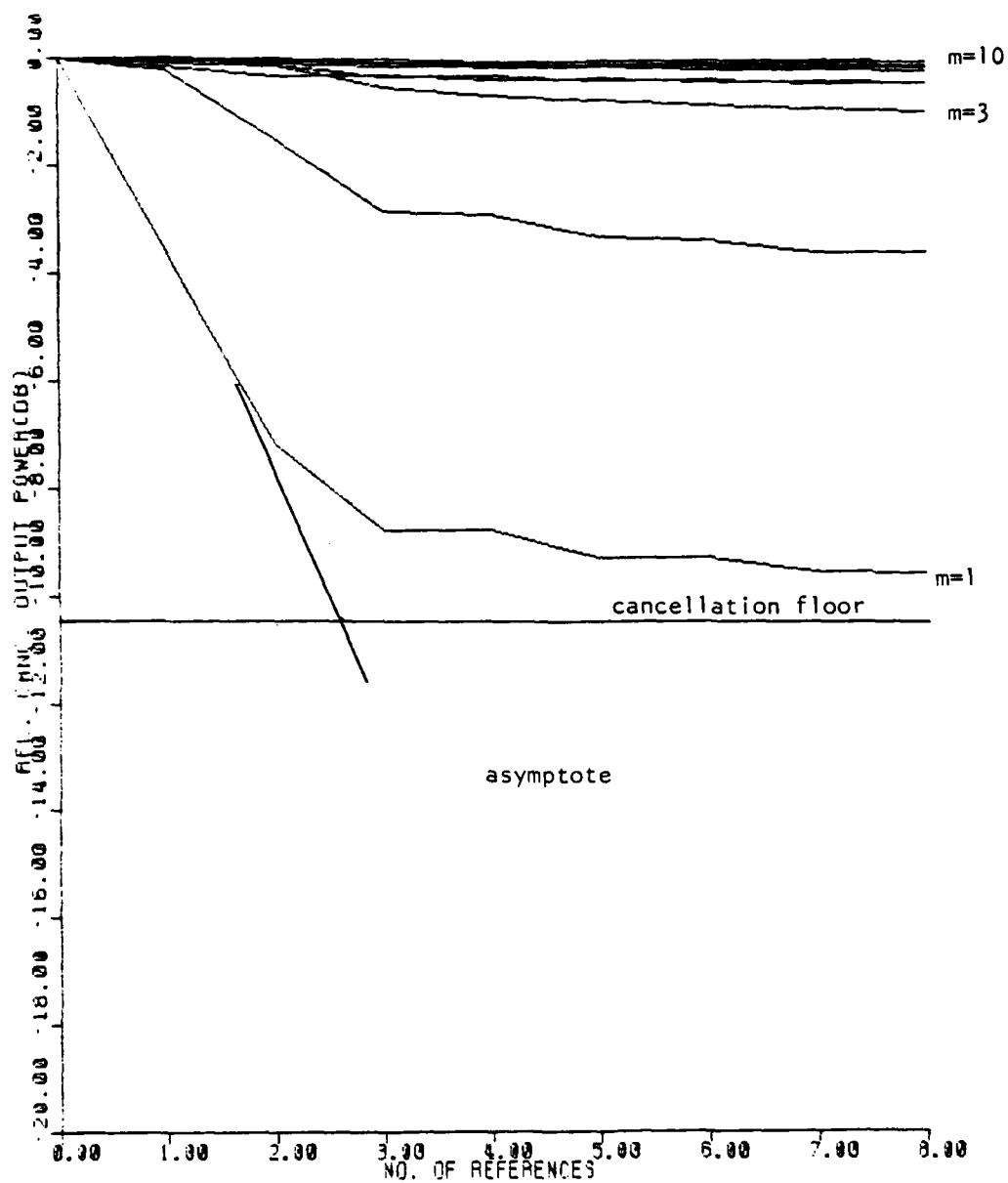
FIGURE K-16

W = .1
INR = 30 dB
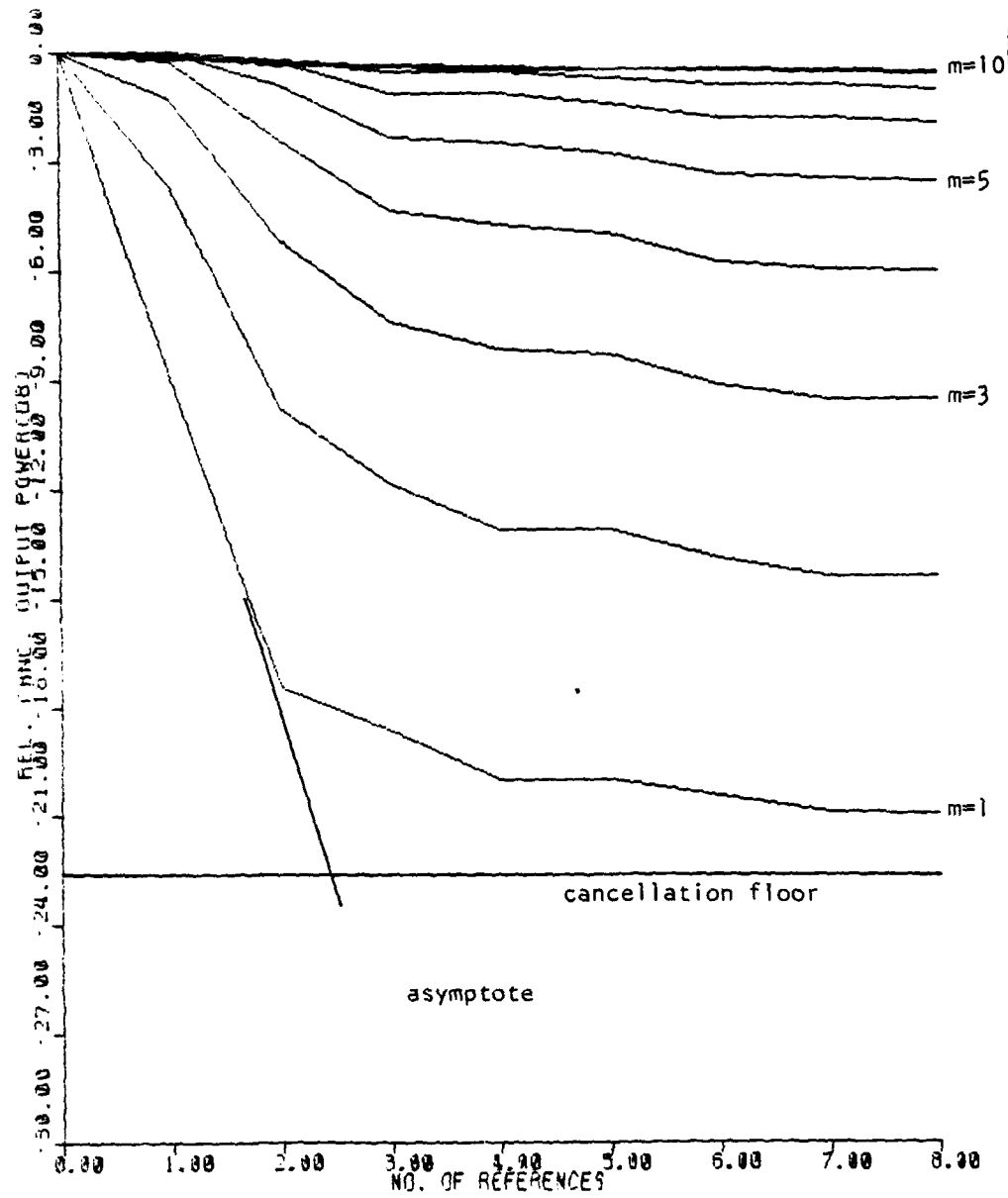
FIGURE K-17

$$W = 10^{-1}$$
$$INR = 20 \text{ dB}$$
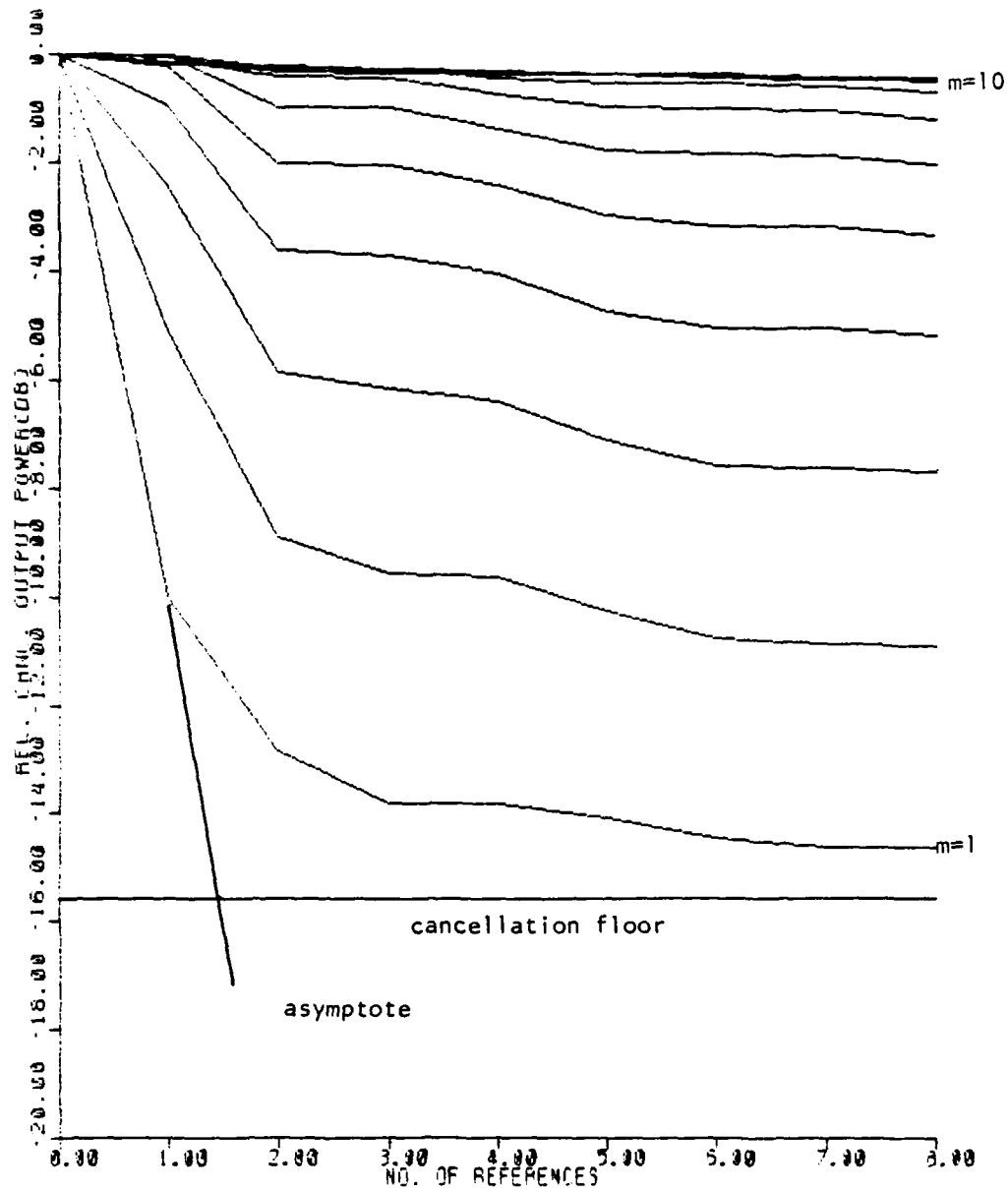
FIGURE K-18

$W \approx 8\times10^{-2}$
INR = 40 dB
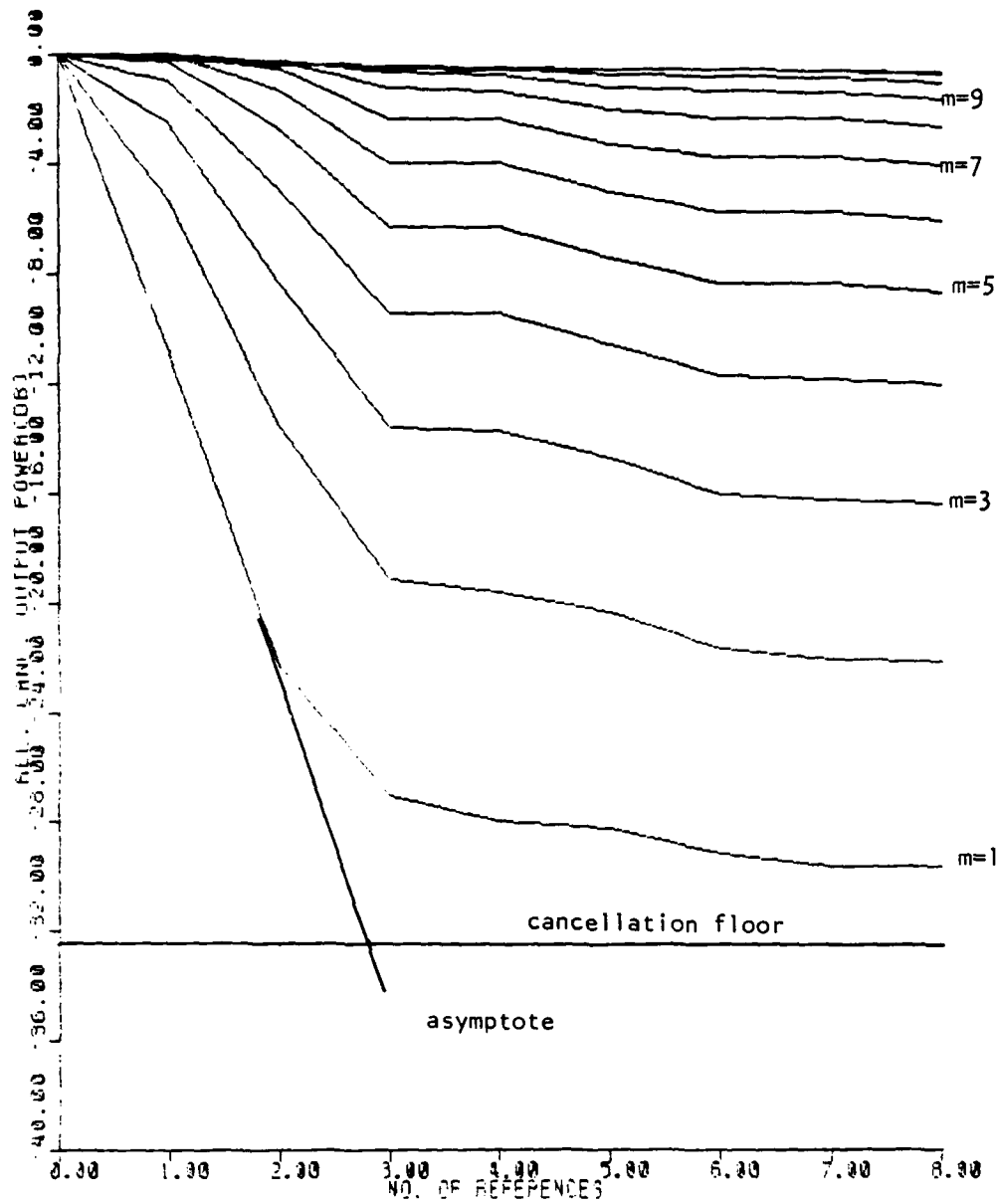
FIGURE K-19

$W = 8 \times 10^{-2}$
$INR = 30$ dB
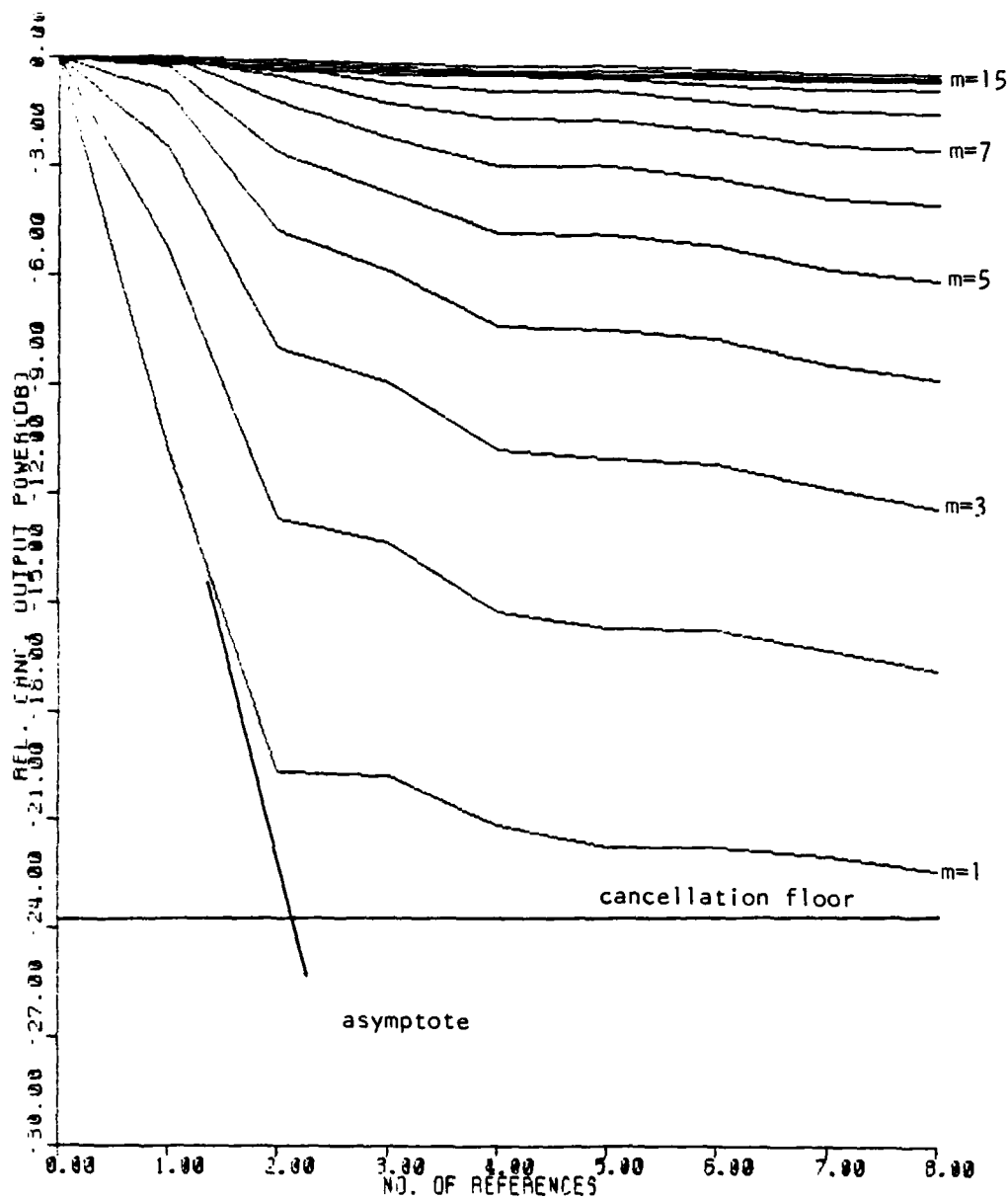
FIGURE K-20

$$W = 8\times10^{-2}$$

$$INR = 20 \text{ dB}$$
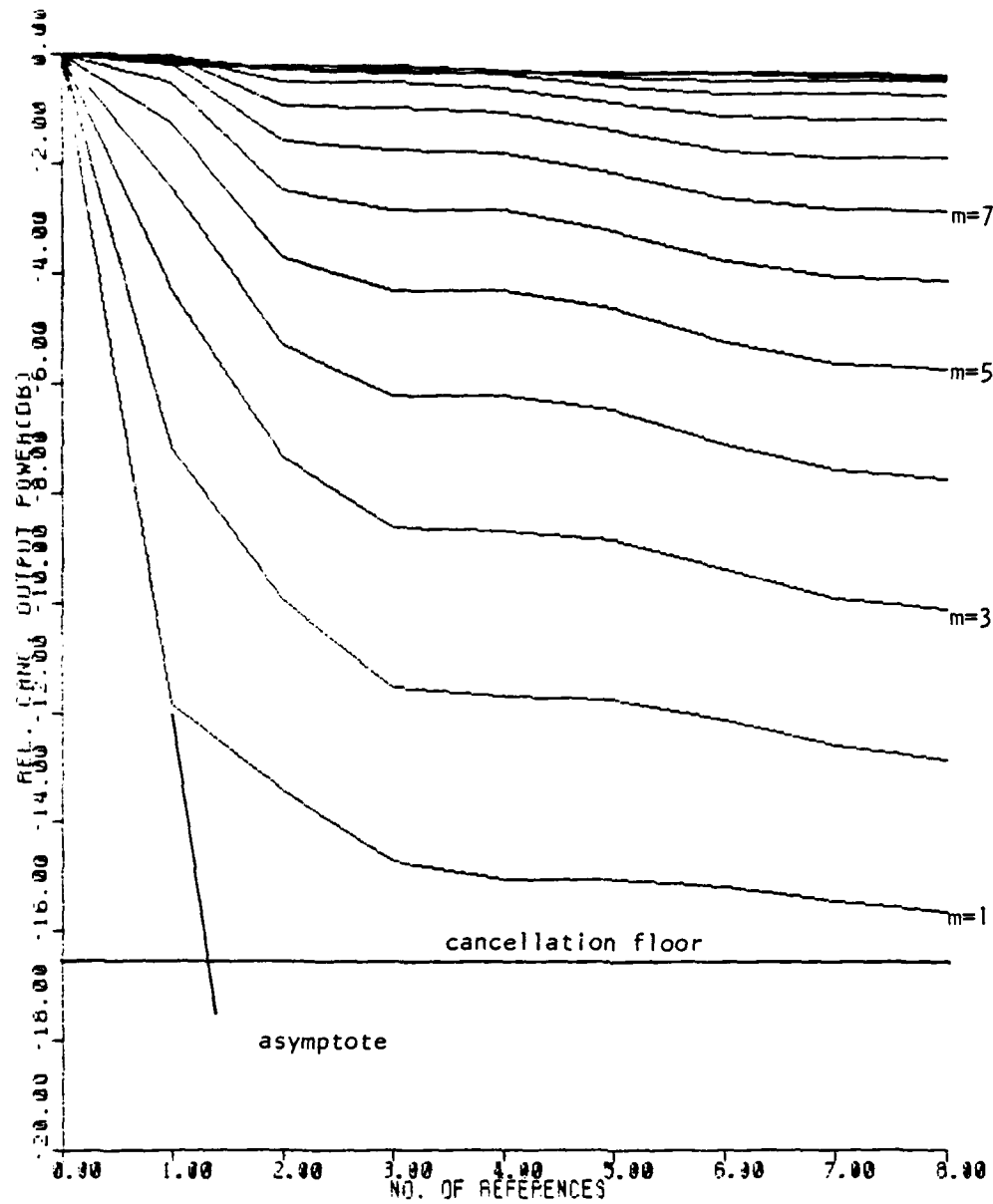
FIGURE K-21

$W = 6 \times 10^{-2}$
INR = 40 dB

cancellation floor

asymptote

REL. CANC. OUTPUT POWER(DB)

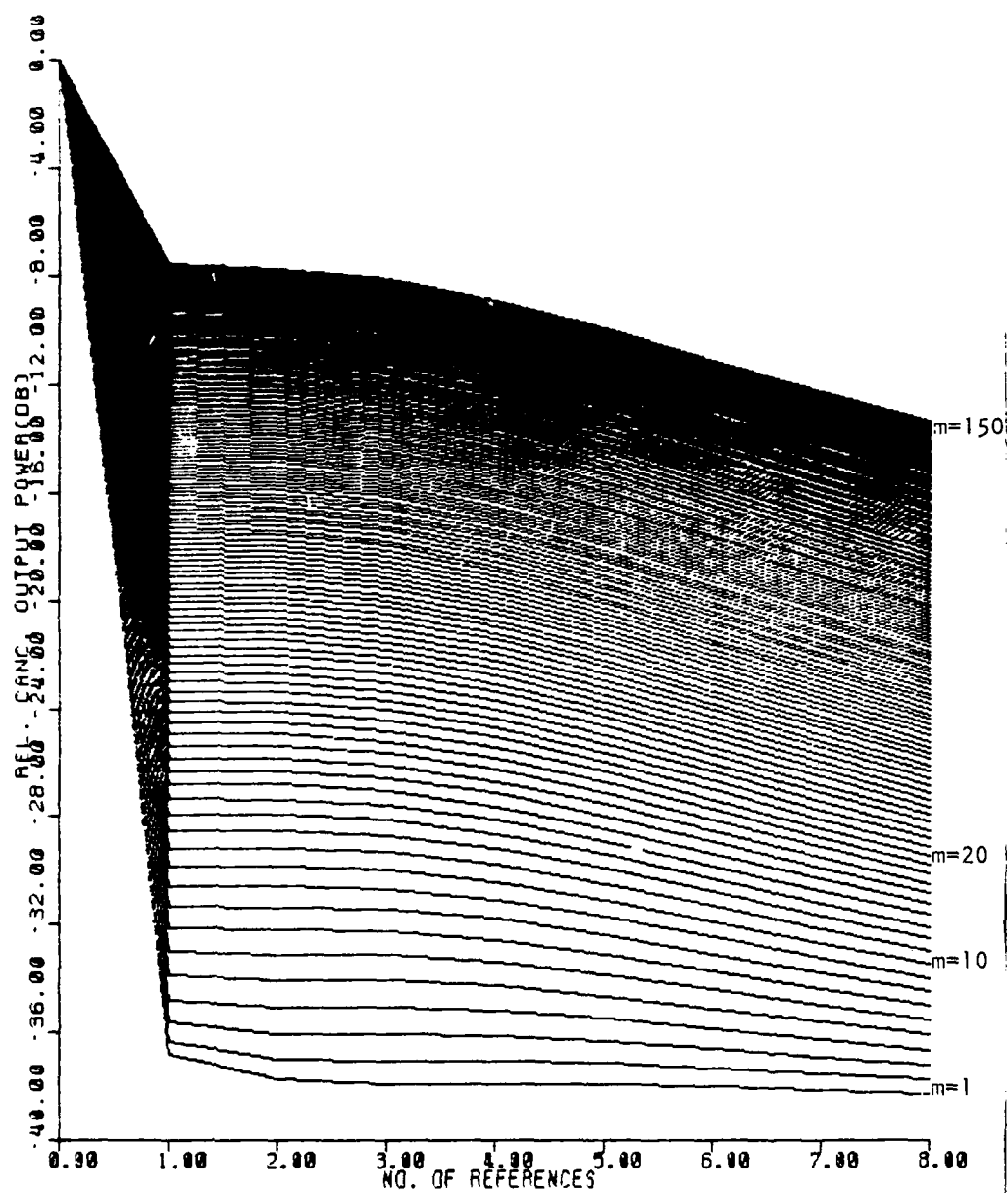NO. OF REFERENCES

m=9

m=7

m=5

m=3
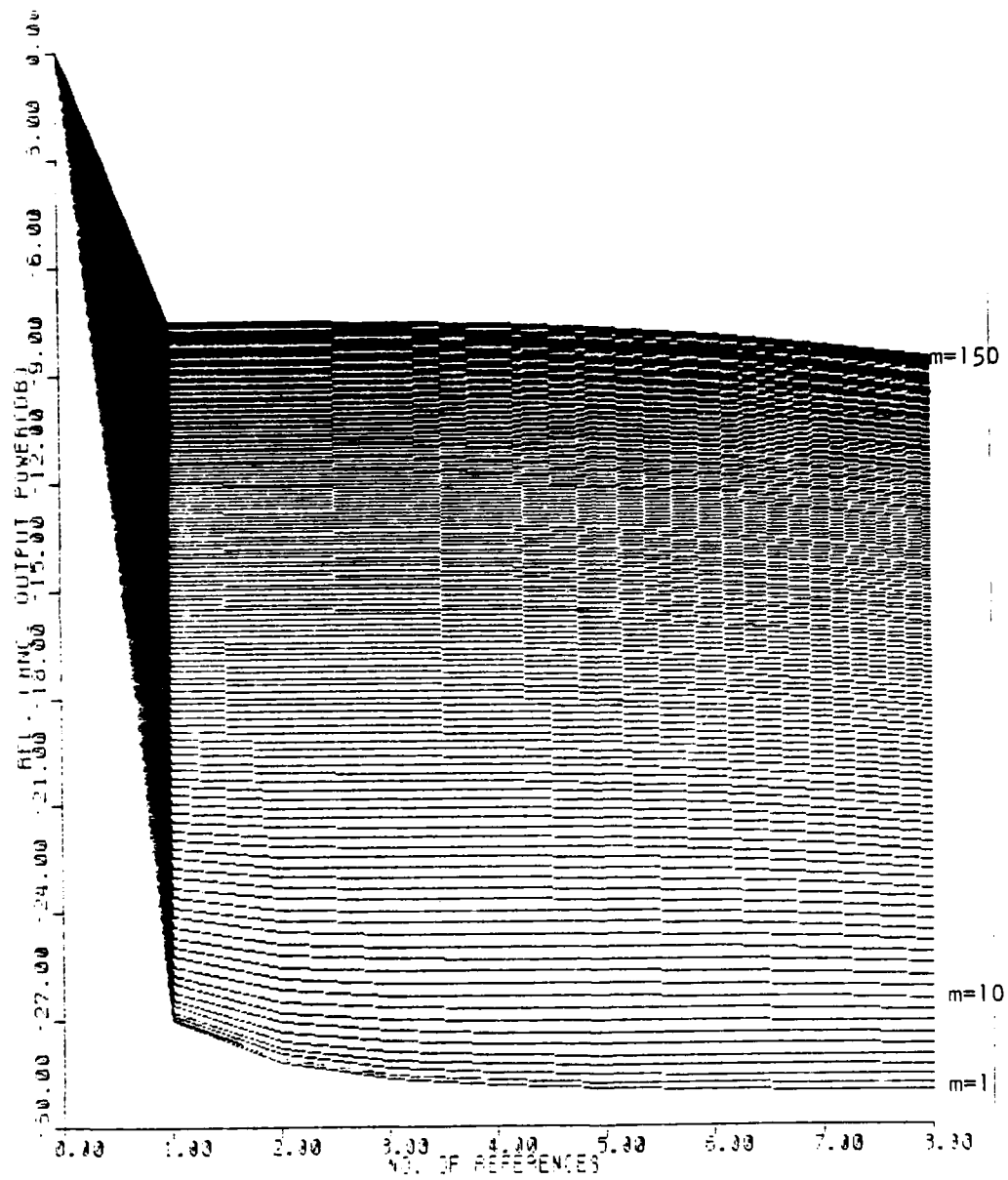
m=1
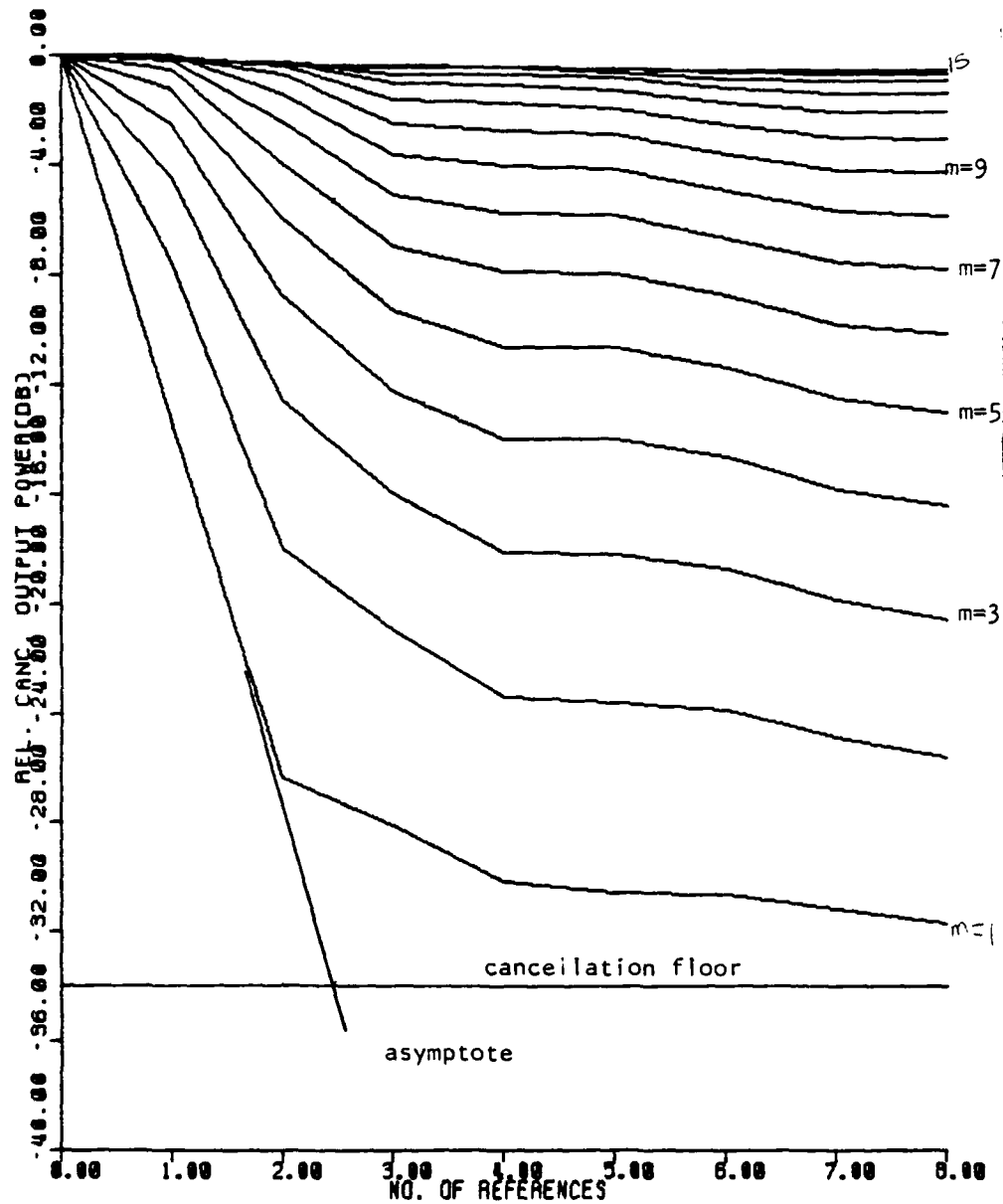
FIGURE K-22

$W = 6 \times 10^{-2}$

INR = 30 dB
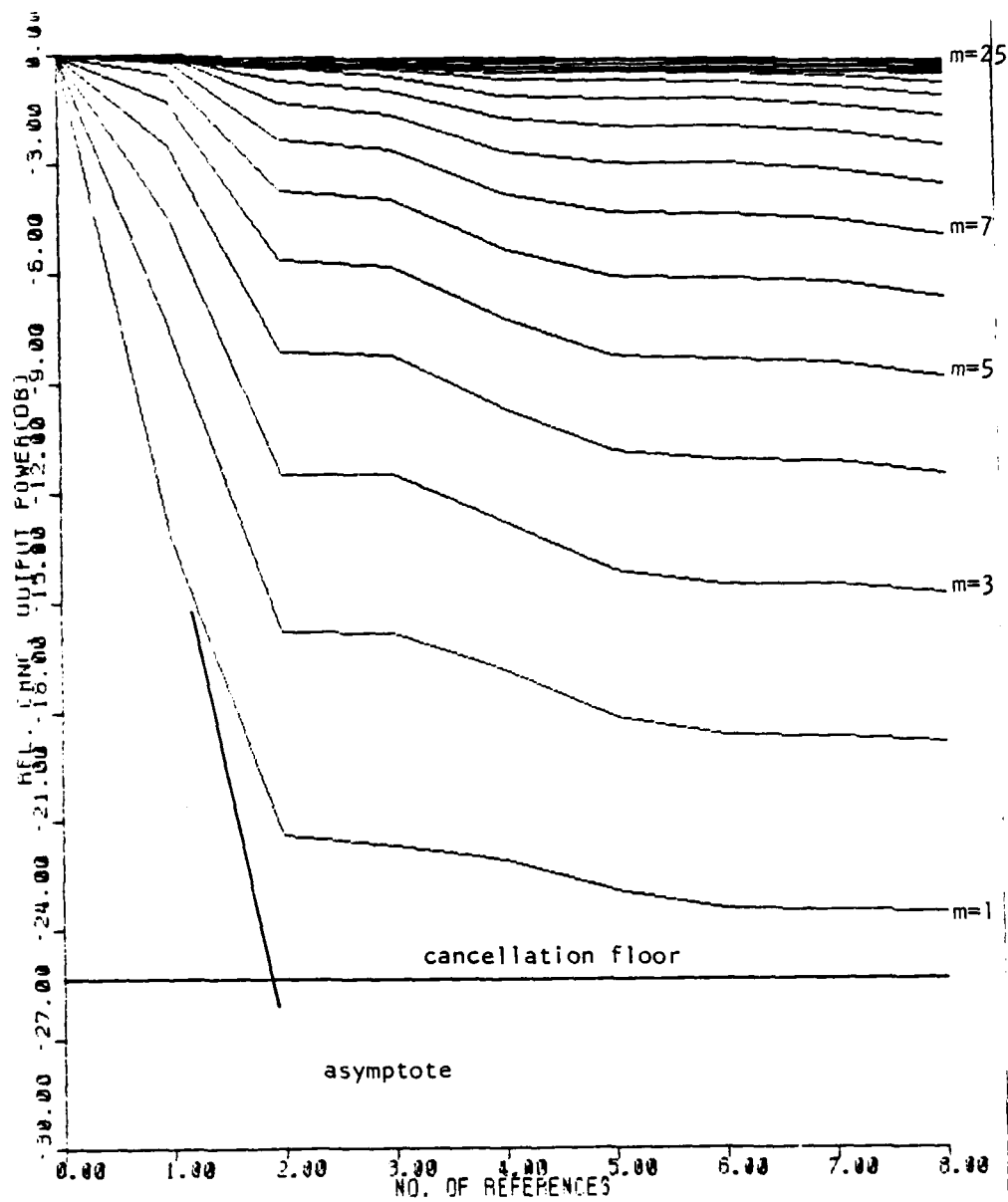
FIGURE K-23

$W = 6 \times 10^{-2}$

$INR = 20$ dB
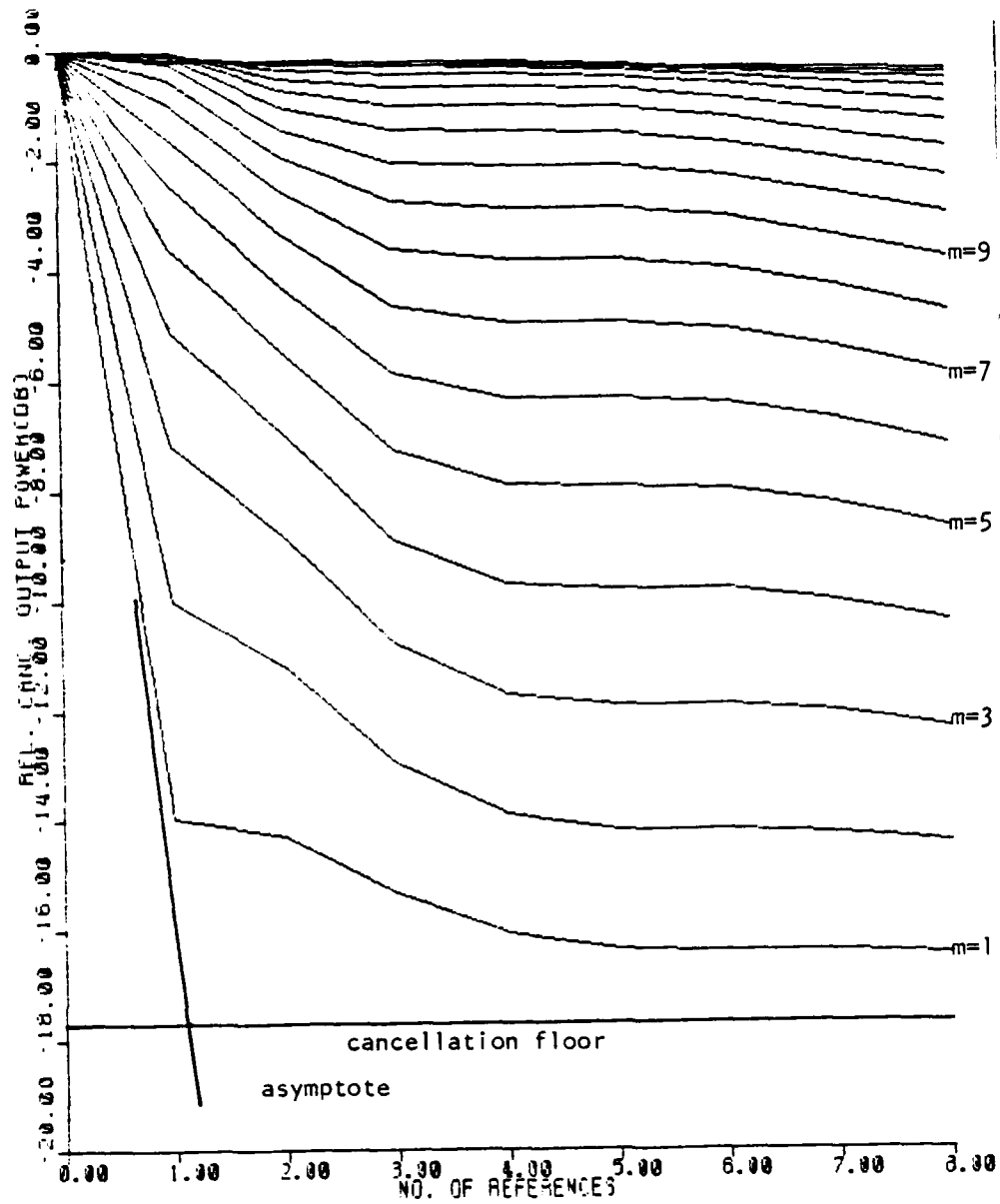
FIGURE K-24

$$W = 4 \times 10^{-2}$$

$$INR = 40 \text{ dB}$$
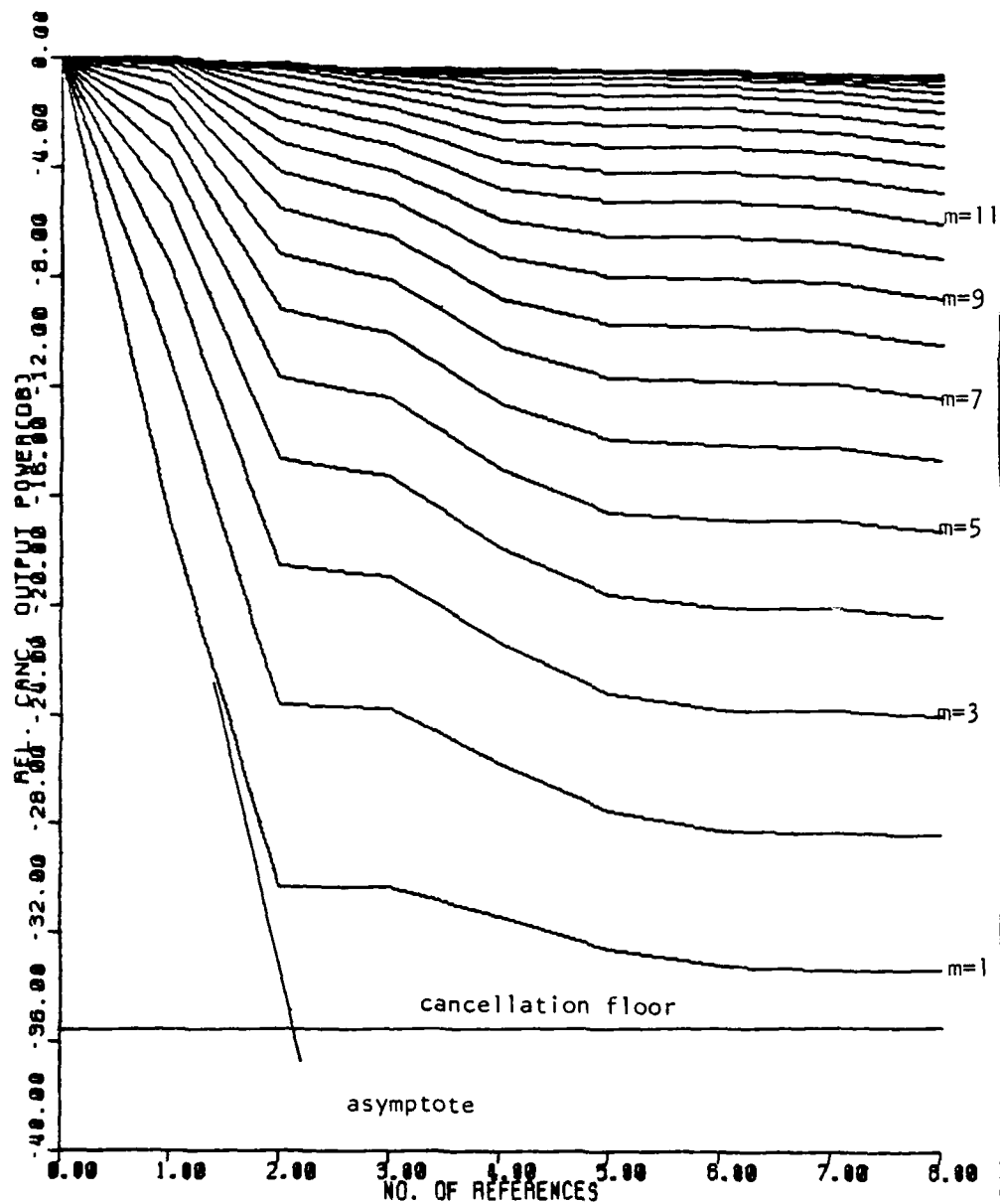
FIGURE K-25

$$W = 4 \times 10^{-2}$$

$$INR = 30 \text{ dB}$$
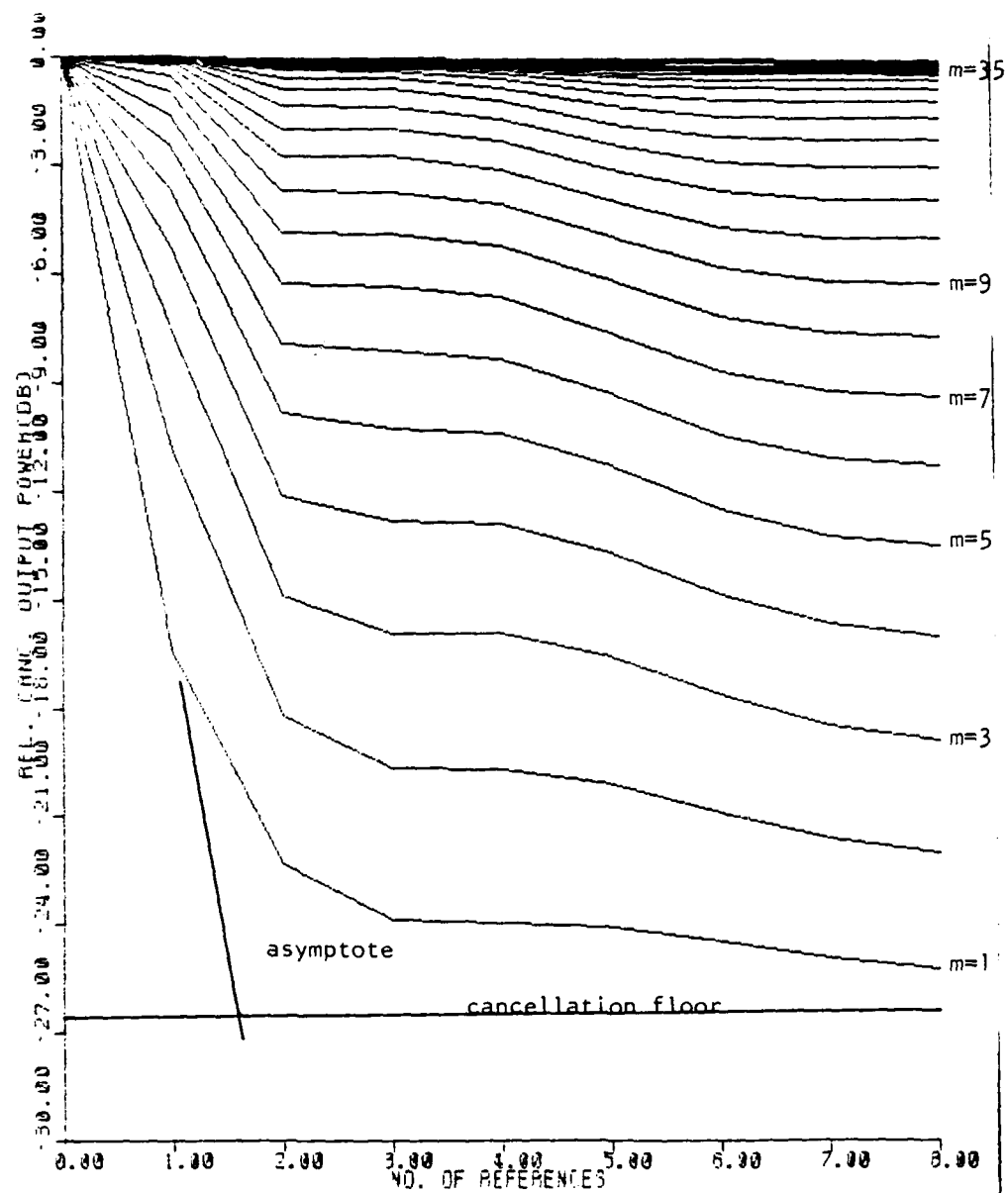
FIGURE K-26

$W = 4 \times 10^{-2}$

INR = 20 dB

m=11

m=9

m=7

m=5

m=3

m=1

cancellation floor

asymptote

NO. OF REFERENCES
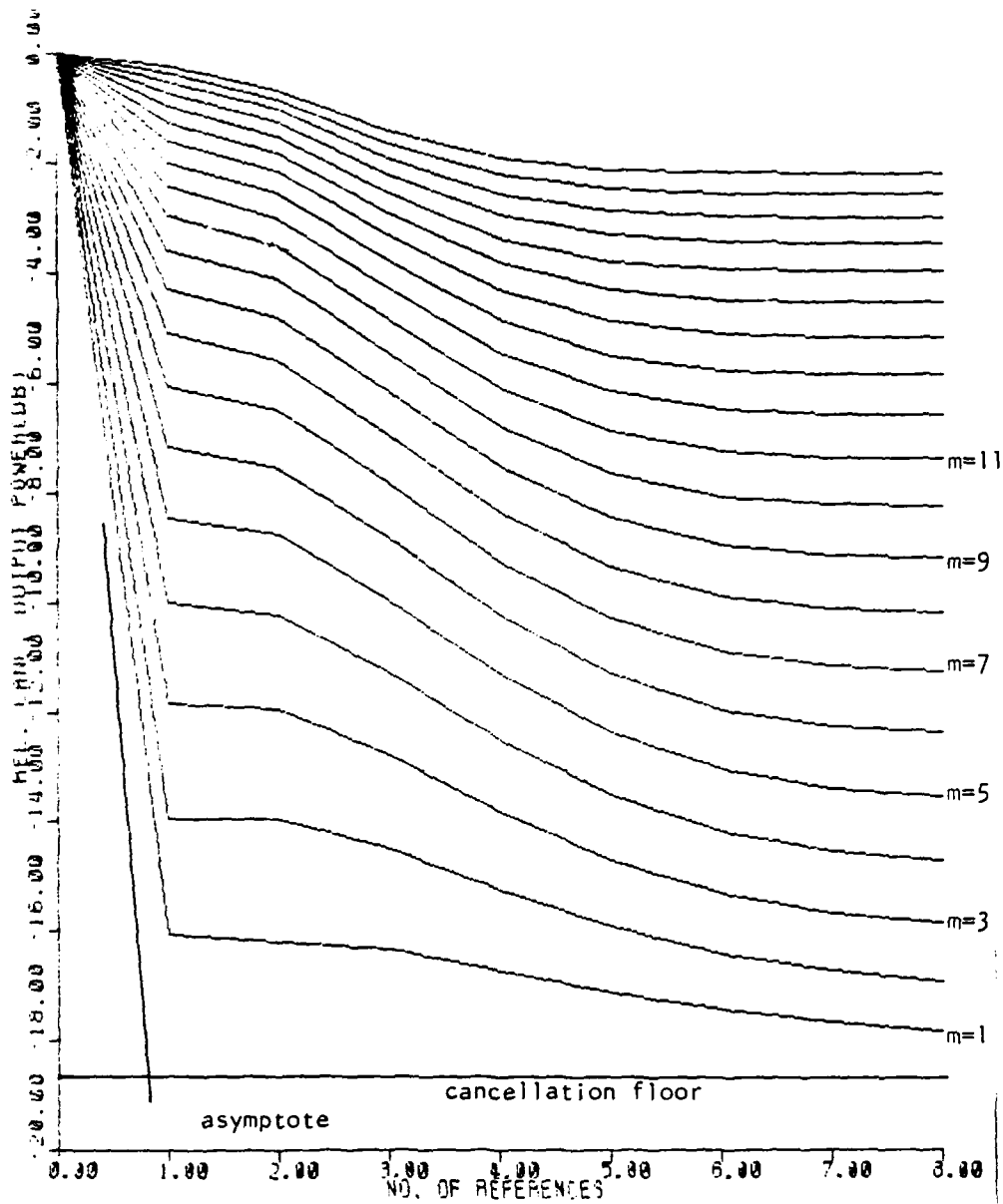
FIGURE K-27

$W = 2 \times 10^{-2}$

INR = 40 dB
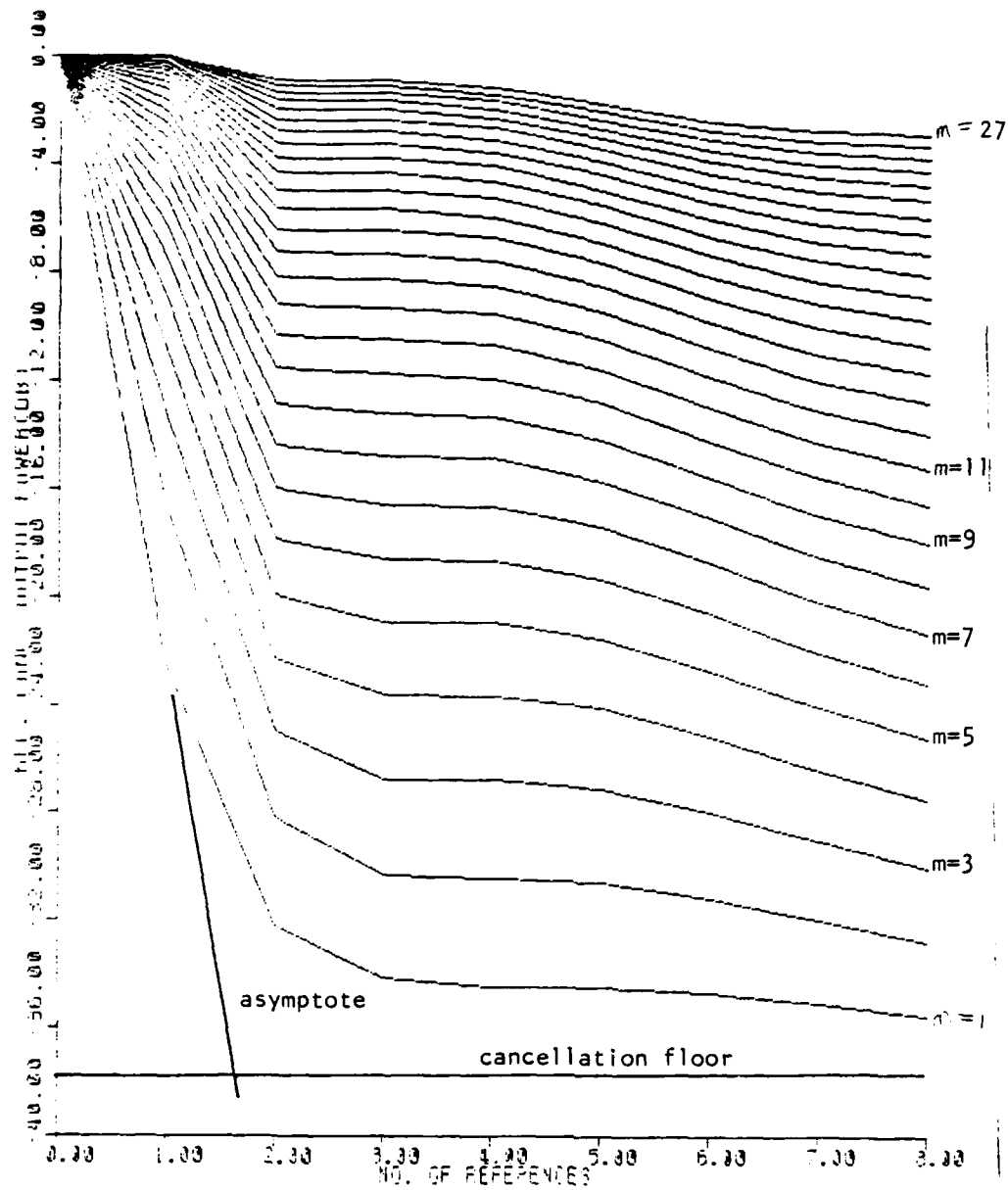
FIGURE K-28

$$W = 2 \times 10^{-2}$$

$$INR = 30 \text{ dB}$$
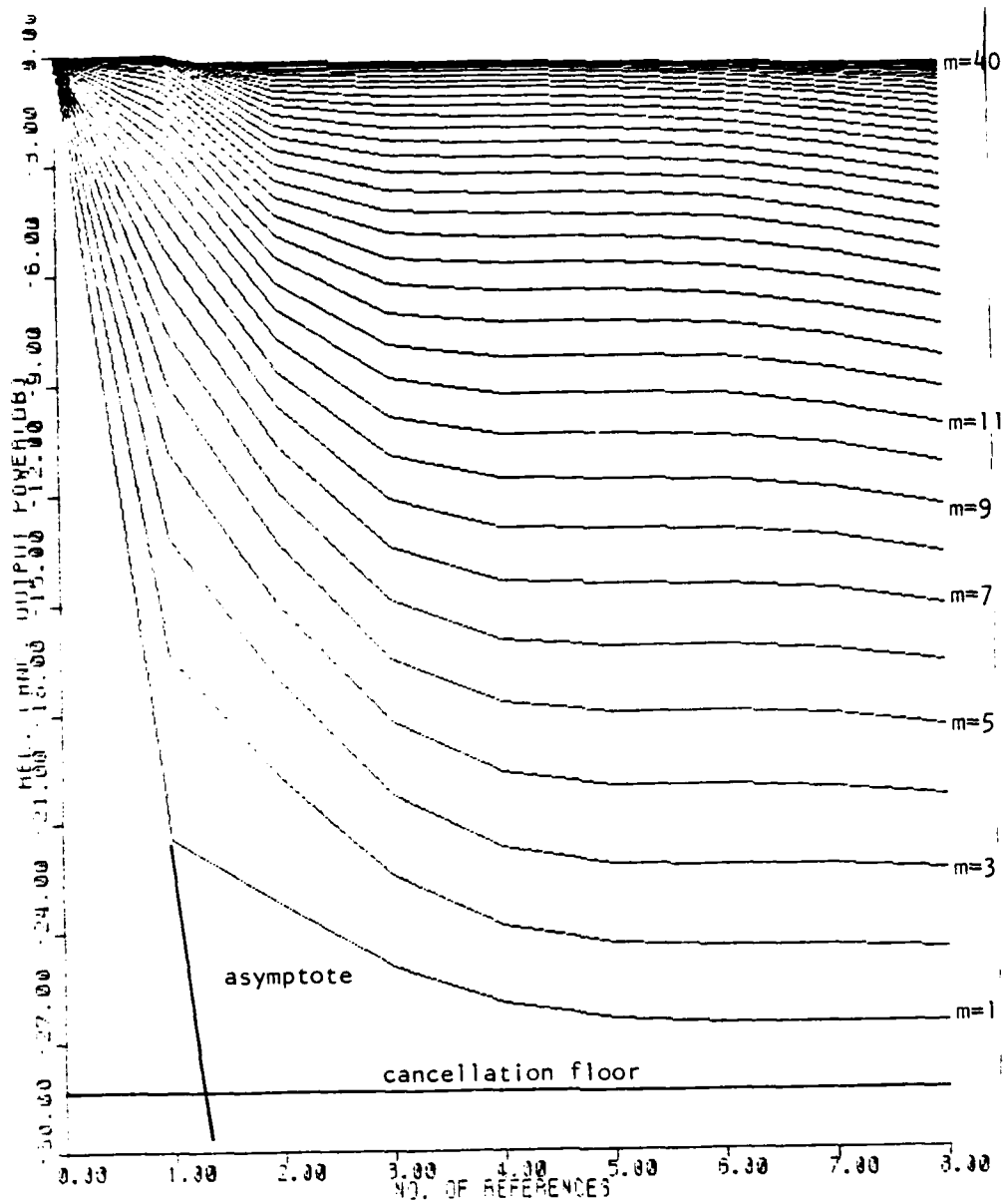
FIGURE K-29

W = .02

INR = 20 dB
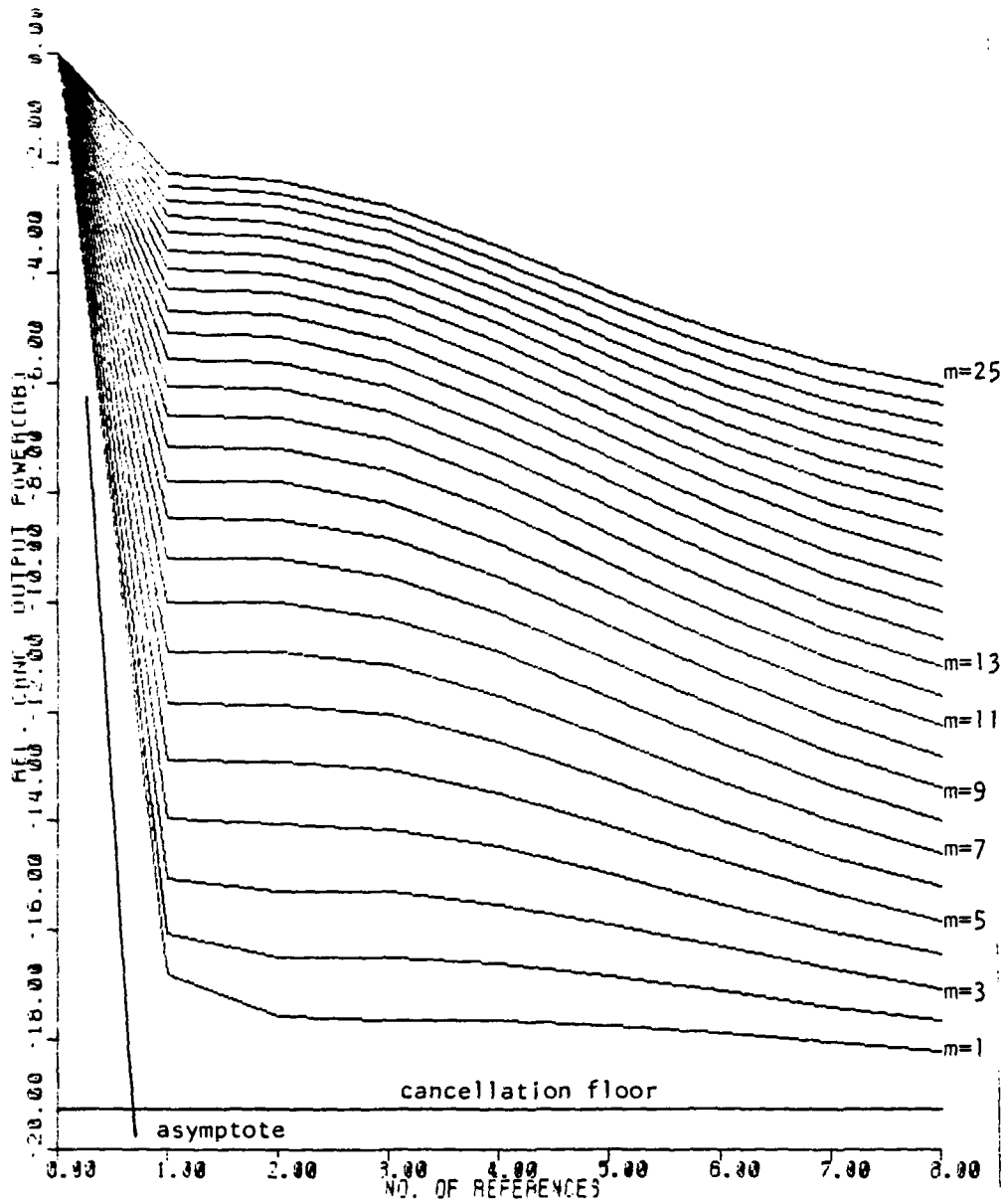
FIGURE K-30

$W = 10^{-2}$

$INR = 40$ dB
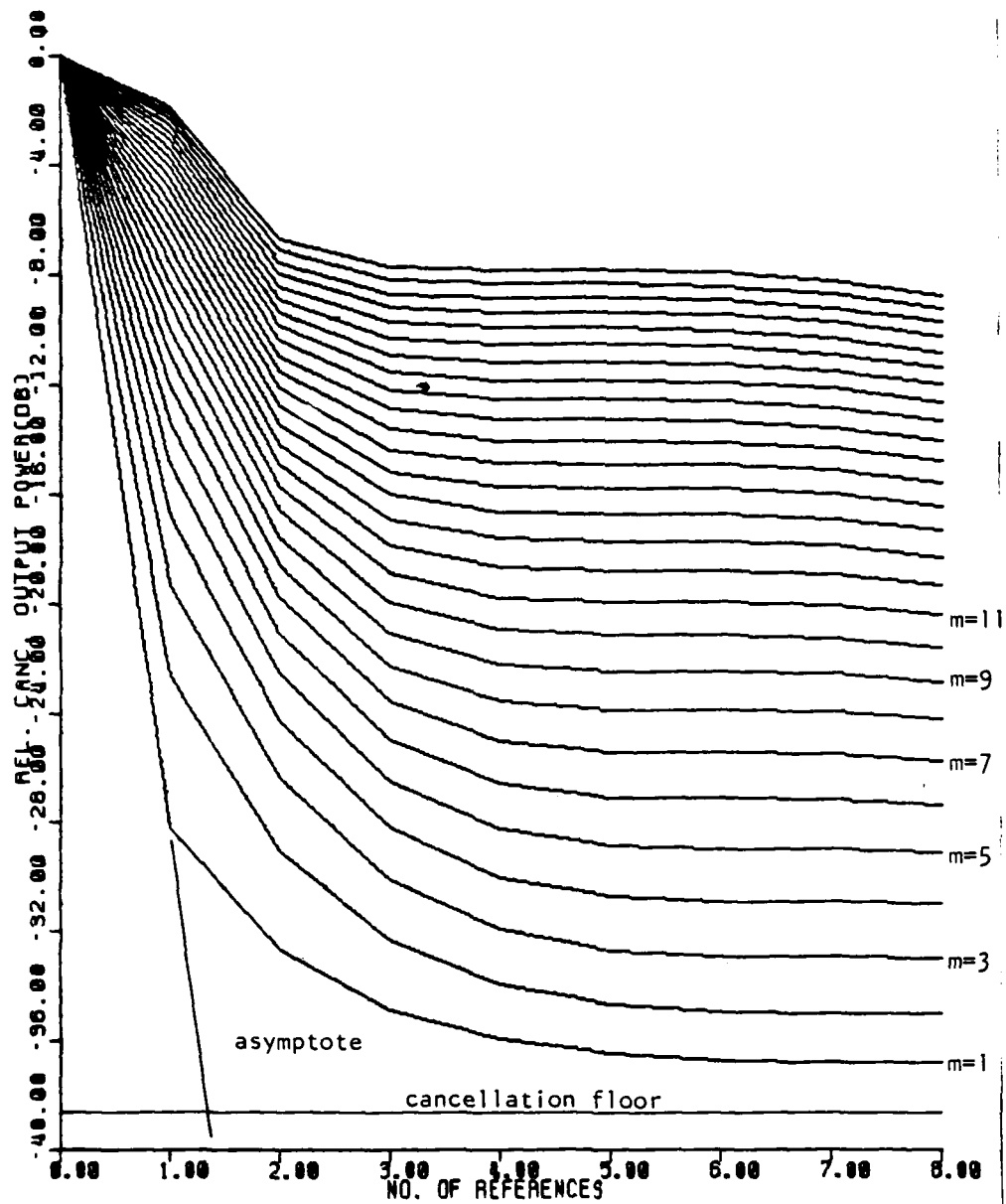
FIGURE K-31

W = .01

INR = 30 dB
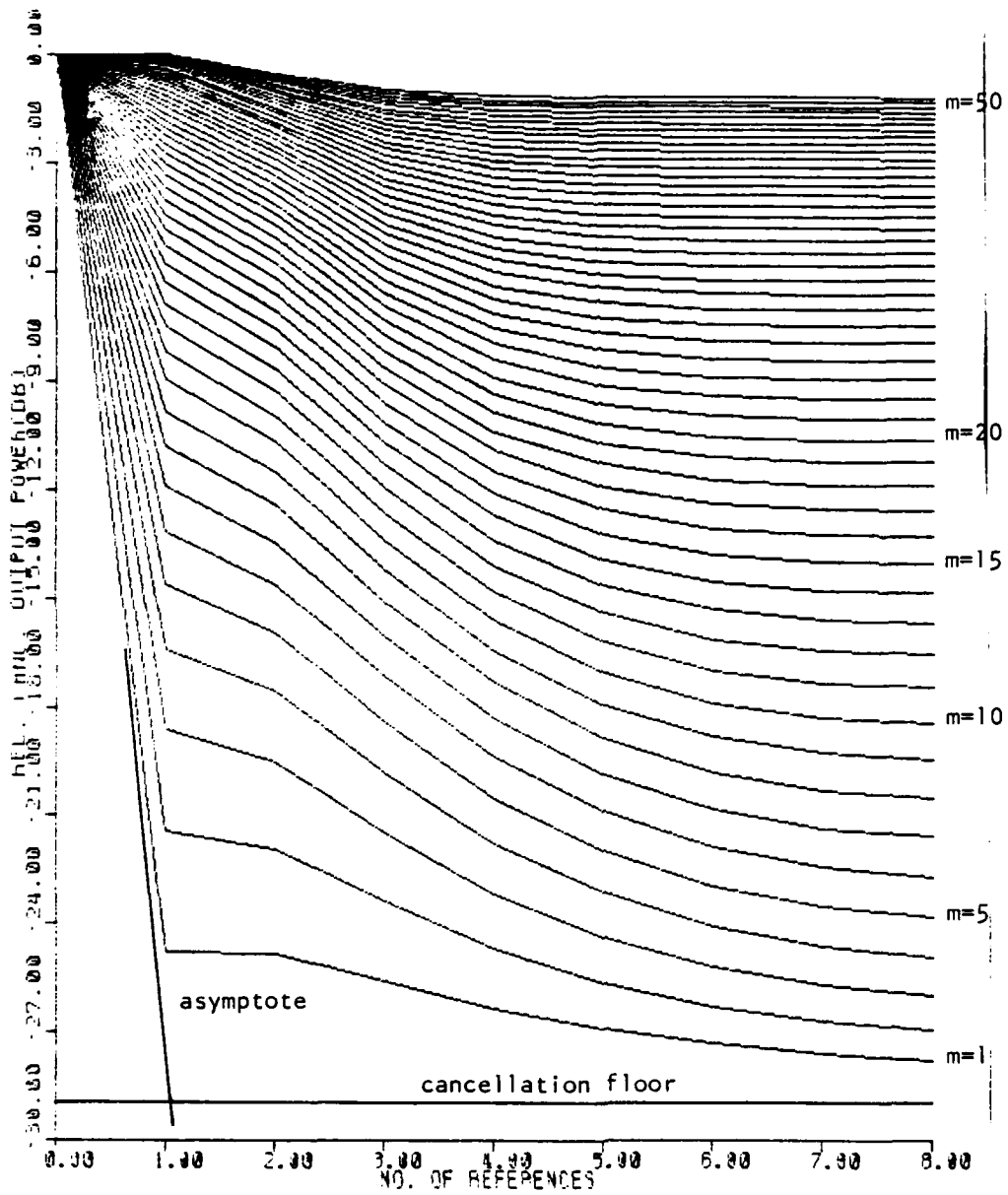
FIGURE K-32

$$W = 10^{-2}$$

$$INR = 20 \ dB$$
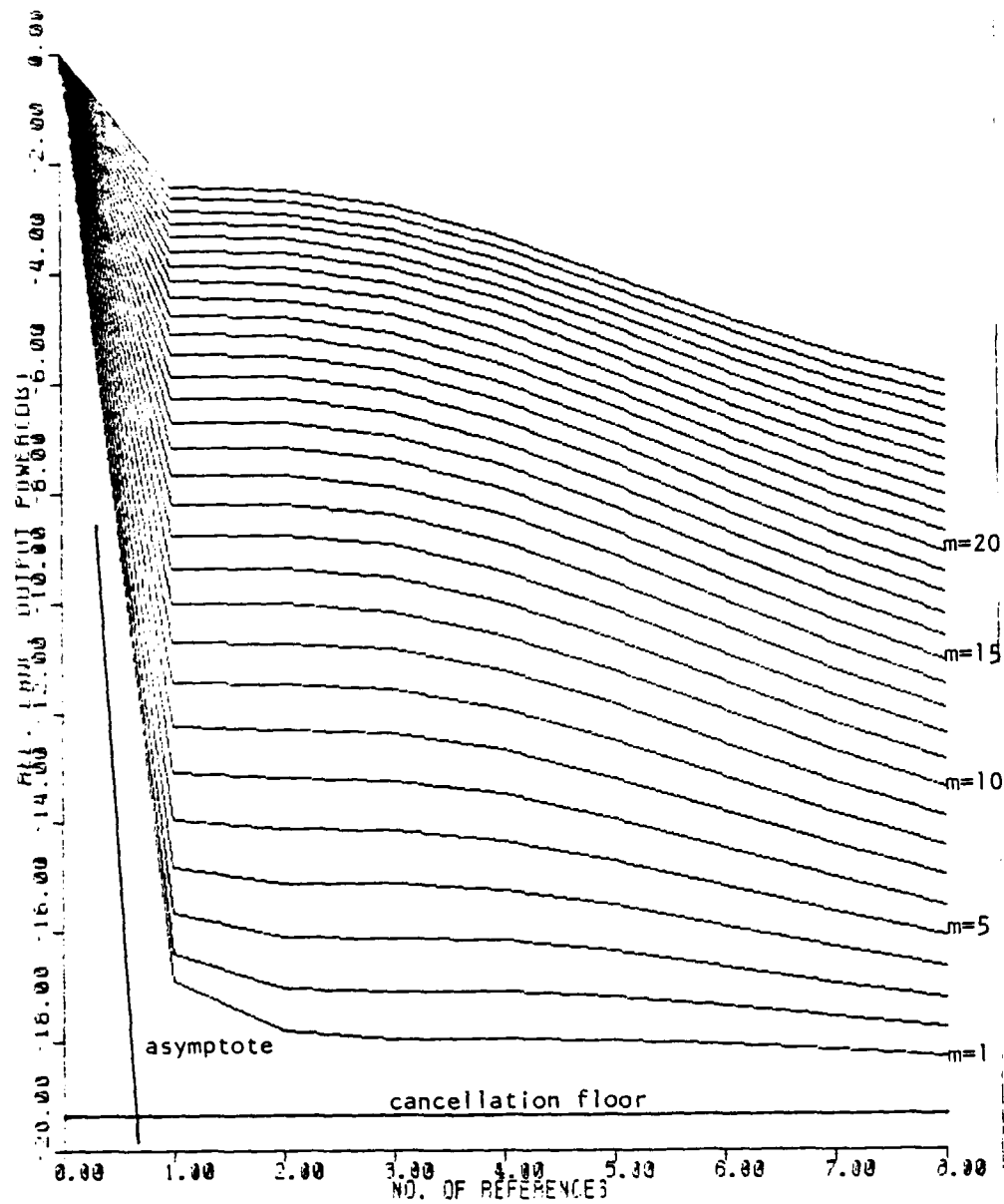
FIGURE K-33

$W = 8 \times 10^{-3}$

$INR = 40$ dB
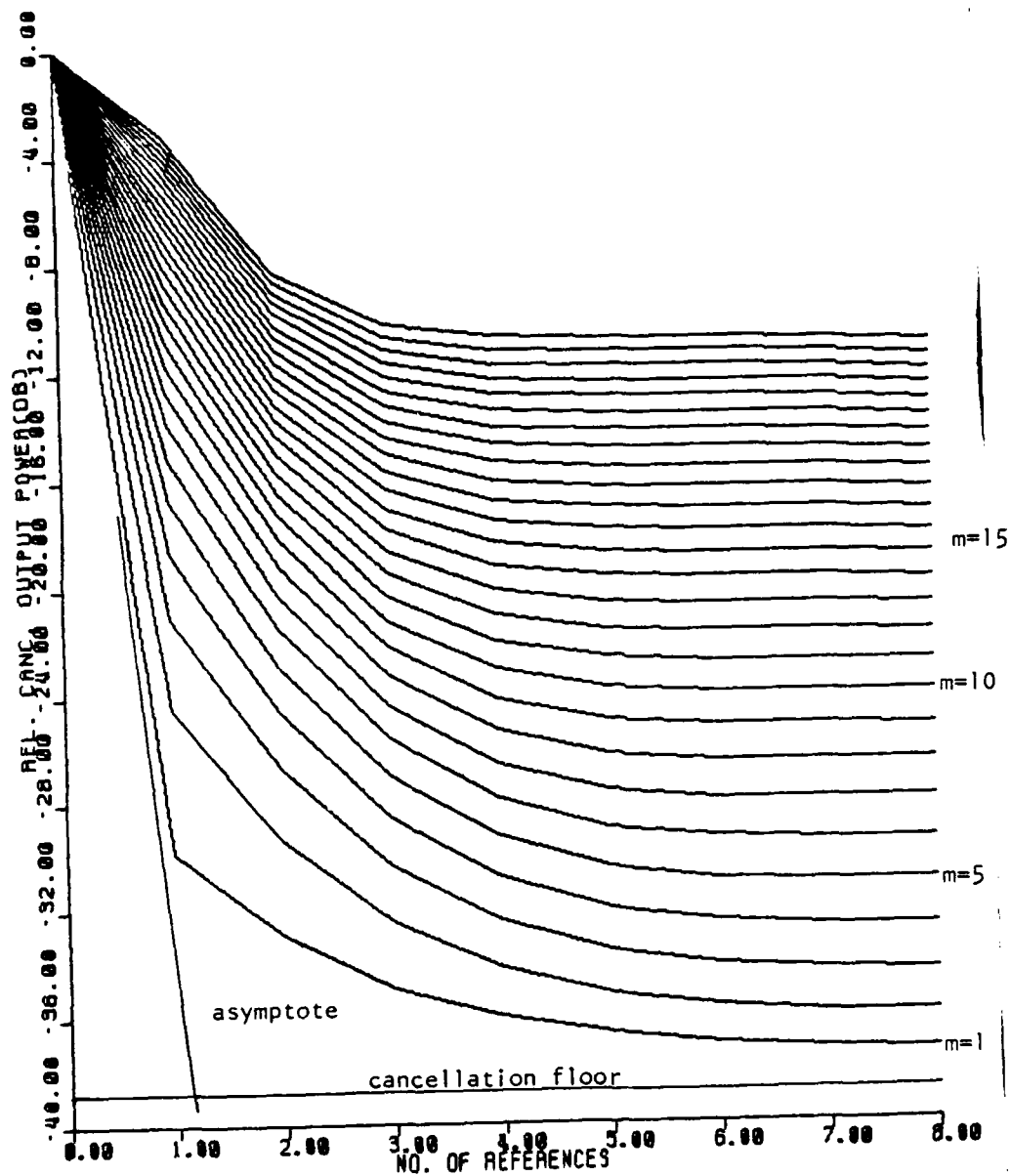
FIGURE K-34

$W = 8 \times 10^{-3}$

INR = 30 dB
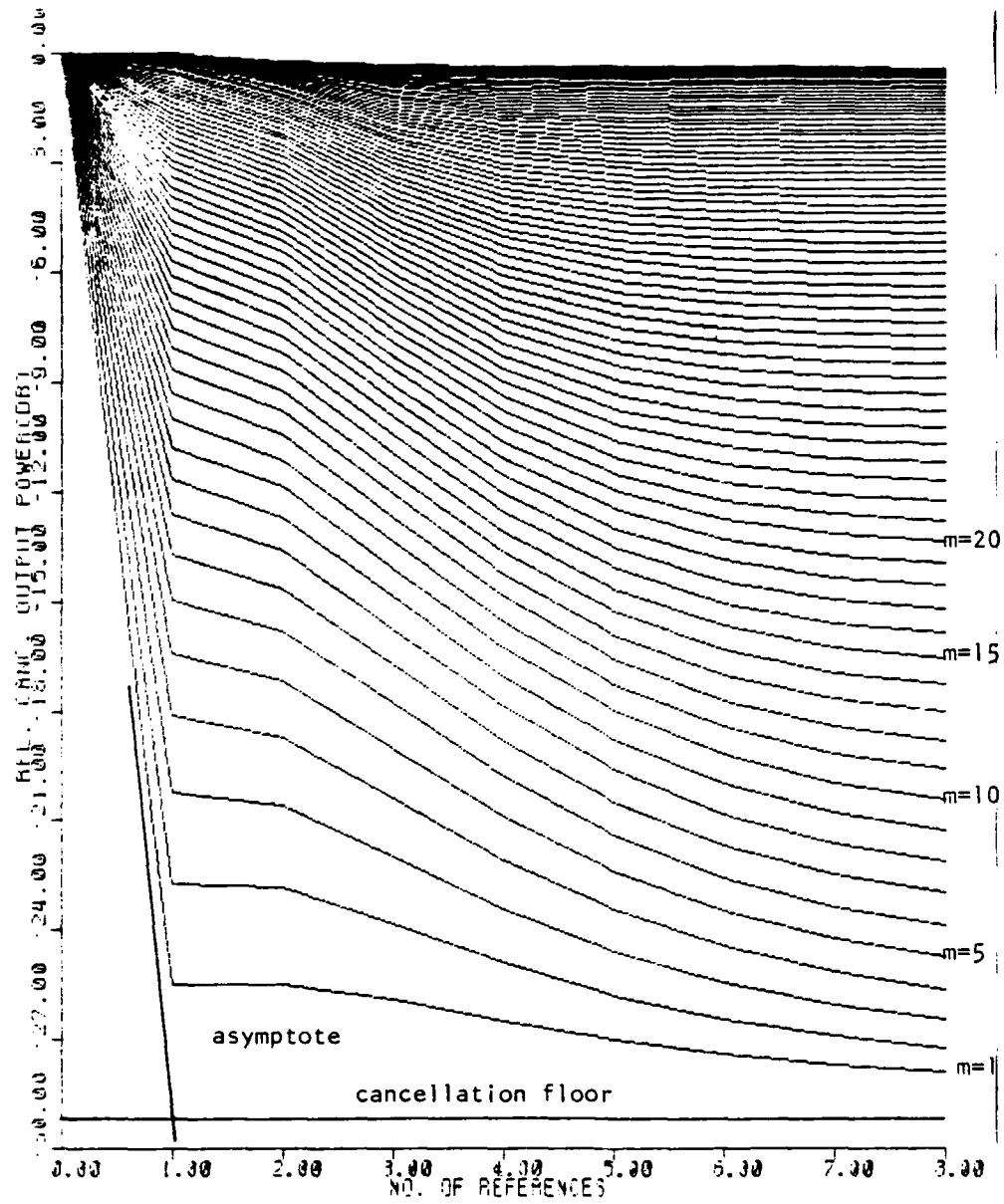
FIGURE K-35

W = .008

INR = 20 dB
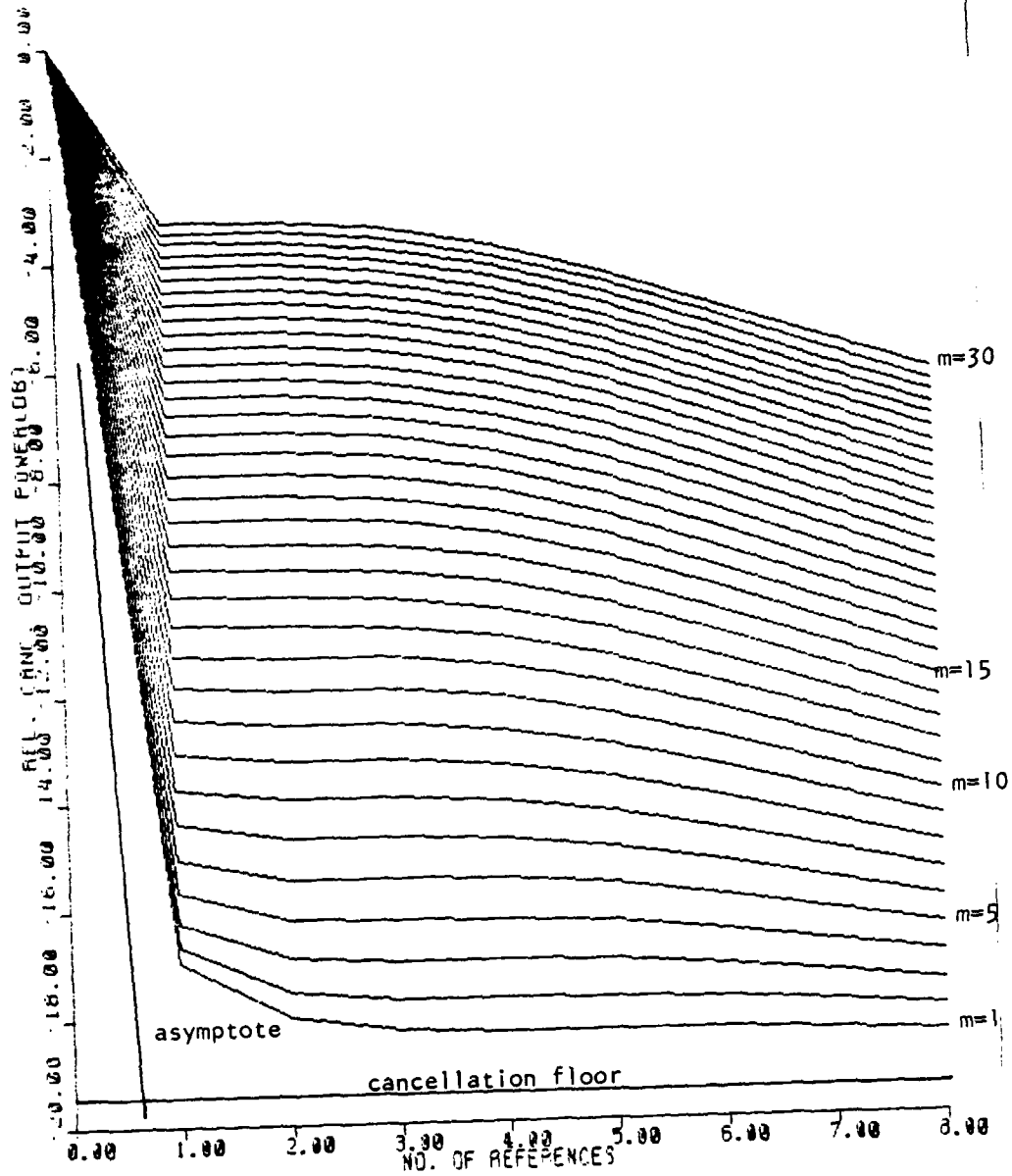
FIGURE K-36

$W = 6 \times 10^{-3}$

INR = 40 dB
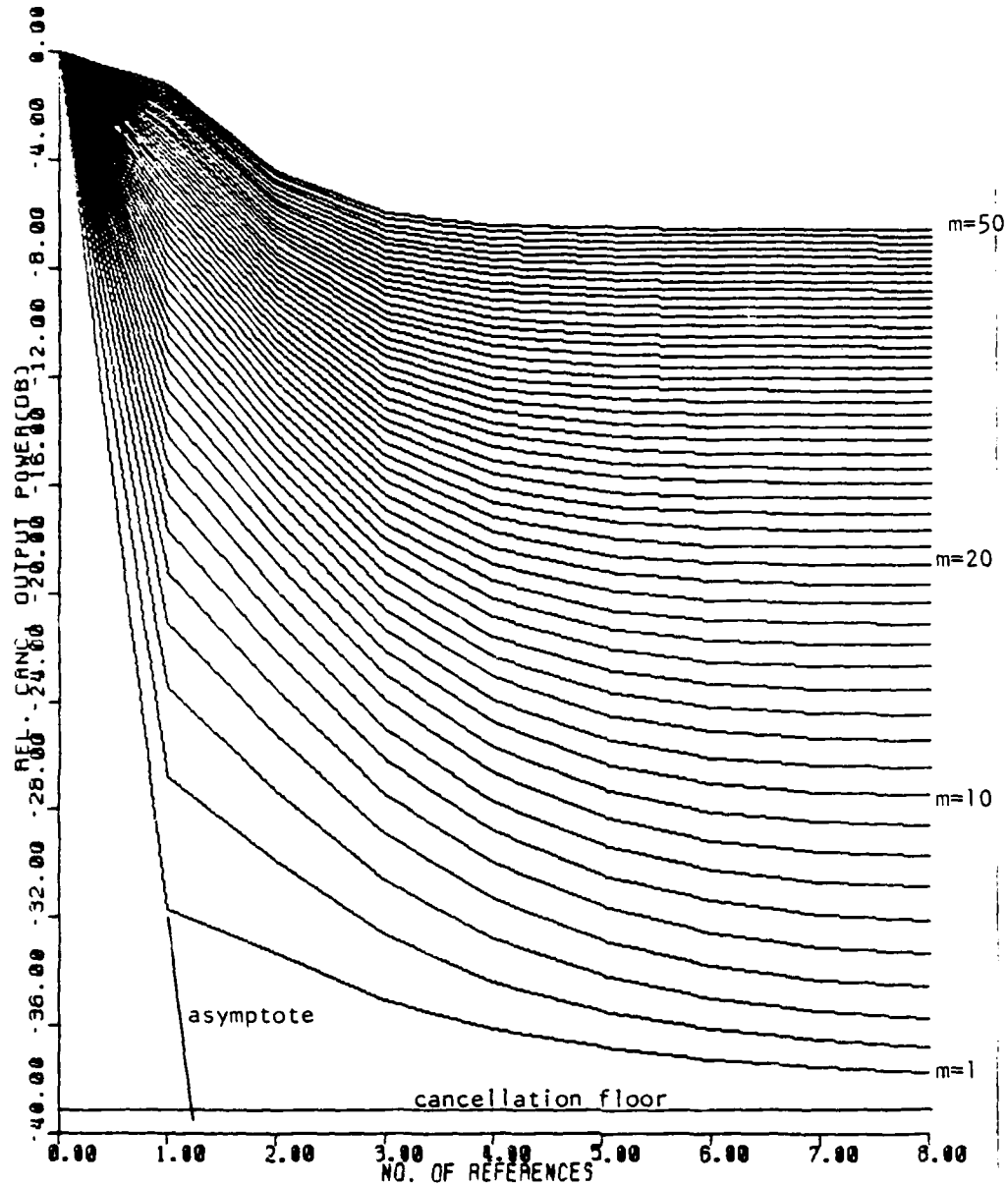
FIGURE K-37

$W = 6 \times 10^{-3}$

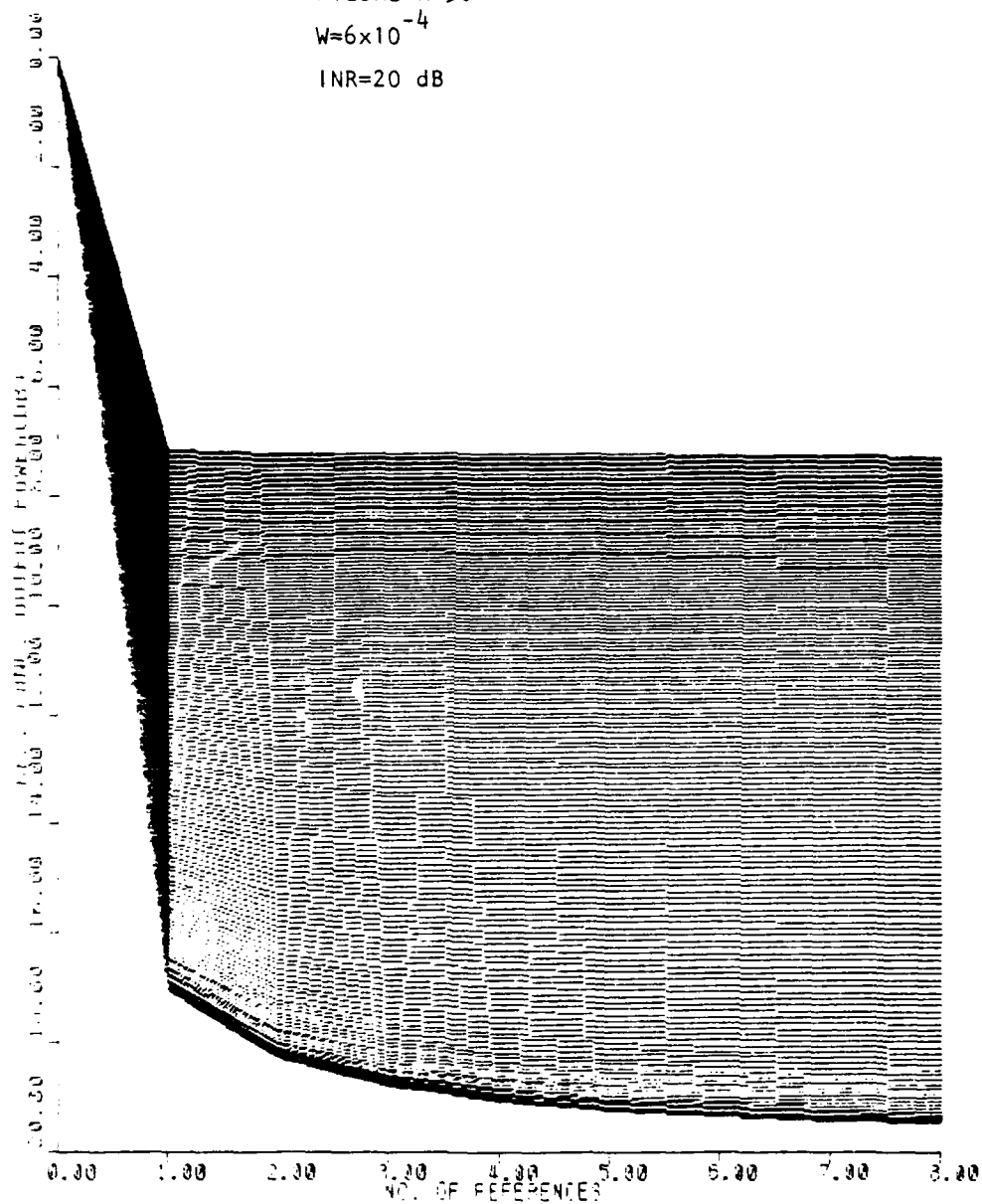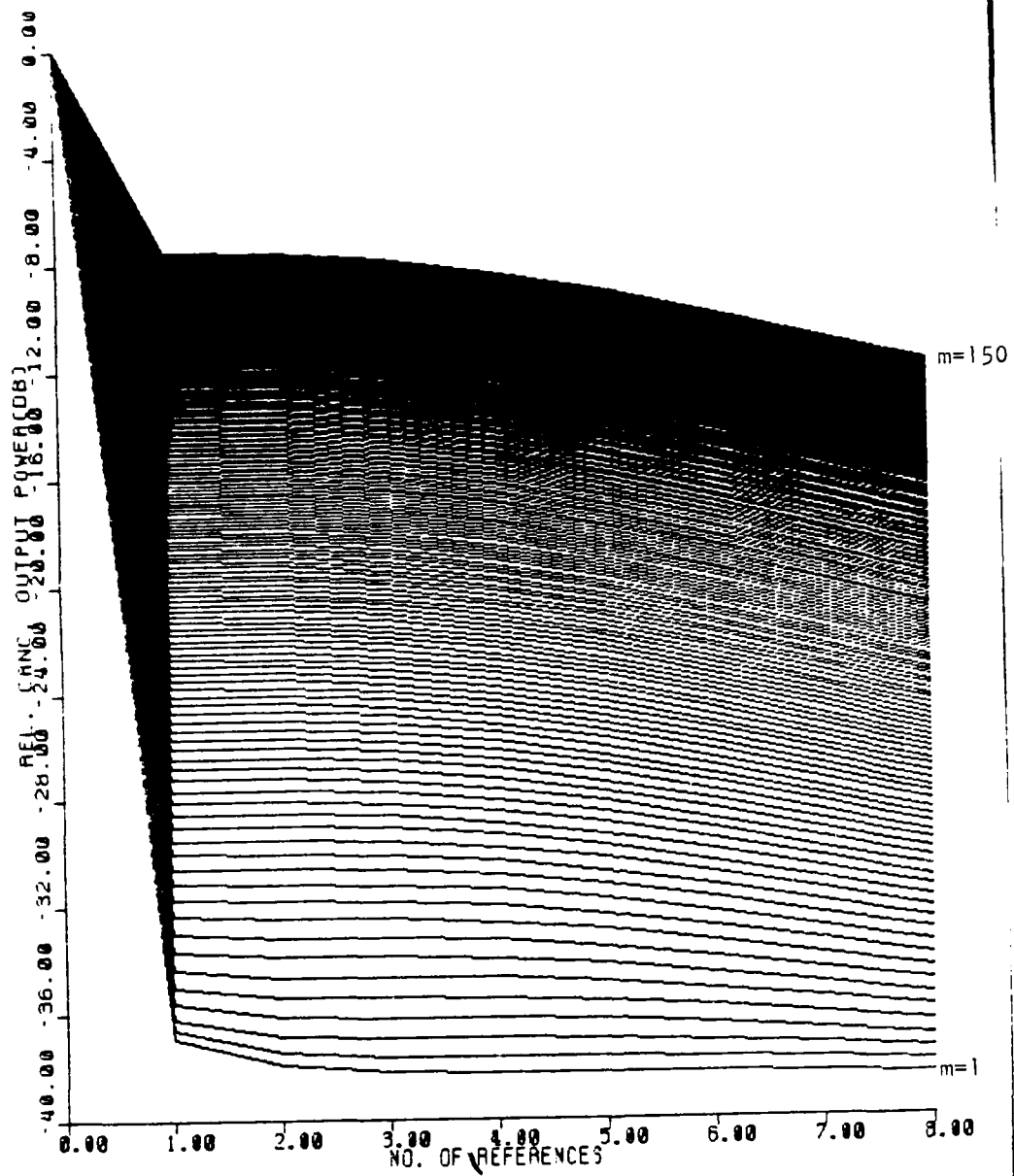INR = 30 dB
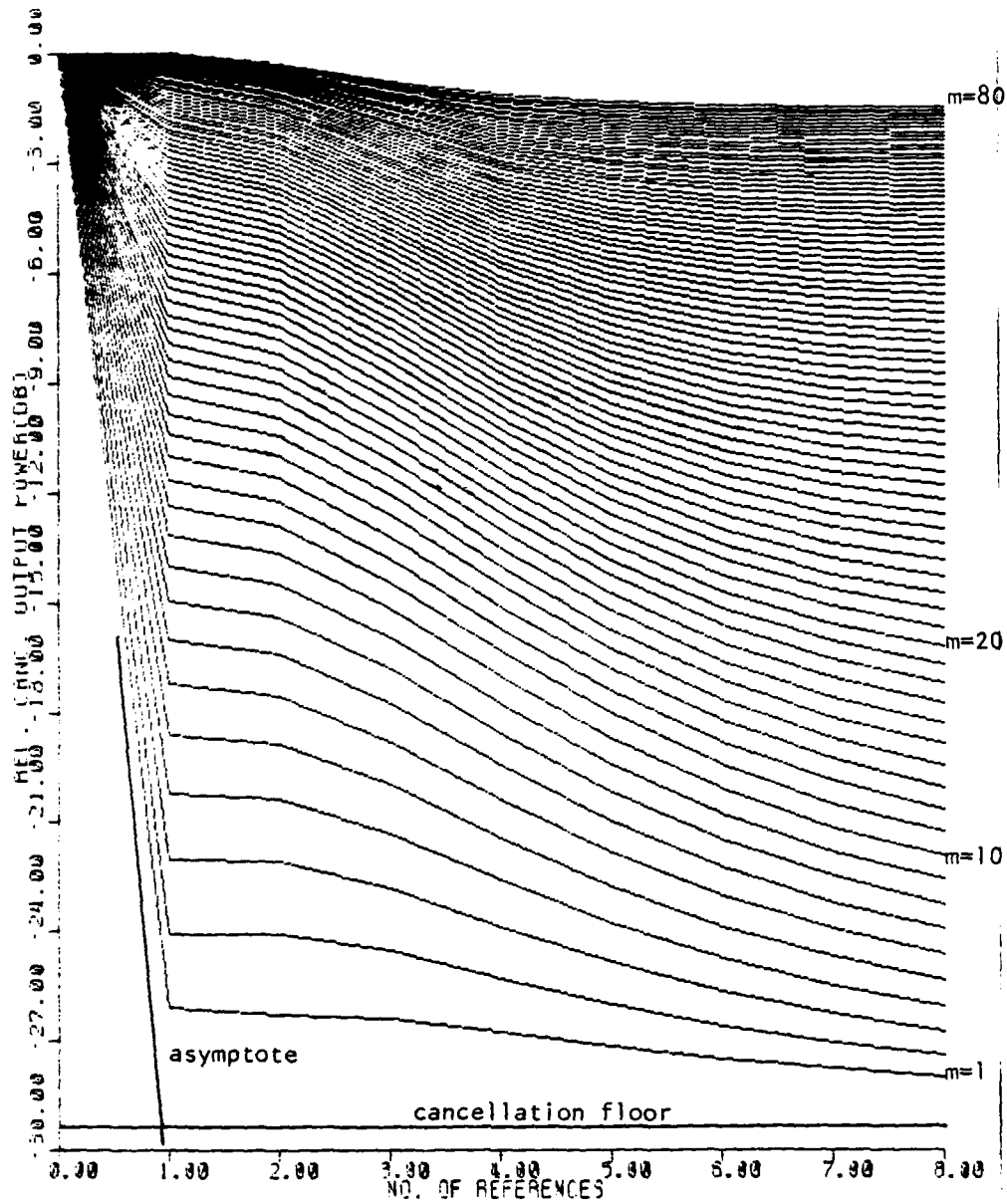
FIGURE K-38

$W = 6 \times 10^{-3}$

INR = 20 dB
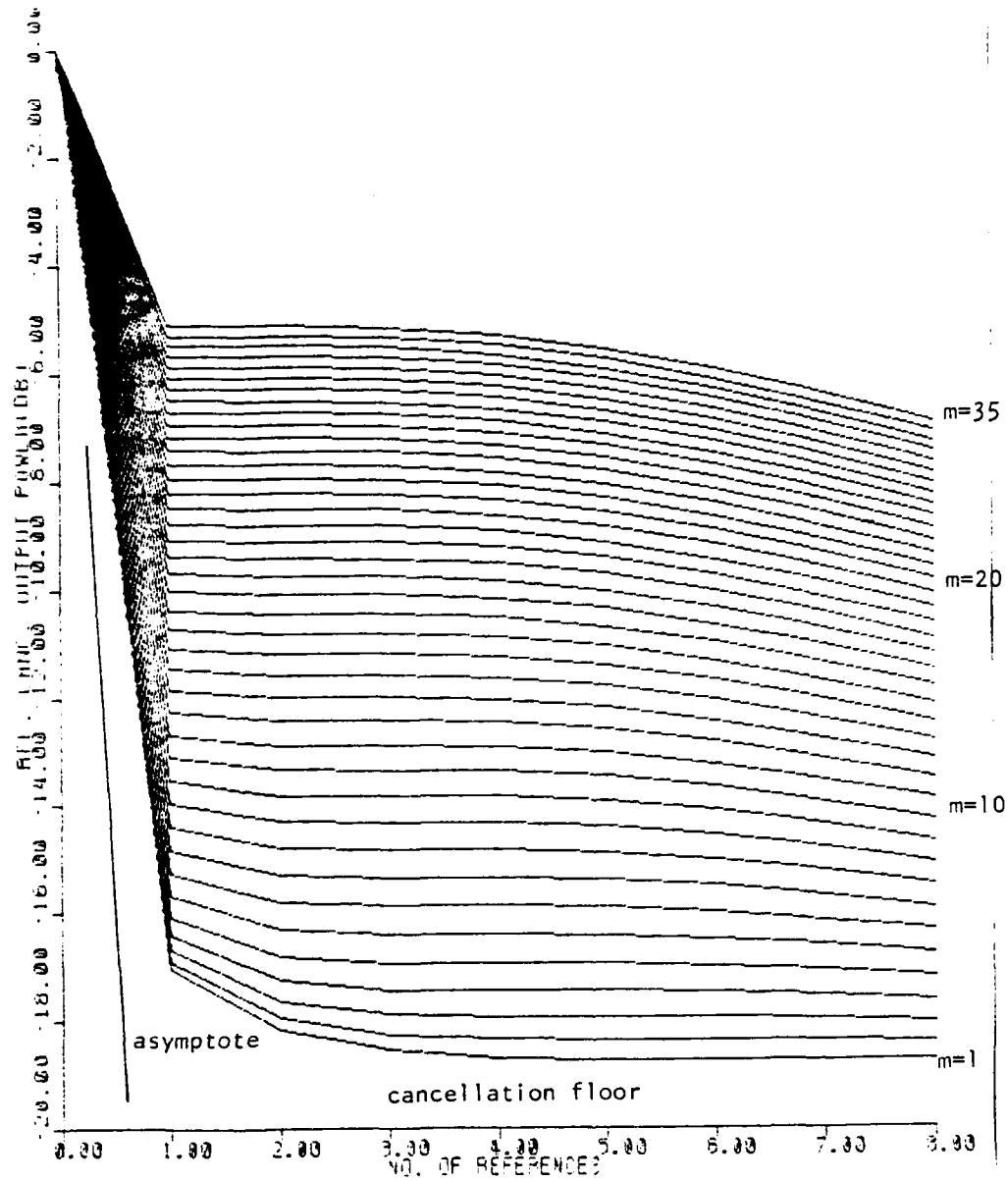
FIGURE K-39

$W = 4 \times 10^{-3}$

INR = 40 dB
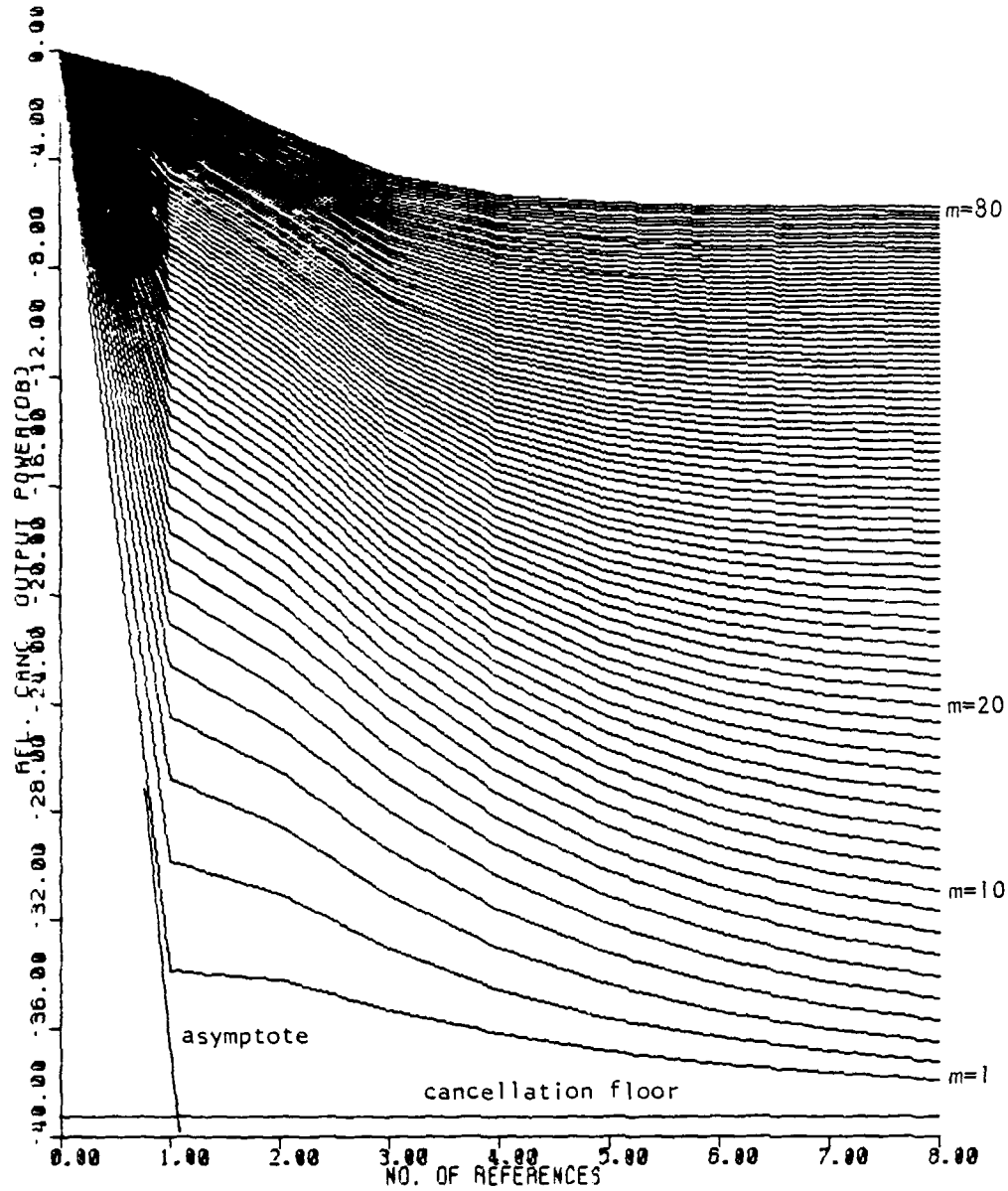
FIGURE K-40

$W = 4\times10^{-3}$

INR = 30 dB
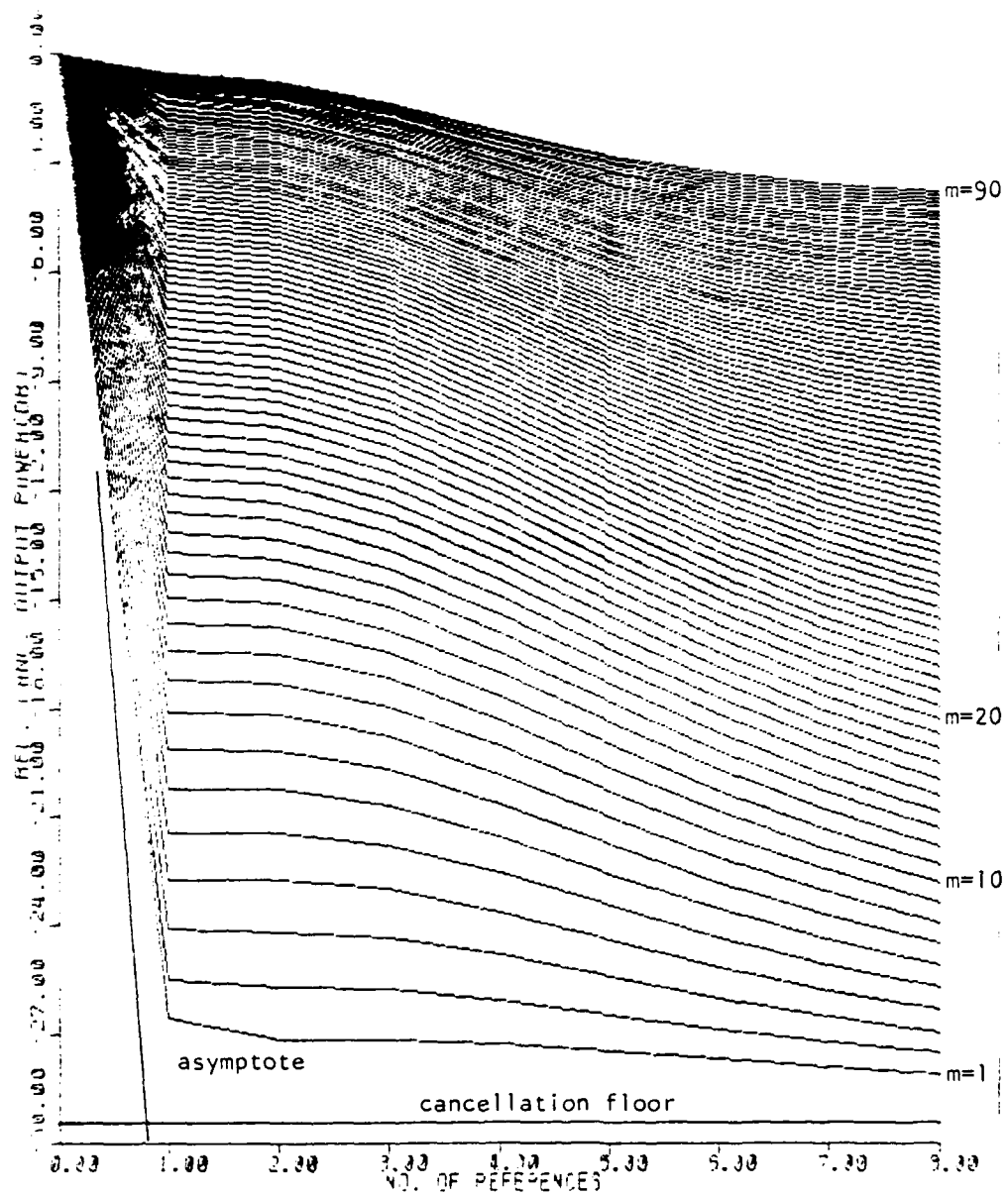
FIGURE K-41

$W = 4 \times 10^{-3}$

INR = 20 dB
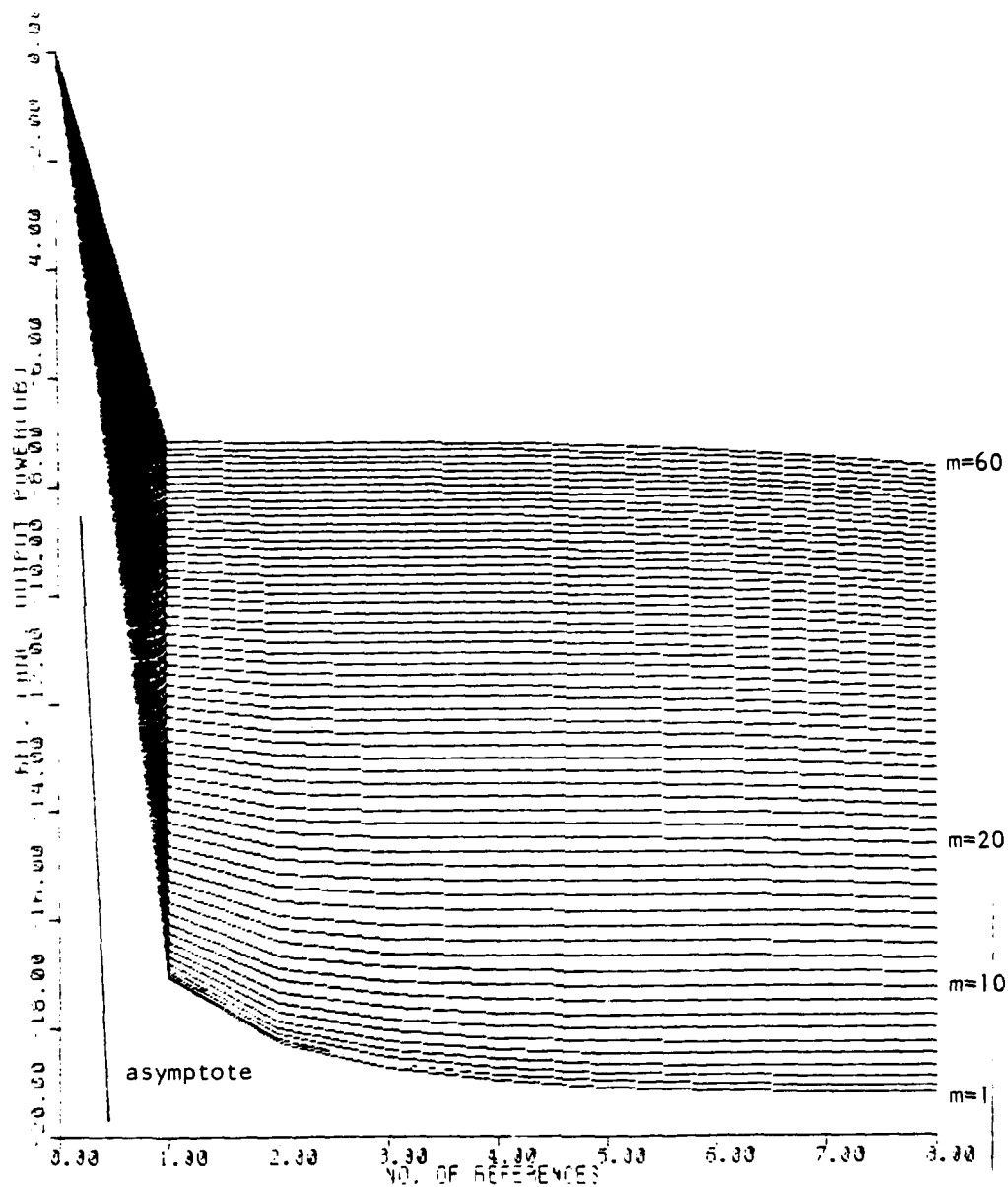
FIGURE K-42

$W = 2 \times 10^{-3}$

$INR = 40$ dB

K-47
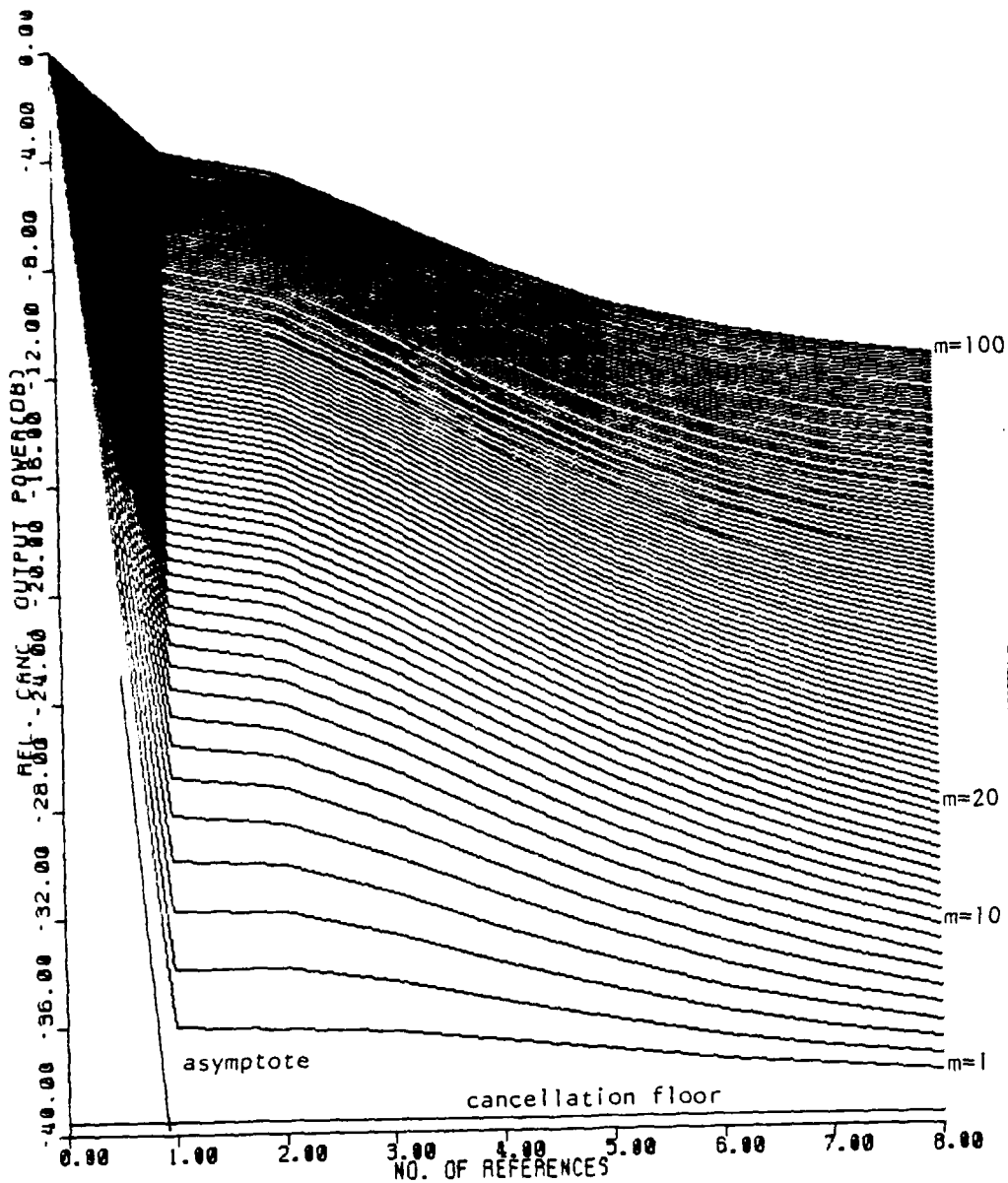
FIGURE K-43

$W = 2 \times 10^{-3}$

INR = 30 dB
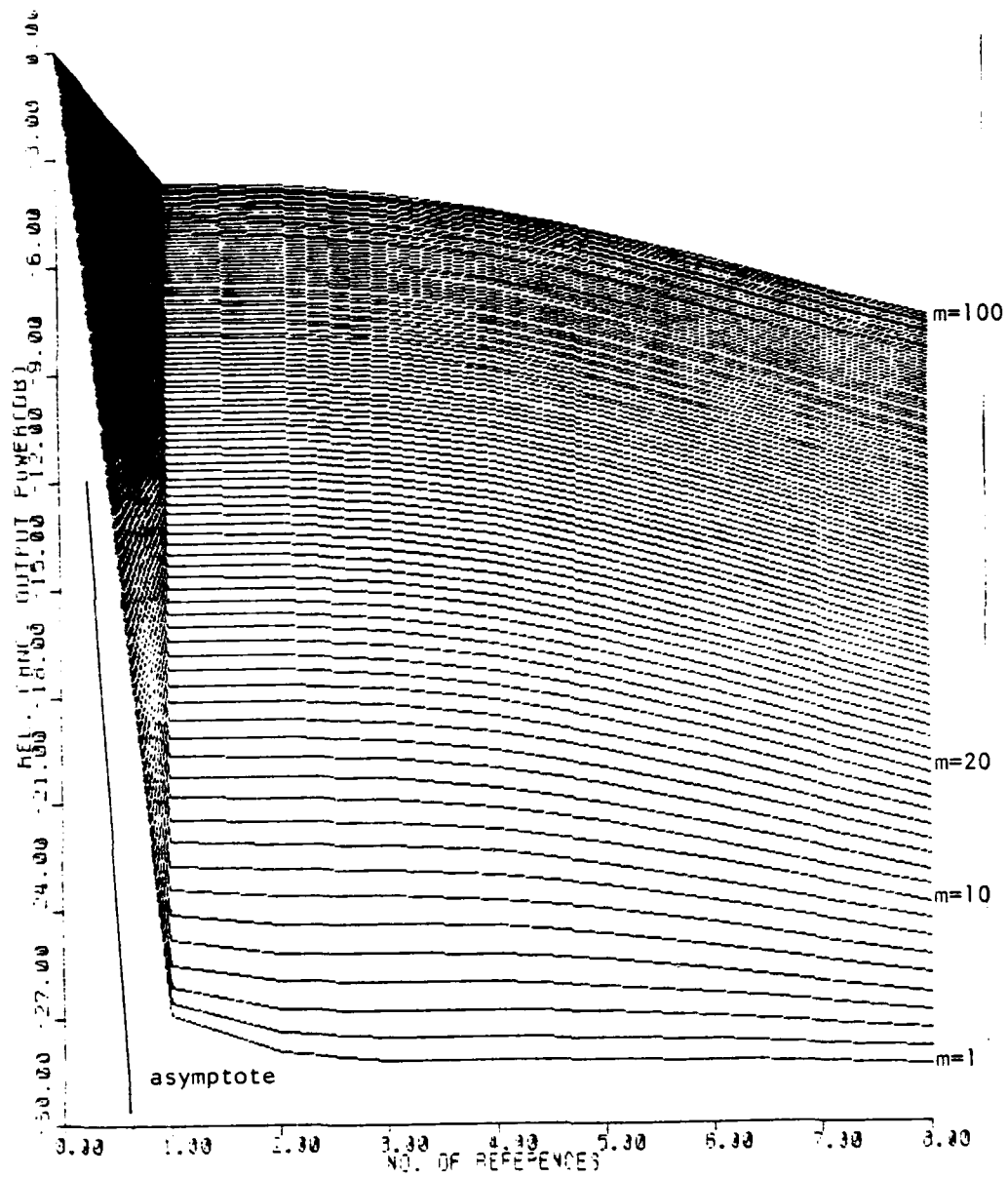
FIGURE K-44

$W = 2 \times 10^{-3}$

$INR = 20$ dB
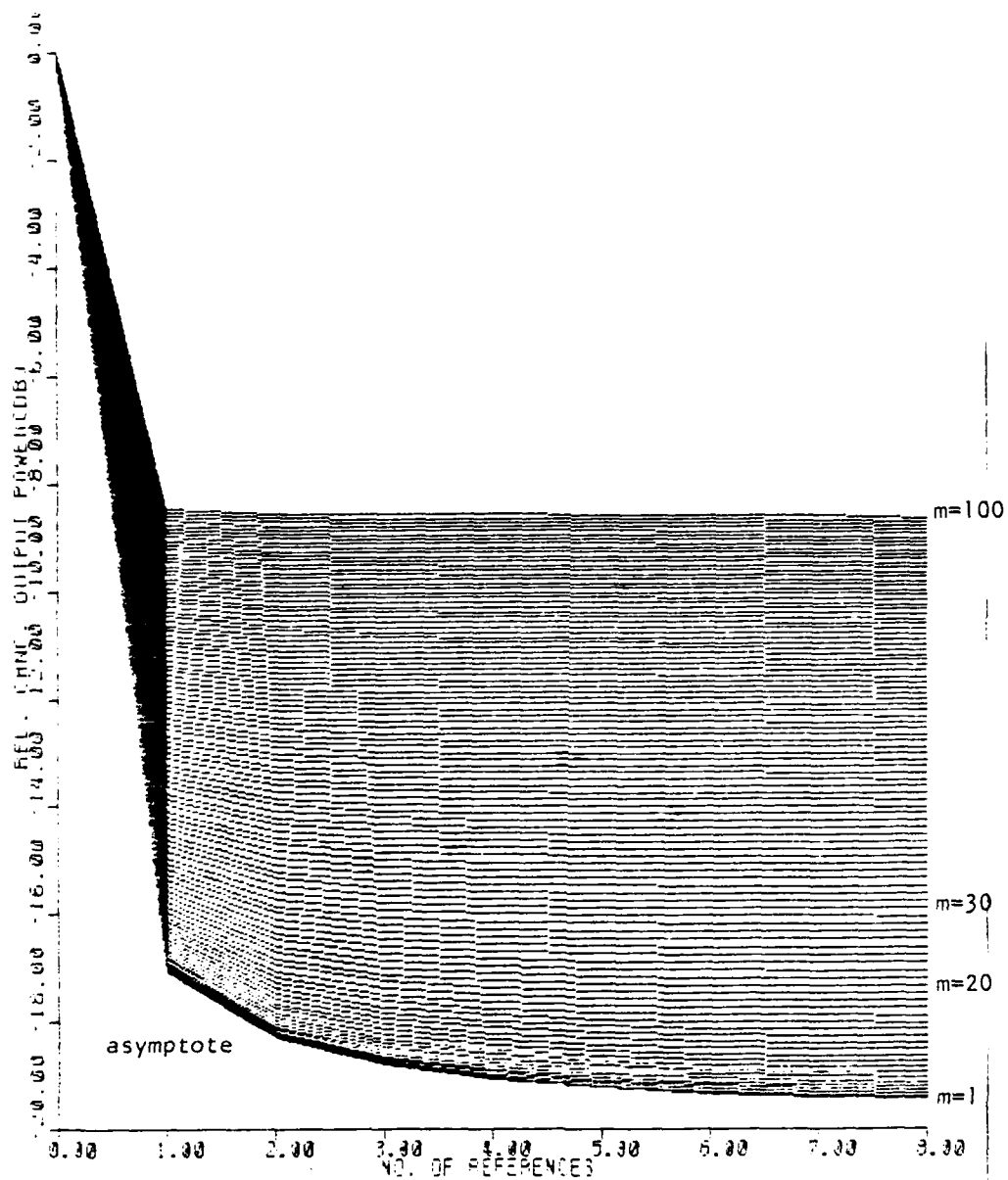
FIGURE K-45

$W = 10^{-3}$

$INR = 40$ dB
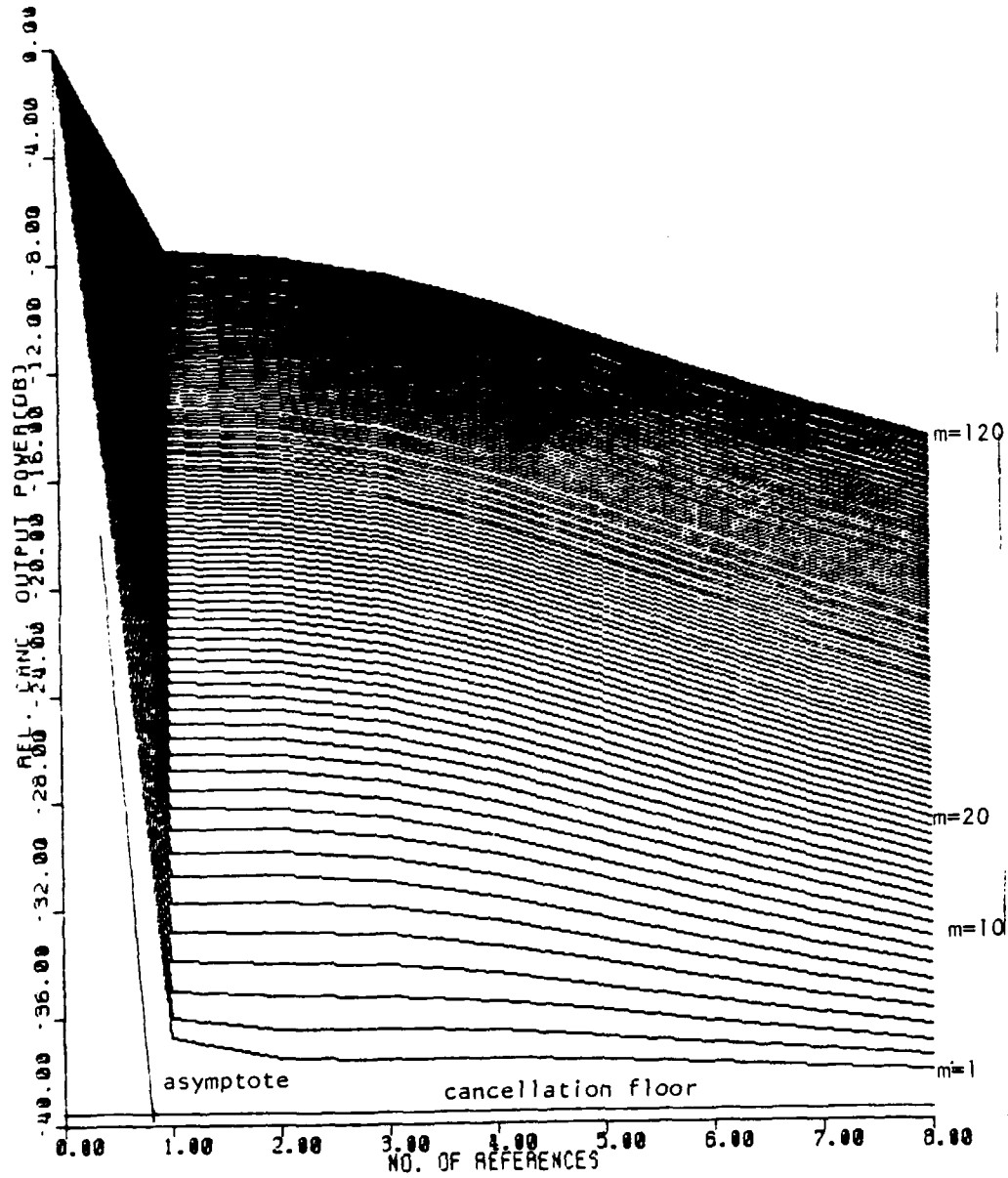
FIGURE K-46

$W = 10^{-3}$

$INR = 30$ dB
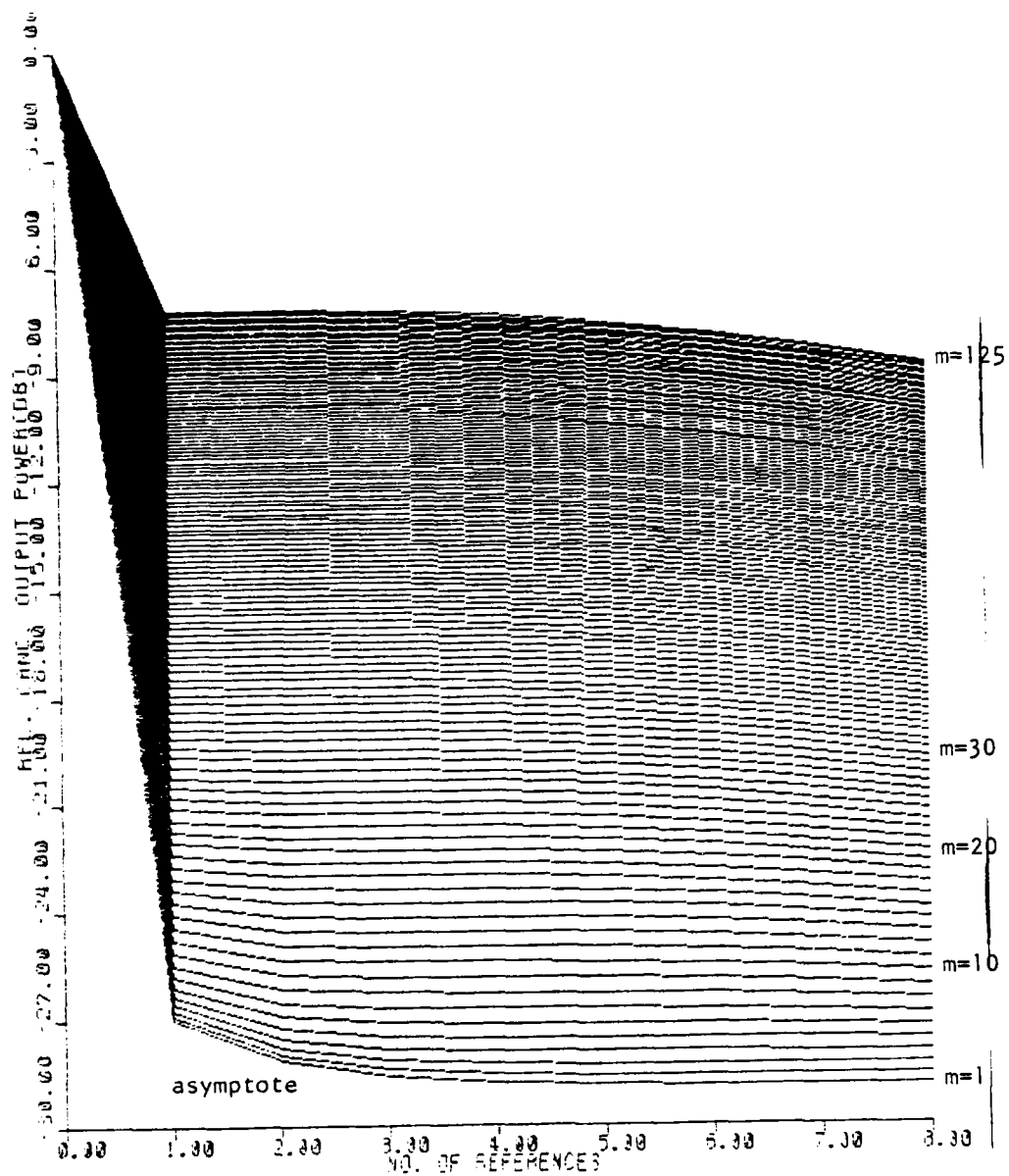
FIGURE K-47

$W = 10^{-3}$

INR = 20 dB

m=140

m=20

asymptote

m=1

0.00   1.00   2.00   3.00   4.00   5.00   6.00   7.00   8.00
NO. OF REFERENCES
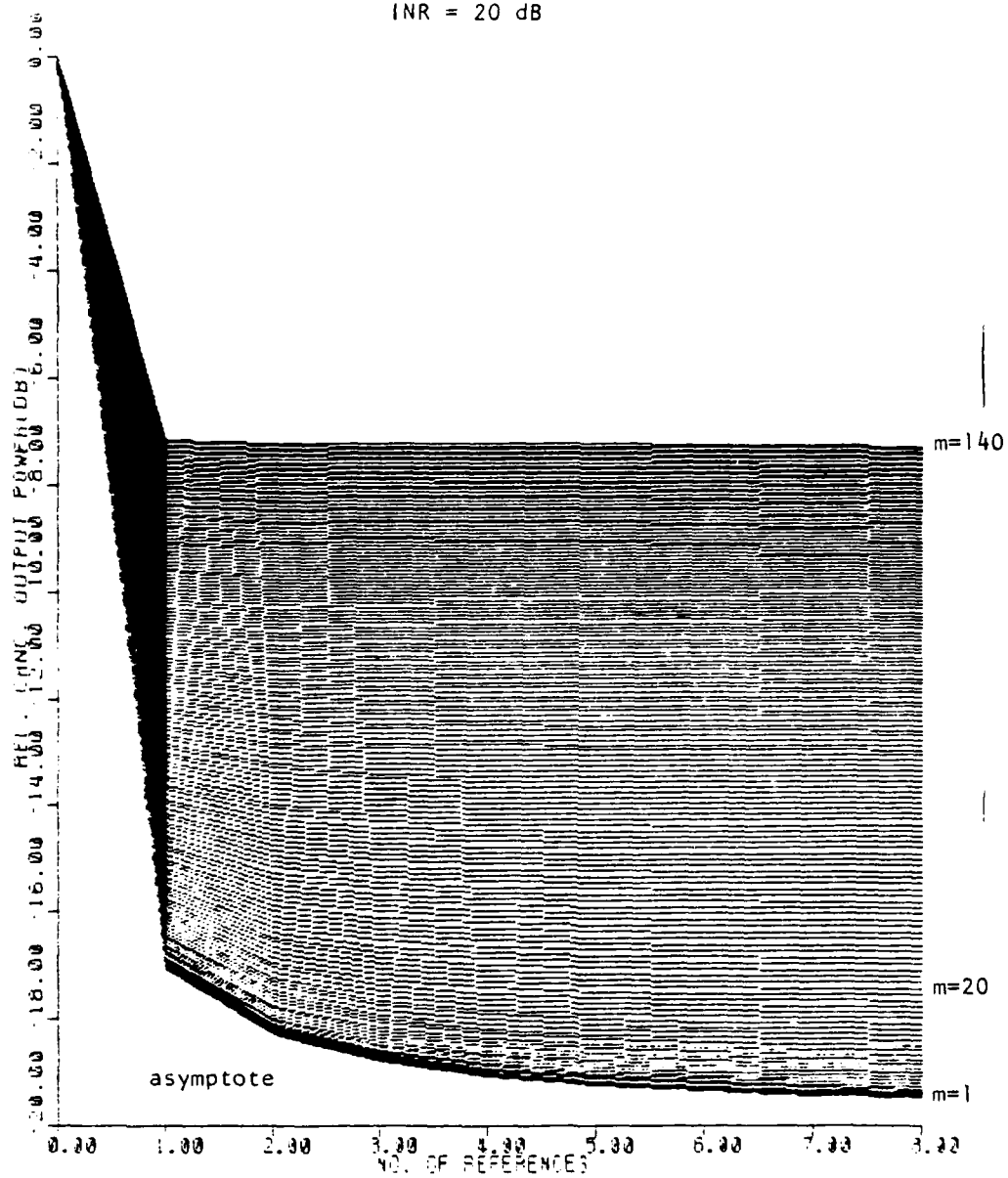
FIGURE K-48

$W = 8 \times 10^{-4}$

INR = 40 dB

FIGURE K-49

$W = 8 \times 10^{-4}$

INR = 30 dB

m=150

m=10

m=1

FIGURE K-50
$W=6\times10^{-4}$
INR=20 dB

FIGURE K-51

$W = 6 \times 10^{-4}$

$INR = 40$ dB

FIGURE K=52

$W = 6 \times 10^{-4}$

INR = 30 dB
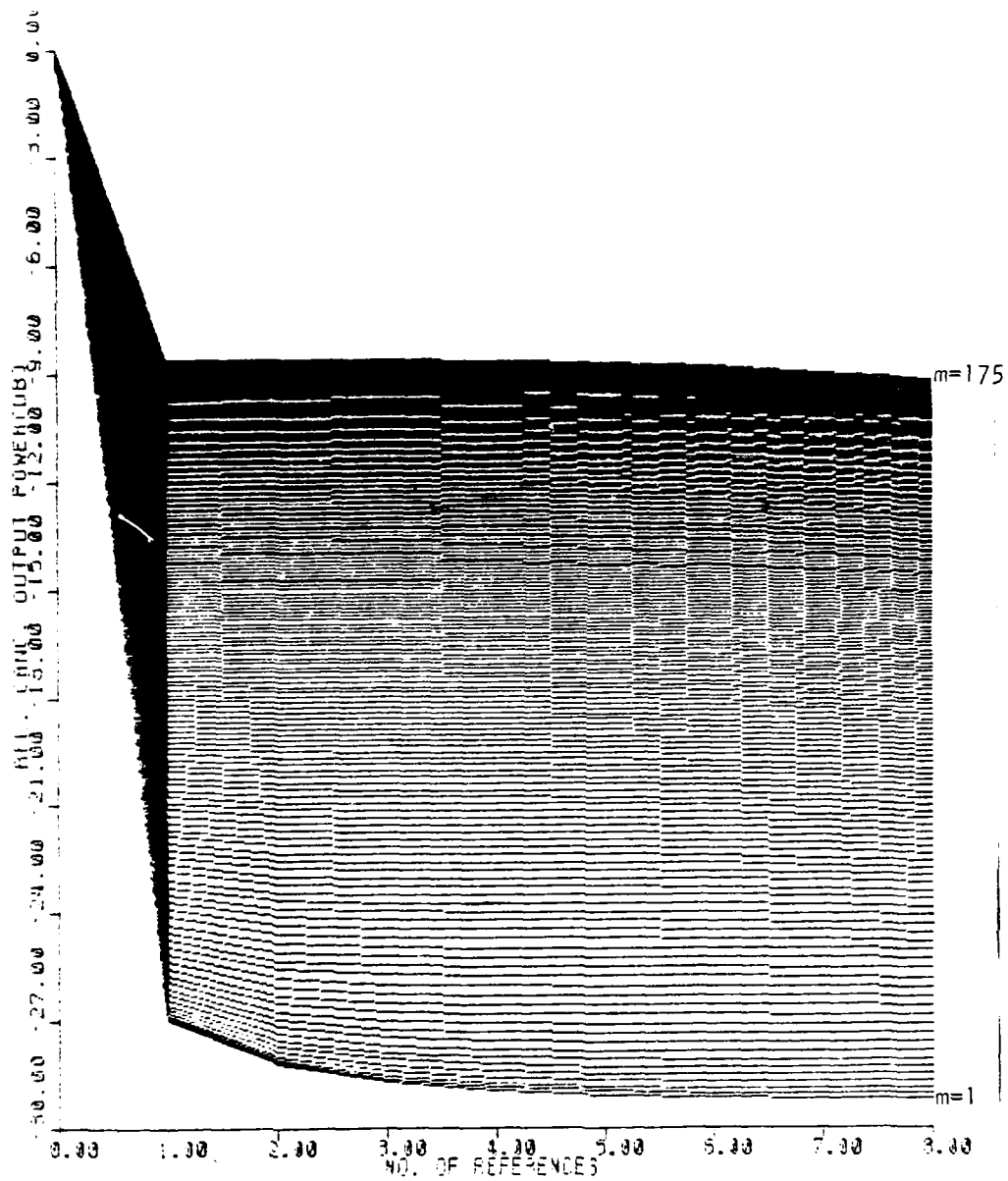
FIGURE K=53

$W = 6 \times 10^{-4}$

$INR = +20$ dB

m=200

m=1

NO OF REFERENCES
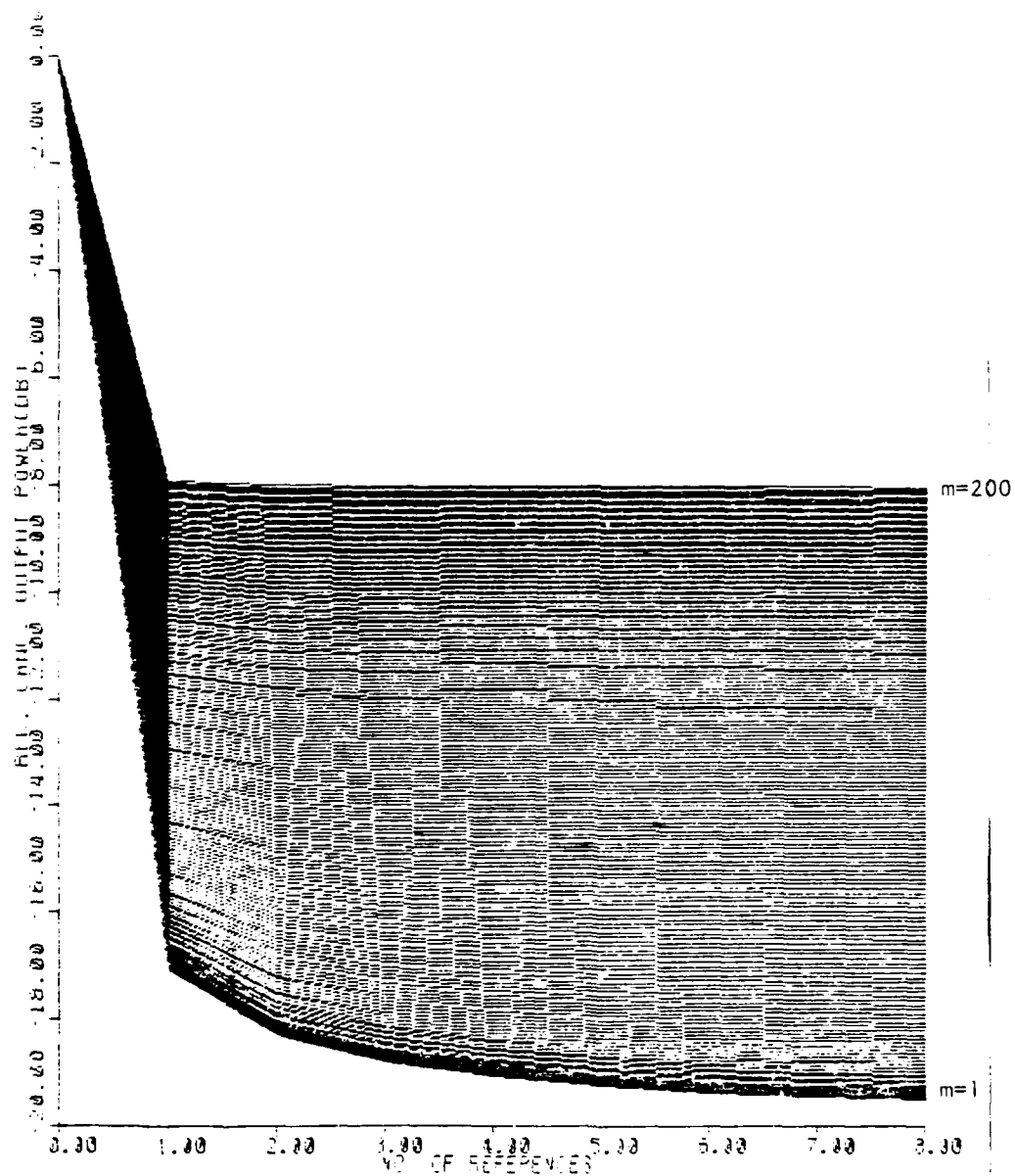
FIGURE K-54

$$W = 4 \times 10^{-4}$$

$$INR = 40 \; dB$$

m=200

m=1

REL. CANC. OUTPUT POWER(DB)

NO. OF REFERENCES
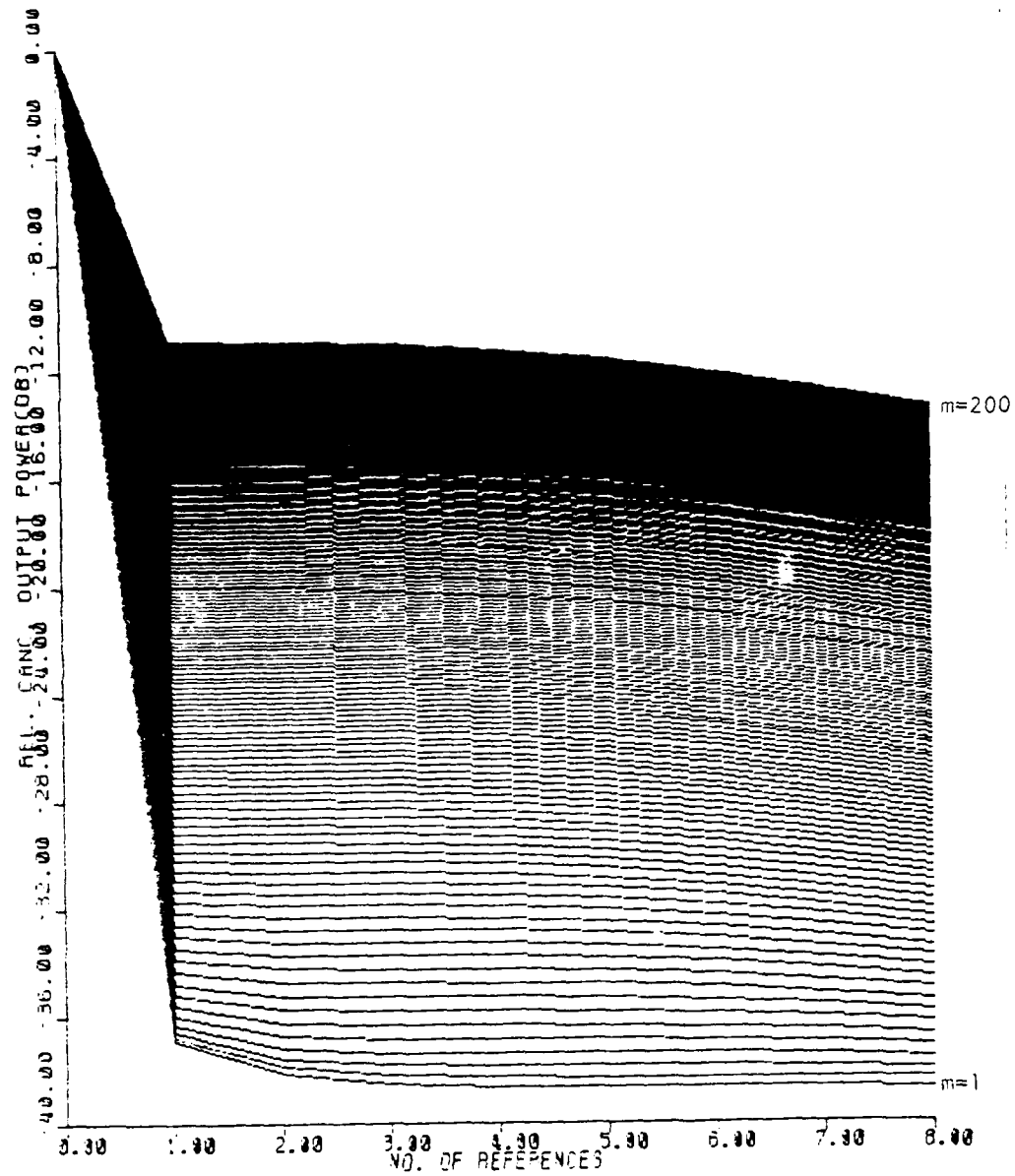
FIGURE K-55

$W = 4 \times 10^{-4}$

$INR = 30$ dB
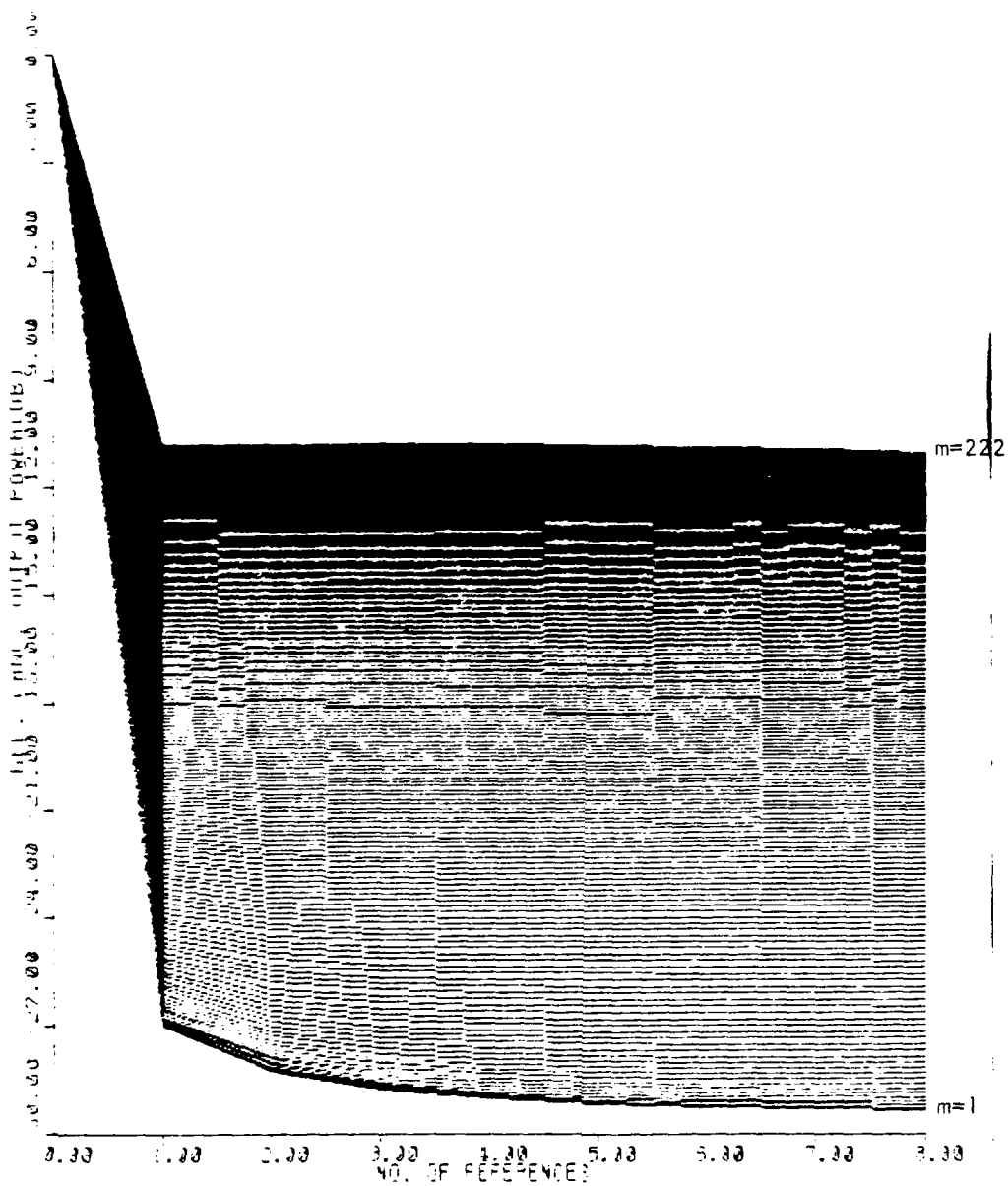
FIGURE K-56

$$W = 4\times10^{-4}$$

$$INR = 20 \text{ dB}$$
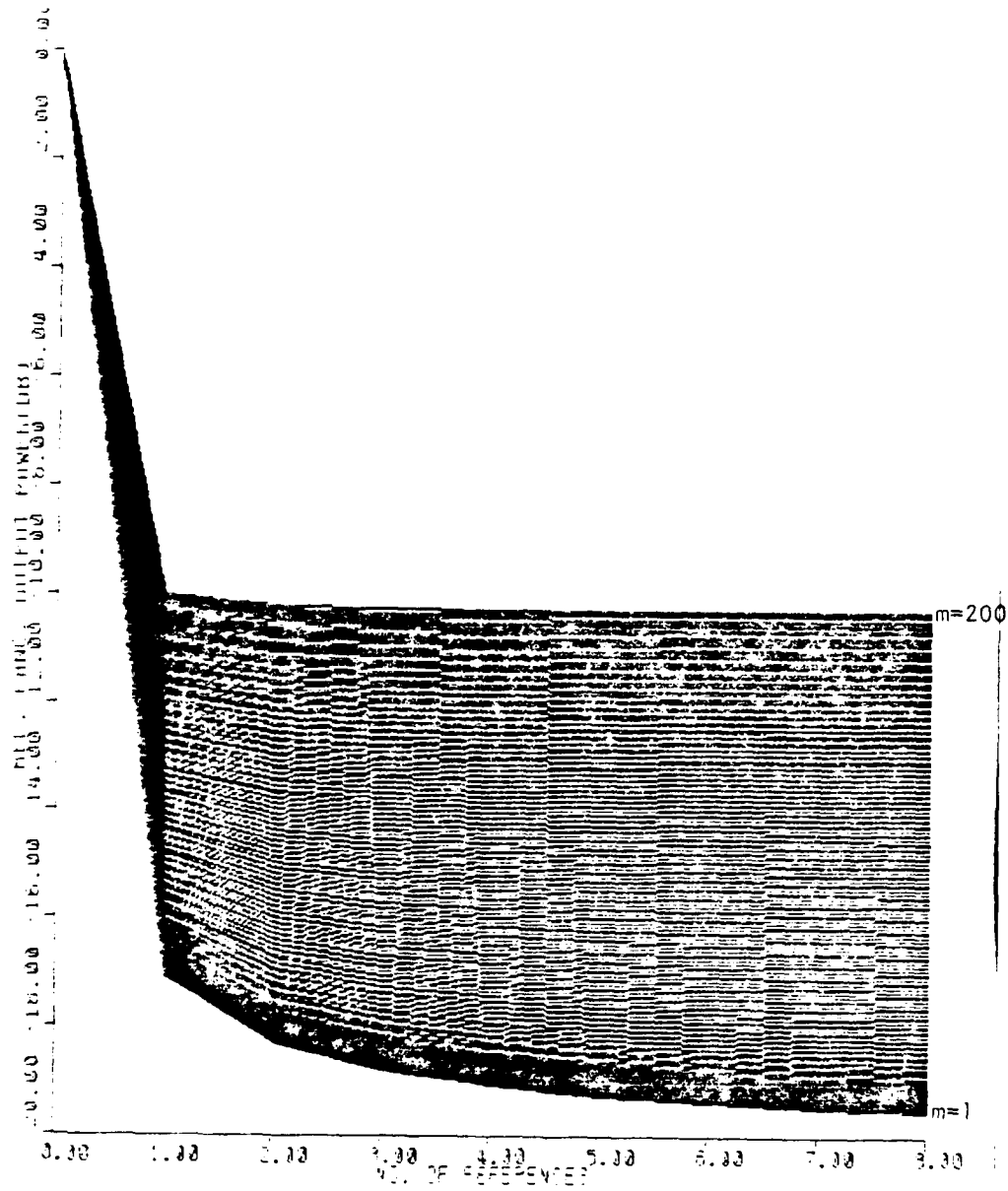
FIGURE K-57

$W = 2 \times 10^{-4}$

$INR = 40$ dB
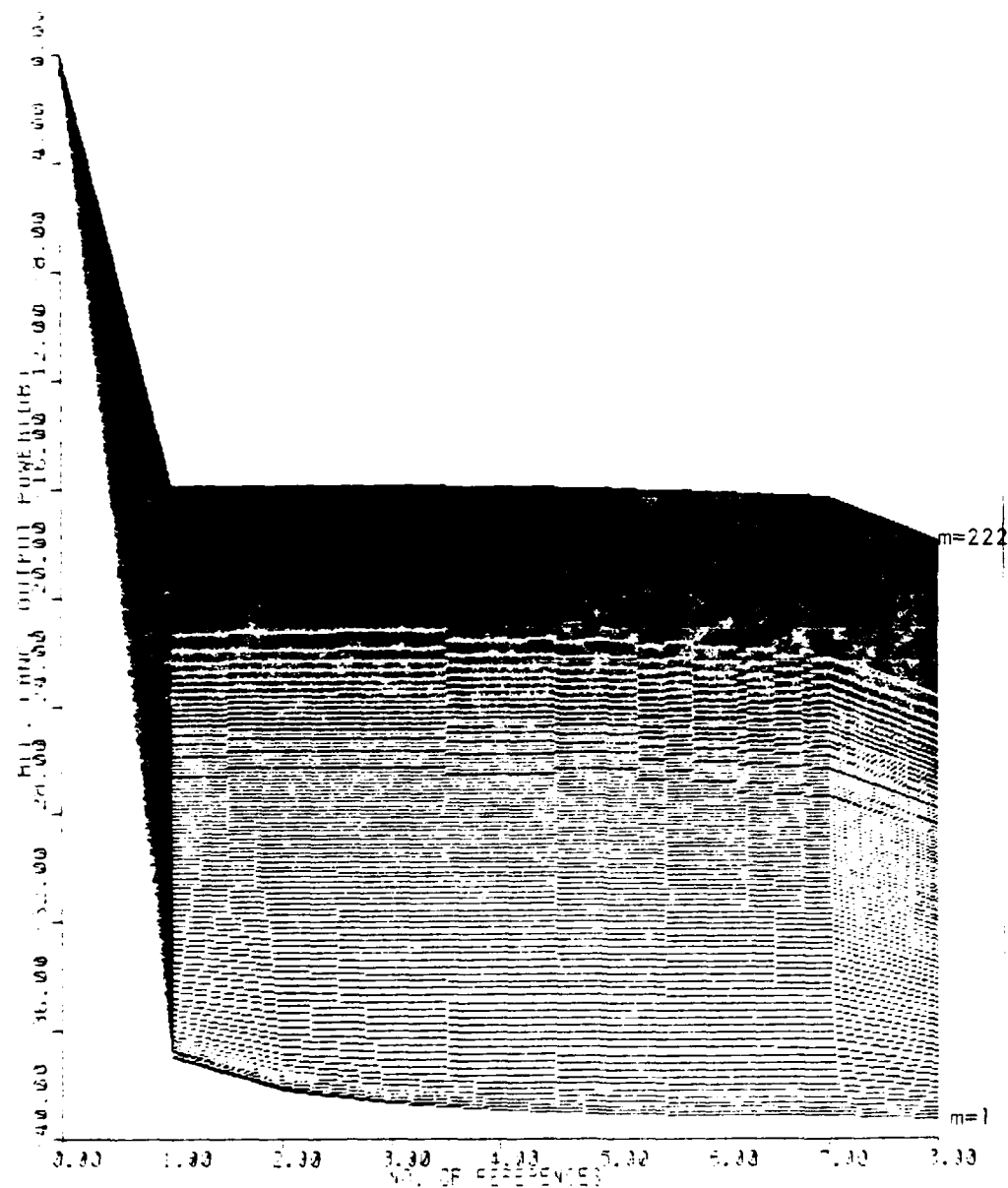
FIGURE K-58

$W = 2 \times 10^{-4}$
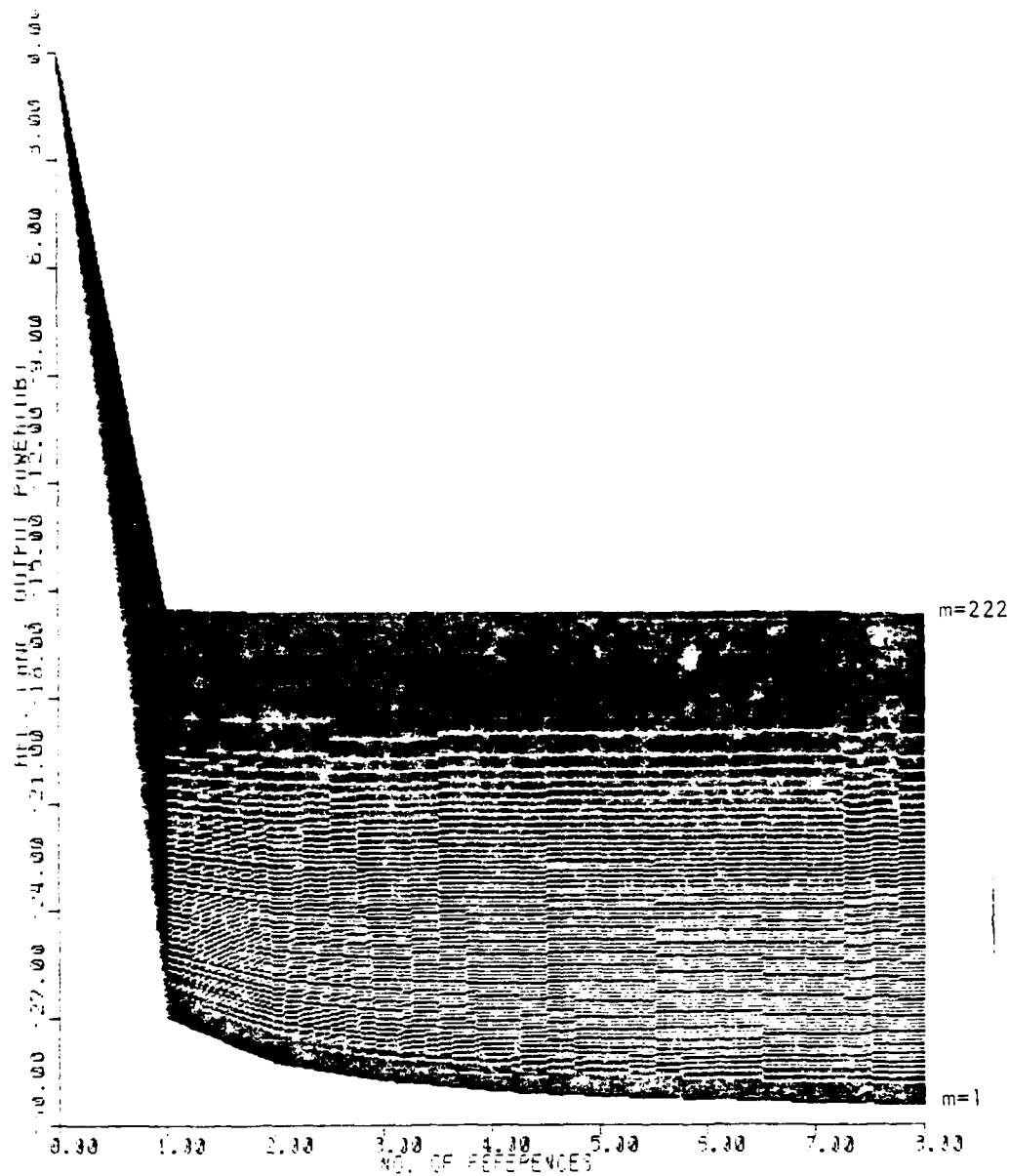
INR = 30 dB

FIGURE K-59

$W = 2 \times 10^{-4}$

INR = 20 dB
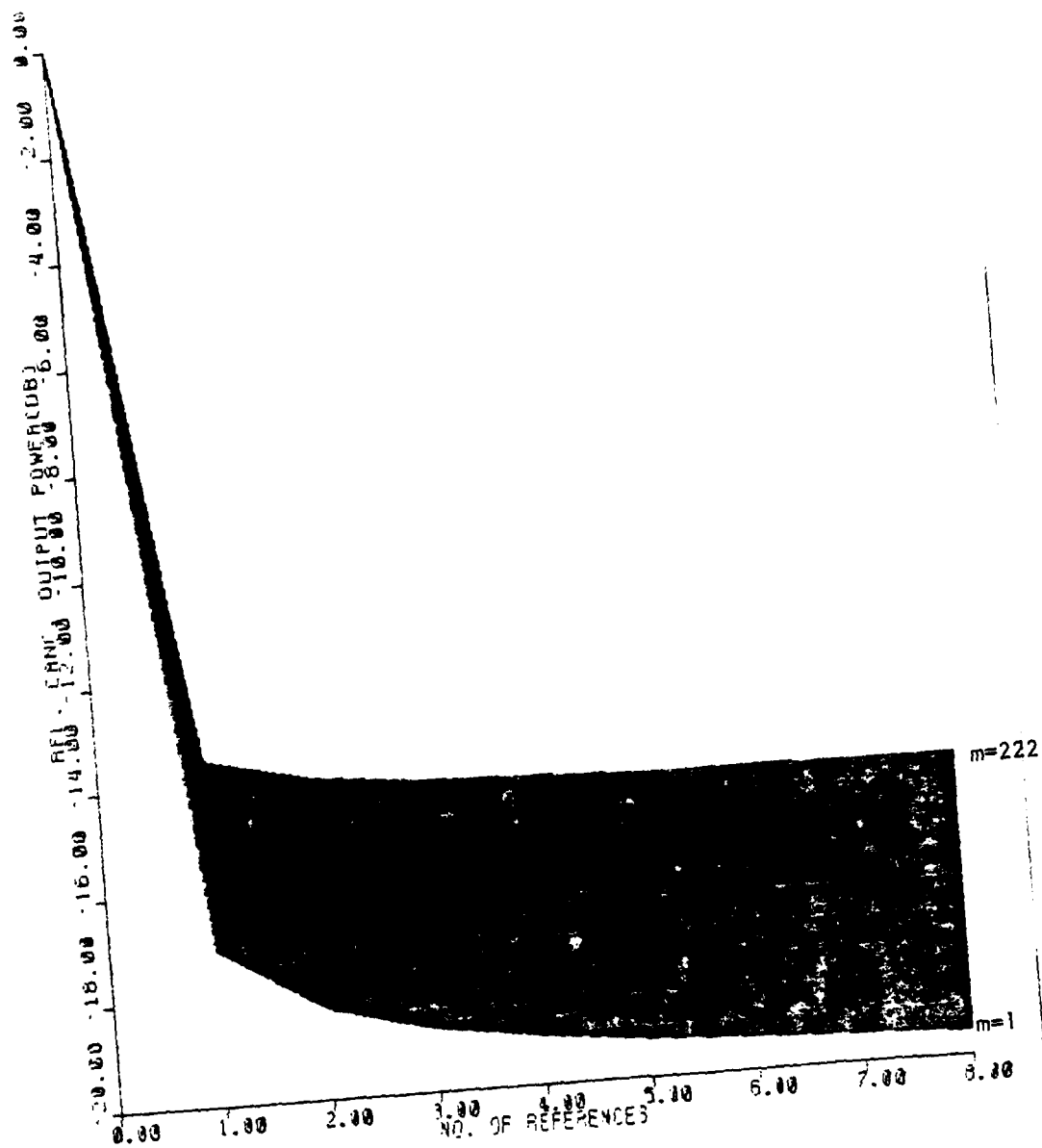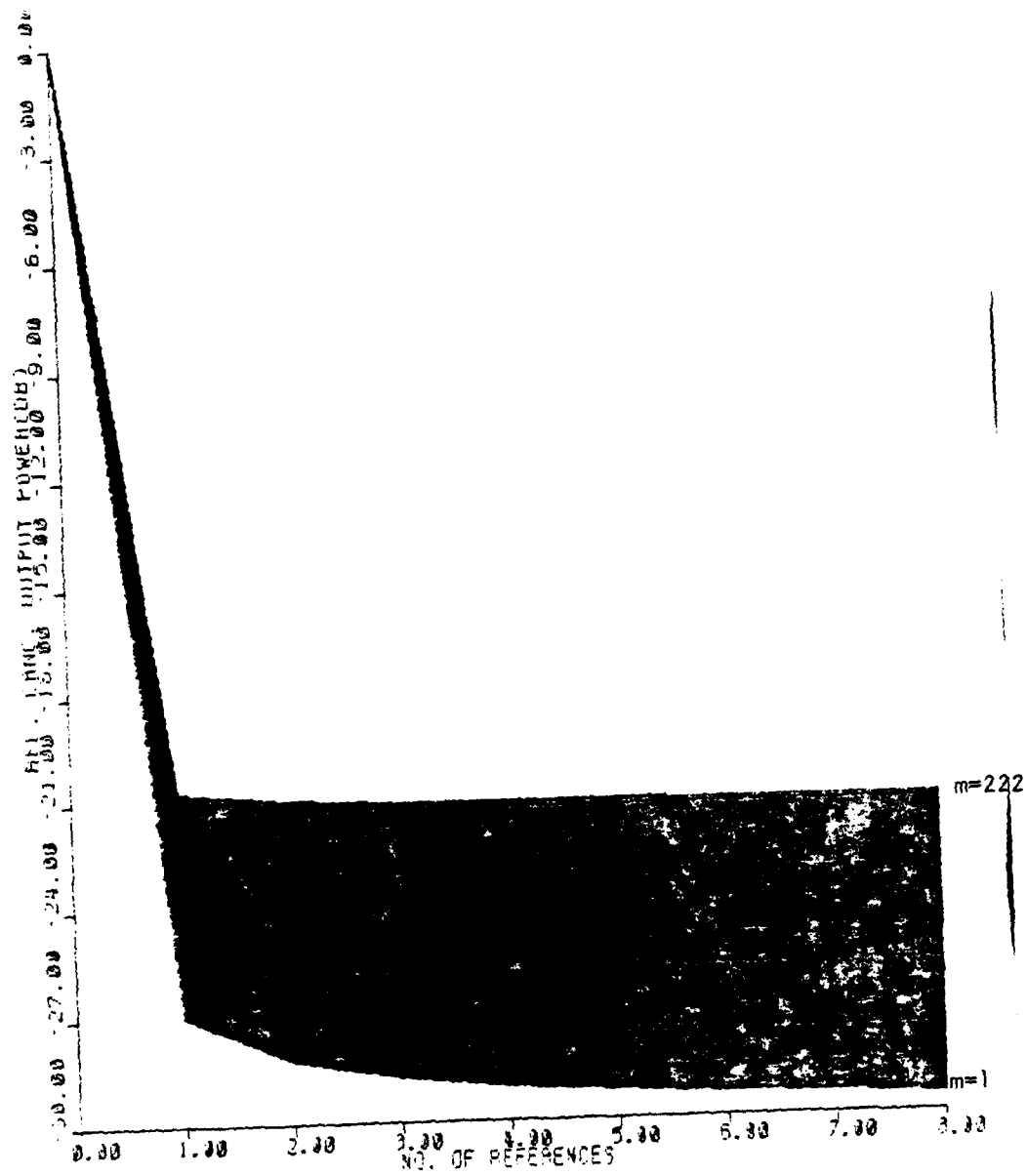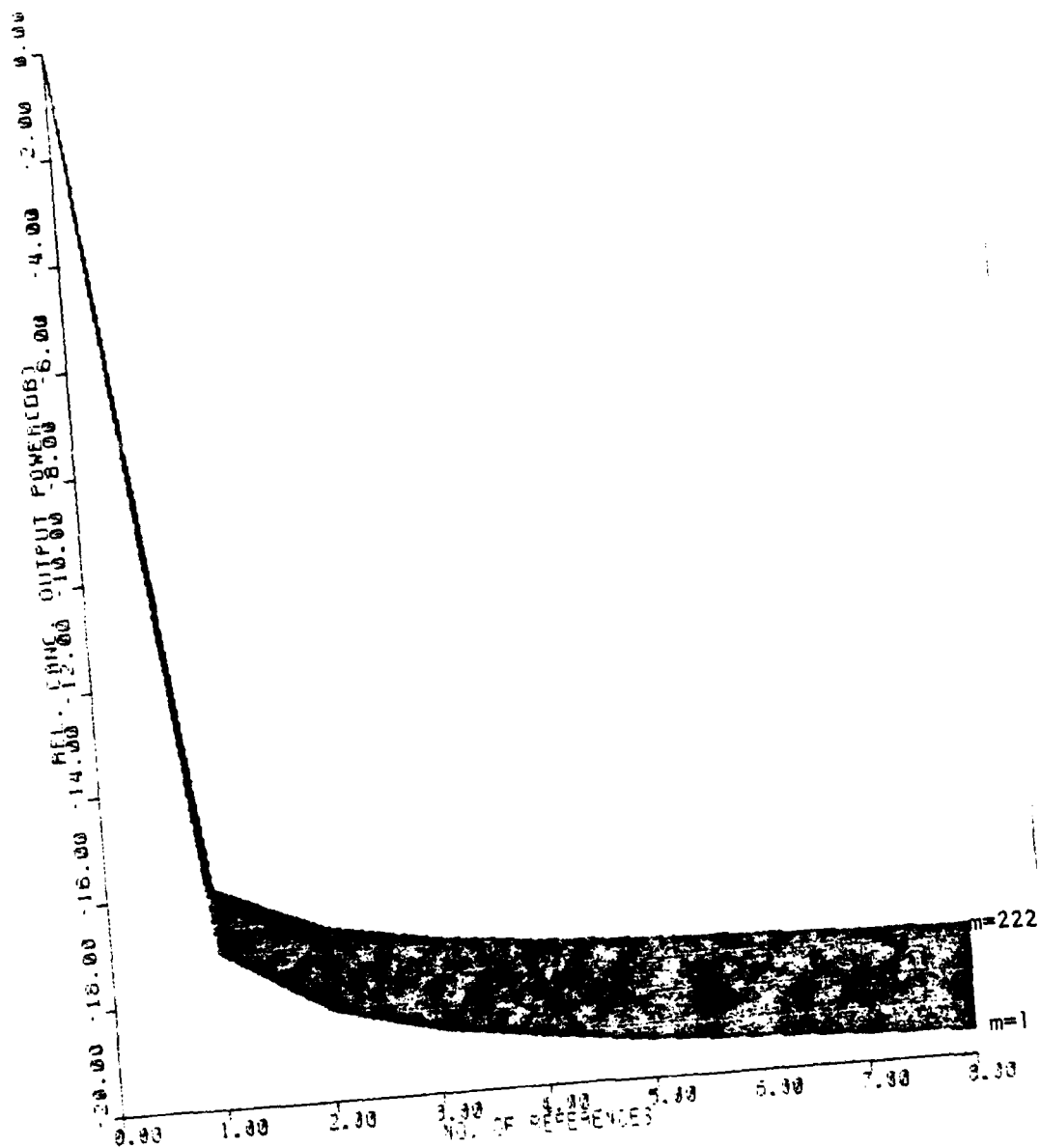
FIGURE K-60

$W = 10^{-4}$

INR = 40 dB
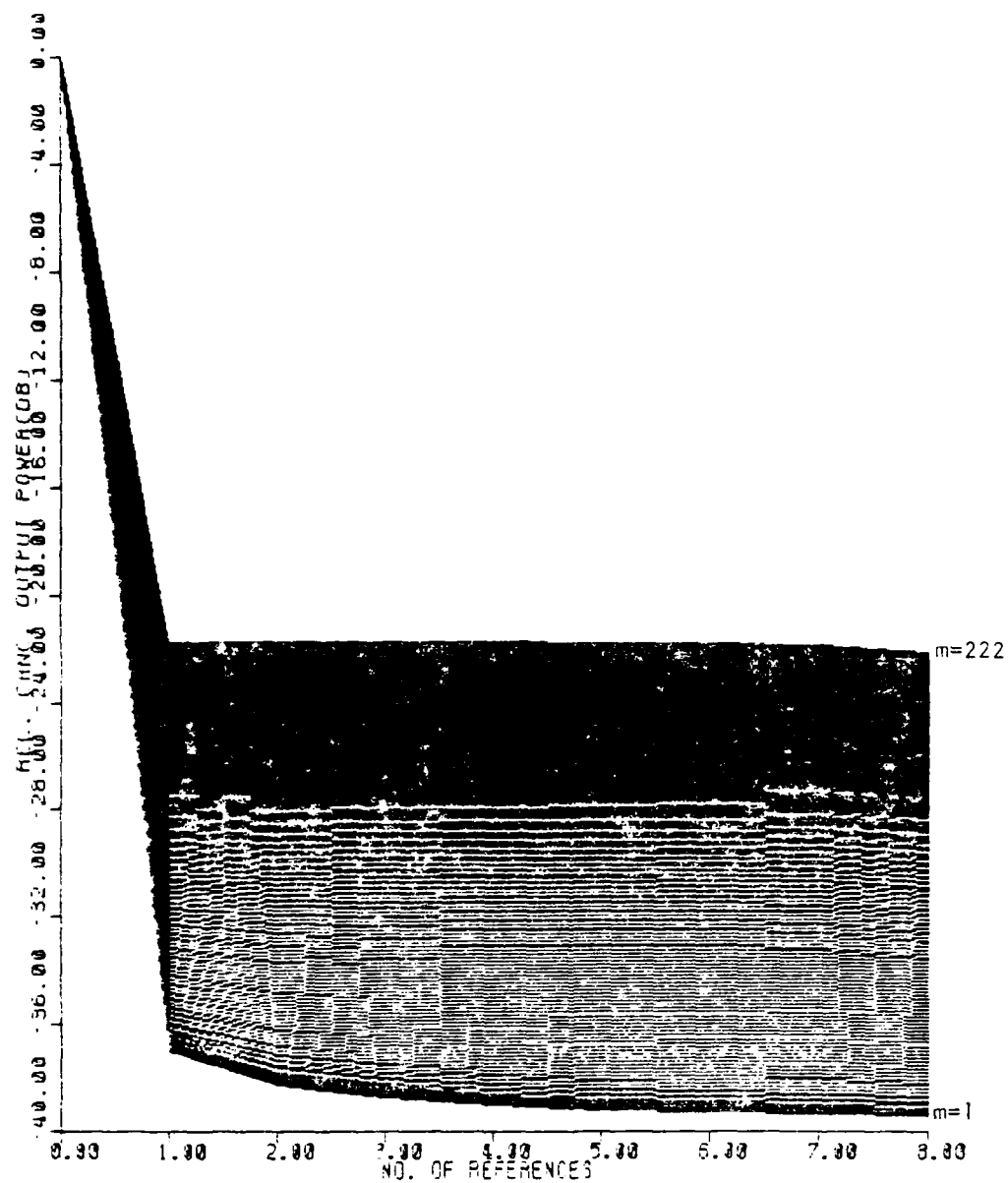
FIGURE K-61

W=10-4

INR = 30 dB

FIGURE K-62

$W = 10^{-4}$

INR = 20 dB

K-67

reference is quite modest. For example, with INR=40 dB and $W=10^{-2}$ (Figure K-30), the first reference gives 28 dB of rejection, the second adds 6 dB more, but the third gives only about 2 dB additional cancellation. The hardware required to incorporate each new reference into the structure is the same, and includes the computational load of computing the weights in an adaptive implementation. Further, in a adaptive canceller, the adaptive loop associated with each reference adds algorithm noise to the system. This algorithm noise can actually offset the improvement due to cancellation improvement. The choice of the number of references must trade off the rejection added by a reference against the additional algorithm noise and computations.

In Appendix F, it was shown that the canceller output spectrum for K references and m=1, that is, $E_K(1,\omega)$ in the noise free case ($\sigma_n^2(\omega)=0$) is asymptotic in K to

$$A(K,W) = \frac{2\Phi\sigma_I^2(\omega)}{2W} [\sin \pi W]^{2K+1} \qquad (K-14)$$

Figure K-63 shows $E_K(1,W)$ for various W plotted along with $A(K,W)$ for $\sigma_n^2(\omega)=0$. It can be seen that $A(K,W)$ is virtually indistinguishable from $E_K(1,\omega)$ when $\sigma_n^2(\omega)=0$ even for small K, so that

$$E_k(1,\omega)\Big|_{\sigma_n^2(\omega)=0} \approx \frac{2\Phi\sigma_I^2(\omega)}{2W} [\sin \pi W]^{2K+1} \qquad (K-15)$$
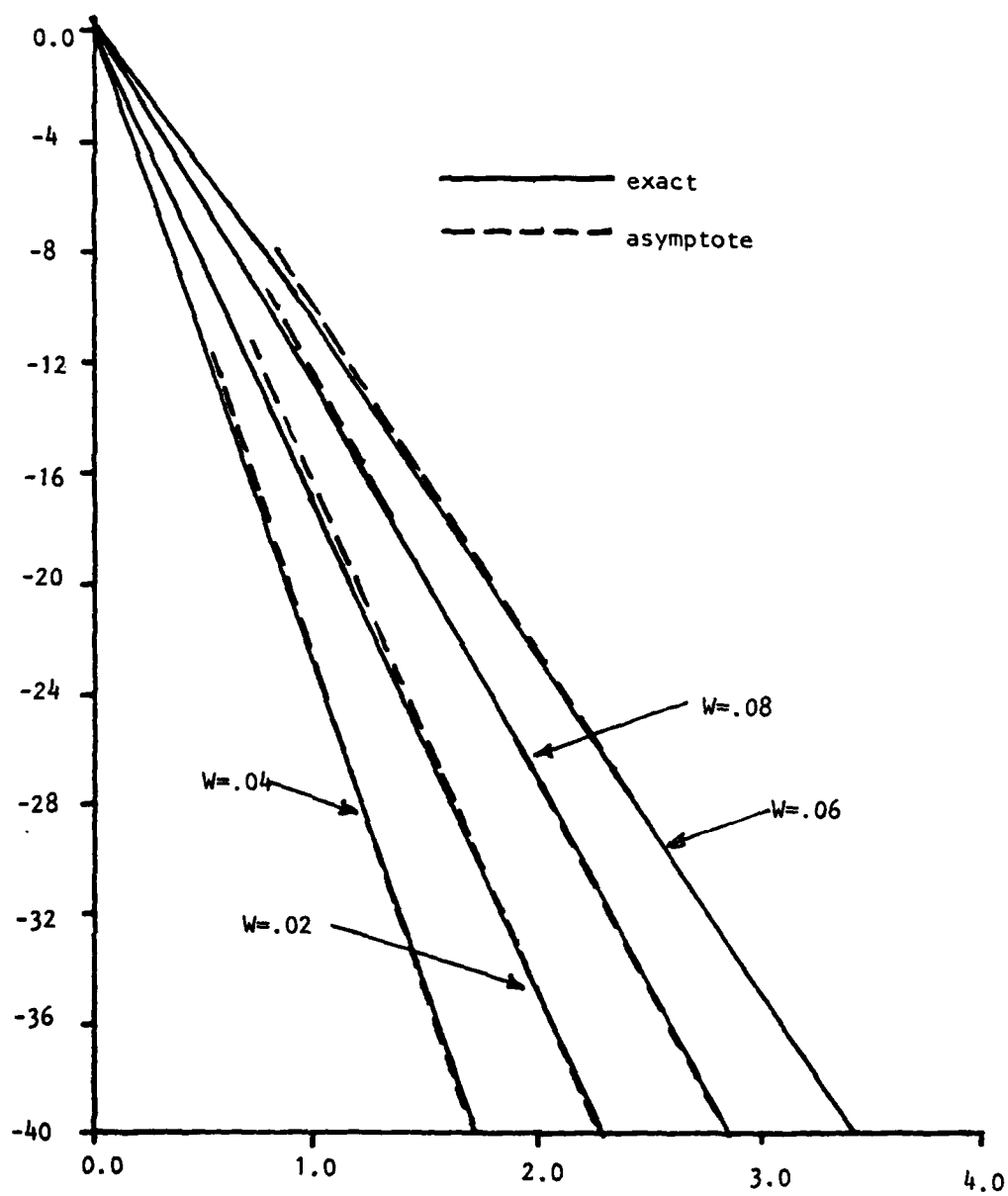
Figure K-63: Comparison of Canceller Output
Spectrum and Asymptote in Ambient Noise
Free Case

K-69

It seems reasonable that as long as INR $\gg$ 1 and the canceller output

spectrum, $E_K(1, \omega)$, is well above the cancellation floor,

$$E_K(1, \omega) \gg E_\infty(1, \omega) \tag{K-16}$$

then the ambient noise present case should behave approximately the same

as the noise free case. The asymptote, $A(K,W)$, is plotted on Figures K-6

through K-62 to test this hypothesis. The agreement between the plots

of $E_K(1, \omega)$ and $A(K,W)$ is quite dependent upon the INR, with excellent

agreement at INR=40 dB, but with $E_K(1, \omega)$ as much as 10 dB higher than

$A(K,W)$ when INR=20 dB. For INR=30 dB the maximum difference is

about 5 dB. Use of (K-14) in the ambient noise present case must be

tempered by knowledge of these errors in the approximation, but it

still provides a useful "rule of thumb".

It would appear from the figures that the value of K at the intersection

of the cancellation floor, (K-12), and the asymptote, (K-14) gives a good

estimate of the transition point at which rapid improvement in cancellation

with additional references is no longer possible (for a given W<1/2 and

INR) for m=1. Using (K-12) and K-14), this intersection occurs at $K=K_I$

where

$$K_I = 1/2 \left\{ [\log (\sin \pi W)]^{-1} [2W \log (1 + \frac{INR}{2W}) - \log (\frac{INR}{2W})]-1 \right\}, \quad W < 1/2$$

$$\tag{K-17}$$

When the interference-to-noise ratio is high, INR $\gg 1$, then (K-17) reduces approximately to

$$K_I \simeq 1/2 \left\{ [\log (\sin \pi W)]^{-1} [(2W-1) \log (\frac{INR}{2W})]-1 \right\}, \quad W < 1/2 \qquad (K-18)$$

Since the selected number of references must be an integer, and taking into account that the intersection given by (K-18) is slightly lower than the transition point in the figures, let

$$K_0 = \lceil K_I \rceil \qquad (K-19)$$

where $\lceil X \rceil$ is the smallest integer greater than or equal to x. Choosing the number of references, K, equal to K_0 for m=1 does not mean that further cancellation is not possible, but that further cancellation is small relative to the increase in computations and algorithm noise. As an example, in Figure K-18 with INR=40 dB and W = .08, (K-19) gives K_0=3 and K=3 produces 27 dB of cancellation. Use of five additional references (K=8) provides only 2.5 dB more rejection of the interference, which would probably not justify the additional computational cost or make up for additional algorithm noise of using five more references.

The number, K_I, provides insight as to how the number of references required in a given situation changes with W and with INR. From (K-18) it can be seen that K_I is linear in 10 log (INR), which is the interference-to-noise ratio in dB. The slope of K_I with respect to 10 log (INR) is

$$\frac{d\ K_I}{d(10\ \log\ (INR))} = \frac{1}{20} \frac{2W-1}{\log(\sin \pi W)} \qquad (K-20)$$

so that approximately $(2W-1)/(20 \log(\sin \pi W)$ references are required per dB of INR. Figure K-64 shows K_I plotted as a function of $10 \log (INR)$ for various W. The dependence on the interference-to-noise ratio is quite weak when $W \lesssim .01$, that is, when the interferences are very narrow.

The dependence of K_I or W is more complicated as shown in Figure K-65, which shows K_I plotted as a function of W for INR=20, 30, and 40 dB. For small W (say, $W < 10^{-2}$) the dependence of K_I on W is very weak, regardless of INR. As W increases above 10^{-2}, the value of K_I begins to increase rapidly with W, going asymptotically to infinity at W=1/2. Recalling from Section 3.3.1.1 that no cancellation is possible when W=1/2, it would be expected that $K_I \to \infty$ at this point.

Now, suppose the criterion $K=K_0$ is used to select the number of references used in a given situation. Figures K-66 shows that the cancellation achieved is within several dB of the cancellation floor, (K-12) for this choice of K. In fact, it can be seen that the value of $E_{K_0}(1,\omega)$ is very nearby log (INR) dB above the floor, so that

$$E_{K_0}(1,\omega) \approx (INR)^{.1} E_\infty(1,\omega) = 2^\Phi \sigma_I^2(\omega)(INR)^{-.9} [1 + \frac{INR}{2W}]^{2W} \qquad (K-21)$$

provided that $(INR)^{.1} E_\infty(1,\omega) \leq 2^\Phi \sigma_I^2(\omega) + \sigma_n^2(\omega)$. This condition just assures that the approximation is not used when it would produce an apparent increase in the interference power relative to the uncancelled primary output. If $INR \gg 1$ and $W < 1$, as it will be in all cases of interest, (K-21) can be approximated as

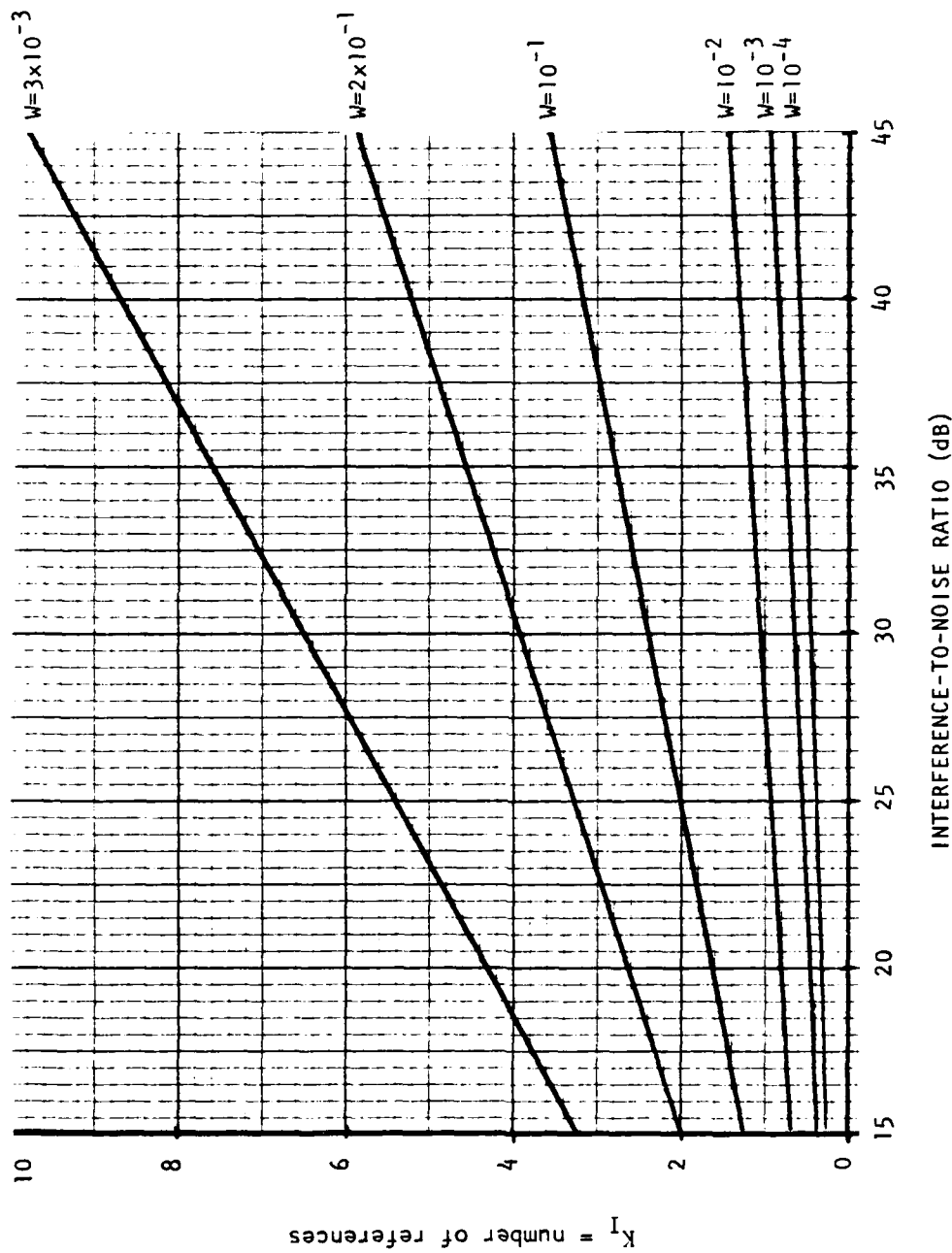$$E_{K_0}(1,\omega) \approx 2^\Phi \sigma_I^2(\omega) (INR)^{2W-.9} (2W)^{-2W}$$
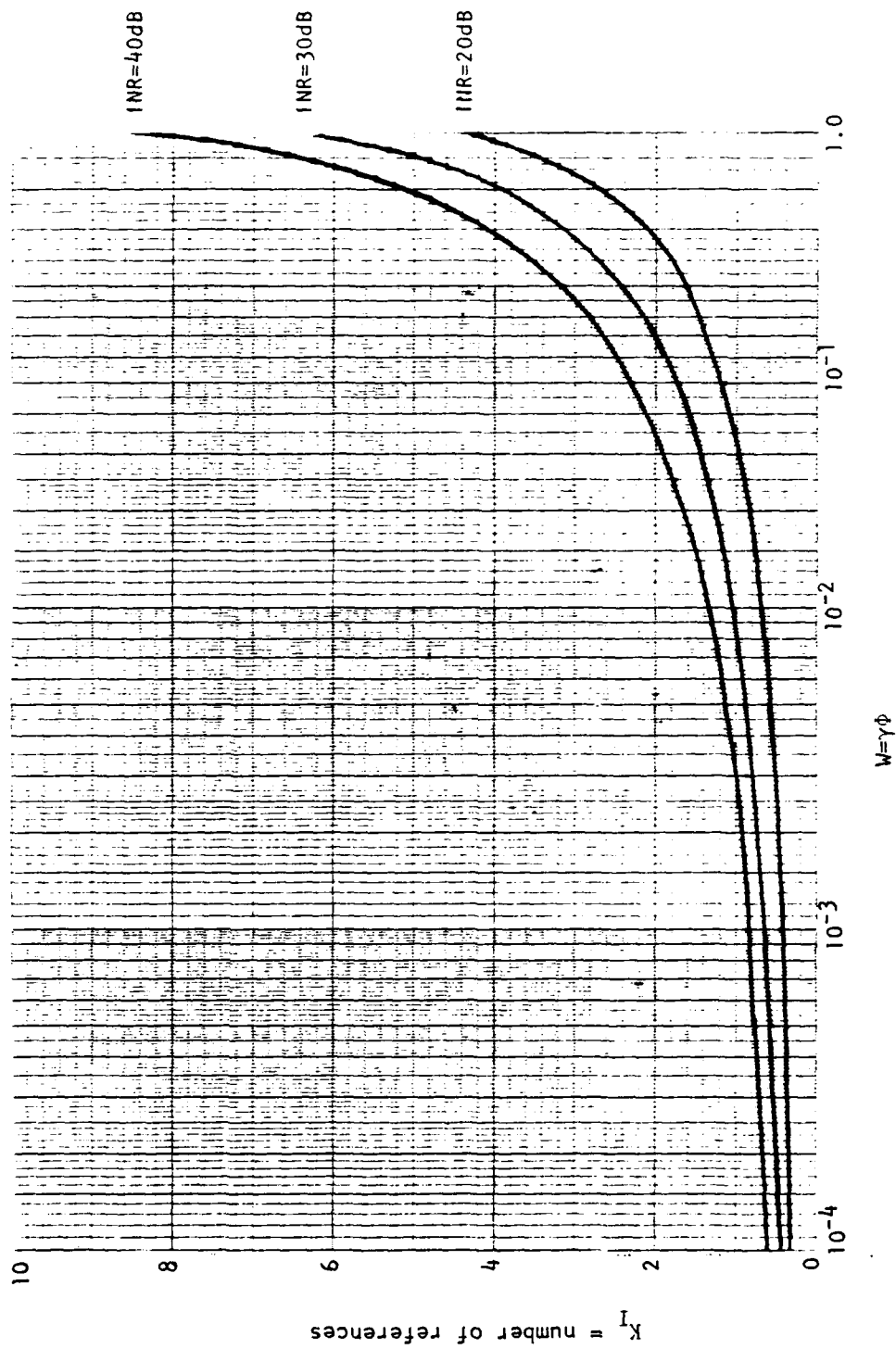
Figure K-64. Change in K_I as a Function of INR
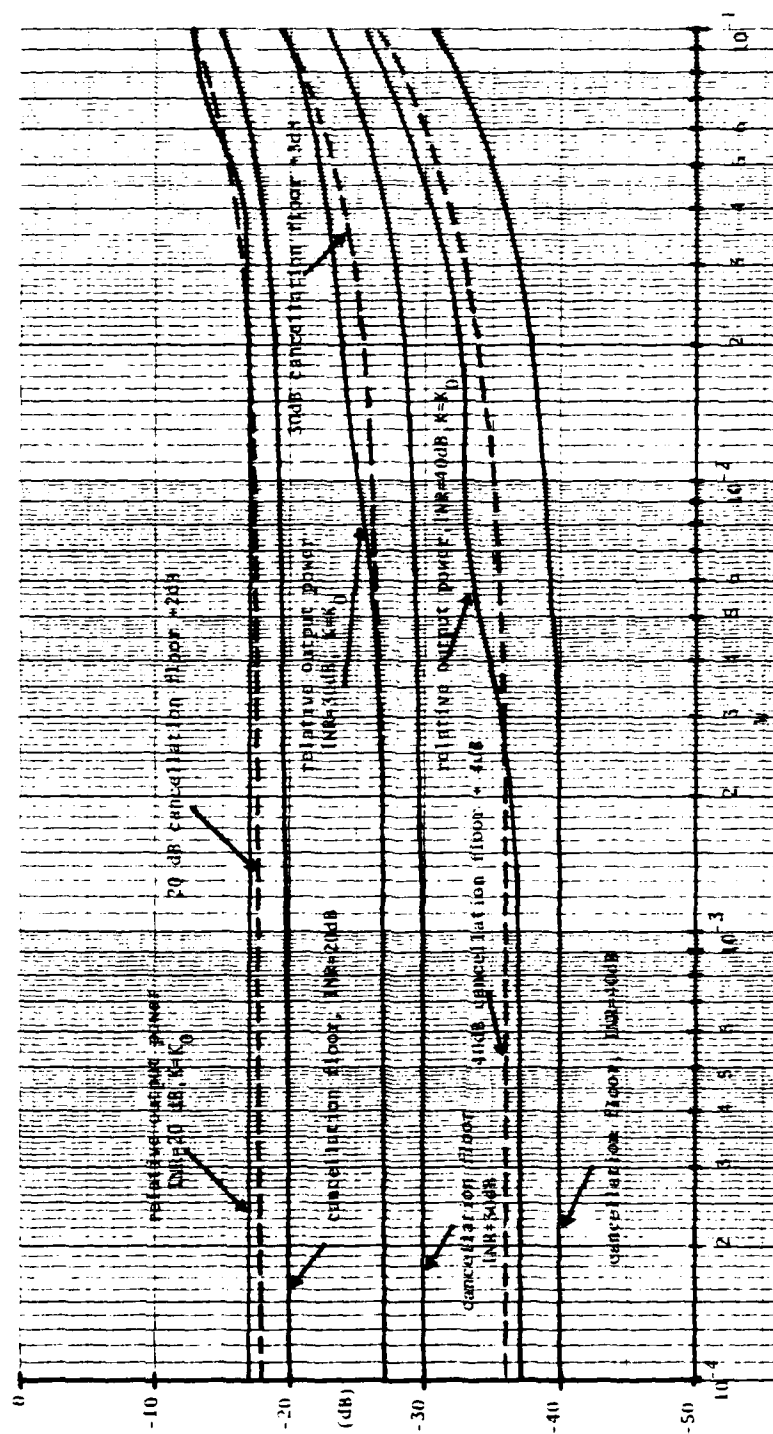
Figure K-65. Change in K_1 as a Function of W

FIGURE K-66. Relative Canceller Outpute Power and Approximation when $K=K_0$

For $0 \leq W \leq 1$, $(2W)^{-2W}$ is within about 1.6 dB of unity, so

$$E_{K_0}(1,\omega) \approx 2\phi \sigma_I^2(\omega) (INR)^{2W-.9} \qquad (K-22)$$

The cancellation achieved is then approximately

$$C_{K_0}(1,\omega) = \frac{E_{K_0}(1,\omega)}{\sigma_n^2(\omega) + 2\phi \sigma_I^2(\omega)} \approx \frac{(INR)^{2W+.1}}{1 + INR} \approx (INR)^{2W-.9} \qquad (K-23)$$

for $INR >> 1$. Expressed in dB, this yields

$$10 \log C_{K_0}(1,\omega) \approx -.9[10 \log(INR)] + 2W[10 \log INR] \qquad (K-24)$$

The interference rejection in dB varies approximately linearly with both the interference to noise ratio in dB and the parameter W. This result is valid over the range $10^{-4} \leq W \leq .45$ and $10^2 \leq INR \leq 10^4$.

Further inspection of Figures K-6 to K-62 shows that for any given values of W and INR, the curves of $E_K(m,\omega)$ have roughly the same shape as that of $E_K(1,\omega)$, and, in particular, have approximately the same transition point in K. This suggessts that K_0 may be a suitable guide for the selection of the number of references, K, even when $m > 1$. It can be seen from the figures that for $m >> 1$, $E_K(m,\omega)$ continues to fall off somewhat faster than $E_K(1,\omega)$ for $K > K_0$. For example, in Figure K-31, with $W = .01$ and $INR = 10^3$, $K_0 = 2$ which yields $10 \log C_2(1,\omega) = -25.5$ dB. Six additional references give $10 \log C_8(1,\omega) = -27.5$ dB of cancellation, so the choice of $K = K_0$ seems justified. However, for $m = 5$, $K = K_0 = 2$ gives $10 \log C_2(5,\omega) = 16$ dB of cancellation, while $K = 3$ yields 19 dB and $K = 5$,

22 dB of cancellation. Of course, there will always be some ambiguity as to how much more rejection must be provided by a new reference to justify its use. Certainly, in any given design situation K_0 can be used as a design guide, with final choices made by consulting the curves in Figures K-6 through K-62.

DEPARTMENT OF DEFENSE FORMS

F-200.1473 *DD Form 1473:* Report Documentation Page

REPORT DOCUMENTATION PAGE		READ INSTRUCTIONS BEFORE COMPLETING FORM
1. REPORT NUMBER	2 GOVT ACCESSION NO.	3. RECIPIENT'S CATALOG NUMBER
4. TITLE (and Subtitle) Final Report on the Cancellation of Surface Reverberation from a Bistatic Sonar		5. TYPE OF REPORT & PERIOD COVERED
		6. PERFORMING ORG. REPORT NUMBER
7. AUTHOR(s) P.L. Feintuch, F.A. Reed, and N.J. Bershad		8. CONTRACT OR GRANT NUMBER(s) N00024-80-C-6292
9. PERFORMING ORGANIZATION NAME AND ADDRESS Hughes Aircraft Company P.O. Box 3310, Fullerton, Ca. 92634		10. PROGRAM ELEMENT, PROJECT, TASK AREA & WORK UNIT NUMBERS
11. CONTROLLING OFFICE NAME AND ADDRESS Naval Sea Systems Command, Code 63R Department of the Navy, Washington, DC 20362		12. REPORT DATE January 20, 1982
		13. NUMBER OF PAGES
14. MONITORING AGENCY NAME & ADDRESS(if different from Controlling Office)		15. SECURITY CLASS. (of this report) Unclassified
		15a. DECLASSIFICATION/DOWNGRADING SCHEDULE
16. DISTRIBUTION STATEMENT (of this Report)		
17. DISTRIBUTION STATEMENT (of the abstract entered in Block 20, if different from Report)		
18. SUPPLEMENTARY NOTES		
19. KEY WORDS (Continue on reverse side if necessary and identify by block number) Adaptive cancellation, bistatic sonar, convergence zone, extended sources, LMS algorithm, LMS adaptive canceller, surface reverberation		

20. ABSTRACT (Continue on reverse side if necessary and identify by block number)

The use of multiple reference LMS adaptive cancellation to suppress surface reverberation from the convergence zone (CZ) in a bistatic sonar is considered. Hydrophones spatially separated from the primary sonar array are used as reference. The surface reverberation is modeled as a narrow, spatially uncorrelated extended source and the cancellation performance determined for such a source. It is shown that the CZ surface reverberation can be suppressed close to the

DD FORM 1473 EDITION OF 1 NOV 65 IS OBSOLETE

Block No. 20

ambient noise floor using a small number of references. To achieve this cancellation, the extent of the source must be taken into account in the design of the canceller. Curves are given for the suppression achieved as a function of reverberation and canceller parameters and guidelines for the selection of canceller design parameters presented.

Distribution List

	Address
NAVSEA 63R-11	Commander Naval Sea Systems Command Department of the Navy Washington, D.C. 20362 Attn: D.E. Porter, 63R-11
NAVSEA 63X3	Commander Naval Sea Systems Command Department of the Navy Washington, D.C. 20362 Attn: 63X3
NAVSEA 63X1	Commander Naval Sea Systems Command Department of the Navy Washington, D.C. 20362 Attn: 63X1
NAVSEA 63Y1	Commander Naval Sea Systems Command Department of the Navy Washington, D.C. 20362 Attn: 63Y3
NAVSEA 63Y3	Commander Naval Sea Systems Command Department of the Navy Washington, D.C. 20362 Attn: 63Y3
NAVSEA 63D	Commander Naval Sea Systems Command Department of the Navy Washington, D.C. 20362 Attn: 63D
NAVSEA 996	Commander Naval Sea Systems Command Department of the Navy Washington, D.C. 20362 Attn: 996
DDC	Defense Documentation Center Defense Services Administration Cameron Station, Building 5 5010 Duke Street Alexandria, Virginia 22314

	Address
DDR&E	Office of the Director of Defense Research and Engineering Room 3C128, The Pentagon Washington, D.C. 20301
AFPRO, CA	AFPRO Hughes Aircraft Company P.O. Box 92463 Los Angeles, California 90009

MED
-8